Tao Jiang

Characterization and Modelling of Soluble Microbial Products in Membrane Bioreactors

Thesis submitted in fulfilment of the requirements
for the degree of Doctor (Ph.D.) in Applied Biological Sciences

to my mother, father, sister
and Heng

Table of Contents

Acknowledgements

My greatest gratitude goes to Peter for all he did for me, from finding me in UNESCO-IHE, giving me the opportunity to start MBR work and being part of the BIOMATH research group. It was not easy to initiate this MBR study completely from scratch. I remember the time (and effort!) that we spent trying to get some additional funds for this research project. I also remember 'fighting' with some of my colleagues to get his time to discuss MBR research – it is not an easy task to get an appointment with a very busy Professor! I also remember his sense of humor, and his kindness in helping me over all the hurdles of a PhD research project.

I want to express my great gratitude to Gary, for taking up the supervision half way through my PhD research project, and giving key suggestions in characterising SMP and pushing me through the UAP research work. His research attitude of 'digging deeper and deeper' has deeply impressed me. I want to express my great gratitude to Prof. Jan Schippers, for his supervision during my MSc and the first two years of my PhD research project. I was impressed by his 'critical' comments throughout both my MSc and PhD studies.

It would not have been possible to perform so many experiments without the financial and technical support of Prof. Dr. ir. Walter van der Meer, Vitens Fryslân & University of Twente, the Netherlands and the technical support of Dr. Harry Futselaar, Norit Membrane Technology (NMT). Thank you so much for your support throughout my MSc and PhD studies! I would like to thank Kiwa Water Research, the Netherlands for allowing the use of their (mini) advanced UF filtration unit. I would also like to thank Dr. Stefan Huber (DOC-LABOR) for his help in interpreting the LC-OCD analyses.

I want to express my sincere gratitude to Maria, who introduced me to the membrane field through my MSc research project. Her patience has encouraged my confidence to live through all the 'hard times' in Europe during the past 7 years. Her broad contacts with companies and universities connected this MBR research project. I want to express my gratitude to Ingmar for organizing, encouraging and supporting

List of abbreviations

AAGR	Average Annual Growth Rate
ABS	Alkyl-Benzene-Sulfonate
AI	Analog Input
AO	Analog Output
AOC	Assimilable Organic Carbon
ASM1	Activated Sludge Model No. 1
ASM2d	Activated Sludge Model No. 2d
ASM2dSMP	Activated Sludge Model No. 2d SMP
ASM3	Activated Sludge Model No. 3
ATU	Allylthiourea
BAP	Biomass Associated Product
BFR	Biofilm Formation Rate
BOD	Biological Oxygen Demand
BSA	Bovine Serum Albumin
CAS	Conventional Activated Sludge
CF	Crossflow
COD	Chemical Oxygen Demand
DAQ	Data Acquisition
DBP	Disinfection By-Products
DOC	Dissolved Organic Carbon
DSVI	Diluted Sludge Volume Index
EBPR	Enhanced Biological Phosphorus Removal
EDC	Endocrine Disrupting Compound
EfOM	Effluent Organic Matter
EMBR	Extractive MBR
EPS	Extracellular Polymeric Substances
F/M	Food to Microorganism ratio
GC	Gas Chromatography
HAA	Haloacetic Acid
HMW	High Molecular Weight
HRT	Hydraulic Retention Time
LAS	Linear-Alkyle-Sulfonate
LC-OCD	Liquid Chromatography - Organic Carbon Detection
LMW	Low Molecular Weight
MABRS	Membrane-Aerated Biofilm Reactor
MBR	Membrane Bioreactor
MF	Microfiltration
MFI-UF	Modified Fouling Index-Ultrafiltration
MLSS	Mixed Liquor Suspended Solids
MLVSS	Mixed Liquor Volatile Suspended Solids
MW	Molecular Weight

MWCO	Molecular Weight Cut-Off
NDMA	N-Nitrosodimethylamine
NF	Nanofiltration
NOM	Natural Organic Matter
OC	Organic Carbon
OCD	Organic Carbon Detector
OND	Organic Nitrogen Detector
OUR	Oxygen Uptake Rate
PAO	Phosphorus Accumulating Organism
PCP	Personal Care Product
PHA	Poly-Hydroxy-Alkanoate
PS	Polysaccharide
PSD	Particle Size Distribution
PT	Protein
PVDF	Polyvinylidene Fluoride
RO	Reverse Osmosis
SCOD	Soluble COD
SDI	Silt Density Index
SEC	Size Exclusion Chromatography
SMP	Soluble Microbial Products
SMPRT	Average Retention Time of SMP
SOC	Synthetic Organic Compounds
SRF	Specific Resistance to Fouling
SRT	Sludge Retention Time
SUVA	Specific UV Absorption
THM	Trihalomethane
TMP	Transmembrane Pressure
TOC	Total Organic Carbon
TSS	Total Suspended Solid
UAP	Utilization Associated Products
UCT	University of Cape Town
UF	Ultrafiltration
UV	Ultraviolet
UVD	UV Detector
VFA	Volatile Fatty Acids
WWTP	Wastewater Treatment Plant

1. Introduction

1.1 Problem definition

Membrane bioreactors (MBRs) refer to the combination of membrane technology and high rate biological process technology for wastewater treatment. The bioreactor is operated similar to a conventional activated sludge (CAS) process but without the need for secondary clarification. MBR technology has received keen interest in recent years and by year 2004, more than 2200 MBR installations were in operation or under construction worldwide (Yang et al., 2006). The global MBR market is currently valued at an estimated US$ 216.6 million, and is rising at an average annual growth rate of 10.9% (BCC, 2006).

MBRs produce excellent effluent quality but require a small footprint. In the EU countries, the driving forces behind the use of MBRs are: 1) the strict EU effluent discharge standards. In many cases, the MBR effluent quality is so good that it can be reused directly in non-potable applications; 2) their small footprint. Many Western European countries suffer from high population density and space limitations in constructing new or expanding existing wastewater treatment plants (WWTP) is a serioius problem; 3) the continuous decrease in membrane costs is increasing the competitiveness of MBR compared with CAS systems.

The investment costs of MBRs have become as low as for CAS system. However, the operating costs are still higher due to membrane replacement costs and the high energy demand for the hydrodynamic control of membrane fouling (Judd, 2006). In addition, membrane fouling occurring on the membrane surface and within the pores reduces the long-term stability of the flux performance. Unfortunately, the understanding of MBR fouling is still limited and many full-scale MBR applications rely on (lengthly) pilot plant testing to evaluate suitable design and operational conditions (van der Roest et al., 2002). At this moment, neither the evolution of

membrane permeability under certain operating conditions nor the effect of cleaning measures can be predicted. These uncertainties therefore cause considerable difficulties in MBR design and operation.

Developing MBR technology requires an interdisciplinary approach and the study of MBR fouling requires knowledge of both biological wastewater treatment (biological background) and membrane filtration (physical-chemical background). Many researchers and projects focus their study on one issure only, i.e., either the biology or the membrane. However, recent progress in the understanding of MBR fouling shows a significant impact of MBR biology on membrane fouling. More and more studies are bridging the two fields, focusing on the interactions between biology and membrane filtration/fouling.

To predict fouling quantitatively, four fundamental questions have to be answered, i.e., 1) what are the main foulants; 2) how are foulants produced and how can the foulant concentrations be predicted; 3) how are foulants deposited onto the membrane; 4) what is the impact of deposited foulants on membrane permeability.

The first fundamental question has been widely studied using various methods, including filtration and filterability tests (te Poele et al., 2004), size exclusion chromatography (SEC) (Drews et al., 2005; Lesjean et al., 2005; Rosenberger et al., 2005; Rosenberger et al., 2006; Zhang et al., 2006a), colorimetric methods (Rojas et al., 2005; Masse et al., 2006) and statistical correlation studies between sludge constituents and membrane fouling (Fan et al., 2006). The results have shown that MBR fouling is mostly related to the MBR sludge water, which is defined as the colloidal and soluble fraction of the MBR sludge. Actually, the major constituent of sludge water is SMP (soluble microbial products) produced by microorganisms. With respect to methodology, nearly all studies used empirical methods, i.e., running MBRs under various conditions, and correlating MBR fouling with certain sludge constituents, e.g., SMP. The results of these studies are therefore constrained to the specific experimental conditions applied.

The second fundamental question that still remains unanswered relates to how SMP are produced and how the SMP concentration can be predicted under certain

operational conditions. Many SMP modelling studies have been conducted in biofilm or CAS systems (Namkung and Rittmann, 1986; Orhon et al., 1989; Boero et al., 1991). More recently, SMP have also been studied in MBR systems (Lu et al., 2001; Lee et al., 2002; Lu et al., 2002; Cho et al., 2003; Ahn et al., 2006). However, most existing SMP models are over-parameterised with strong parameter correlation, and in many cases, the only available measurement used for parameter estimation is the soluble COD concentration of the MBR sludge water. Therefore, the results of parameter estimations are questionable and these models should be applied with caution. To quantify the SMP concentration in MBRs, efforts should be spent on developing and calibrating a simple but adequate SMP model with reliable parameter estimation, for a feasible experimental effort.

The third fundamental question related to the foulant deposition under crossflow conditions has been partially studied but further studies are needed. The deposition of particles onto the membrane is impacted by the hydrodynamic conditions of the membrane module (Belfort et al., 1994). Early hydrodynamic studies in MBRs have focused on large particles (Tardieu et al., 1998; Tardieu et al., 1999), but the significance of SMP on MBR fouling requires the study of submicron particles under various flux and crossflow conditions.

The fourth fundamental question related to the prediction of membrane permeability is probably the most difficult one, as it is related to the first three fundamental questions but also many other operational conditions of the MBR. Typical long-term filtration behaviour (transmembrane pressure vs. time) often shows a gradual increase in TMP followed by a rapid TMP jump (Ognier et al., 2002; Zhang et al., 2006a). The gradual increase of TMP in the early filtration stage has been attributed to soluble EPS (extracellular polymeric substances), while the rapid fouling afterwards has been attributed to the deposition of biomass (Cho and Fane, 2002). A combined pore blocking and cake filtration model originally developed by Ho and Zydney (2000) has been applied to model the TMP transition in an unstirred batch filtration test with alginates as a model soluble EPS (Ye et al., 2006). However, the applied operational conditions are far from the MBR field conditions, i.e., crossflow, periodical backwashing/relaxation, and actual MBR sludge. Therefore, considerable efforts are spent to answer this question.

In summary, the lack of fundamental understanding of membrane fouling is putting the rapidly growing MBR market at risk. There is an urgent need to improve this understanding and to develop a tool to predict MBR fouling quantitatively.

1.2 Goal and objectives

The goal of this thesis is to characterise the foulants in MBRs and develop a mathematical model to predict both membrane fouling and effluent quality. The main objectives of this work are as follows.

- To calibrate a lab-scale MBR using the activated sludge model No. 2d (ASM2d) for biological nutrient removal and to predict the sludge characteristics and effluent quality. The biological model is regarded as the backbone of the SMP model.

- To study the characteristics of SMP, i.e., the composition, molecular weight distribution (MWD), hydrophobicity, and biodegradability and to identify the fractions of BAP and UAP, that correlate with membrane fouling.

- To develop and calibrate an ASM2dSMP model with reasonable parameter estimation that can predict the SMP concentration in the bioreactor.

- To further develop existing hydrodynamic models by incorporating energy consumption and evaluate the cost-effectiveness of crossflow in the control of submicron particle deposition.

- To develop a mathematical filtration model under crossflow conditions and predict the TMP change over short-term (within one filtration cycle) and long-term (between two chemical cleanings) operation.

1.3 Outline

An outline of this thesis, showing the links between the 5 main chapters, is presented in Figure 1-1. This thesis aims to improve our understanding of SMP, and in particular to show that SMP is the link between MBR biology. The chapters containing significantly new approaches and findings are highlighted in bold.
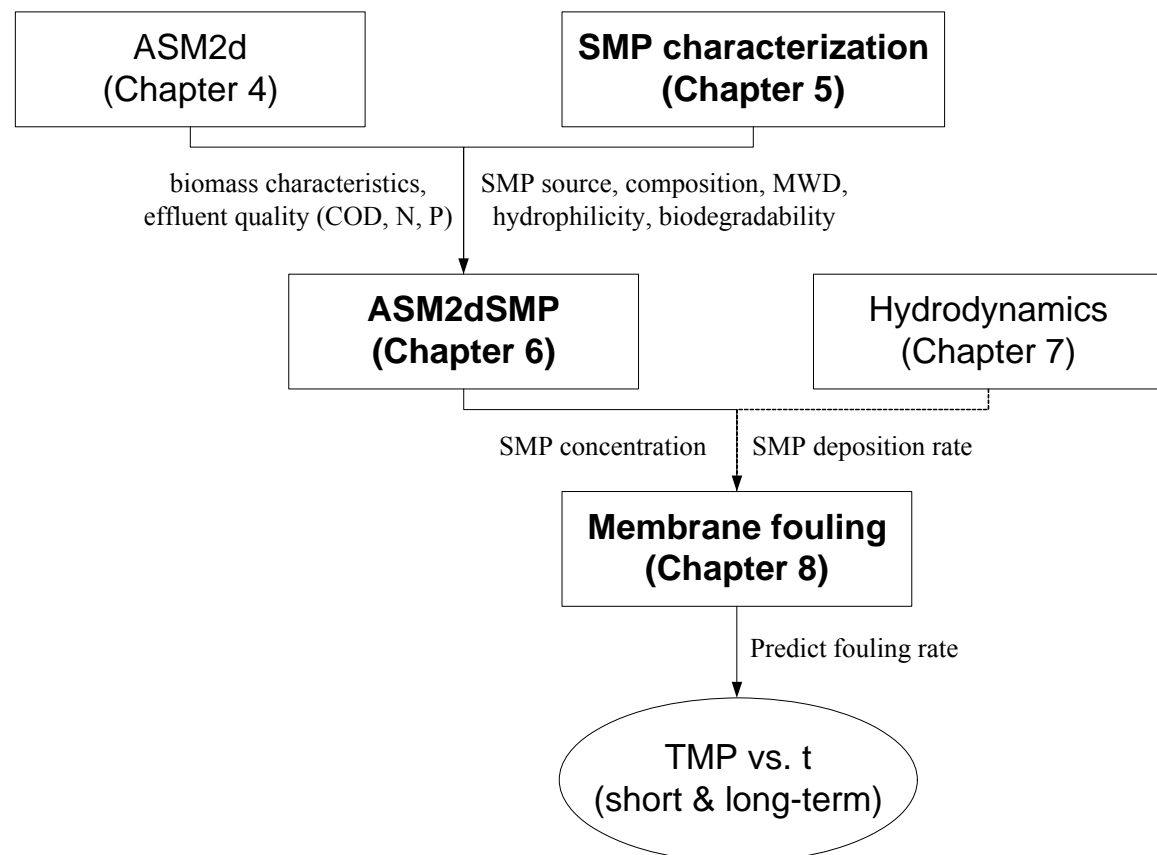
Figure 1-1 Outline of thesis chapters

Chapter 4 is the basis of modelling MBR biology. The activated sludge model No. 2d (ASM2d) is adapted to describe the MBR system with the aim of predicting biomass characteristics and effluent quality. The characteristics of SMP, e.g., source, composition, molecular weight distribution (MWD), hydrophilicity, biodegradability and fouling potential are studied in Chapter 5 using a new analytical tool, LC-OCD (liquid chromatography - organic carbon detection) equipped with organic carbon, UV and organic nitrogen detectors. The significant impact of SMP on MBR fouling requires a tool to predict the SMP concentration in MBRs, and this is achieved by developing a simple and identifiable mathematical model called ASM2dSMP in Chapter 6. The model is developed, calibrated and validated with the power to predict

the SMP concentration under various SRT (sludge retention time) and HRT (hydraulic retention time) conditions.

The deposition rate of particles on membranes is described by a hydrodynamic model in Chapter 7. Finally, in Chapter 8, a pore blocking and cake filtration model incorporating a simplified description of hydrodynamics was developed. This integrated model is able to predict the MBR fouling rate with respect to both short-term (between two backwashings) and long-term (between two chemical cleanings) operation.

2.
Literature review

2.1 Membrane bioreactors

2.1.1 Definition of MBRs

Membrane bioreactors (MBRs) refer to the combination of membrane technology and the high rate biological process for wastewater treatment (Stephenson et al., 2000). It has been undergone rapid development in the last decade and is becoming a promising alternative to conventional biochemical wastewater treatment processes.

MBRs can be classified into three groups: biomass separation MBRs, membrane aeration bioreactors - also called membrane-aerated biofilm reactors (MABRs) and extractive MBRs (EMBRs) (Figure 2-1). At this moment, full-scale biomass separation MBRs are extensively applied for domestic and industrial wastewater treatment. However, MABRs and EMBRs have only been operated up to pilot-scale for industrial wastewater treatment (Stephenson et al., 2000).
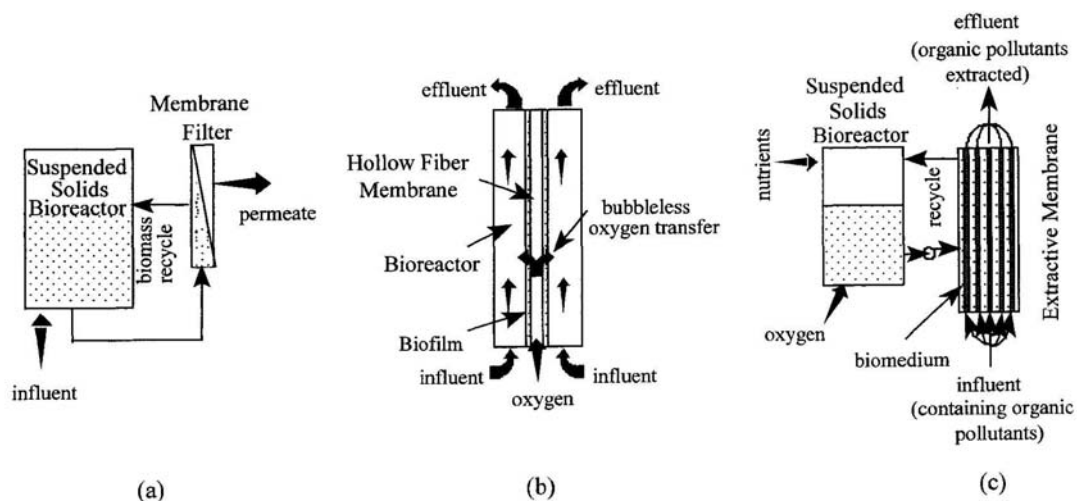
Figure 2-1: Three types of MBR processes: (a) Biomass separation MBRs, (b) membrane aeration bioreactors, (c) Extractive MBRs (Stephenson et al., 2000)

Membrane aeration bioreactors use gas permeable membranes to directly supply high purity oxygen without bubble formation to a biofilm growing on the external side of

the membranes. Due to the oxygen concentration/partial pressure gradient, the oxygen passes through the membrane pores (from internal to external) and reaches the biofilm. Organic pollutants are biodegraded within the biofilm under aerobic conditions. The most interesting feature of MABRs is the possibility to control the oxygen supply such that all supplied oxygen is utilised for biodegradation. Therefore, no oxygen bubbles are formed on the biofilm side. High oxygen utilisation efficiency (almost 100%) and high biomass concentration (high reaction rate) can be maintained. MABRs are an attractive alternative to the conventional process for the treatment of high oxygen demanding wastewater (Brindle and Stephenson, 1996; Brindle et al., 1998; Casey et al., 1999; Terada et al., 2006). MABRs have been used for the treatment of contaminates such as xylene (Debus and Wanner, 1992), phenol (Woolard and Irvine, 1994), chlorophenols (Wobus et al., 1995) and for nitrification (Brindle et al., 1998; Terada et al., 2003; Terada et al., 2006).

Some industrial wastewater has high concentrations of inorganic materials, such as high salinity, extreme pH values, etc., which may inhibit the biodegradation process. Extractive MBRs selectively extract specific organic pollutants from the water and the extracted pollutants can be biodegraded in a separated bioreactor under optimised conditions. A range of technologies have been recently developed to remove hydrophobic organics from aqueous solutions, including membrane-based options such as pervaporation (Wijmans et al., 1990) and membrane supported solvent extraction (Kiani et al., 1984). However, extractive MBRs appear to be a new promising technology (Livingston, 1994; Liu et al., 2001). The membranes used in EMBRs (e.g., solid silicone rubber membranes) can selectively extract certain organic (e.g., phenol, nitrochlorobenzene, dichloroaniline, dichloroethane, monochlorobenzene and hydrogen sulphide, etc., sometimes even inorganics), but retain the inorganic composition (Livingston et al., 1998; Chuichulcherm et al., 2001; Liu et al., 2001). Therefore, the target organic pollutants can be concentrated into an optimised bioreactor and biodegraded without the effect of those inorganic materials or extreme pH conditions. The driving force of the target organic pollutants is their concentration gradient, which is high on feed wastewater side but low on the bioreactor side.

Biomass separation MBRs are the most often used MBRs. Their key feature is to use a microfiltration (MF) or ultrafiltration (UF) membrane to replace the conventional secondary settling tank in an activated sludge process to separate the biomass from the water phase. Only biomass separation MBRs are studied in this thesis and all MBRs refer to biomass separation MBRs, unless otherwise indicated.

2.1.2 Short history of MBR developments

The concept of an activated sludge process coupled with an ultrafiltration membrane for biomass separation was first developed and commercialized in the late 1960s by Dorr-Oliver (Smith et al., 1969). In the 1970s the technology first entered the Japanese market through a license agreement between Dorr-Oliver and Sanki Engineering Co. Ltd, where MBRs had a rapid development. In 1980s MBRs were widely applied in Japan for domestic wastewater treatment and decentralized wastewater reuse in skyscrapers. During the early development, the side-steam MBR was the original configuration, which used external membrane modules. However, MBRs were associated with high membrane cost and high energy.

The submerged MBR was introduced in the late 1980s to reduce the high energy costs (Yamamoto et al., 1989). Since then the MBR technology has developed rapidly. A Japanese company, Kubota developed flat sheet MBRs and a Canadian company, Zenon Environmental, developed capillary MBRs. As of the year 2004, there are more than 2200 MBR installations in operation or under construction worldwide. In North America, 258 full-scale MBR plants have been constructed (Yang et al., 2006).

2.1.3 Configuration of MBRs

According to the configuration, MBRs can be classified as side-stream and submerged (Figure 2-2). In side-stream MBRs, the membrane module is separated from the main bioreactor. The sludge in the bioreactor is pumped into a membrane module, where a permeate stream is generated and a concentrated sludge stream is retained by the membrane and returned to the bioreactor. In the early development of side-stream MBRs, both of the transmembrane pressure (TMP) and crossflow velocity were generated by the recirculation pump. However, a few modifications were made to

reduce the high energy consumption associated with the side-stream configuration. Firstly, a suction pump was added on the permeate side, which increased the operation flexibility and decreased the crossflow rate and energy consumption (Shimizu et al., 1996). The latest side-stream MBRs even introduced an air flow in the membrane module, which intensified the turbulence in the feed side of the membrane and reduced the fouling and operational costs.

Aiming to reduce energy consumption associated with the recirculation pump in the side-stream configuration, the submerged MBRs were first introduced by Yamamoto et al. (1989). A membrane module was directly submerged in the bioreactor, which avoided the recirculation pump. Consequently, only a suction pump was used on the permeate side to create the transmembrane pressure (TMP). In some circumstances (e.g., MF membrane and very low filtration fluxes), the permeate side is placed in a lower position, and the gravity itself is the only driving force for the filtration (Ueda and Hata, 1999).

Side-stream MBR   Submerged MBR
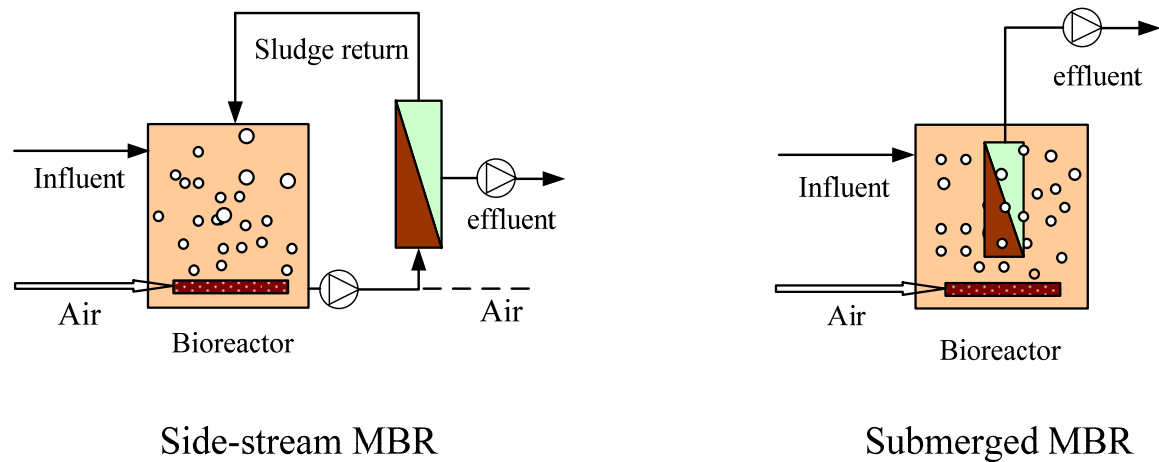
Figure 2-2: Configuration of side-stream and submerged MBRs

The comparison between the side-stream and submerged MBRs is summarized in Table 2-1. The submerged MBR has a simpler configuration, since it needs less equipment. The coarse bubble aeration in the membrane tank is multifunctional. In addition to the membrane fouling control, it also supplies oxygen to the biological process (although the oxygen utilisation efficiency is low). The biggest advantage of submerged over side-stream configuration is the energy saving by using coarse bubble aeration and lower fluxes (10-30 L/(m^2·h)), instead of high rate recirculation pump

and high fluxes (40-100 L/(m^2·h)) in side-stream MBRs. The capillary and hollow fibre membranes used in many submerged MBRs have very high packing density and low cost, which make it feasible to use more membranes and operate at lower fluxes. However, typical tubular membranes used in side-stream MBRs have low packing density and they are very expensive. Gander et al. reviewed 4 side-stream and 4 submerged MBR systems and concluded that the side-stream MBRs have a higher total energy cost, by up to two orders of magnitude, mainly due to the high recycle flow velocity (1-3 m/s) and head loss within the membrane module. In addition to the energy saving, the submerged MBRs suffered less fouling and could be cleaned easier than the side-stream MBRs (Gander et al., 2000).

However, the side-stream MBRs have the advantage of having more robust physical strength, more flexible crossflow velocity control and hydraulic loading rate and allowing easier chemical cleaning. They are now mostly used in industrial wastewater treatment and small scale WWTPs, where influent flow rate and composition has larger variation and operational conditions are tough (e.g., at high temperature conditions).

Table 2-1: The comparison of side-stream MBRs and submerged MBRs

	Side-stream	Submerged
Complexity	Complicate	Simple
Flexibility	Flexible	Less flexible
Robustness	Robust	Less robust
Flux	High (40-100 L/(m^2·h))	Low (10-30 L/(m^2·h))
Fouling reducing methods	- Crossflow - Air lift - Backwashing - Chemical cleaning	- Air bubble agitation - Backwashing (not always possible) - Chemical cleaning
Membrane packing density	Low	High
Energy consumption associated with filtration*	High (2-10 kWh/m^3)	Low (0.2-0.4 kWh/m^3)

2.1.4 Advantage and disadvantage of MBRs

The MBR technology is actually a new development of the conventional activated sludge (CAS) process. The invention of MBRs is to overcome a few limitations in the CAS process, where the often occurring bottle-neck is the biomass separation in the secondary clarifier. The secondary clarifier uses gravity to settle the flocs. However

the specific gravity of the activities sludge (1.02) (Tchobanoglous et al., 2003) is so close to that of water that poor settling is a common phenomenon in the normal range of the hydraulic retention time (2-3 hrs) of a secondary clarifier. The settling problem is often associated with small flocs (< 10 μm), open structure flocs and highly concentrated sludge (> 5 g/L). So called sludge bulking is one of the most common settling problems in the operation of an activated sludge process. The causes are very complex, e.g., low loading rate, low DO, nutrient deficient, nitric oxide or nitrite build up, toxic compounds, shock loading, denitrification in the secondary clarifier and process dynamics and process configuration, etc. (Casey et al., 1995; Eikelboom et al., 1998; Musvoto et al., 1999; Jenkins et al., 2004).

MBRs exploit the separation ability of membrane technology to eliminate the biomass separation problem. Membrane filtration has a much higher separation ability compared to the gravity settling, especially for the separation of small flocs and colloidal particles. In the secondary clarifier, the driving force, i.e., the density difference between flocs and water, is only related to the floc mass and structure, which is not directly controllable. However, the driving force in membrane filtration is transmembrane pressure, which is directly controllable using the suction pump. As a result, it is possible to use a higher sludge concentration (up to 60 g/L), a short hydraulic retention time (HRT) and a long solid retention time (SRT). In addition, the HRT and SRT appear to be independent in MBRs, since the MLSS concentration can go beyond 4-5 g/L without any problem. This key feature results in many new characteristics of MBRs. The advantages and disadvantages of MBR are summarised in Table 2-2, where the reference process is the CAS process.

Table 2-2: Advantages and disadvantages of MBRs

Advantages	Disadvantages
Excellent effluent quality (reusable)	Inevitable membrane fouling
Independence between HRT and SRT	High capital cost, no economy scale
High loading rate	Complicated control system
Small foot print	Low oxygen transfer efficiency
No sludge bulking risk	
Low sludge production	
Possibility to grow specific microorganisms	
Treat wastewater under extreme conditions	
Flexible modular design	

In EU countries, the driving forces of using MBRs are: 1) strict effluent EU discharge standard. In many cases, the MBR effluent quality is so good that it can be reused directly for non-potable purposes, e.g., for landscape and irrigation; 2) small footprint. Many Western European countries suffer high population density and space limitation in constructing new or expanding existing WWTPs. In these cases, MBR processes often beat CAS processes in space saving; 3) continuously decreasing in membrane costs is making MBR more competitive compared with CAS systems.

The investment costs of MBRs are as low as for CAS system with secondary clarification. However, operating costs are still higher due to membrane replacement costs and high-energy demand for hydrodynamic control of membrane fouling (Judd, 2006). Fouling phenomena on the membrane surface and within the pores reduces the long-term stability of flux performance. Permeate back flushing and chemical cleaning are standard procedures applied to minimise these effects and stabilise overall permeability of the membrane systems, but result in losses of net filtration efficiency and possible damage to the membrane by cleaning agents. Neither the evolution of membrane permeability under certain operating conditions or the effect of cleaning measures can currently be predicted. These uncertainties cause considerable difficulties in plant layout, design and operation.

2.1.5 Perspectives of MBR market

According to the most recent technical market research report of a US-based Business Communications Co Inc. (BCC, 2006), the global MBR market is currently valued at an estimated US$216.6 million, and is rising at an average annual growth rate (AAGR) of 10.9%. It is expected to approach $363 million in 2010. This market is growing faster than the larger market for advanced wastewater treatment equipment, at about 5.5% AAGR, and more rapidly than the market for other types of membrane systems, which are increasing at rates from 8% to 10%, depending on technology.

2.2 Filtration process in MBRs

2.2.1 Overview of membrane filtration processes

The basic principle of all membrane operations is the separation of a mixture of substances with a selective thin film. The transport of matter through a selective barrier is caused by a chemical potential difference between two phases, i.e., the feed and the permeate (Mulder, 1996). In pressure-driven membrane filtration systems, which have been widely applied in water and wastewater treatment systems, the driving force is a pressure difference across the membrane. Typically, four types of membranes are distinguished according to their separation range (molecular weight cut-off or pore size) and the applied transmembrane pressure: reverse osmosis (RO), nanofiltration (NF), ultrafiltration (UF), and microfiltration (MF) (Figure 2-3).

Size μm	Ionic /molecule	macromolecular	colloids	suspended	settable
	0.001 0.01 0.1		1.0	10	100
Approx. MW	100 1K 10K 100K				
Relative size of various materials in water	Salts / Fatty acids / Humics	Viruses / Polysaccharide / Protein	Cell fragments	Bacteria	Protozoa / Algae
Pressure [bar] 100 / 10 / 1 / 0.1	Reverse osmosis / Nanofiltration		Ultrafiltration	Microfiltration	

Figure 2-3: Classification of membrane and colloidal/macromolecular organic matter in ground and surface water (adapted from Mallevialle et al., 1996)

In MBRs, a tight microfiltration or a lose ultrafiltration membrane is often applied. The most often used membrane materials in MBRs are organic polymers, e.g., polyethylene, polypropylene and polyvinylidene fluoride (PVDF) membranes (Judd, 2006). Some of them are blended with other materials to change their surface charge or hydrophobicity (Mulder, 1996). Inorganic membranes (e.g., ceramic membranes) are only used in special applications e.g., solvent resistance and thermal stability are

required, due to their high costs (Baker, 2004). The ultrafiltration membrane often has a supporting layer (e.g., a microfiltration membrane), onto which a thin skin layer, i.e., a true ultrafiltration membrane, is attached.

2.2.2 Membrane fouling

Membrane fouling refers to the deposition or adsorption of material on the surface of the membrane or within the pores. It is a common and costly problem in membrane filtration applications. Fouling may cause a decline in permeate flux, increase in TMP, loss of permeate quality and deterioration of the membrane, etc. In conjunction with the forming of a filter cake, a shift in the effective pore size or molecular weight cut-off (MWCO) to smaller sizes is common, which can result in a MF process displaying the characteristics of UF membranes (Lee et al., 2001b; LaPara et al., 2006).

2.2.3 Fouling of pressure driven membrane filtration systems

The common compounds that foul a membrane can be the following four categories: particulate fouling caused by colloids and suspended solids, organic fouling caused by adsorption of organic matter, biofouling caused by deposition or growth of microorganism, and scaling caused by salt precipitation (Table 2-3).

Table 2-3 Characteristics of four types of membrane fouling

	Particulate fouling	Organic fouling	Biofouling	Scaling
Foulants	Colloids Suspended solids	Organic matter	Microorganism	Salt Metal cations
Major Factors affect fouling	Concentration Particle size distribution Compressibility of particles	Concentration Charge Hydrophobicity pH Ionic strength Calcium	Temperature Nutrients	Temperature Concentration pH
Indicator of fouling prediction	Silt density index (SDI) Modified fouling index (MFI) Specific resistance to fouling (SRF)	DOC UV_{254} SUVA	Assimilable organic carbon (AOC) Biofilm formation rate (BFR)	Solubility
Feed water pretreatment	Coagulation MF and UF	Adjustment of pH Coagulation	Sand filtration Biofilter Coagulation Flocculation UF and MF	Acid Anti-scalent

- **Particulate fouling**

Small particles can accumulate on the membrane surface, thereby forming a filter cake, which is referred to as particulate fouling. The particulates can either be suspended solids, colloids and even microorganisms. Particulate fouling is the dominant type of fouling in most MF and UF systems. However, MBRs using MF and UF membranes suffer more colloidal and organic fouling, which will be addressed intensively in this thesis.

- **Organic fouling**

Organic fouling refers to the adsorption of dissolved organic substances on the membrane surface or in its pores due to the intermolecular interactions between the membrane and organic matter (Zeman and Zydney, 1996). Natural organic matter (NOM) fouling in drinking water filtration processes is a well-known problem (Combe et al., 1999; Jones et al., 2000; Lee et al., 2004). Humic substance is a major fraction of NOM. However, the filtration of wastewater and activated sludge has been applied more recently and soluble microbial products (SMP) fouling has been the main concern (refer to section 2.2.11.2).

- **Biofouling**

Biofouling refers to the adhesion and growth of microorganisms on the membrane surface, i.e., the formation of a biofilm, which results in a loss of membrane performance. Basically a biofilm can occur on all kinds of surfaces, natural and synthetic, due to the fact that bacteria have developed elaborate adhesion mechanisms. RO and NF processes suffer more of biofouling due to their low flux and limited membrane cleaning options (Flemming et al., 1996; Flemming, 1997; Baker and Dudley, 1998).

- **Scaling**

The formation of a scaling on the membrane surface may occur if dissolved salts exceed their solubility product. Typically, over-saturation is of concern in reverse osmosis and nanofiltration operations with regard to $CaCO_3$, $CaSO_4$, $BaSO_4$, $SrSO_4$, $MgCO_3$, and SiO_2 Baker, 2004. However, RO plants can operate at super-saturation

condition (e.g., $BaSO_4$) without scaling (Bonne et al., 2000). Scaling is not dominating in MBR fouling. However, iron or calcium precipitation may occur in some cases. Acid cleaning should be considered if oxidant cleaning is not sufficient to restore the membrane permeability (te Poele and van der Graaf, 2005).

However, one has to keep in mind that there are overlaps in the above four types of foulants, e.g., organic fouling due to the deposition of suspended solids can be particulate fouling, so is the biofouling due to the seeding and growing of a biofilm. In addition, the different types of fouling can occur simultaneously and form hybrid fouling, which can be more difficult to clean (te Poele and van der Graaf, 2005).

2.2.4 Interactions between foulant and membrane

The affinity of foulant to the membrane can significantly influence the membrane fouling and permeate quality. The interaction between the foulant and membrane is more pronounced for the colloidal and macromolecular organic matter rather than the particulates due to the fact that they have smaller sizes. There are many factors which can influence this interaction, e.g., charge, pH, hydrophobicity, multivalent ions (Ca^{2+} and Mg^{2+}), ionic strength, and membrane morphology.

- **Charge**

If the colloids/macroorganics and the membrane surface have the same charge, the colloids/macroorganics will be repelled by the membrane due to electrostatic forces. Consequently, the adsorption of colloids/macroorganics is less (Nystrom et al., 1995; Hong and Elimelech, 1997; Schafer et al., 2004). Many colloids and macroorganics are negatively charged at neutral pH conditions (Lee et al., 2003), therefore, the MF/UF membranes in water and wastewater filtration processes are often manufactured or modified to be negatively charged. However, it should be noted that the charge of the membrane can be modified by the adsorption and deposition of colloids/macroorganics and eventually, the membrane may have the similar charge as the deposited colloids/macroorganics eventually (Hong and Elimelech, 1997).

- **pH**

The pH can influence the charge of colloids/macroorganics. Colloids/macroorganics are more negatively charged at high pH conditions due to the deficiency of protons, which promotes the dissociation of protons from the colloids/macroorganics into the solution (Simpson et al., 1987; MunozAguado et al., 1996; Hong and Elimelech, 1997; Matsumoto et al., 2003; Schafer et al., 2004; Kuzmenko et al., 2005). However, the filtration of water and wastewater is mostly performed at neutral pH conditions, and it is not feasible to adjust the pH for the fouling control purpose only.

- **Hydrophobicity**

If the colloids/macroorganics and the membrane surface have opposite hydrophobicity, the colloids/macroorganics may be repelled by the membrane (Hong and Elimelech, 1997). Many membranes for drinking water treatment are made hydrophilic (Mulder, 1996), which has the advantage of high membrane permeability and low affinity with the aromatic foulants (e.g., many NOMs). Fang and Shi conducted the filtration of MBR sludge and reported that the MCE membrane suffered more pore blocking than the PVDF membranes because the former is more hydrophobic (Fang and Shi, 2005). However, it should be noted that the hydrophobicity of the membrane can be modified by the adsorption and deposition of colloids/macroorganics and eventually, the membrane tends to have similar hydrophobicity to the deposited colloids/macroorganics eventually (Hong and Elimelech, 1997).

- **Multivalent ions (Ca^{2+} and Mg^{2+})**

The presence of multivalent ions, e.g., Ca^{2+} and Mg^{2+}, often facilitates membrane fouling. This can be attributed to the fact that, 1) the charge of colloids/macromolecular organic matter may be increased (less negative) by the binding between calcium ions and negative charged functional groups (Schafer et al., 2004; Lee et al., 2005); 2) the charge of the membrane may be increased (less negative) by the binding between calcium ions and negative charged membrane surfaces; 3) a calcium ion can form a bridge between the negatively charged molecules and the negatively charged membranes (Hong and Elimelech, 1997; Schafer et al., 2004; Lee et al., 2005).

- **Ionic strength**

Filtration with low ionic strength feed water may reduce the adsorption of colloids/macroorganics. The impact of ionic strength is indirect. In the filtration of proteins, screening of the charges of the proteins is reduced at low ionic strength. Therefore protein molecules strongly repel each other, especially at the membrane surface, where the concentration of protein is high (Kuzmenko et al., 2005). A similar phenomenon was also observed in NOM filtration (Lee et al., 2001a).

- **Membrane morphology**

Membrane morphology, e.g., pore opening, pore size distribution and surface roughness can affect membrane fouling. Generally, a narrower membrane pore size distribution can reduce the amount of fouling (Mulder, 1996). Fang and Shi conducted the filtration of MBR sludge using a few different MF membranes with similar nominal membrane pore sizes (i.e., 0.2–0.22 μm). The PES membrane with large pore openings (18–20 μm) suffered significant more pore blocking than other membranes. The latter had a smooth surface and a more uniform pore size distribution, which suffered less pore blocking (Fang and Shi, 2005).

2.2.5 Concentration polarization

Membrane fouling always starts from the concentration polarization (Figure 2-4). Due to the continuous transport of feed water and solutes to the membrane surface and the selective retention of certain solutes, some solutes accumulate on and near the membrane surface. Hence, their concentration increases over the filtration time and results in a boundary layer of higher concentration with its maximum at the membrane surface (c_m). The concentration build-up causes a particle backtransport flux ($D \cdot (dc/dx)$) into the bulk (c_b). Under steady state conditions, the convective solute flow towards the membrane ($J \cdot c$) is equalised by the solute flux through the membrane ($J \cdot c_p$) and the diffusive backtransport (Mulder, 1996). The crossflow operation is able to enhance the particle backtransport and reduce fouling (i.e., the increased diffusion coefficient D, due to the combination of Brownian diffusion, shear-induced diffusion and inertial lift mechanisms) (Belfort et al., 1994).
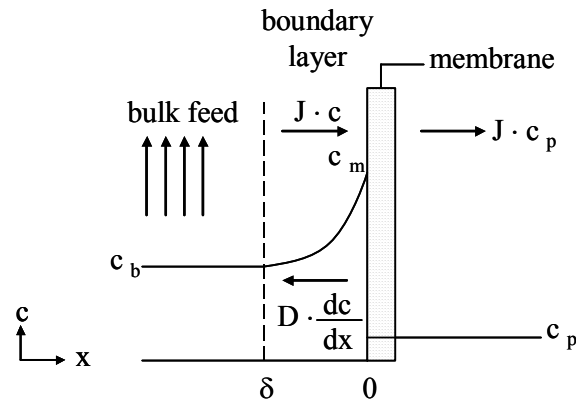
Figure 2-4 Concentration profile in the concentration polarization boundary layer, adapted from Mulder (1996)

2.2.6 Fouling mechanism

Ideally, there are four types of fouling mechanisms, complete blocking, standard blocking, intermediate blocking and cake filtration (Hermans and Bredée, 1936; Carmen, 1937). They are schematically depicted in Figure 2-5 and explained as follows.

1) Complete blocking assumes that each particle arriving at the membrane participates in blocking some pore with no superposition of particles. The particles which participate complete blocking should have sizes comparable to the membrane pore size. 2) Standard blocking assumes that each particle arriving at the membrane is deposited onto the internal pore walls leading to a decrease in the pore volume. Therefore, particles which participate standard blocking are small colloids or macromolecular organic matter, which are small enough to enter the membrane pores. In addition, the colloidal matter and membrane surface interaction can play an important role here. 3) Cake filtration assumes that each particle locates on the others, which have already deposited and blocked some pores. In this case, there is no room for particles to directly obstruct the membrane area. 4) Intermediate blocking is the intermediate step between the complete blocking and the cake filtration. It assumes that each particle can settle on the other particles previously arrived or it can directly block some membrane area. The possibility of pore blocking depends on the proportion of available pores to total amount of pores (Bowen et al., 1995).
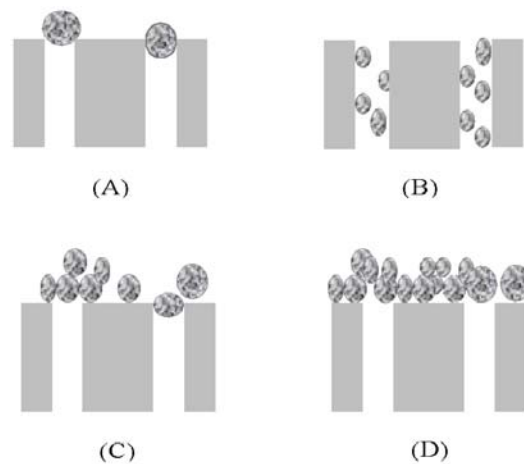
Figure 2-5 Schematic drawing of the fouling mechanisms: (A) Complete blocking; (B) Standard blocking; (C) Intermediate blocking; (D) Cake filtration, adapted from Bowen (1995)

In an actual filtration process, the four fouling mechanisms may take place simultaneously and one mechanism may dominate at different filtration stages. Membrane fouling always starts from concentration polarization. In the initial filtration stage, the complete blocking mechanism may dominate, followed by the standard blocking and intermediate blocking. With the progress of filtration and deposition of particles, the surface of the membrane is eventually completely covered by a deposition layer and there is no room for direct blocking and a thin filter cake has been formed. In such a situation and afterwards, cake filtration will dominate the subsequent filtration stage. In addition, the cake layer can act as a secondary dynamic "membrane", which can retain colloids and macromolecular organic matter and reduces the direct contact to the membrane. The membrane pore size appears modified and some colloids smaller than the membrane pore size may be retained by this secondary dynamic "membrane" (Lee et al., 2001b).

2.2.7 General filtration models

Filtration flux (J) is defined as the volume flowing through the membrane per unit area and time. If the membrane is clean, the clean water flux can be determined by Darcy's law:

$$J = \frac{dV}{Adt} = \frac{\Delta P}{\eta_p R_m} \qquad (2.1)$$

Where: J — flux [$m^3/(m^2 s)$]

V — filtrate volume (m^3)

A — filter membrane surface area (m^2)

t — filtration time (s)

ΔP — differential pressure applied across the membrane (Pa)

η_p — viscosity of the permeate (Pa.s)

R_m — membrane resistance (m^{-1})

When membrane fouling occurs, in addition to the clean membrane resistance (R_m), the blocking resistance (R_b) and cake resistance (R_c) also need to be taken into account when calculating the total filtration resistance. This can be modelled as the simple well known multi-resistance law:

$$Flux(J) = \frac{\Delta P}{\eta_p(R_m + R_b + R_c)} \qquad (2.2)$$

If the filter cake is rigid (incompressible), the cake resistance in Eq.(2.2) can be estimated by either the cake mass density (Eq.(2.3)) or the cake thickness (Eq.(2.4)).

$$R_c = \alpha \frac{w}{A} \qquad (2.3)$$

Where α — specific cake resistance according to cake mass density (m/kg)

w — dry cake mass (kg)

$$R_c = r_c \delta \qquad (2.4)$$

Where r_c — specific cake resistance according to cake thickness ($1/m^2$)

δ — cake thickness (m)

If the particles are spherical and rigid and the formed filter cake has a constant porosity, the specific cake resistance α can be estimated by the Carman-Kozeny equation (Eq.(2.5) and (2.6)) as follows:

$$\alpha = \frac{180(1-\varepsilon)}{\rho_s d_s^2 \varepsilon^3} \tag{2.5}$$

$$r_c = \frac{180(1-\varepsilon)^2}{d_s^2 \varepsilon^3} \tag{2.6}$$

Where ε —— Cake porosity (-)

d_s —— Diameter of particles deposited (m)

ρ_s —— Particle density (kg/m^3)

However, when the cake is compressible, the cake porosity may be reduced due to the pressure applied. The most often used is the power law by introducing a cake compression factor n as in Eq.(2.7) and (2.8). If n=0, the cake is incompressible, a high n value indicates a highly compressible cake.

$$\alpha = \alpha_0 \, \Delta P^n \tag{2.7}$$

$$\text{or } r_c = r_{c0} \, \Delta P^n \tag{2.8}$$

Where: α_0 —— initial specific cake resistance (m/kg)

r_{c0} —— initial specific cake resistance (1/m^2)

n —— cake compression factor (-)

The blocking resistance in the multi-resistance model is more difficult to estimate, which will be described in the section 2.2.8.

2.2.8 Single mechanism filtration models

A number of fouling models exist to describe each fouling mechanism encountered during the filtration process. For the constant pressure filtration, Hermia (1982) presented a unified power law model as Eq.(2.9), where four different mechanisms are modelled using parameter k and n. The complete blocking has the highest fouling rate (n=2) and the cake filtration has the lowest fouling rate (n=0). The summary of model parameters is listed in Table 2-4.

$$\frac{d^2t}{dV^2} = k\left(\frac{dt}{dV}\right)^n \tag{2.9}$$

Where: t — filtration time

V — total filtered volume

k — rate constant depending on filtration mechanism i.e., n

n — filtration constant characterizing the filtration mechanism

Table 2-4 Summary of parameter k and n for constant pressure filtration laws under dead-end mode, adapted from Hermia (1982)

Fouling mechanism	k	n
Complete blocking	$\sigma_d \dfrac{Q_0}{A}$	2
Standard blocking	$\dfrac{2\Phi_d}{LA} Q_0^{1/2}$	1.5
Intermediate blocking	$\dfrac{\sigma_d}{A}$	1
Cake filtration (incompressible)	$\dfrac{\alpha \rho_p C_b \eta_p}{A^2 \Delta P (1 - mC_b})$	0

In the case of constant flux filtration, a similar integrated power law model can be proposed (Eq.(2.10)). The values of k and n are summarised in Table 2-5 (Jiang, 2002).

$$\frac{d\Delta P}{dt} = k\Delta P^n \qquad\qquad (2.10)$$

Table 2-5 Summary of parameter k and n for constant flux filtration laws under dead-end mode, adapted from Jiang (2002)

Fouling mechanism	k	n
Complete blocking	$\dfrac{\sigma_d}{\eta_p R_m}$	2
Standard blocking	$2\Phi_d \sqrt{\dfrac{JA}{8\pi\eta_p NL^3}}$	1.5
Intermediate blocking	$\sigma_d J$	1
Cake filtration (incompressible)	$\eta_p \alpha_0 C_b J^2$	0

2.2.9 Combined pore blocking and cake filtration model

Single mechanism filtration models cannot model the filtration process satisfactory due to the complicity and the transition of filtration mechanisms in a filtration process. Some researchers divided the filtration into a few stages and model each stage separately using single mechanism models Bowen et al., 1995. However, it is arbitrary to divide the stages and the transition between the stages is not smooth. More recently, Ho and Zydney (2000) developed a combined pore blocking and cake filtration model for protein fouling during microfiltration. A simplified analytical form is given in Eq. (2.11). The first term in the bracket is equivalent to the classical pore blocking model and gives a simple exponential decay in the volumetric flow rate. At long time runs ($t >> \dfrac{\eta_p R_m}{\alpha \Delta P C_b}$), the volumetric flow rate is dominated by the second term (classical cake filtration model). This combined model provides a smooth transition from pore blocking to cake filtration behaviour during the course of filtration, eliminating the need to use completely separate mathematical descriptions in these fouling regimes. The combined model was able to model the filtration process of synthetic particles (Ho and Zydney, 2000; Ye et al., 2005b; Ye et al., 2006). However, it was only implemented in batch filtration with artificial foulant so far.

$$Q = Q_0 [\exp(-\frac{\alpha \Delta P C_b}{\eta_P R_m} t) + \frac{R_m}{R_m + R_p}(1 - \exp(-\frac{\alpha \Delta P C_b}{\eta_p R_m} t))] \qquad (2.11)$$

Where: Q — volumetric flow rate at time t (m^3/s)

Q_0 — initial volumetric flow rate at time t=0 (m^3/s)

α — pore blocking parameter (m^2/kg)

C_b — bulk foulant concentration (g/l)

R_m — membrane resistance (1/m)

R_p — resistance of the foulant deposit (1/m), which is a function of filtration time

2.2.10 Hydrodynamic model

Basically the single mechanism filtration model summarized in section 2.2.8 is only valid for dead-end filtration processes, where the particles move towards the membrane only due to the permeation flow. The particle backtransport is limited due

25

to the negligible shear applied on the membrane surface. However, in crossflow filtration processes, as in the case of MBRs, the particle backtransport is intensified in order to the control membrane fouling. Predicting the amount of particle deposition and modelling of membrane fouling requires a hydrodynamic model in addition to the filtration model. A brief review of the existing models is given below and the more detailed model development and application for MBRs will be given in Chapter 7.

There are a few mechanisms of particle backtransport. The most classic one is the Brownian diffusion model, sometimes called concentration polarisation model, Eq.(2.12). Brownian diffusion is a certain type of random movement resulting from the bombardment of particles by water molecules. The backtransport of particles with a small radius (colloids and macroorganics) are more influenced by the Brownian diffusion.

$$J_B = 0.185(\frac{\gamma_0 k^2 T^2}{\eta_f^2 a^2 L} \frac{\Phi_w}{\Phi_b})^{1/3} \qquad\qquad (2.12)$$

Where: J_B — backtransport velocity due to Brownian diffusion (m/s)

γ_0 — shear rate (s^{-1})

k — Boltzmann constant ($k = 1.38 \times 10^{-23}$ kg m^2/s^2)

T — absolute temperature (K)

η_f — feed sludge viscosity (Pa s)

a — particle radius (m)

L — membrane tube length (m)

Φ_b and Φ_w — particle volume fraction in the bulk and at the edge of the cake layer (-)

Brownian diffusion model underestimated the particle backtransport, the deviation was more pronounced for large particles and at high shear rate condition. Some backtransport mechanism might be overlooked. As a possible new mechanism, Zydney and Colton (1986) introduced the shear-induced hydrodynamic diffusivity first measured by Eckstein et al. (1977). The Shear-induced diffusion occurs because individual particles undergo random displacements from the streamlines in a shear flow as they interact with and tumble over other particles. The backtransport of

particles with medium to big radius (a few micrometers) are more influenced by the shear-induced diffusivity. More recently, Davis and Sherwood (1990) performed a similar solution of shear-induced model (Eq. (2.13)).

$$J_S = 0.072\gamma_0(\frac{a^4}{L}\frac{\Phi_w}{\Phi_b})^{1/3} \qquad\qquad (2.13)$$

Where: J_s — backtransport velocity due to shear-induced diffusion (m/s)

In addition to the introduction of shear-induced diffusion mechanism, an inertial lift mechanism was also proposed by Belfort and co-workers (Green and Belfort, 1980; Drew et al., 1991) (Eq.(2.14)). Inertial lift provides a lateral migration of particles, which transports particles away from the membrane. The backtransport of particles with big radius (bigger than 10 μm) are more influenced by the inertial lift mechanism.

$$J_I = 0.036\frac{\rho_L a^3 \gamma_0^2}{\eta_f} \qquad\qquad (2.14)$$

Where: J_I — backtransport velocity due to inertial lift (m/s)

However, it should be noted that the hydrodynamic models reviewed here are simplifications of the real complex world. They do not consider the physical-chemical interactions between solutes, colloids and particles; They do not consider the possible aggregation or breakage of particles (due to high local concentrations and high shear rates); And they do not consider the role of solutes on cake structure (binding between particles). Therefore, these simple hydrodynamic models are actually only applicable to mono-dispersed suspensions. Care should be taken in the application of complex mixtures, e.g., activated sludge.

2.2.11 Foulant identification in MBRs

2.2.11.1 The composition of activated sludge

In membrane bioreactors, the feed to the membrane module is not domestic wastewater, but an activated sludge. The composition of the activated sludge in a

27

biological domestic wastewater treatment process is very complex. Generally, it comprises 1) bio-flocs, dispersed microorganisms, cell fragments, protozoa, rotifers, 2) natural organic matter (NOM) present in drinking water, disinfection by-products (DBP) produced during the disinfection process of the drinking water treatment process, 3) synthetic organic compounds (SOC) introduced by the consumers, 4) soluble microbial products (SMP) produced by the microorganisms in the biological wastewater treatment and 5) salts (Chudoba et al., 1986; Hejzlar and Chudoba, 1986a; Hejzlar and Chudoba, 1986b; Rittmann et al., 1987; Drewes and Fox, 1999; Jarusutthirak et al., 2002; Tchobanoglous et al., 2003).

Most organics in the activated sludge are flocculated, so called bio-flocs. Most microorganisms in activated sludge are flocculated in settable flocs. Bacteria are the main fraction, which play the most important role in the degradation of organic matters. Protozoa and rotifers act as effluent polishers. Protozoa feed on bacteria including the free dispersed bacteria and rotifers consume bio-flocs including the small non-settable flocs. In the flocs of an activated sludge, a small amount of filamentous bacteria function as the backbone of bio-flocs. Extracellular polymeric substances (EPS) act as a "glue" to connect different microbes and biomass debris (Bitton, 1999; Grady et al., 1999; Tchobanoglous et al., 2003).

According to the size of the activated sludge, the mixed liquor can be classified into: 1) settable particulates (> 5-10 μm), 2) non-settable particulates (0.45 – 5-10 μm), 3) colloids (1 nm- 0.45 μm), 4) solutes (< 1 nm). The particulates are mostly bio-flocs. The colloids are biomass debris, cell fragments, big NOM, big SOC, SMP, etc. The solutes are mostly small NOM, DBP and small SOC. A small amount of volatile fatty acids (VFA), short chain sugars and amino acids may also present. However, these compounds are readily biodegradable and their concentrations present in the activated sludge to the feed of the membrane are normally very low. Figure 2-6 summarizes the composition of an activated sludge.

It should be noted that there is no strict classification of particulates, colloids and solutes. According to the definition of International Union of Pure and Applied Chemistry (IUPAC), colloids are in the range of 0.001 to 1 μm, above which, the compounds are defined as particulates, and below which, the compounds are

considered as truly soluble. However, there are many other definitions of colloids. Tchobanoglous et al. (2003) defines colloids in the range of 0.01 to 1 μm. Some researchers differentiate macromolecular organic matter from colloids as such that colloids are in the range 0.1 -1 μm and macromolecular organic matter are in the range of 0.001-0.1 μm. In activated sludge models of IWA, 0.45 μm filters are often used to classify the particulates from the colloids and solutes (Henze et al., 1987; Henze et al., 1999; Tchobanoglous et al., 2003). In summary, this thesis defines colloids in the range of 0.1-0.45 μm and macroorganics in the range of 0.001-0.01 μm. Everything above 0.45 μm are particulates and everything below 0.001 μm are solutes.
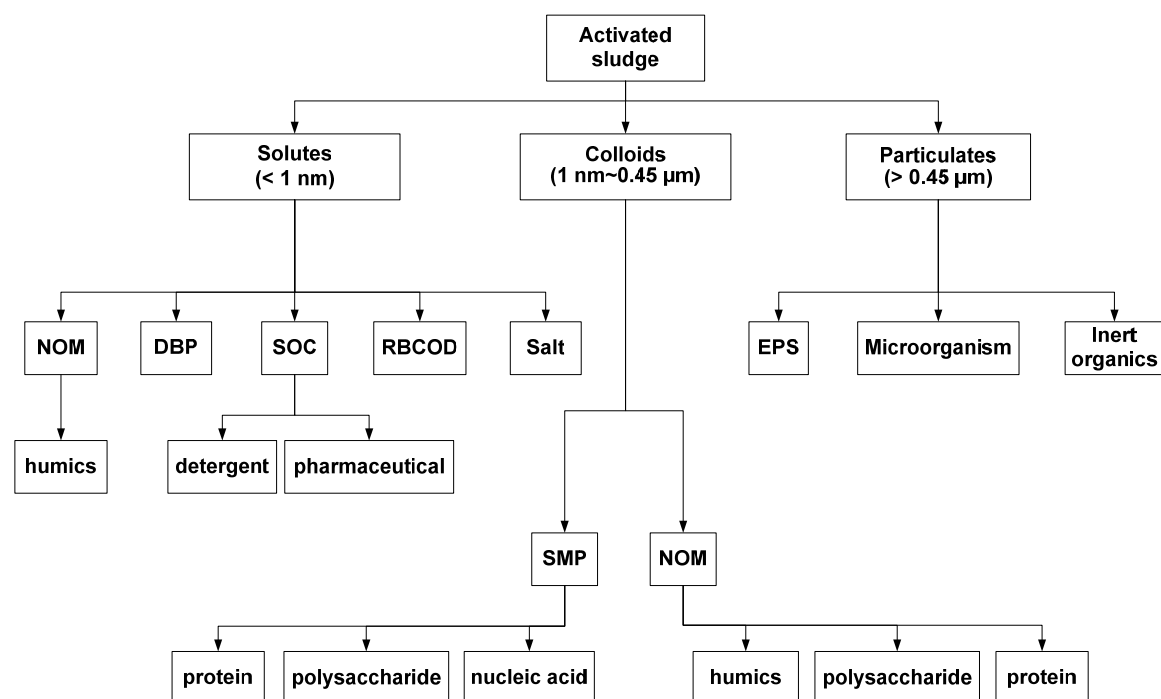
Figure 2-6: Composition of activated sludge with respect to sizes

2.2.11.2 Source and fate of potential foulants in MBR

The complex composition of activated sludge has different contributions to membrane fouling. It is essential to find the major contributor to membrane fouling and the fouling mechanism in MBRs. The components of activated sludge summarized in section 2.2.11.1 and the interaction with the membrane are discussed below.

- **Particulates**

The particulates in activated sludge are mostly flocs containing bacterial cells as well as inorganic and organic particles. Biopolymers, e.g., EPS, are excreted by biomass and "glue" individual bacterial cells together (Bitton, 1999). Table 2-6 summarizes the PSD of MBR and CAS sludge and important operational parameters. The bio-flocs in activated sludge showed a very wide particle size distribution (PSD) from very small flocs, i.e., approximately 1 μm (single cell) up to 500-1000 μm in CAS processes. In addition to the influence of influent type, configuration, MLSS concentration, SRT, and shear rate, the PSD are also influenced by measurement device, sampling method, and dilution rate, etc.

A few interesting points are worth to point out. 1) The MBR sludge flocs are generally smaller than the CAS sludge flocs. The most convinced results were obtained at the same influent characteristics, process configuration, MLSS concentration, SRT, and using the same device measuring PSD Manser et al., 2005b; Masse et al., 2006. However, Sperandio reported the maximum number of flocs (in volume) of MBR flocs (240 μm) were larger than the CAS flocs (160 μm) (Sperandio et al., 2005). 2) Some MBR sludge exhibited two peaks, i.e., one in the large size range and the other one in the small size range (1-10 μm) (Luxmy et al., 2000; Wisniewski et al., 2000; Sperandio et al., 2005). This could probably be attributed to the intensifies shear rate in the MBRs, which increased particle breakage rate (Kim et al., 2001). 3), Masse et al. (2006) increased the SRT from 10, 37, 53 and 110 days in a MBR and resulted in smaller (from 120-220 to 70-100 μm) but more compact sludge flocs. However, the turbidity of the MBR supernatant after 30 minutes settling increased from 50-70 to 120-150. The MBR sludge had always much higher non-flocculated small flocs and higher DSVI than the CAS sludge, which can be attributed to the loss of selection pressure based on the sludge settling property in MBR systems. These rheological characteristics of MBR sludge will certainly influence its filterability.

The protozoa and metazoa in activated sludge feed on small flocs. It is often assumed the predators are roughly an order of magnitude larger than preys. Moloney and Field (1991) reported on average, prey organisms ranged from 4-13% of its body size

calculated in linear dimensions and the optimum prey size estimated was 6% of predator's linear dimension. The reduction in small flocs and single cells is able to reduce the sludge production, which is often lumped into the reduced the biomass decay rate from the viewpoint of process engineering (Van Loosdrecht and Henze, 1999). In addition, the reduction in single cells (approximately μm) may also improve the filterability of the MBR sludge.

Table 2-6 Comparison of the particle size of MBR sludge and conventional activated sludge

Source	Avg. floc size (μm)	Influent	MLSS (g/l)	SRT (day)	Configuration	Process
Manser et al., 2005b	35 ± 9	real WW	n.a.	20	SMBR	pre-denitrification
	307 ± 72		n.a.		CAS	
Sperandio et al., 2005; Masse et al., 2006	1st peak: 120-220 2nd peak: 1-10	real WW	1.9	10	SMBR	n.a.
	70-100		3.7	37		
	70-100		7.2	110		
	160		1.6	9.2	CAS	
Zhang et al., 1997	30-40	synthetic	2.5	infinity	SMBR	intermittent aeration
	7-8	Domestic + food	8	16.8	SSMBR	continuous aeration
	80-100	real WW	1-1.2	3.4-3.6	CAS	n.a.
Luxmy et al., 2000	1st peak: 50-90 2nd peak: < 10	real WW	n.a.	n.a.	SMBR	continuous aeration
Huang et al., 2001	15	real WW	1	5	SMBR	continuous aeration
	48		3	20		
	31		6.5	40		
Defrance et al., 2000	50	real WW	9-12	60	SSMBR (4m/s)	continuous aeration
Wisniewski et al., 2000	1st peak: 100 2nd peak: 1-2	synthetic	n.a.	n.a.	SSMBR (1.3 m/s)	Anoxic

n.a. = not available

Luxmy et al. (2001) performed an interesting metazoa study in a submerged MBR. The low fouling was attributed to the metazoa, which was abundant on the membrane surface and probably played a role in removing accumulated sludge from the membrane surface.

- **SMP**

The role of soluble microbial products (SMP) will be reviewed in Chapter 5-8.

- **NOM**

Natural organic matter (NOM) refers to the organic matter originating from plants and animals present in natural (untreated or raw) waters, and undergo a wide variety of alteration processes such as physical degradation and aggregation, microbial remineralization, diagenesis, and photochemical reactions. The large number of different primary sources, coupled with the various alteration processes, leads to large variations in NOM composition (Sannigrahi, 2005). The NOM characteristics are source specific. In general the main composition of NOM is humic substances. Conceptual models for NOM structures include aromatic and aliphatic carbon with carboxyl, phenol, hydroxyl or carbonyl functional groups (Larson and Weber, 1994). NOM are often negatively charged in the normal pH range due to the dissociation of carboxylic (and phenolic) functional groups (Hong and Elimelech, 1997). The organics are amphipathic in nature, i.e., contain both hydrophobic and hydrophilic moieties (Lee et al., 2004).

Membrane fouling due to NOM is a well known problem in the filtration of natural waters. NOM adsorbs both inside pores and on the membrane surface (Combe et al., 1999; Jones et al., 2000; Lee et al., 2004), and forms a gel layer (Yuan and Zydney, 1999). Howe and Clark reported a relatively small size range of inorganic and organic colloids (3–20 nm) but represented an important foulant in membrane filtration (Howe and Clark, 2002). The colloidal and non-colloidal hydrophilic NOM were identified as being more problematic than the other components, exhibiting relatively higher biodegradability and reactivity toward DBP formation potential. A higher biodegradability especially can provide a high risk of membrane biofouling, if a membrane is fouled by highly biodegradable NOM (Kwon et al., 2005).

- **DBP**

Disinfection by-products (DBPs) are formed when disinfectants used in water treatment plants react with bromide and/or NOM. DBPs include the compounds formed in chlorination, e.g., trihalomethanes (THMs), haloacetic acids (HAAs), trichlorophenol, and aldehydes. More recently, N-nitrosodimethylamine (NDMA) has been found in the effluent of WWTPs, which is produced in the chlorination of the effluent of WWTPs (Tchobanoglous et al., 2003). These organic DBPs are toxic and

poor or slow biodegradable (Shukairy and Summers, 1992). However, their concentrations in domestic wastewater are low and molecular sizes are very small. Therefore, it is reasonable to expect that the contribution of DBPs to membrane fouling in MBRs is minimal.

- **Detergents**

Detergents are surfactants and they are commonly composed of a strong hydrophobic group combined with a strongly hydrophilic group. They are introduced into the wastewater by the consumers in the washing process. Alkyl-benzene-sulfonate (ABS) was the main group of detergent in the past. However, ABS is poorly biodegradable in biological WWTPs and recently replaced by more biodegradable linear-alkyle-sulfonate (LAS) (Eichhorn and Knepper, 2002). In biological WWTPs, detergents tend to collect at the air-water interface with the hydrophilic in the water and the hydrophobic group in the air (Tchobanoglous et al., 2003).

De Wever et al. (2004) performed a direct comparison of LAS removal in a MBR and a CAS process. The results showed that both MBR and CAS processes was able to achieve over 97% removal. Biodegradation was concluded to be the main removal mechanism, which is in line with other studies (Schleheck et al., 2000; Eichhorn and Knepper, 2002). In addition, the LAS concentration in the MBR effluent was only 0-30% lower than the supernatant, which suggested that the size exclusion due to the ultrafiltration membrane was not a significant mechanism of LAS removal in MBRs. This can be explained by the fact that the MW of LAS (a few hundred Daltons) is significantly lower than the pore size of the UF membrane (0.03 μm). The advantage of MBR in LAS removal was the quick adaptation to the changes in operational conditions and more robust performance.

In addition, the concentration of detergent present in domestic wastewater typically ranges from 1 to 5 mg/L (De Wever et al., 2004). Therefore, it is reasonable to expect that the contribution of LAS to membrane fouling in MBRs is minimal.

- **Pharmaceutical products**

Pharmaceutical products including endocrine disrupting compounds (EDCs) (hormones and chemicals, which are suspected to have an impact on humans and wildlife hormonal systems) and personal care products (PCPs) are introduced by the households into the domestic wastewater stream (Heberer, 2002; Clara et al., 2005b). The pharmaceutical products are mostly soluble with MW of a few hundred Daltons. The negative adverse health effects on aquatic organisms have been well documented in many studies (Sonnenschein and Soto, 1998).

The direct comparison of a few pilot and full-scale CAS and MBR systems showed that the ultrafiltration membrane employed in MBRs did not allow additional retention of the pharmaceutical products by the mechanism of size exclusion. Slightly lower total emissions can be achieved in MBRs compared to CAS processes due to the mechanism of adsorption (Clara et al., 2005a; Clara et al., 2005b). Biodegradation was still the main removal mechanism in MBRs (Clara et al., 2004; Wintgens et al., 2004; Clara et al., 2005a; Clara et al., 2005b). However, the long SRT often applied in MBRs was an advantage. The SRT was reported to be an important parameter for the removal of pharmaceutical products and a minimum SRT of 10 days at 10 °C is suggested Clara et al. (2005b). Nevertheless, some studies showed MBRs did achieve significant higher removal of Pharmaceutical products than CAS systems. Kimura et al. reported that MBRs exhibited much better removal of ketoprofen and naproxen compared to the CAS process. With respect to the other compounds, comparable removal was observed between the two types of treatment. Removal efficiencies were dependent on their molecular structure such as the number of aromatic rings or inclusion of chlorine (Kimura et al., 2005).

As a result, it is reasonable to expect that the contribution of pharmaceutical products to membrane fouling in MBRs is minimal due to their small sizes and low concentrations (typically ng up to mg/L).

- **Pesticides and herbicides**

Pesticides, herbicides and other agricultural chemicals are not common constituents of domestic wastewater but result primarily from surface runoff from agricultural, vacant,

and park lands. Pesticides and herbicides are very toxic, however, most pesticides and herbicides widely applied now are slowly biodegradable (Aksu, 2005). In addition, their concentrations present in domestic wastewater are low and molecular sizes are very small. Therefore, it is reasonable to expect that their contribution to membrane fouling in MBRs is minimal.

2.2.11.3 Fouling mechanisms in MBR

The pore size of most MBR membranes is in the range of 0.03-0.4 μm. Comparing the particle size in the feed sludge with the membrane pore size, the particulates can only form a filter cake. The colloids and macroorganics can either form a filter cake or block the membrane pores (complete blocking or standard blocking). The solutes are unlikely to form a filter cake. They may be either be absorbed on the membrane pores and result in standard blocking or pass the membrane and end up in the permeate without any interaction with the membrane.

The relative contribution of particulates, colloids/macroorganics and solutes to membrane fouling are influenced the filtration flux and hydrodynamic conditions, which determine the tendency of particle deposition. If the flux is high but the crossflow velocity is low, the permeation velocity can be higher than the backtransport velocity. The particulate fouling and cake filtration may dominate. However, if the filtration flux is low and the crossflow velocity is high, the permeation velocity can be lower than the backtransport velocity and only colloids/macroorganics and solutes may deposit/absorb on the membrane. The role of organic fouling and pore blocking becomes important (Tardieu et al., 1998; Tardieu et al., 1999).

However, most full-scale MBRs run under sub-critical flux condition to limit the deposition of particulates and only colloids/macroorganics and solutes may deposit. Many studies concluded that cake filtration is the dominant fouling mechanism in MBRs. Lee et al. reported that the membrane resistance, cake resistance, blocking and irreversible fouling resistance contributed 12%, 80% and 8% to the total resistance, respectively in a submerged MBR using 0.1 μm UF membrane (Lee et al., 2001b). Chang and Lee (1998) reported that cake resistance was the major contributor to the

resistance of membrane coupled activated sludge systems especially under low sludge age conditions.

During the filtration process of MBR, the formed filter cake may function as a dynamical membrane layer and reduce direct contact of foulant with the membrane. In addition, the colloidal/macromolecular organic matter could be rejected/adsorbed and biodegraded by the dynamic "membrane". As a result, pore blocking is alleviated and membrane cleaning becomes easier (Lee et al., 2001b).

The role of a dynamic membrane layer in MBRs was confirmed in many MBR studies. Chiemchaisri et al. (1992) reported that two MBRs equipped with 0.03 and 0.1 μm pore size membranes attained the same log reduction of coliphage virus, and that improved rejection occurred with time owing to the build-up of a dynamic membrane layer. Chang et al. (2001) studied the contribution of soluble COD removal within the cake layer and membrane pores and attributed the predominant solute removal to the sieving and adsorption by the filter cake. Huang et al. (2000) analysed the soluble organic compounds in a submerged MBR and attributed the accumulation of soluble organic matter within the bioreactor to the dynamic membrane layer above the real membrane.

However, colloidal and soluble foulants are important as well. Organic fouling due to the adsorption of colloids and macroorganics are often more difficult to clean hydraulically than the filter cake. Bouhabila et al. (2001) reported the supernatant of MLSS had 20-30 times higher specific resistance than the sludge suspension, which represented the high fouling potential of soluble and colloidal fraction.

In summary, to reduce the membrane fouling, MBRs should be designed in a way to reduce the pore blocking and allow a certain amount of filter cake formation. This is due to the fact that pore blocking results in quicker loss of permeability and more difficulties in membrane cleaning. Fang and Shi studied the MBR fouling using different membranes and suggested that the MBR system should use the cake dominant type of membranes, but avoid the blocking dominant type of membranes, such as PES (Fang and Shi, 2005).

2.2.12 MBR fouling control

Membrane fouling control is the most important aspect in MBR design and operation. It should plan and implement in an integrated way, including many physical, chemical and biological aspects. Some of them are in the design stage and some are in the operational stage. The major aspects of membrane fouling control are summarized below.

2.2.12.1 Membrane selection

MF or UF membranes are often used in MBRs. The selection of membrane should consider the pore size, morphology, surface charge, hydrophobicity, chemical stability, mechanical strength, packing density and, eventually, costs.

The selection of membrane material (determining charge, hydrophobicity and chemical stability) and pore size can influence the membrane fouling. The optimised membrane pore size should not be too big to facilitate pore blocking (Lee et al., 2004; Fang and Shi, 2005) and it should not be too small to reduce the membrane permeability (Stephenson et al., 2000). Furthermore, a narrow pore size distribution can reduce fouling (Mulder, 1996). Choo and Lee (1996) found that a membrane pore size of 0.1 μm resulted in minimum fouling compared to 0.02, 0.5 and 1 μm membrane pore size for the filtration of anaerobic digestion broth.

In general, negatively charged membrane has the less fouling potential in the MBR application. The particles in wastewater effluents are mostly colloidal in nature and negatively charged, thus repelling each other (Adin, 1999). Furthermore, the use of hydrophilic rather than hydrophobic membranes can also help to reduce fouling (Mulder, 1996). Madaeni et al. (1999) reported higher critical flux using hydrophilic membranes. Chang and Lee (1998) and Chang et al. (2001) compared the filterability of activated sludge through a hydrophobic and a hydrophilic membrane and reported more fouling for the hydrophobic membrane. The filtration of normal and foaming sludge was also compared. The result showed that the foaming sludge generated much more fouling, probably due to its hydrophobic nature, which had higher affinity with the hydrophobic membrane.

2.2.12.2 MBR biology

- **Influent characteristics**

The biodegradable organics in typical domestic wastewater can be classified into ready biodegradable (often soluble) and slowly biodegradable (often colloidal and particulates) compounds. In addition, the inert organics in the influent will either pass the membranes or be wasted through the excess sludge depending on the relative size compared to the membrane pores.

It is reasonable to hypothesize that the amount of organic matters in the domestic wastewater, their size and degradability can influence the MBR fouling. In addition, the intermediate products of slowly biodegradable organics and the SMP produced by the biomass may also be substrate specific. MBRs fed on simple substrate may suffer less from fouling compared to the ones fed on high molecular weight and slowly biodegradable substrate.

LaPara et al. (2006) reported substantial performance differences between the starch-fed and acetate-fed MBRs with respect to the rate, at which the membrane fouled and the rate at which carbohydrate accumulated in the bioreactor. Starch-fed system had significant more fouling than the acetate-fed one, which appears that either the underrated starch or the produced SMP resulted in more significant fouling in starch-fed system.

- **Sludge age and F/M**

Sludge age (or solid retention time, mean cell residence time, SRT, θ_c) is defined as the total mass of microorganisms in the bioreactor divided by the mass of microorganisms removed from the system daily in both the waste sludge and effluent. In MBRs, there is no sludge lost from the effluent and consequently SRT can be well controlled by the waste sludge. SRT is an important design parameter due to the fact that at steady state it is related in a simple way to the growth rate μ_H (Eq. (2.15)). Before the widespread use of SRT as an independent variable for design of activated sludge processes, the food to microorganism ratio (F/M) (or process loading factor, sludge loading) was the most used variable (Grady et al., 1999). However, F/M cannot

directly connect to the growth rate (μ_H) without the knowledge of the active biomass fraction (f_A). However, it is rather easy to make a conversion between them. An approximate form of F/M is given in Eq. (2.16), by assuming that effluent substrate concentration is much lower than influent. The active fraction of biomass (f_A) can be estimated by Eq. (2.17). Combining Eq. (2.15)-(2.17) by cancelling μ_H and f_A can result in the relation between F/M and SRT as in Eq. (2.18), where Y_H is the true yield of heterotrophic biomass, b_H is the decay rate of the heterotrophic biomass (traditional decay model not the regrowth model adopted in ASM1, ASM2 and ASM2d), and f_D is the yield of biomass debris in the decay process. It is obvious that a low F/M is associated with a high SRT although the relation is not linear.

$$\mu_H = \frac{1}{\theta_C} - b_H \tag{2.15}$$

$$F/M \approx \frac{Q_{in}*(S_{SO}-S_S)}{V*MLSS} = \frac{f_A \mu_H}{Y_H} \tag{2.16}$$

$$f_A = \frac{1}{1+f_D*b_H*\theta_C} \tag{2.17}$$

$$F/M = \frac{1-b_H*\theta_c}{Y_H*\theta_c*(1+f_D*b_H*\theta_c)} \tag{2.18}$$

Where: Q_{in} — influent flow rate (m^3/s)

S_{SO}, S_S — substrate concentration in the influent and in the reactor (mg COD/L)

f_D — fraction of biomass debris generated in biomass decay (-)

It is well-known that SRT influences the effluent quality (COD). However, if the SRT is above 3-5 days, there is no further reduction of effluent COD using higher SRT. In activated sludge processes, nitrification is often the limiting step determining the minimum SRT. Nitrifiers are slow growing microorganisms and very sensitive to temperature, pH, toxic compounds, etc. The minimum SRT for complete nitrification is 20 days at 10 °C in practice.

However, the influence of SRT on membrane fouling is controversial. Some of the most comprehensive studies of SRT on membrane fouling are summarized in Table

2-7. Most studies showed that a moderate to high SRT resulted in less MBR fouling, i.e., Grelier et al. studied SRTs of 8-40 days; Trussell et al. studied SRTs of 2-10 days; Zhang et al. studied SRTs of 10-30 days; Chang and Lee studied SRTs of 3-33 days. However, Han et al. reported more fouling at very higher SRT in the range of 30-100 days.

It is hypothesized that there exists an optimal SRT. Operating below the optimal SRT can result in high sludge loading, high biomass growth rate and incomplete substrate biodegradation. Operating above the optimal SRT can result in excess biomass decay and accumulation of biomass debris from the decay process.

Table 2-7 Summary of the influence of SRT and F/M on membrane fouling

Rference	Fouling rate		WW	SRT (d)	HRT (hr)	MLSS (g/L)	F/M (gCOD/ (gMLSS·d))	Conf.	Proc.
	unit	value							
Han et al., 2005	Critical flux (L/m^2/hr)	47	synth. WW	30	12	7	0.15	SMBR	SBR (BNR)
		43		50		10	0.1		
		42		70		14	0.07		
		36		100		18	0.05		
Grelier et al., 2006	Fouling rate (1/m/day)	2.3×10^{11}	Real WW	8	12	3.2	0.3	SMBR	Biosep
		1.4×10^{11}		15		4.9	0.2		
		0.3×10^{11}		40		7.7	0.1		
	Fouling rate (1/m/day)	4.1×10^{11}		8	4.5	7.8	0.3		
		1.1×10^{11}		15	6	6.8	0.2		
		0.7×10^{11}		40	12	7.3	0.1		
Trussell et al., 2004	Fouling rate (LMH/bar/day)	3.6	Real WW	2	1-4	8	1.41	SMBR	aerobic
		1.6		3			0.84		
		0.6		4			0.73		
		0.4		5			0.55		
		0.2		10			0.34		
Zhang et al., 2006b	Fouling rate (dTMP/dt)	higher	synth. WW	10	6	5	0.12 (in TOC)	SMBR	aerobic
		lower		30	6	9.2	0.07 (in TOC)		
Chang and Lee, 1998	Total Resistance (×10^{11}/m)	94[a]	synth. WW	3	n.a.	n.a.	n.a.	CAS sludge	SBR
		52[a]		8					
		30[a]		33					
		116[b]		3					
		59[b]		8					
		29[b]		33					
		125[c]		3					
		61[c]		8					
		33[c]		33					

[a b c]: batch filtration resistance with YM30 membrane, XM50 membrane, PM30 membrane

SMBR = submerged MBR

- **MLSS**

The general trend found in the literature is that membrane fouling was intensified with increasing MLSS concentrations. However, some other studies reported no effect or no effect at all up to a certain threshold concentration. Rosenberger and Kraume (2002) reported that MLSS concentration between 2-24 g/L had little impact on sludge filterability. Some others reported no impact from 3.6-8.4 g/L (Harada et al., 1994) and up to 30-40 g/L (Yamamoto et al., 1989). More recently, Le-Clech et al. (2003) reported there was little difference in critical flux for the concentrations of MLSS ranging form 4 to 8 g/L but there was a significant increase in critical flux when the MLSS was increased to 12 g/L.

2.2.12.3 Filtration flux control

In MBR systems, filtration flux is a critical operational parameter determining membrane fouling. Nagoka et al. (1998) observed that when the flux was less than 4.2 $L/(m^2 \cdot h)$, fouling was minimised, and the membrane could run for months without cleaning. Furthermore, when the flux was too high, neither decreasing the volumetric organic loading rate nor increasing the shear force was effective in reducing the fouling.

For crossflow filtration, there exists a flux below which no fouling is observed, such a flux is the so called critical flux concept (Field et al., 1995). In addition, filtration flux affects the fouling reversibility as well. Defrance and Jaffrin (1999a) found that in a side-stream MBR, when the permeate flux was set below the critical flux, the TMP remained stable and the fouling was reversible. On the contrary, when the critical flux was exceeded, the TMP increased and the fouling formed was partly irreversible when the flux was lowered again. Howell et al. (2004) reported the fouling was reversible at a low flux as 10 $L/(m^2 \cdot h)$, even when air flow was as low as 10 mm/s. However, at a higher flux of 25 $L/(m^2 \cdot h)$, fouling was observed even at a high aeration rate as 201 mm/s and 220 mm/s.

The critical flux is often determined by the flux-step method, in which the flux is step-wise increased and the impact recorded as fouling rate (Le Clech et al., 2003). More

recently, Howell et al. determined critical flux using the hysteresis method at a function of aeration flow at fixed MLSS concentration. The advantage of this method is that it also reveals the information of the reversibility of fouling (Howell et al., 2004). However, a close examination of flux-step data often reveals that small increase of TMP even at very low fluxes, indicating slight fouling at sub-critical fluxes (Le Clech et al., 2003). In this context, the critical flux value is a strict definition as dP/dt=0. Nevertheless, it is practically defined rather arbitrary to allow a certain amount of fouling (Le Clech et al., 2003). In addition, the long-term operation under sub-critical flux showed very different behaviour from the short-term operation. Le Clech et al. (2003) reported that the fouling rate measured for long-term experiments were always lower than the equivalent values measured for the short-term flux-step experiments. The critical flux value indicated the point at which fouling starts to become severe, but does not yield predictive absolute permeability data for extended operation. Critical flux actually represents the boundary between fouling by the dissolved/colloidal components and suspended matter of the biomass (Cho and Fane, 2002). Sub-critical fouling in MBRs is mainly caused by organic macromolecules such as SMP and EPS (a few dozens of mg COD/L). Operation above sub-critical flux may results in the deposition of particulates (a few thousands of mg COD/L), and rapid loss of membrane permeability.

The critical flux depends on membrane characteristics, feed characteristics and operational conditions. Madaeni et al. (1999) reported critical flux depended on feed concentration and crossflow velocity and membrane type, being higher for higher crossflow velocity, lower feed concentration and hydrophilic membranes. More recently, Howell et al. reported the critical flux increased as the air flow rate was increased in a submerged MBR (Figure 2-7), which suggests the potential energy saving by varying the air flow rate according to the influent flow rate (filtration flux) in a truly dynamic MBR system. However, the degree to which the critical flux was increased by gas flow was limited (saturated at high air flow rate). The change of critical flux as a function of crossflow velocity (by recirculation pump in side-stream MBRs or air flow in submerged MBRs) can be well interpreted by the particle backtransport model (see section 2.2.10).
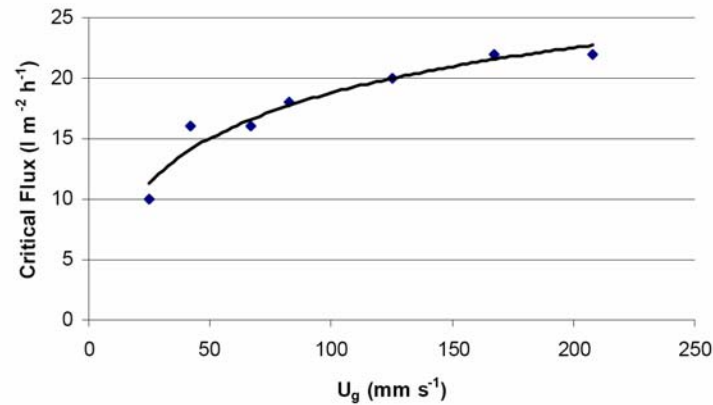
Figure 2-7 Critical flux as a function of air flow rate, MLVSS=17.15 g/L (Howell et al., 2004)

Most recently, a comprehensive study was performed in a pilot MBR to correlate the critical flux with sludge characteristics, i.e., sludge DSVI (diluted sludge volume index), time to filer (TTF), MLSS concentration, permeate TOC, colloidal TOC (water phase of sludge obtained by 30 minutes centrifugation at 2000 g) and bound EPS (Fan et al., 2006). The critical flux could be almost exclusively correlated to the concentration of colloidal particles, even though other characteristics of the tested sludge samples varied widely (Figure 2-8). As the concentration of colloidal particles increased from 5 to 50 mg/L, the critical flux decreased rapidly initially and then levelled off. Finally an empirical relationship was built to link the critical flux (Jc) to colloidal concentration (C_{TOC}) and temperature (T) as Eq. (2.19).

$$Jc = 51.2 \ (1\text{-}0.43 \ logC_{TOC}) \ 1.025 \ ^{(T\text{-}20)} \hspace{3cm} (2.19)$$
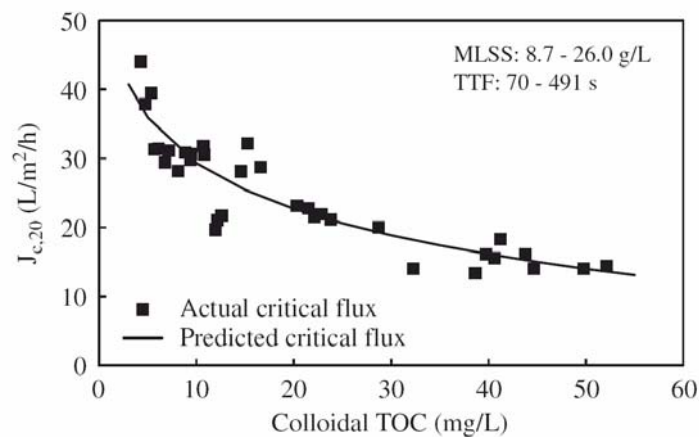
Figure 2-8 Relationship between colloidal particle concentration and critical flux (Fan et al., 2006)

2.2.12.4 Crossflow operation

Shear applied on the membrane surface can improve the backtransport of particles into the bulk solution. In submerged MBRs, shear is created by the coarse air bubble agitation on the membrane surface; while in side-stream MBRs, it is created by the high velocity generated by the crossflow of sludge or sludge/air mixture (air lift).

Numerous studies concluded that operation under high crossflow velocity is beneficial for membrane fouling control in both side-stream and submerged MBRs (Defrance and Jaffrin, 1999a; Madaeni et al., 1999; Howell et al., 2004). This can be well interpreted by the particle backtransport model (see section 2.2.10).

However, excess shear may break up microbial flocs. Excess shear created by a centrifugal pump resulted in floc breakage and possible EPS release (Kim et al., 2001). Ghyoot et al. (1999) reported a significant reduction of nitrification and denitrification using a centrifugal pump compared with a positive displacement pump. Brockmann and Seyfried (1996) reported a destruction of sludge flocs due to unsuitable pumps or to a high TMP in an anaerobic MBR. In several crossflow systems, an increase of the specific cake resistance was reported due to a selective deposition of small particles producing a less permeable filter cake (Lu and Ju, 1989; Tarleton and Wakeman, 1994; Field et al., 1995).

Finally, creating shear on the membrane consumes energy. Recirculating the sludge to create a crossflow is the main energy consumption and main drawback in side-stream MBRs and coarse bubble membrane aeration is very costly in submerged MBRs (Côte et al., 1998; Gander et al., 2000).

2.2.12.5 Membrane cleaning

Almost all pressure driven membrane filtration systems suffer from membrane fouling. However membrane fouling is more pronounced in MF and UF systems due to its feed characteristics. In the application of MBRs, the following methods are commonly applied in membrane cleaning.

- **Relaxation**

Relaxation refers to the periodical stop of the filtration process (e.g., 10-20 seconds every 2-5 minutes). Relaxation allows the removal of the deposited foulants in a "relaxed" condition. Relaxation has the advantage of no consumption of production water and easy implementation in all MBR configurations.

- **Forward flushing**

Forward flushing refers to the periodical creation of a high crossflow velocity along the membrane surface. Membrane forward flushing is beneficial for the removing of filter cake and has the advantage of no consumption of production water. Forward flushing is a unique cleaning method for tubular membranes.

- **Backwashing**

Backwashing (sometimes called backpulsing, backflushing) refers to the reversion of the filtration flow from the permeate side to the feed side for hydraulic membrane cleaning (Mulder, 1996). Backwashing is an effective method to control the membrane fouling. It is easy to automate and can be performed frequently in MBR systems. However, backwashing consumes product water and creates a filtration down time.

Not all membrane modules can apply backwashing. It is feasible for tubular, hollow fibre and capillary membranes (e.g., X-flow, Zenon, and Mitsubishi MBRs). However, it is practically difficult for the flat plate membranes (e.g., Kubota MBRs), due to the lack of mechanical support to the flat sheet membranes. Therefore, the flat plate membranes normally run at a lower flux to limit the membrane fouling.

The parameters controlling the backwashing include: backwashing frequency, duration and flux, which can vary in a wide range for different configurations of MBRs. Generally tubular membranes modules can backwash at a higher flux (3-10 times filtration flux) but a shorter duration (8-20 seconds) due to their strong mechanical strength. The hollow fibre and capillary membranes are normally backwashed at a lower flux (1-2 times) but for a longer time (0.5-2 minutes).

- **Chemical cleaning**

Chemical cleaning is the strongest form of cleaning. It is used to clean the membrane fouling, which cannot be removed hydraulically. Chemicals can be used to displace, dissolve or chemically modify the foulant depending on the characteristics of the foulant and chemicals. Chemicals should be carefully selected according to the type of fouling and the stability of the membrane material. An ideal chemical should be effective to remove the target foulant, minimise the damage to the membrane material, environmental friendly, and, finally, cheap. Unfortunately, due to the complexity of the membrane fouling, selecting a suitable chemical is often a trial and error process, if there is no experience on the specific feed water characteristics.

In MBRs, the most common fouling is organic fouling due to the adsorption of proteins, polysaccharides, etc. Therefore bases, e.g., sodium hydroxide, are often used to "loosen" the organics. In addition oxidants, e.g., sodium hypochlorite and hydrogen peroxide, are the most often used chemicals to destroy the organics. Acids, e.g., citric acid, are used in the case of iron, etc. salt precipitation. Proteases are also used in the case of protein fouling, if conventional base and oxidants cleaning are not effective (MunozAguado et al., 1996; te Poele and van der Graaf, 2005).

In the chemical cleaning process, a few factors are essential to the cleaning efficiency, i.e., chemical concentration, contact time, temperature (Bartlett et al., 1995; Bird and Bartlett, 2002), crossflow velocity (Lee et al., 2001a; Bird and Bartlett, 2002), and TMP (Bartlett et al., 1995; Bird and Bartlett, 2002).

Chemical cleaning can be applied in different ways in MBRs, e.g., in backwashing (chemical enhanced backwashing), lower concentration but in-situ (maintenance chemical cleaning) and high concentration but offline (intensive chemical cleaning).

2.3 Modelling the biological performance of MBRs (ASM model)

2.3.1 Activated sludge model (ASM)

Activated sludge models (ASM) proposed by IWA are basically white-box models, or deterministic models. ASMs are based on first engineering principles, meaning that the model equations were developed from general balance equations applied to mass and other conserved quantities, resulting in a set of differential equations. A few well-known ASM models are reviewed below. The detailed description of model structure is complex and out of the scope of this thesis. Only the extension of these basic models and the unique features in MBRs are described in the corresponding chapters of this thesis.

ASM1 was primarily developed for municipal activated sludge WWTPs to describe the removal of organic carbon compounds and N, with simultaneous consumption of oxygen and nitrate as electron acceptors (Henze et al., 1987). Two groups of microorganisms, i.e., heterotrophic and autotrophic microorganisms were introduced. The introduction of ASM1 has been widely applied and proven to be a success and it is often considered as a reference model for further development.

ASM2 extends the capabilities of ASM1. In addition to the COD and nitrogen removal, ASM2 includes the description of phosphorus removal (both bio-P and chemical P removal) (Henze et al., 1995). A new group of microorganisms, so called phosphorus accumulating organisms (PAO) was introduced. The ASM2d model is only a small extension of ASM2, introducing an anoxic denitrification process of the PAO using cell internal stored organic products poly-hydroxy-alkanoates (PHA) (Henze et al., 1999).

The ASM3 model was also developed for biological nitrogen removal, with basically the same goals as ASM1. The major difference between the ASM1 and ASM3 models is that the latter recognises the importance of storage polymers in the heterotrophic activated sludge conversions. In addition, in the decay/lysis processes, ASM3 uses the

47

traditional decay concept to replace the circular death–regeneration concept in ASM1. As a result, the model calibration is easier (Gujer et al., 1999).

In addition to the IWA ASM models, some research groups developed their own models for various purposes, e.g., the TUDP model (Van Veldhuizen et al., 1999; Brdjanovic et al., 2000) and the EAWAG BIO-P model (Rieger et al., 2001) to tackle the complicated bio-P process.

It should be noted that all of these reviewed models are basically aiming for biological nutrient removal. The SMP and EPS are not included in these models, since the COD removal of domestic wastewater using an activated sludge process is generally satisfied. As a result, the produced SMP in an activated sludge process is often lumped into the influent inert soluble COD (S_I) (Henze et al., 1987) from the practical viewpoint of overall COD mass balance. However, as reviewed in section 2.2.11.2, the true inert soluble COD in the domestic wastewaters are mostly NOM, but the soluble COD in effluent WWTPs are mostly NOM and SMP. Another important issue is that secondary clarifiers are used to in these ASMs for biomass separation.

2.3.2 Modelling the biological performance of MBRs

Modelling the biological performance of MBRs involves some new features compared to the modelling of CAS processes. In addition to the obvious differences, i.e., replacement of the secondary clarifier by a membrane, no loss of sludge in the effluent and high MLSS, some other features are involved, i.e., the uneven distribution of sludge mass fraction due to the lack of concentrated underflow sludge from the second clarifier (Ramphao et al., 2005), the low oxygen transfer efficiency due to high MLSS (Günder, 2001; Krampe and Krauth, 2003), the additional oxygen supply from the aeration of membrane modules, etc.

The traditional ASM can be adapted to model the biological performance of MBR systems. However, the complete retaining of biomass may have some impact on the biological performance, i.e., 1) in a CAS process, the selection pressure on the biomass population is SRT and sludge settling property. However, the latter criterion disappears in the case of MBRs. Nevertheless, the substrate uptake at substrate

deficient conditions may become a new criterion; 2) The modelling of troublesome secondary clarifier is no longer necessary, from this point of view, biological modelling of MBRs is even simpler than with a traditional ASM employing a secondary clarifier; 3) The high shear stress imposed on the MBR sludge for membrane fouling control has an impact on particle size distribution, which eventually may influence the substrate and oxygen diffusion into the flocs (Manser et al., 2005b). On the other hand, excess shear stress may also negatively impact the biological activity (Brockmann and Seyfried, 1996; Ghyoot et al., 1999).

Both black-box and mechanistic models are adopted to model the biological performance of MBRs. Gehlert and Hapke (2002) developed black-box models to simulate the effluence organic concentration. Hasar and Kinaci (2004) developed a regression model to model the specific OUR. More recently, Ren et al. (2005) constructed a regression model to predict the COD removal from the MLSS and HRT However, none of the models included the nutrient removal features.

One of early attempt to mechanistically model MBR performance was performed in a lab-scale single reactor MBR treating domestic wastewater (Chaize and Huyard, 1991). ASM1 was used with default parameters. The method of influent wastewater characterisation was not reported. The model successfully simulated the effluent COD and TKN, but failed to simulate the MLSS concentration. The measurement MLSS was 10 and 36 g/L at HRT of 8 and 2 hr, respectively, however, the model predicted 16 and 65 g/L. The authors attributed the deviation to the fact that ASM1 does not incorporate the maintenance phenomena. Nevertheless, to my knowledge, the deviation is mostly due to the incorrect wastewater characterisation, i.e., the over estimation of inert particulate COD in the influent wastewater. The MBR run at a very high SRT (100 days) but a very short HRT (2 and 6 hrs). A small error in influent X_I characterisation will be magnified by a factor of SRT/HRT.

Rittmann and co-workers built a model to simulate the SMP production and degradation in MBRs (Furumai and Rittmann, 1992; de Silva et al., 1998; Urbain et al., 1998). Lu and co-workers extended ASM1 and ASM3 with SMP components (Lu et al., 2001; Lu et al., 2002). Ahn and co-workers also extended ASM1 model with SMP components and further linked them to membrane fouling (Lee et al., 2002; Cho

et al., 2003; Cho et al., 2004). More recently Ahn et al.(2006) included EPS into the ASM1 model. Yoon et al. (2004) built a kinetic model to estimate the sludge production and aeration requirement. However, all of them (except Ahn, 2006) used parameters directly taken from literature derived from CAS systems or even biofilm system. Although the simulation had a good agreement with the measurement, the evidence is not enough to conclude that a MBR system has the same stoichiometric and kinetics parameters as a CAS system (Dochain and Vanrolleghem, 2001).

Few groups studied the stoichiometric and kinetics parameters in MBRs. Results are summarized in Table 2-8. The default parameters of ASM2d in CAS systems were also included in the table for easy comparison. The MBR parameters obtained by various groups had a large variation, which can be influenced by both the nature of the MBR system and the method used in parameter estimation. The only studies conducted in ASM models in a systematic way were Jiang et al and Ahn et al. using ASM1. In addition, many studies did not report the temperature, which is a well-known factor influencing the kinetic parameters of biological processes. There clearly is a strong need to study the influence of complete sludge retention on the change of sludge biological characteristics, e.g., 1) to evaluate whether the ASM models mostly used in CAS systems are still valid in MBRs 2) the difference of parameters of CAS and MBRs.

Manser et al. performed interesting studies on the influence of membrane separation on the nitrifers by running a membrane bioreactor (MBR) and a conventional activated sludge (CAS) plant in parallel (same wastewater and same SRT), i.e., the population dynamics (Manser et al., 2005a), the kinetics and mass transfer (Manser et al., 2005b) and the decay process (Manser et al., 2006).

The community composition of ammonia-oxidizing bacteria and nitrite-oxidizing bacteria appeared only minor difference according to the FISH (fluorescent in situ hybridization) results. Both systems exhibited the same maximum nitrification rates. It appeared that the membrane separation itself does affect neither the nitrifying community composition nor the nitrification performance (Manser et al., 2005a).

Table 2-8 Stoichiometric and kinetic parameters obtained in MBRs

Reference	Overall biomass / Heterotrophic biomass				Autotrophic biomass			ww	Temp (°C)	SRT (d)	MLSS (g/L)	Config.	Process
	Y	μ_m	K_d	K_s	Y	μ_m	K_d						
Wen et al., 1999	0.56	n.a.	0.08	n.a.	n.a.	n.a.	n.a.	real	30	5,15,30	1.8-10.1	SSMBR	aerobic
Jiang et al., 2005b	0.72	n.a.	0.25[a]	n.a.	0.25	n.a.	0.080	real	22-28	20	8-12	SSMBR	aerobic
Lobos et al., 2005	0.72	3.12	0.06-0.15	n.a.	0.72	3.12	0.06-0.15	n.a.	n.a.	n.a.	n.a.	n.a.	n.a.
Al-Malack, 2006	0.487	1.28	0.151	289	0.487	1.28	0.151	Synth	n.a.	2.1-25	3	Mesh MBR	aerobic
	0.567	1.40	0.062	326	0.567	1.40	0.062			2.8-17	5		
	0.571	5.52	0.037	1967	0.571	5.52	0.037			3.4-31	10		
	0.583	6.46	0.026	2933	0.583	6.46	0.026			4.4-23	15		
Ahn et al., 2006	0.43	1.17	0.77*	n.a.	0.30	0.48	0.18	Synth	n.a.	90	n.a.	SBMR	aerobic
Henze et al., 1999[b]	0.625	6/3	0.4/0.2*	4	0.24	1/0.35	0.15/0.05		20/10				

[a] Decay rate of death-regeneration model
[b] default ASM2d values for conventional activated sludge process
SSMBR= side-stream MBR
SMBR= submerged MBR

The half-saturation coefficients for the substrate were low in both MBR and CAS process and did not differ significantly between the two processes (K_{NH4} = 0.13±0.05 and 0.147±0.10 mg N/L and K_{NO2} = 0.17±0.06 and 0.287±0.20 mg N/L for the MBR and CAS process, respectively). However, the half-saturation coefficients for oxygen exhibited a major difference between the two processes for both the ammonia-oxidizing (AOB) and nitrite-oxidizing (NOB) bacteria. The experiments yielded $K_{O,AOB}$ = 0.18±0.04 and 0.79±0.08 mgO$_2$/l as well as $K_{O,NOB}$ = 0.13±0.06 and 0.47±0.04 gO$_2$/l (substrate only NO$_2$) for the MBR and CAS process, respectively. The higher K_o values of the CAS process were attributed to mass transfer effects within the large flocs prevailing in the conventional system. In contrast, the sludge from the MBR consisted of very small flocs for which the diffusion resistance can be neglected (Manser et al., 2005b).

The decay rates of ammonia and nitrite oxidizing bacteria and heterotrophic bacteria were compared between a MBR and a CAS system. No significant differences were detected between the two systems. The aerobic decay rates of AOB, NOB and heterotrophic bacterial were 0.15±0.02, 0.15±0.01, 0.28±0.05 and 0.14± 0.01, 0.14±

0.01, 0.23± 0.03 1/d for CAS and MBR, respectively. However, the anoxic decay rates were significantly lower, i.e., 0.015±0.004, <0.001, 0.033±0.002 and 0.01±0.003, 0.02±0.009, 0.064±0.002 1/d, respectively (Manser et al., 2006).

2.4 Integrated MBR model

An integrated MBR model refers to a model integrating the biological process with a membrane filtration unit, i.e., to model the impact of MBR biology on membrane fouling and the impact of membrane filtration on MBR biology. An integrated model needs a few sub-models, i.e., probably an activated sludge model (refer to section 2.3), a hydrodynamic model (refer to section 2.2.10), and a filtration (resistance) model (refer to section 2.2.7-2.2.9). The key of integration is to select suitable variables to link these sub-models. Due to the lack of fundamental understanding of the interactions between different sub-models, there are no truly mechanistic integrated MBR models developed so far. However, a few efforts have been reported, and they are reviewed below.

Wintgens et al. (2003) proposed a simple model to simulate the increase in transmembrane pressure in a pilot MBR operating at constant flux conditions. The resistance in series model was used, as in Eq.(2.20), including the membrane resistance (R_m), the cake resistance $R_c = k_c C_b \exp[F(t)/k_p]$ and the fouling resistance $R_f = S_f [1 - \exp(-k_F \int_0^t F(t)dt)]$. The cake resistance was estimated by the combination of traditional concentration polarisation model ($J=k_p \ln(C_M/C_b)$) for the estimation of C_M and a very empirical cake filtration model ($R_c=k_C C_M$), where C_M and C_b are the particle concentration at the membrane surface and in the bulk, respectively. The fouling resistance R_f was assumed to be dependent on the total permeate volume produced in a filtration interval under consideration, e.g., between two chemical cleanings.

$$\Delta P = F(t)\{R_m + k_c C_b \exp[F(t)/k_p] + S_f [1 - \exp(-k_F \int_0^t F(t)dt)]\} \qquad (2.20)$$

Where, F(t) is the flux (L/(m^2·hr, m/s); k_c is the model parameter cake layer (m^2/kg); k_p is the mass transfer coefficient (m^3/m^{2}s); S_f is the model parameter fouling saturation (1/m); k_f is the model parameter fouling (1/m).

The simulated and measured TMP had reasonable agreement. However, it is not a truly integrated model, because there is no link between the biological process and the filtration process. In addition, 1) the hydrodynamic effects is not included in the model and the shear stress due to the membrane aeration (in submerged MBRs) or crossflow velocity (in side-stream MBRs) on particle backtransport is not incorporated; 2) this model does not include the membrane cleaning effects (such as backwashing and chemical cleaning); 3) it uses many lumped filtration parameters (e.g., k_c and k_f), which are too empirical and cannot capture the influence of dynamic sludge characteristics on membrane fouling.

More recently, Broeckmann et al. (2006) extended the model of Wintgens. It considered the particle and membrane pore size distributions as well as adhesion forces between the particles and the membrane surface. In addition, a simple description of backwashing was also incorporated empirically. However, the model still misses the hydrodynamic effects and the impact of biological process on membrane fouling.

Ahn and co-workers linked biology to membrane fouling using a single variable, i.e., the total suspended solid (TSS) concentration (Lee et al., 2002; Cho et al., 2003; Cho et al., 2004). In their model, a modified ASM1 including SMP (BAP only) was used to simulate the TSS concentration and a simple cake filtration model was used to predict the membrane fouling as in Eq. (2.21) and (2.22). Unfortunately, the SMP concentration was not linked to the membrane fouling in their model, and only used to predict effluent quality.

$$J = \frac{\Delta P}{\eta_p (R_m + m\alpha)} \qquad (2.21)$$

$$m = k_m \frac{V_p X_{TSS}}{A} \qquad (2.22)$$

Where m is the mass of cake accumulating on the membrane surface (kg); α is the specific cake resistance $(1/(m \cdot kg))$; k_m is the coefficient reflecting the crossflow effect ranging from 0 (no deposition in crossflow filtration) to 1 (complete deposition in dead-end filtration); V_p is the filtrate volume (m^3).

The obvious limitation of this model is that 1) it overlooks the importance of SMP on membrane fouling but overstressed the impact of TSS (refer to section 2.2.11.2-2.2.11.3); 2) only cake resistance was incorporated and there is no differentiation of the reversibility of membrane fouling; 3) Backwashing was not incorporated. However, in spite of the simplification and obvious limitations, this is probably the first mechanistic integrated MBR model.

3.
Lab-scale MBR and methods of foulant identification

3.1 Lab-scale MBR system

A lab-scale MBR system for biological COD, nitrogen and phosphorus removal was built in the lab of BIOMATH, Ghent University. A tubular membrane with a side-steam configuration was applied. The reason of choosing a side-steam configuration instead of the popular submerged one is due to the fact that: 1) tubular membrane are easier to calculate hydrodynamic conditions, which can reduce some unknowns in hydrodynamics; 2) good contact existed with the tubular membrane supplier (X-Flow, the Netherlands) and the surface area of the MBR module (0.17 m^2) is suitable for a lab-scale setup. Significant efforts were put into the design, construction and automation of the setup to mimic a real MBR system treating domestic wastewater. A computer code was programmed using the LabVIEW 7.1 software (National Instruments, USA) for automated data acquisition and control.

3.1.1 Model based design of lab-scale MBR

The design of the lab-scale MBR was based on simulations using ASM2d model (Henze et al., 1999) in WEST software (MOSTforWATER NV, Kortrijk, Belgium). The model based design helped to determine the process configuration, reactor volumes and operational conditions with the goal of achieving optimal effluent quality. The design criteria included: the membrane surface area (0.17 m^2), SRT (17 days), MLSS concentration (8-12 g/L) and filtration flux (30-40 L/(m^2·h)). The SRT was set close to that (SRT = 15 days) of a SBR reactor running in the lab. The MLSS concentration was set in the common range of full-scale MBRs. The filtration flux referred to the lower end of the filtration flux of side-stream MBRs.

Three reactors (anaerobic, anoxic/aerobic and aerobic) in serials were configured in WEST (Figure 3-1). The bioreactor was divided into three compartments, i.e., an anaerobic compartment, an aerobic/anoxic compartment with alternating aeration and a membrane loop. The membrane module operated under air-lift mode. Thus, the membrane loop and the volume in pipes were also considered as a completely aerobic reactor with an active sludge holding volume of 3.8 L. A cooling machine was connected to both the bioreactor compartments and the membrane loop keeping constant temperature at 15 °C.
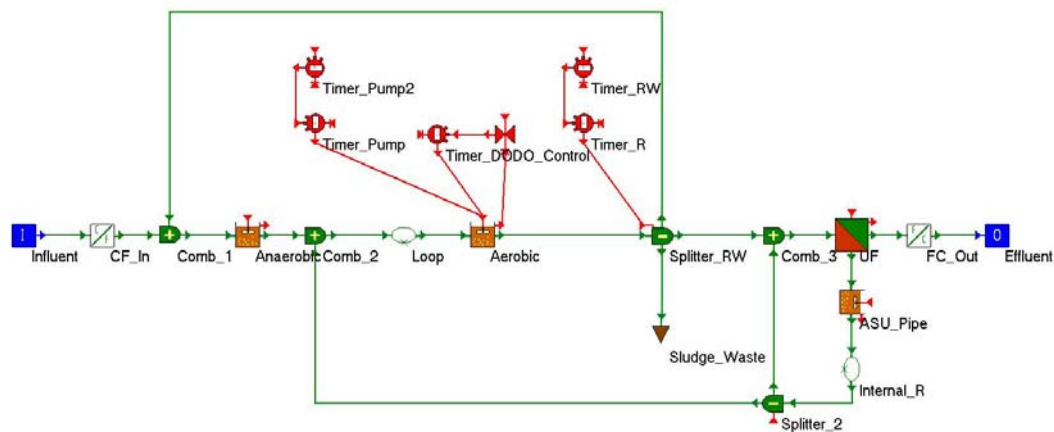
Figure 3-1 lab-scale MBR configuration in WEST

Default ASM2d parameters were used in simulation. The influent wastewater characterisation was straight forward since a synthetic wastewater with known composition was used (see section 3.1.2). The influent flow rate (108 L/day) was determined by the size of the membrane module and filtration flux (31.8 L/(m^2·h)). The total volume of the three compartments (28.8 L) was determined by the influent flow rate and the chosen MLSS concentration (10 g/L). The anaerobic compartment size (8 L), aerobic/anoxic compartment size (16 L) and the time ratio of aerobic : anoxic phase (17 : 23 minutes) were optimised by simulations using trial and error with the goal of achieving full nitrification and minimum achievable nitrate and phosphorus concentration in the effluent. A detailed description of the system and operational parameters are presented in section 3.1.3. A detailed calibration using the results of daily measurements and a measurement campaign is presented in Chapter 4.

3.1.2 Composition of synthetic influent wastewater

A municipal-like synthetic wastewater was used to reduce the disturbance and unknown factors of real influent variation. The synthetic wastewater has the advantage of known and stable composition. However, it suffers the drawback that it always differs somehow from real domestic wastewater. Care should therefore be taken to transfer the results from lab-scale treating synthetic wastewater to full-scale treating real wastewater.

The influent wastewater recipe was adapted from Boeije et al. (1999) with modifications (refer to Appendix A). Both soluble and colloidal components (e.g., acetate, milk powder, peptone and starch, etc.) were used as COD source, which is expected to be more representative than using completely soluble COD source, e.g., acetate or glucose. To challenge the capability in nutrient removal, the nutrient : COD ratio was set at a ratio higher than real municipal wastewater (COD : N : P = 100 : 13.7 : 2.76).

To minimize the effort of preparing influent, a concentrated influent was prepared at pH=3 (to avoid the growth of microorganisms) for 3-4 days use. The concentrated influent was diluted on-line with a ratio of concentrated influent:tap water = 1:14. The dilution was performed using a 3-way solenoid valve switching alternately between 12 seconds concentrated influent and 168 seconds tap water.

3.1.3 Scheme of lab MBR setup

A picture, a scheme and the operational conditions of the MBR system are presented in Figure 3-2, Figure 3-3 and Table 3-1, respectively. The list of equipments used is summarized in 0.

Figure 3-2 A view of lab-scale MBR system
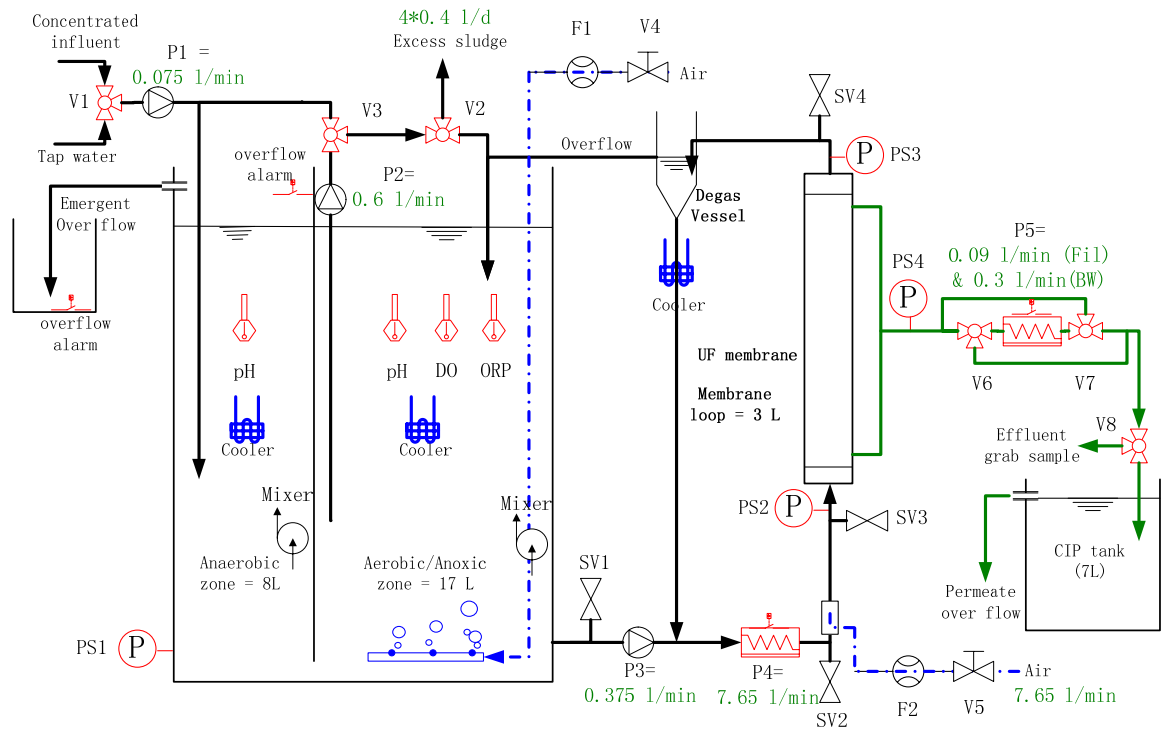
Figure 3-3 Scheme of lab-scale MBR system

Table 3-1 Summary of operational conditions of lab-scale MBR

Variable	Reference values
Influent flow rate	0.075 L/min
Recirculation flow rate from aerobic/anoxic to anaerobic compartment (= sludge waste rate)	0.9 L/min
Recirculation flow rate from reactor to membrane	0.375 L/min
Aerobic duration	17 min every 40 min
Anoxic mixing duration	11 min every 40 min
Anoxic recirculation duration	12 min every 40 min
sludge waste duration	40 sec every 6 hr
SRT	17 days
Aerobic SRT	7.2 days
Filtration flux	31.8 L/(m^2·h)
Backwashing flux	106 L/(m^2·h)
Filtration duration	450 sec every 475 sec
Relaxation duration	7 sec every 475 sec
Backwashing duration	18 sec every 475 sec
Sludge superficial velocity (in membrane tubes)	0.5 m/s
Air superficial velocity (in membrane tubes)	0.5 m/s
Mean velocity (in membrane tubes)	1 m/s
Reynolds number (in membrane tubes)	2060
Temperature	15 °C

The synthetic wastewater was pumped (P1, 0.075 L/min, Watson Marlow 323U/RL, UK) into the anaerobic compartment, where PAOs (phosphorus accumulating organisms) took up the VFAs and released phosphate. Subsequently, the sludge flowed into the aerobic/anoxic compartment (17 L) under a baffle, where COD degradation, nitrification, phosphate uptake and denitrification (by switching off aeration) took place. The aerobic/anoxic compartment was aerated intermittently to create alternating aerobic/anoxic conditions (17 minutes DO = 2 mg/L, 23 minutes DO = 0). During the first 11 minutes of the anoxic phase, the sludge was mixed within the aerobic/anoxic compartment by pump P2 (Watson Marlow 505 U, UK). During the last 12 minutes of the anoxic phase, the sludge from the aerobic/anoxic compartment was recirculated to the anaerobic compartment by pump P2 (0.6 L/min, 8×Q_{in}). The switching was performed by a 3-way valve V3. Every 6 hours, 0.4 L excess sludge was wasted from the aerobic/anoxic compartment via P2 during the last 40 seconds of the aerobic phase.

The sludge in the aerobic/anoxic compartment was pumped by P3 (0.375 L/min, 5×Q_{in}, Watson Marlow 505 U, UK) to the inside of the membrane tubes, where the sludge was recirculated through the membrane by a positive displacement pump P4 (Seepex BN 2-6L, Germany, 7.65 L/min) without pulsation. Together with the

injected air (7.65 L/min), an air/liquid slug flow (1 m/s) was created in the membrane tubes to control the membrane fouling. A small portion of the feed sludge was withdrawn as permeate by a positive displacement pump P5 (Seepex MD 003-12, Germany) without pulsation at a flow rate of 0.090 L/min, with corresponding gross filtration flux of 31.8 L/(m^2·h), to fill a CIP (Clean In Place) tank (7 L). Meanwhile the majority of the feed sludge pumped into the membrane inlet (> 98%) overflowed out of the membrane module outlet and was directed to a degassing device to remove the air from the sludge. The extra concentrated sludge (0.3 L/min, 4×Q_{in}) pumped into the membrane loop was returned to the aerobic/anoxic compartment of the bioreactor.

Every 450-second filtration, the membrane was backwashed for 18 seconds followed by a 7 seconds relaxation period (stop P5). The backwashing flow was 0.3 L/min, i.e., a flux of 106 L/(m^2·h) or 3.3 times the filtration flux. The reverse of the flow direction was controlled by two 3-way valves, i.e., V6 and V7, and the backwashing flux was controlled by a suction pump P5.

The MBR system was operated under constant flux conditions, The permeate flow rate was determined by the rotating speed of a positive displacement pump (P5), whose flow rate hardly changes with increasing pumping head. The liquid level (setpoint = 62.5 cm) in the bioreactor was controlled by varying the speed of the permeate pump P5. A pressure sensor (PS1) was installed at the bottom of the anaerobic compartment, which read an on-line pressure signal. The level signal was transferred to the permeate pump P5 and the filtration flow rate was adjusted correspondingly every filtration cycle (around 8 minutes) by a proportional level control algorithm.

Two temperature switches were installed on pump P4 and P5, respectively to protect the pumps from accidental dry running. In case of too high temperature (> 40 °C), the corresponding pump can be switched off automatically. Three liquid detection sensors were installed in two safety tanks, where the reactors and pumps were placed in. In case of sludge overflow and touched any of the liquid detection sensors, the VI could automatically stop all pumps and switch the MBR to an emergent mode keeping alternating aeration only.

3.1.4 Mixing in the reactor (tracer test)

The height of the reactor was 62.5 cm but the cross sections of the anaerobic and aerobic/anoxic compartment were only 10×6 cm 10×12 cm, respective. This design provided a sensitive detection of the water level and a good control of the reactor active volume, but it was vulnerable to insufficient mixing and creating dead zones. Therefore, a tracer test was performed to check whether both compartments can be modelled as completely mixed reactors.

During the tracer tests, the mixing pump was kept running but the recirculation flow and aeration were switched off. This can be considered as the worst mixing condition. The tracer test was only performed in the anaerobic compartment, since the aerobic/anoxic compartment obviously has better mixing than the anaerobic one due to the cyclic aeration and internal recirculation.

Sodium chloride was used as a tracer. Conductivity and temperature (Kemotron 9222 conductivity sensor and Knick Stratos 2402 Cond transmitter) were measured on-line every second. Three different tracer tests were conducted, i.e., 1) pulse addition of NaCl, 2) step-up (add NaCl solution to the reactor originally filled with tap water) and 3) step-down (add tap water to the reactor originally filled with NaCl solution). The conductivity sensor was calibrated with NaCl solutions. In addition, the tap water conductivity and the influence of temperature on conductivity were corrected.

Curve fitting with assumption of one tank and 2 equal size tank in series were performed using the optimisation tool box in Matlab (Mathworks, USA). The recovery of the NaCl (recovered/added NaCl) was estimated by integrating the measured NaCl flux in the effluent. An example of curve fitting (step-down) using 1 tank and two-tank in series (equal size) model are given in Figure 3-4. Clearly, the one tank model provided a much better fitting.
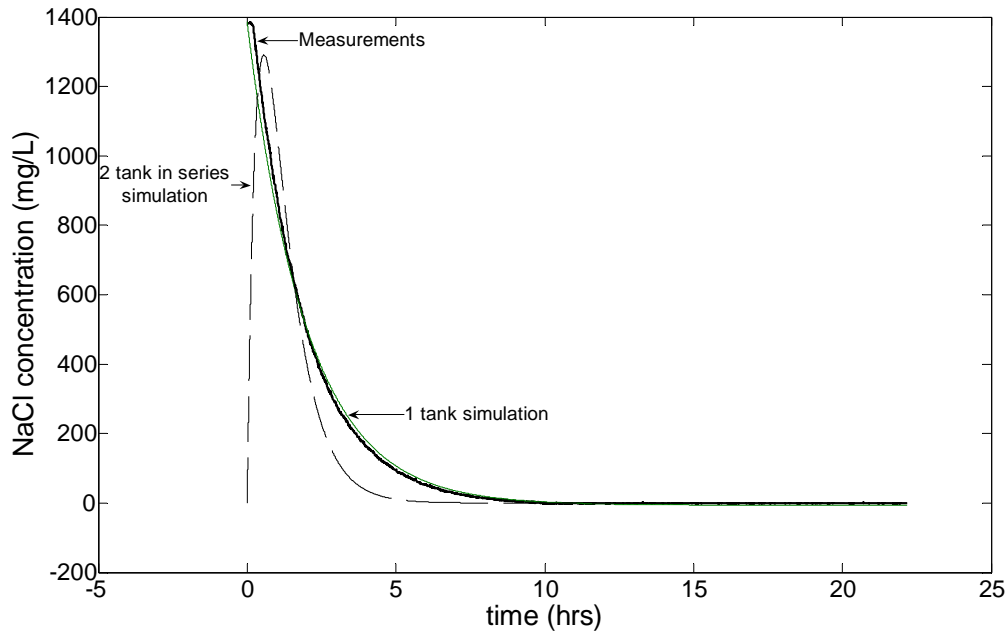
Figure 3-4 Comparison of simulated NaCl concentration using one tank and two tank in series model with experimental results (t step-down experiment)

The results of the 3 types of tracer tests presented are summarized in Table 3-2. There was 10-17% error in estimating the reactor residence time (HRT was underestimated in pulse test but overestimated in the step tests). The recovery was 0.877-1.03, which is acceptable. In conclusion, both compartments in the reactor can be modelled as completely mixed reactors.

Table 3-2 Results of tracer test in the anaerobic compartment (one tank)

Test type	Estimated influent concentration (mg/L)	Estimated hydraulic residence time (min)	recovery
Pulse	4346 (4781)	90 (108)	0.877
Step-up	1381 (1324)	125 (108)	1.03
Step-down	6.1 (0)	120 (108)	1.05

* Results in parentheses are the true values.

3.1.5 Oxygen transfer coefficient (K_La) under clean water conditions

The oxygen transfer coefficient (K_La) in the aerobic/anoxic compartment, the membrane module operating at air-lift mode and the surface aeration in the anaerobic and aerobic/anoxic compartment were estimated under clean water conditions. The step aeration method was used as follows: 1) sodium sulfite (Na_2SO_3) was added to

remove dissolved oxygen, with potassium cobalt chloride ($CoCl_2.6H_2O$) as catalyst; 2) the aeration was switch on and the DO concentration was measure on-line every second; 3) the DO concentration was corrected by considering the time constant of the DO probe. 4) A simple curve fitting was performed in WEST software (MOSTforWATER NV, Kortrijk, Belgium) to estimate both K_La and the saturated oxygen concentration. 5) The estimated K_La values were standardised to 15 °C using Eq. (3.1) (ASCE, 1993 and Mueller et al., 2002). The experiment conditions and results are summarized in Table 3-3.

$$K_La_{,15} = K_La\, \theta^{(15-T)} \tag{3.1}$$

Table 3-3 Experimental conditions and results of clean water K_La test (Values in parenthesis are 95% confidence interval)

Type	Replicate	Q_{air} (L/min)	Temp. (°C)	$K_La_{,t}$ (1/d)	$K_La_{,15}$ (1/d)	Avg $K_La_{,15}$ (1/d)
Coarse bubble aeration in aerobic/anoxic compartment	1	20	22	846 (6)	717 (5)	
	2	20	22	830 (6)	703 (5)	691
	3	20	22	770 (5)	652 (4)	
Air lift in membrane module	1	10	31	1182 (14)	809 (10)	792
	2	10	31	1134 (15)	776 (10)	
Surface aeration in anaerobic compartment	1	0	15	7.07 (0.006)	7.07 (0.006)	7.07
Surface aeration in aerobic/anoxic compartment	1	0	15	7.24 (0.009)	7.24 (0.009)	7.24

Generally, the K_La obtained in field conditions can be much lower than the clean water K_La. A simple correction method by measuring the so-called alfa factor (α) is normally performed, which is the ratio of K_La_sludge and K_La_clean water (ASCE, 1993 and Mueller et al., 2002). The K_La_sludge was only 223 1/d (see section 3.2.3), resulting in a very low alfa factor of only 0.32. The low alfa factor measured in the MBR sludge is consistent with some field MBR studies (Günder, 2001; Krampe and Krauth, 2003).

3.1.6 Membrane characteristics

The characteristics of the membrane used for the lab MBR are listed in Table 3-4. The PVDF membrane has a tubular configuration with a nominal pore size of 0.03 μm and 200 kDa. The exact same membrane tube is used for pilot and full-scale MBR installations, which creates similar hydrodynamic conditions in different scale MBRs. In addition, the flat sheet membrane used in batch filtration tests (see section 3.4) has the same membrane characteristics as the tubular ones. The similar membranes used in batch, lab, pilot and full-scale MBRs makes the filtration results more transformable.

Table 3-4 Membrane characteristics of lab-scale MBR

Characteristics	Value
Membrane module	X-flow, 11PE
Membrane tube	X-flow, F 4385
Membrane material	Polyvinylidene fluoride (PVDF)
Membrane hydrophobicity	Hydrophilic
Structure	Asymmetric / microporous
Membrane carrier	Composite polyester fabric
Geometry	Tubular
Nominal pore size (μm)	0.03
Hydraulic diameter (mm)	5.2
Tube length (m)	1
Number of tubes in each module	12
Diameter of module (inch)	1
Membrane surface area for each module (m^2)	0.17
Initial flux L/(m^2·h) (distilled water at 25°C and 100kPa)	1200
Transmembrane pressure (kPa)	-100 ~ +300
pH tolerance	2-10
Maximum chlorine exposure (ppm×h)	250,000
Temperature (°C)	1-70

3.1.7 Air distribution in the membrane module

The crossflow inside the membrane tubes (feed sludge) was generated by a mixture of air and sludge. Each module has 12 membrane tubes (5.2 mm in diameter). To obtain a uniformed air distribution in the tubes, care was taken in designing the air injector in the membrane loop. An air injector with 4 small holes was installed just at the outlet of the recirculation pump (P4). The mixture of air and sludge had to travel 70 cm in a pipe and go through a few bends before reaching the inlet of the membrane module (Figure 3-5).
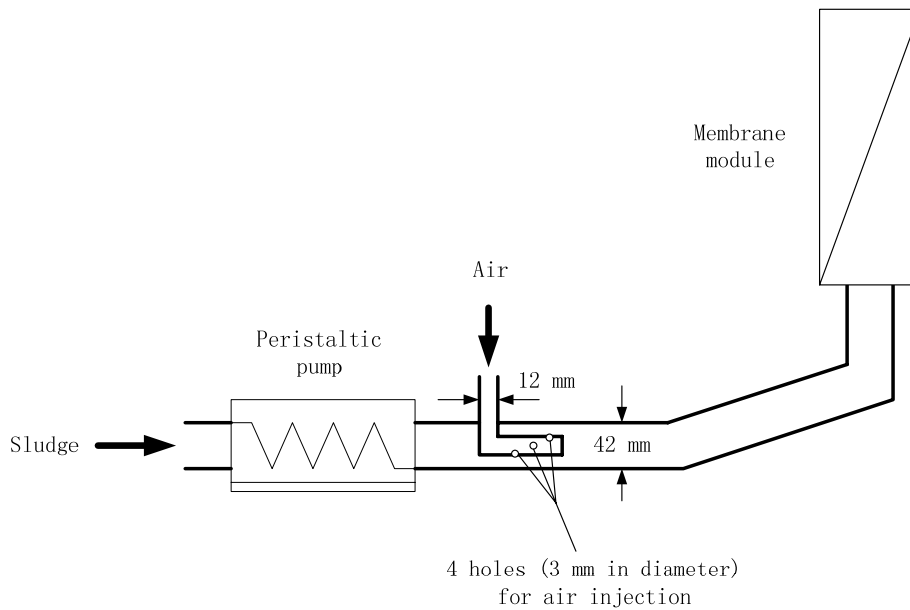
Figure 3-5 Schematic drawing of air injection into the membrane module

The air distribution in the membrane module was evaluated by visualization. The outlets of the 12 membrane tubes were connected to 12 transparent hoses. In the test range of mean velocities (1-2 m/s) and an air/sludge ratio (1:1), visual inspection showed that air was evenly distributed among the 12 membrane tubes and good air/sludge slugs were formed.

3.1.8 Procedure of membrane chemical cleaning

Chemical cleaning was performed when the TMP reached approximately 15 kPa. The cleaning frequency was once per month on average. A few chemicals, i.e., NaOH, NaOCl, HCl and citric acid were used in cleaning. Softened water was used to avoid calcium precipitation on the membrane at room temperature (around 20 °C) and the general cleaning procedure is as follows.

- Remove the membrane module from the MBR setup and flush the membrane tubes one by one using the pressure of tap water.
- Recirculate the NaOH solution (pH=11.5) inside the membrane tube at a flow rate of 2 L/min, mean while suck from the permeate side at a flow rate of 0.075 L/min. The TMP during the cleaning was monitored on-line. This cleaning step was performed for around 30 min or until the TMP is stabilised.

- Clean with 600 mg/L (as active chlorine) of NaOCl solution using the same procedure as step 2. Repeat if necessary in case fouling is significant.
- Clean with softened water for 10 minutes to remove residual chemicals.
- Clean with HCl (pH=1.5).
- Clean with softened water for 10 minutes to remove residual chemicals.
- Put the membrane back into the reactor.

3.1.9 Data acquisition and control using LabVIEW

A computer code was programmed using the LabVIEW 7.1 software for the automated data acquisition and control. The DAQ card (NI PCI-MIO-16XE-50) channel configuration is summarized in Appendix C. Nine AI (analog input) channels were used to obtain analog input signals, i.e., reactor level, pressure at the membrane inlet, membrane outlet and membrane permeate, anaerobic pH, aerobic/anoxic DO, aerobic/anoxic pH, aerobic/anoxic ORP and temperature. The speed of the permeate pump (P5) and recirculation pump (P4) were regulated by frequency invertors via two AO (analog output) channels, respectively. Six digital output channels were used to control valves, i.e., aeration, influent mixture, waste sludge, sludge mix/recirculation, backwashing, grab sampling of effluent. One digital output channel was used to stop three peristaltic pumps (P1, P2 and P3) in the case of danger of reactor overflow.

3.2 On-line and off-line monitoring of lab-scale MBR

3.2.1 On-line monitoring

LabVIEW acquired on-line data every second and stored in a text file, including anaerobic pH (METTLER TOLEDO Inpro4250, Knick stratos-E 2402 pH) aerobic ORP (METTLER TOLEDO Pt4805-DXK-58/120, Knick stratos-E 2402 pH), aerobic pH (METTLER TOLEDO Inpro4250, Knick stratos-E 2402 pH) and aerobic DO (METTLER TOLEDO InPro6050, Knick stratos-E 2402 oxygen), aerobic temperature, reactor level (PS1, 142PC02D, Honeywell), feed pressure (PS2 and PS3, 142PC15D, Honeywell) and permeate pressure (PS4, 143PC15D, Honeywell).

An example of online MBR data (DO, pH in aerobic/anoxic compartment and TMP) is given in Figure 3-6. On the left figure, the DO concentration was controlled at 2 mg/L using (on-off control) during the aerobic phase. The nitrification process was activated and the production of protons decreased the pH. On the right figure, the filtration phase can be clearly identified from the backwashing and relaxation phase with a slow increase in TMP. Backwashing was visible as negative TMP; however relaxation (7 seconds) cannot be clearly identified due to the too short duration.
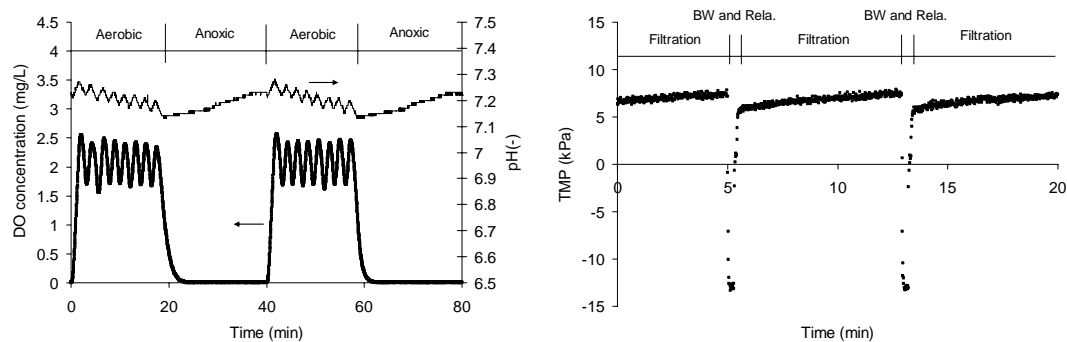
Figure 3-6 Online MBR data (DO, pH in aerobic/anoxic compartment and TMP)

3.2.2 On-line estimation of OUR

The oxygen uptake rate (OUR) of the MBR was estimated on-line using LabVIEW. When reactor phase was switched from the aerobic to anoxic and the aeration was switched off, the linear part of DO values (0.7-1.4 mg/L) were stored in an array every second. A linear regression was performed automatically using the stored DO vs. time data and the estimated slope was the OUR. However, one has to bear in mind that the OUR in the reactor was not constant during the aerobic phase. The on-line OUR estimation can only be considered as an approximation, due to the fact that: 1) the oxygen uptake rate is a function of the DO concentration. The growth rate of biomass will be reduced if DO drops below 1 mg/L and the reduction is more pronounced for nitrifiers (Henze et al., 1987); 2) The oxygen uptake rate is a function of the substrate concentration. The readily biodegradable COD and ammonium are more abundant at the start up of an aerobic phase than the end of it; 3) The biomass may need a certain time to adapt to the switch of electron acceptors between nitrate and oxygen, e.g., to prepare the related enzymes. Therefore, there may exist some delay, which can influence the oxygen uptake rate profile (Vanrolleghem et al., 2004).

3.2.3 On-line estimation of $K_L a$

The $K_L a$ value was estimated from the increasing profile of DO using Eq.(3.2), when the compartment phase was switched from anoxic to acerbic conditions. The left side of the equation (DO gradient) can be estimated as the slope of the DO profile from 0.5 mg/L to the moment that aeration was stopped. The OUR term (r_{O2}) on the right side of the equation is assumed constant throughout the aerobic phase and taken the value from the previous cycle (40 minutes before). Again, the on-line $K_L a$ estimation was only a rough estimation, since the OUR changes over time and the range of DO data used in the calculation was too small (0.5-2 mg/L).

$$\frac{dC_o}{dt} = K_L a (C^* - C_o) - r_{O2} \tag{3.2}$$

The on-line OUR and $K_L a$ estimation were useful tools in fault detection, e.g., in the case that the influent tube was clogged, the on-line OUR dropped and this failure was discovered quickly. The OUR data were also used for an overall COD mass balance (Ekama et al., 1986).

3.2.4 Sampling and off-line measurement

The offline effluent monitoring included COD, BOD_5, NH_4^+-N, NO_2^--N, NO_3^--N, TN, PO_4^{3-}-P, TP, proteins and polysaccharides. The offline sludge monitoring included MLSS, MLVSS, SMP of sludge water phase (as protein, polysaccharide and COD), extracted EPS (as protein, polysaccharide and COD), viscosity and particle size distribution. The effluent COD, NO_3^--N, and PO_4^{3-}-P were monitored daily. The effluent NH_4^+-N, NO_2^--N, TN, TP, MLSS, MLVSS, proteins, polysaccharides and SMP were monitored twice per week. EPS extraction and measurement were performed every two weeks. The others were monitored irregularly if necessary.

The effluent sample was collected in the CIP tank, which had a hydraulic residence time of 1.8 hours. This way of sample collection reduced the variation due to the alternating aeration in the aerobic/anoxic compartment on effluent sampling.

The sludge water for SMP measurements was separated by centrifugation and one or two-step filtration. First, the sludge was centrifuged (Sorvall RC-5B, Du Pont Instruments) at 2000 rpm (534 G) for 5 minutes to remove suspended solids. Afterwards, if the sludge sample volume was small (e.g., 20 ml), the collected supernatant was filtered directly using a Millex 0.45μm PVDF filter (Millipore, USA). If the volume was large (a few litres for filterability test), the collected supernatant was first filtered through a glass microfibre filter (GF/C, 1.2μm, Whatman, UK) and followed by the second step filtration using a flat sheet microfiltration membrane (DURAPORE 0.45 μm PVDF, Millipore, USA) on a stirred cell (Stirred Cell 8200, Millipore, USA). The final permeate is defined as the sludge water. The two-step filtration avoided the build up of a thick filter cake. All filters were pre-rinsed with Milli-Q water before use to remove residual TOC (see section 3.5 for the procedures of rinsing filters). All samples were stored in a fridge at 4 °C for maximum 4 days before analysis.

The COD and nutrient concentrations, i.e., TN, NH_4^+-N, NO_2^--N, NO_3^--N, PO_4^{3-}-P and TP were measured by Dr Lange kits using colorimetric methods. BOD_5 was measured with an Oxitop apparatus (WTW, Germany). MLSS and MLVSS were measured by standard methods (APHA, 1998).

The protein content of SMP and extracted EPS samples were measured using the Lowry method (Originally proposed by Lowry et al. (1951) and modified by Raunkjaer et al. (1994)). Humic substances can interfere with the measurement (Frølund et al., 1995). However, since a synthetic wastewater was used in the lab-scale MBR, no humic substances would be expected to be produced at the SRT of only 17 days. Consequently, no corrections on humic substances were made.

The polysaccharide content of SMP and extracted EPS samples were measured using the phenol method (Dubois et al., 1956). Nitrate can interfere with the measurement. To quantify the absorbance of nitrate in the polysaccharide measurement, a calibration curve of nitrate was constructed as in Figure 3-7 and Table 3-5. The 95% of confidence interval in the nitrate calibration curve is not wide with an absorbance error less than 0.01. In addition, the slope of the nitrate calibration curve (0.0017) is much lower than that of polysaccharides (0.0141). Thus, an error in estimating the

nitrate absorbance won't have a significant impact on polysaccharide measurement (e.g., 0.01 unit absorbance error in nitrate will only result in 0.001 unit equivalent absorbance error in polysaccharide). To subtract the absorbance due to nitrate from the sample absorbance, nitrate was measured using Dr. Lange kits independently. This correction is essential in case the polysaccharide concentration is low, and the nitrate concentration is high, e.g., in the effluent and in the BAP batches (see section 3.3).
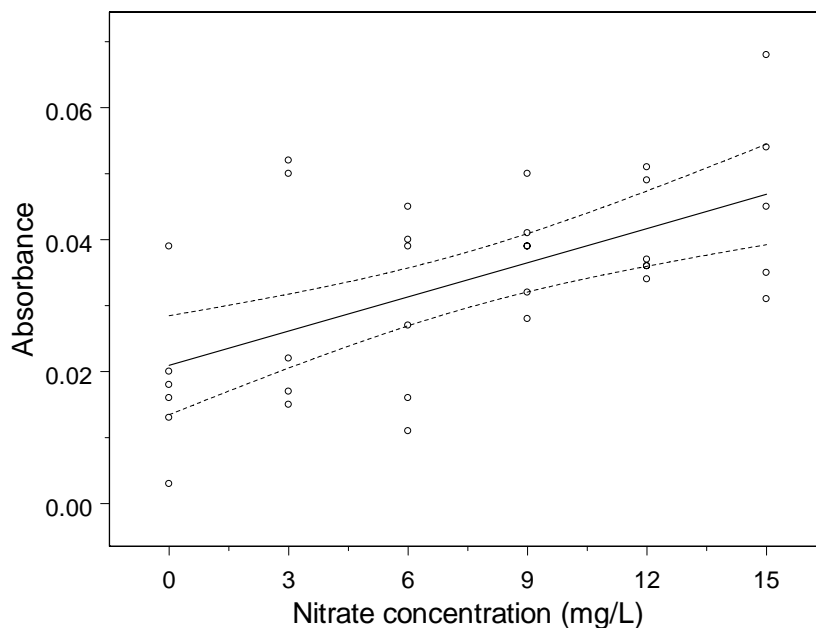
Figure 3-7 Calibration curve of nitrate using the phenol method (— regression curve; - - - 95% confidence region)

Table 3-5 Inference of nitrate on polysaccharide measurements (linear regression of nitrate using the phenol method)

	Value	Std. Error	t value	Pr(>|t|)
Slope	0.0017	0.0004	4.2061	0.0002
Intercept	0.0210	0.0037	5.6927	0.0000

EPS was extracted by a cation exchange method described by Frølund et al. (1996). A small modification was made in the last step. To remove the particulates, in addition to centrifugation, the extracted EPS was filtered through a 0.45 μm PVDF Millex filter (Millipore, USA) to ensure that no suspended flocs/resin remained in the water phase. The extracted EPS was measured as COD, polysaccharides and proteins.

3.2.5 LC-OCD analysis

The LC-OCD analysis was performed by a commercial lab (DOC-LABOR Dr. Huber, Germany, Huber and Frimmel, 1991; Huber and Frimmel, 1992). Both fine and coarse size exclusion chromatography (SEC) columns (Alltech, Germany) were used. The SEC column was filled with Toyopearl resin (HW-50S or HW-65S with pores size of 12.5 and 100 nm respectively). The HW50S column has a good resolution in a LMW region (<20 kDa) and the HW65S column has a good resolution in a HMW (high molecular weight) region (50-2000 kDa). Therefore the combination provided a clear MW profile of SMP. Three detectors were installed in series in a sequence of UVD, OCD and OND. The UV detector (UVD, Knauer K200, Germany) measured the SAC (Spectral Adsorption Coefficient) at 254 nm. The OCD detector oxidized all organic matters in a thin film UV reactor, thus the organic carbon present in the sample could be quantified from the amount of produced CO_2 (OCD, DOC-LABOR, Germany). Afterwards a second capillary UV reactor was connected to ensure than all organic nitrogen (Norg.) was oxidized into nitrate. Finally a UVD (Knauer K2001, Germany) was equipped to quantify the amount of nitrate from SAC, due to the fact that nitrate is the only strongly UV-absorbing compound (measured at 220 nm) potentially present after oxidation.

The size-exclusion chromatograph separates compounds according to their MW. In a properly operated chromatographic column, the larger MW compounds elute before the smaller ones. An example chromatogram of a surface water sample is presented in Figure 3-8. The first peak at approximately 30 minutes is the biopolymer peak, which is composed of polysaccharides, proteins and organic colloids associated with cellular debris with a MW larger than 20 kDa (upper limit of column separation). Humics (HS) follows a tight definition based on the retention time, peak shape and SUVA (specific UV absorbance), and appear as a broad peak at approximately 46 minutes. Building blocks (HS-Hydrolysates) are assumed to be sub-units ("building blocks") of HS with broad shoulders and molecular weights between 300-450 g/mol, and appear as a compressed at approximately 49 minutes. LMW (low molecular weight) organic acids are all aliphatic (< 300-450 g/mol) showing a peak at 53 minutes. However, a small amount of HS may fall into this fraction. A software program was used (FIFFIKUS, DOC-LABOR) to correct this error on the basis of standard humic substances

obtained through IHSS. Neutrals are LMW weakly charged hydrophilic or slightly hydrophobic compounds, like monosaccharides, oligosaccharides, alcohols, aldehydes, ketones, and amino acids.
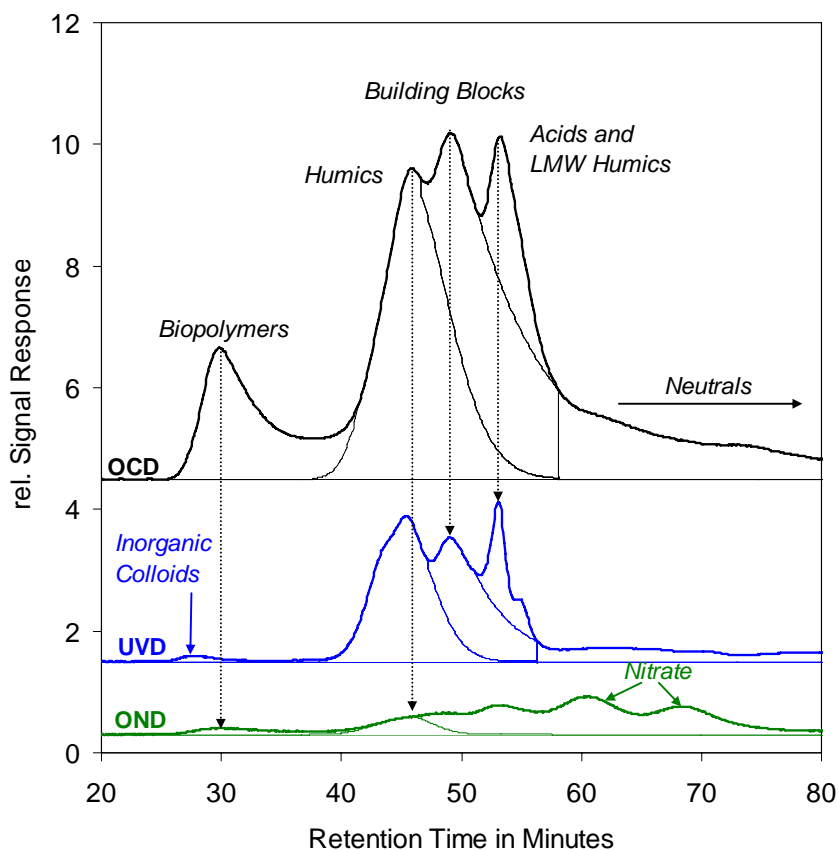
Figure 3-8 Idea LC-OCD chromatogram of a surface water sample with HW50S column (the thick line represents total signal, and the thin line represents the separation of each fraction using a software FIFFIKUS)

However, the interpretation of LC-OCD chromatograms should be with caution. First, inorganic colloidal compounds (e.g., polyelectrolytes, polyhydroxides and oxidhydrates of Fe, Al or Si) also absorb UV at 254 nm and unfortunately their elution time is close to that of the biopolymers. In this sample, it is slightly earlier at 28 minutes. Theoretically, polysaccharides have no UV adsorption at all. However some proteins can have a low UV adsorption, e.g., the SUVA value of amino acid such as L-tryptophan or L-Tyrosine is about 1.7 L/(mg·m), but BSA (bovine serum albumin) has a very low SUVA value as 0.1-0.2 L/(mg·m) (Nam, 2006). Thus, the biopolymer fraction normally has hardly any UV adsorption. Second, if a large amount of nitrate is present in the sample, the OND will not be able to differentiate the nitrate produced after oxidation of Norg. Thus, the chromatograms of Norg. in this region (after 55 minutes) have to be interpreted with caution.

The LC-OCD chromatograms showed very precise and reproducible results. A UAP sample was analyzed two times in consecutive days using the HW-65S column, the maximum relative error, defined as $|OC_1-OC_2|/OC_1$, in time series (every 5 sec) was only 3%, and in the region of main OC peaks, the relative error was less than 1%.

3.3 BAP and UAP production in batch reactors

BAP and UAP were produced in two different batch experiments. Producing BAP and UAP in different batches made it possible to characterise and filter them separately (Chapter 5). The SMP dynamics measured during the batch reactors also provided dynamic data for the calibration of BAP and UAP models (Chapter 6).

The BAP was produced under starvation conditions as follows. 2.2 L of sludge was taken directly from the aerobic/anoxic compartment of the lab-scale MBR and centrifuged at 2000 rpm (534 G) for 5 minutes. The supernatant was replaced with a synthetic inorganic solution, which had the same inorganic composition as the sludge water but no ammonium and organic constituents (no substrate) and diluted using Milli-Q water. The washing and replacing of supernatant was performed 3 times to ensure that the sludge water was completely replaced. The washed sludge was then resuspended to 2 L and placed in a temperature (15 °C) and pH (7.5 by dosing NaOH and HCl automatically) controlled batch reactor. The batch temperature and pH were the same as those in the sludge fed to the membrane of the lab-scale MBR. Alternating aeration was performed in the batch reactor at the same ratio as the lab-scale MBR (49.4 minutes on with DO setpoint of 2 mg/L, 70.6 minutes off). The alternating aeration in the BAP batch is essential due to the fact that the biomass decay rate is influenced by the electron acceptor condition. An aerobic decay using oxygen typically has a higher decay rate than anoxic decay using nitrate (Manser et al., 2006). Sludge was undergoing starvation in the BAP batch reactor for 19 days, during which, 20 mL of sludge sample was taken from the batch reactor every 1-2 days and BAP was separated from the sludge using the method described in section 3.2.4. By the end of the BAP batch experiment (19 days), the sludge water (BAP) was completely harvested and the filterability of BAP was studied in an unstirred cell filtration unit.

The UAP was produced in the biomass growth phase with substrate (sodium acetate) addition as follows. 4.4 L of sludge was taken directly from the lab-scale MBR and centrifuged at 2000 rpm (534 G) for 5 minutes. The sludge water was replaced with a synthetic inorganic solution in the same way as the BAP experiment. The washed sludge was then resuspended to 4 L and divided into two parts: a reference batch without sodium acetate addition and a UAP batches with sodium acetate addition representing a readily biodegradable COD substrate. The batch experiment was performed under constant temperature (15 °C) conditions and pH (7.5) was controlled by dosing NaOH and H_2SO_4 automatically. However, both The UAP and the reference batches were performed under completely aerobic conditions with a DO setpoint of 2 mg/L. The completely aerobic condition was used to estimate OUR (oxygen uptake rate). One hour before the substrate addition, ATU (Allylthiourea) and nutrients were dosed into both batches to reach initial concentrations of 10 mg/L ATU, 37.5 mg-N/L NH_4Cl and 7.5 mgP/L KH_2PO_4. The NH_4Cl and K_2HPO_4 were supplied as nutrients for biomass growth and the ATU was used to inhibit nitrification to avoid oxidation of NH_4Cl by nitrifiers. Sodium acetate was dosed into the UAP batch to form an initial substrate concentration of 1000 mg COD/L and a substrate/biomass ratio (S_0/X_0) ratio of 0.097. Sludge samples (20 mL each) were taken from the each batch reactor every 1-2 hr in the initial 8 hrs plusing the last sample at 23.2 hrs. UAP was separated from the sludge using the method described in section 3.2.4. The added acetate was depleted in approximately 4 hrs. By 23.2 hrs, the sludge water (UAP) was completely harvested and the filterability of UAP was studied in an unstirred cell filtration unit. By comparing the water phase of the UAP and the reference batches, the net UAP production can be quantified.

3.4   Batch filtration experiment of SMP samples

All batch filtration runs were performed at the room temperature (21 ± 2 °C) and the temperature was recorded manually to correct the viscosity. Before the filtration, the pH of the samples was adjusted to 7.5 (same as the lab-scale MBR) using HCl or NaOH.

The BAP, UAP and SMP samples were filtered using a constant pressure filtration unit equipped with a stirred cell unit (Stirred Cell 8200, Millipore, USA) operating

under unstirred conditions (dead-end). A flat sheet 0.03 μm PVDF membrane was manufactured for this batch filtration (X-flow, the Netherlands) with exactly the same material, structure and morphology as the tubular one used in the lab and full-scale MBRs. The feed to the unit was supplied by a high level tank (TMP = 14.3 kPa, close to the practical TMP in full-scale MBRs). The permeate was collected on a precision balance (PB602-L, METTLER TOLEDO, Switzerland). The weight signal of the balance was transferred to a PC every second via a RS232 port. A computer code was programmed using LabVIEW 7.1 (National Instruments, USA) for data acquisition. The weight and flux can be visualized on a screen instantaneously during the filtration process. With this fully automated filtration device, it is possible to record the initial flux decline accurately.

Each constant pressure batch filtration started with Milli-Q water to estimate the clean membrane resistance. When a constant flux was reached, the feed was switched from Milli-Q water to sample. Each filtration run lasted for 10 hours, and by the end, the permeate (approximately 80-150 mL) was collected for analysis.

The sludge water separated directly from the lab-scale MBR was also filtered using a constant flux filtration unit equipped with a pen membrane module (0.0049 m^2) made by X-Flow (the Netherlands). The membrane module used the same PVDF membrane tubes as the one used in lab and full-scale MBRs. The filtration was performed at the same constant flux as the lab-scale MBR, i.e., 31.8 L/(m^2·h). The membrane was backwashed automatically for 45 sec every 450 sec filtration. The backwashing flux was the same as the filtration flux. A pressure sensor collected the TMP every second, with data saved in a MS-Excel sheet by a Visual Basic program (Microsoft, USA). This operational scheme created the same net flux as the lab-scale MBR, i.e., 26.0 L/(m^2·h).

Each constant flux batch filtration started with Milli-Q water to estimate the clean membrane resistance. When a constant pressure was reached, the feed was switched from Milli-Q water to sludge water. Each filtration run lasted for 2 hours (approximately 250 mL), and the permeate and backwash water were collected for analysis (see section 3.2.4). After 2 hrs filtration, the feed was again switched from

sludge water to Milli-Q water and until TMP was stabilized. The TMP difference between the sludge water feed and Milli-Q water feed can be used to evaluate the fouling reversible by rinsing. Afterwards, a prolonged backwashing (20 minutes) was applied at 31.8 L/(m^2·h), and finally a Milli-Q water filtration was again performed. The difference of TMP before and after the prolonged backwashing provided an indication of the fouling reversibility.

3.5 Data quality assurance

3.5.1 Millex filter

Some membrane filters can release COD, since many MF and UF filters are made of organic polymers. The Millex 0.45μm PVDF 33mm filter (Millipore, USA) was used throughout the study, due to its low protein bounding properties. They were tested prior to use with the following objectives: 1) to estimate the amount of Milli-Q water needed to wash away the residual COD; 2) to evaluate the potential COD adsorption on the filter.

Procedure for objective 1 (filer rinsing)

- Measure the COD of Milli-Q water.
- Wash the filter with 20 mL Milli-Q water; measure the COD of the next 5 mL of filtrate.
- Wash the same filter with 75 mL Milli-Q water; measure the COD of the next 5 mL of filtrate.

Procedure for objective 2.1 (protein adsorption)

- Prepare the standard protein solution (20 mg/L BSA (bovine serum albumin)), measure the absorbance of the feed standard protein solution.
- Wash the filter with 20 mL Milli-Q water, followed by the second wash using 5 mL of protein solution.
- Measure the absorbance of the next 5 mL of filtrate.
- Filter 20 mL of protein, measure the absorbance of the next 5 mL of filtrate.

The procedure for objective 2.2 (glucose absorbance) was similar to the protein adsorption test, except that 40 mg/L glucose was used instead of 20 mg/L of BSA.

The results are summarized in Table 3-6,
Table 3-7 and Table 3-8. The COD of Milli-Q water was below the detection limit of Dr. Larnge kits (5 mg/L). The filter rinsing tests showed that pre-rinsing with 20 mL of Milli-Q water was sufficient to remove the residual COD in the filter. Pre-rinsing with 20 mL of Milli-Q water was standardised throughout the entire study. The adsorption test of polysaccharide and protein showed that the filter did not absorb protein nor glucose. It is safe to use this type of filter to separate remove residual suspended solids from the sludge water.

Table 3-6 Millex filter leaking of COD (feed with Milli-Q water)

	COD (mg/L)		
	Replicate 1	Replicate 2	Average
Milli-Q water	2.11	1.60	1.86
Filtrate after 20 mL of Milli-Q washing	1.96	2.39	2.18
Filtrate after 100 mL of Milli-Q washing	3.18	3.30	3.24

Table 3-7 Millex filter adsorption of proteins (feed with BSA)

Absorbance of Protein (20 mg/L)	Absorbance			
	Replicate 1	Replicate 2	Average	Subtracted with blank
Blank	0.034	0.040	0.037	
Feed protein solution	0.171	0.179	0.175	0.138
After 5 mL of protein through filter 1	0.179	0.188	0.184	0.147
After 5 mL of protein through filter 2	0.178	0.185	0.182	0.145
After 20 mL of protein through filter 1	0.183	0.187	0.185	0.148
After 20 mL of protein through filter 2	0.175	0.183	0.179	0.142

Table 3-8 Millex filter adsorption of polysaccharides (feed with glucose)

Absorbance of glucose (40 mg/L)	Absorbance			
	Replicate 1	Replicate 2	Average	Subtracted with blank
Blank	0.037	0.039	0.038	
Feed protein solution	0.799	0.792	0.796	0.758
After 5 mL of glucose through filter 1	0.816	0.72	0.768	0.730
After 5 mL of glucose through filter 2	0.727	0.784	0.756	0.718
After 20 mL of glucose through filter 1	0.734	0.723	0.729	0.691
After 20 mL of glucose through filter 2	0.771	n.a.	0.771	0.733

3.5.2 Sample storage

The SMP was measured as COD, polysaccharides and proteins. A sample storage test was performed to check whether the sample composition changes during storage. A SMP sample was stored for 1, 2, 4 and 16 days in the fridge at 4 °C. The COD, polysaccharide and protein concentrations were measured and the results are summarized in Table 3-9.

Table 3-9 Change of SMP composition during sample storage

Storage days	COD (mg/L)	Polysaccharide (mg/L)	Protein (mg/L)
day 1	123	34.4	7.42
day 2	n.a.	32.7	5.20
day 4	126	35.6	11.4
day 16	125	35.7	9.92

n.a. = not available

The COD and polysaccharide concentration hardly changed within 16 days. However, the protein concentration showed some variation, but without general trend probably due to measurement errors. In conclusion, SMP sample storage for maximum 4 days at 4 °C did not induce significant changes in composition.

4.

Comparison of modelling approach between MBR and conventional activated sludge (CAS) processes

4.1 Introduction

The membrane bioreactor (MBR) technology is a new development of the conventional activated sludge (CAS) process. The introduction of membrane filtration to replace secondary clarifiers overcomes several limitations in the CAS process, e.g., many settling problems from filamentous bulking to foaming, rising sludge and pinpoint sludge (Casey et al., 1995; Jenkins et al., 2004), a low MLSS (mixed liquor suspended solid) concentration in the bioreactor and a large footprint, etc.

The use of a membrane and a higher MLSS concentration in MBRs also creates other differences with the CAS process. First, the MBR has a lower oxygen transfer efficiency due to the higher MLSS concentration (Günder, 2001; Krampe and Krauth, 2003). In aeration systems, a correction factor (α) is defined as the ratio of the $K_L a$ obtained in the activated sludge mixed liquor and the one obtained in clean water. The α factor decreases as a function of the MLSS concentration, e.g., Krampe and Krauth (2003) employed a power law, $\alpha = \exp(-0.08788\ X_{TSS})$, to estimate the α factor of MBR sludge over a MLSS range of 1-28 g/L. Second, the sludge concentration in the front of the MBR bioreactor (often an anaerobic zone) is often much lower than that at the rear of the bioreactor (often the aerobic zone), where a membrane module is submerged (submerged configuration) or connected (side-stream configuration). However, the CAS system often has a concentrated sludge flow returning from the secondary clarifier to the front of the bioreactor. As a result, the sludge mass in MBRs is no longer proportional to the bioreactor volume as in a CAS system. The consequent advantage is that the sludge mass distribution can be manipulated flexibly by adjusting the internal recirculation flow rate (Ramphao et al., 2005).

It is hypothesized that the complete sludge retention in a MBR changes the selection pressure on the biomass population from the sludge settling properties (in CAS) to growth kinetics (in MBR). Biomass with a high substrate affinity and low growth rate may obtain a competitive advantage over those with a low substrate affinity and high growth rate. However, this hypothesis still needs more experimental confirmation. Unfortunately, studies on direct comparison of MBR and CAS under the same feed wastewater and operational conditions are rare. Gao et al. (2004) have reported that a submerged MBR develops significantly more nitrifiers than a reference CAS system, and its nitrification performance was more effective and stable. Conversely, Manser et al. (2005b) have reported that the community composition of ammonia-oxidizing bacteria and nitrite-oxidizing bacteria exhibits only a minor difference as indicated by FISH (fluorescent in situ hybridization) results. Both systems exhibited the same maximum nitrification rates.

Some kinetic parameters of MBR sludge have been compared with those of CAS systems. Manser et al. (2005a) have studied the substrate and oxygen affinity of nitrifiers. With respect to ammonia-oxidizing (AOB) and nitrite-oxidizing (NOB) biomass, the half-saturation coefficients for the substrate do not differ significantly between MBR and CAS processes (K_{NH4} = 0.13±0.05 versus 0.15±0.10 mg N/L and K_{NO2} = 0.17±0.06 versus 0.29±0.20 mg N/L for the MBR and CAS, respectively). However, the half-saturation coefficients for oxygen exhibit a major difference. The experiments yield $K_{O,AOB}$ = 0.18±0.04 versus 0.79±0.08 mg O_2/l and $K_{O,NOB}$ = 0.13±0.06 versus 0.47±0.04 mg O_2/l for the MBR and CAS, respectively. The lower K_O values obtained in the MBR are attributed to the smaller size of activated sludge flocs (35 μm vs. 307 μm) developed under conditions of the absence of settling pressure and increased shear rate. Hence, the floc size characteristic implies a lower substrate diffusion limitation for MBR sludge. Jiang et al. (2005) have reported that decay rates of both heterotrophic and autotrophic biomass in a completely aerated MBR at T=23°C (b_H=0.25 1/d and b_A=0.080 1/d, at 23°C) do not differ significantly from the default ASM1 parameters (b_H=0.40 1/d and b_A=0.12 1/d, at 20°C in ASM1, Henze et al., 2000) recommended for a CAS system.

MBRs operate under conditions of high SRT/HRT ratio. Colloidal and macromolecular organic compound in MBRs can be partially retained by the membrane and build up to a high concentration (Huang et al., 2000; Shin and Kang, 2003). The impact of these organics on the kinetics of MBR sludge remains unknown. Backwashing and relaxation are often applied in MBRs for membrane fouling control. These cleaning methods change the hydraulic conditions in MBRs, e.g., introducing a mixing of MBR permeate with the sludge during the backwashing. The impact of neglecting these cleaning methods, which is often done in simple MBR models, on model accuracy is often overlooked. The objectives of this study are: 1) to calibrate an ASM2d model to describe the biological performance of a lab-scale MBR and compare the MBR model parameters with the default ASM2d parameters suggested for CAS systems; and 2) to identify the difference in modelling MBR and CAS systems subject to the same influent and similar operating conditions.

In this chapter, first, the equipment and methods used in the lab-scale MBR and model calibration are presented. Second, the steady state performance of the MBR is presented. Third, a phosphorus and nitrogen mass balance is conducted as a check of the data quality. Fourth, the influent wastewater characterisation, as ASM2d fractions, is presented. The results are used as model input. Fifth, a measurement campaign with monitoring of in-cycle behaviour of the MBR is presented. The results are used in the model parameter estimation. Finally, a discussion of the differences in ASM modelling approach between MBR and CAS process is summarized. The calibrated ASM2d model is the backbone of the biological model and it will be further extended with SMP-related processes in Chapter 6 addressing the ability to predict the SMP concentration in the MBR system.

4.2 Materials and methods

A side-stream lab-scale MBR system was setup for biological COD, nitrogen and phosphorus removal. A municipal-like synthetic influent was adapted from Boeije et al. (1999) with modifications. To challenge the MBR capability in nutrient removal, the nutrient : COD ratio was set at a ratio higher than real municipal wastewater (COD : N : P = 100 : 13.7 : 2.76). The lab MBR had an influent flow rate of 108 L/day and was operated under constant flux filtration conditions (31.8 L/(m^2·h)). The

HRT, total SRT and aerobic SRT were controlled at 6.4 hrs, 17 days and 7.2 days, respectively. A tubular UF module with a total membrane surface area of 0.17 m^2 (X-Flow, the Netherlands) was used. The PVDF membrane had a nominal pore size of 0.03 μm or 200 kDa, as specified by the manufacturer. A detailed description of the MBR system and operation is presented in section 3.1.

Separation of sludge water (soluble and colloidal component) from the whole activated sludge was performed by centrifugation followed by membrane filtration. First, the sludge was centrifuged (Sorvall RC-5B, Du Pont Instruments) at 2000 rpm (534 G) for 5 minutes to remove suspended solids. Afterwards, the collected supernatant was filtered using a Millex 0.45μm PVDF filter (Millipore, USA). The permeate is defined as the sludge water.

The COD, NH_4^+-N, NO_3^--N, NO_2^--N and TN concentrations were measured using colorimetric methods (Dr. Lange, Germany). Proteins were measured using the Lowry method (Lowry et al., 1951; Raunkjaer et al., 1994) and polysaccharides were measured using the phenol method (Dubois et al., 1956) with corrections for nitrate absorbance. The BOD was measured using an Oxitop (WTW, Germany) at 20 °C. The EPS (extracellular polymeric substances) were extracted using the cation exchange method adapted from Frølund et al. (1995). The extraction was performed at 600 rpm for 2 hrs and the extracted EPS was filtered using a Millex 0.45μm PVDF filter. The VFA (volatile fatty acids) were analyzed with a capillary FID (flame ionization detector) gas chromatograph (GC, 8000 Carlo Erba Instruments, Wigan, UK). The VFA are defined here as the sum of VFA with 6 or less carbons. The LC-OCD analysis was performed by a commercial lab (DOC-LABOR Dr. Huber, Germany, Huber and Frimmel, 1991; Huber and Frimmel, 1992).

A temperature (15 °C) and pH controlled (7.5±0.1) respirometer (2 L) was used to determine the OUR (oxygen uptake rate) of the activated sludge. The respirometer was equipped with a dissolved oxygen sensor (Mettler Toledo, Inpro 6400) and a pH sensor (Mettler Toledo HA 405-DXK-S8/225). The reactor pH was controlled at the setpoint by automated acid (HCl) or base (NaOH) addition. The DO was controlled between 3-4 mg/L by on/off aeration using a solenoid valve and OUR was estimated

from the linear part of the DO decline profile using linear regression when the aeration was switched off. A computer code was programmed using LabVIEW (National Instruments, USA) for the automated data acquisition and process control of the respirometer.

Decay rate of the autotrophic biomass (b_{aut}) was determined from batch respirometric experiments (Spanjers and Vanrolleghem, 1995). The sludge was daily spiked with ammonium chloride ($S_0/X_0 = 0.0005$). Biomass activities (alive biomass) were assumed proportional to the exogenous OUR. However, the spiked substrate produced new biomass and corresponding OUR, that were estimated and subtracted from the gross exogenous OUR. A non-linear curve fitting (exponential decrease in the correct exogenous OUR) was performed to estimate the decay rate. The detailed experimental procedures are as follows.

During the 6-day experiment, alternating aeration (49.4 min aerobic with DO setpoint of 2 mg/L and 70.6 min anoxic) was used to keep the batch experiments having the same aerated and non-aerated mass ratio as that of the lab-scale MBR. Before start up of the batch experiments, Potassium dihydrogen phosphate (end concentration 5 mg P/L) was added to prevent phosphorus deficiency. Every day, before the spiking with ammonium chloride (end concentration 5 mg N/L), the sludge was aerated for one hour (DO = 3-4 mg/L) to ensure that all readily biodegradable substrate, produced during the anoxic phase, was consumed.

The impact of SMP concentration on nitrification was evaluated by two comparative batch tests. 4 L MBR sludge was collected from the reactor and equally divided into two parts. The first part of the sludge (SCOD = 86 mg COD/L) was directly used for a respirometer test. The second part of the sludge was washed using a centrifuge (Sorvall RC-5B, Du Pont Instrument, 2000 rpm (534 G) for 5 minutes) to replace the sludge supernatant with MBR effluent. The washed sludge had only a SCOD = 24 mg COD/L indicating a much lower concentration of SMP. Both raw and washed sludge were spiked using ammonium chloride (10 mg NH_4^+-N/L), and the corresponding endogenous and exogenous OUR were estimated.

To calibrate the ASM2d model, a measurement campaign was carried out to capture the in-cycle dynamics, e.g., phosphate release & uptake and nitrification & denitrification, in the reactor due to the alternating aeration and periodical recirculation. Samples were taken from the anaerobic, aerobic/anoxic compartment, membrane loop and effluent every 5-17 minutes during a 40 minutes cycle. The sludge samples were centrifuged and filtered immediately to obtain the sludge water for further analysis.

The software WEST (MOSTforWATER NV, Kortrijk, Belgium) was used to perform the model simulations and parameter estimations.

4.3 Results and discussion

4.3.1 Steady state mass balance

To check the experimental data quality under steady state conditions, mass balances of phosphorus and nitrogen were verified using the method of Ekama et al. (1986). The sludge age is considered as the most important operational variable in activated sludge modelling, and a closed phosphorus mass balance should be achieved if the sludge age and experiment data are correct (Nowak et al., 1999; Meijer et al., 2002). The nitrogen mass balance is more difficult to verify due to the fact that nitrogen gas production during denitrification is a nitrogen sink that is difficult to measure. In this lab-scale MBR, the amount of denitrified nitrate and nitrite was estimated from the nitrate and nitrite mass balance over the anaerobic compartment and the anoxic phase of the aerobic/anoxic compartment using measurement campaign results (see section 4.3.5). The mass balance of total phosphorus and nitrogen showed that only 0.42% phosphorus and 2.05% nitrogen were lost (Table 4-1), which is an indication of good data quality and correct control of sludge age.

Table 4-1 steady state mass balance of phosphorus and nitrogen

Phosphorus mass balance		Nitrogen mass balance	
TP in the influent (mg P/day)	1351	TN in the influent (mg N/day)	6774
TP in the effluent (mg P/day)	618	TN in the effluent (mg N/day)	1083
TP in the waste sludge (mg P/day)	727	TN in the waste sludge (mg N/day)	1286
		Nitrate denitrified (mg N/day)	4265
loss of TP	0.42%	loss of TN	2.05%

4.3.2 Steady state performance

The sludge and effluent characteristics of the MBR under steady state conditions (4-month average and standard deviation) are summarized in Table 4-2.

Table 4-2 Comparison of experimental and model simulation results under steady state conditions

Sample (sampling location)	Variable (unit)	Values			
		4-month average	Standard deviation	Simul_1	Simul_2
Waste sludge (from aerobic/anoxic compartment)	MLSS (g/L)	8.86	1.13	-	
	MLVSS (g/L)	7.47	0.72	-	
	MLVSS/MLSS	0.84	-	-	
	COD (g/L)	10.90	0.65	10.83	10.94
	COD/MLVSS	1.46	-	-	
EPS (extracted from waste sludge)	Polysaccharides (mg/L)	87.0	6.4	-	
	Proteins (mg/L)	152	22	-	
	COD (mg/L)	532	81	-	
	PS+PT (COD eq.) / COD	0.55	0.41	-	
Sludge water (separated waste sludge using 0.45μm filter)	Polysaccharides (mg/L)	32.8	6.8	-	
	Proteins (mg/L)	13.8	4.1	-	
	COD (mg/L)	87.4	22.7	4.5	4.1
	BOD_5 (mg/L)	1.7	-	-	
	BOD_{17} (mg/L)	4.6	-	-	
Effluent (from permeate)	COD (mg/L)	11.0 (97.6%)	3.1	5.0	4.4
	TN (mg/L)	10.2 (83.7%)	2.8	8.8	8.0
	NH_4^+-N (mg/L)	0.18	0.42	0.18	0.20
	NO_3^--N (mg/L)	7.0	1.7	8.6	7.8
	NO_2^--N (mg/L)	0.30	0.21	-	
	Norg. (mg/L)	2.6	1.4	0.0	0.0
	PO_4^{3-}-P (mg/L)	5.6 (49.3%)	2.2	5.3	5.6
	TP (mg/L)	5.8	2.2	5.4	5.7

1, The values in parenthesis are removal percentage

2, PS+PT(COD eq.) = COD equivalent of polysaccharides and proteins by assuming 1 g PS = 1.5 g COD (starch) and 1g PT = 1.07 g COD (bovine serum albumin)

3, Norg. = TN − NH_4^+-N − NO_2^--N − NO_3^-N

4, Simul_1 = Simulation using ASM2d without considering the membrane hydraulic cleaning (backwashing and relaxation)

5, Simul_2 = Simulation using ASM2d including the membrane hydraulic cleaning (backwashing and relaxation)

An excellent COD removal was achieved (97.6%), which is attributed to the biodegradation and physical retention by the membrane. The SCOD at the feed side of the membrane was approximately 1.25 times that in the reactor, i.e., 107.4 mg/L. Thus, the membrane retained 89.7% of the SCOD. This suggests that a large portion of the SCOD retained by the membrane was not truly soluble, but colloidal with MW (molecular weight) corresponding to a size larger than the membrane pore sizes (0.03 µm or 200 kDa). The retained SCOD is primary composed of SMP (soluble microbial products), since most SCOD compounds originating from the influent is readily biodegradable and the SMP are of microbial origin (Grady et al., 1972; Daigger and Grady, 1977). The BOD value of the sludge water was very low (1.7 and 4.6 mg/L for 5 and 17 days, respectively), resulting in a very low BOD_5/COD ratio (0.019 only), suggesting that the SMP is refractory. Given the high retention percentage, and low biodegradability, the "SMP retention time" in the MBR is likely to be much longer than the HRT (hydraulic retention time). As a result, a build up of a high concentration of SMP has been commonly observed in many MBRs.

The removal of total nitrogen and phosphorus was 83.7% and 49.3%, respectively. It is well known that the denitrification by heterotrophic biomass and phosphorus uptake by PAO (phosphorus accumulation organisms) compete for volatile fatty acids (VFA), more specifically, acetate. The good biological nitrogen removal but unsatisfactory EBPR (enhanced biological phosphorus removal) in the MBR suggests that the heterotrophic biomass obtained an advantage over PAO for VFA uptake. This can be explained as follows. First, anoxic and aerobic conditions were achieved in one compartment by alternating aeration. The return sludge from the membrane loop ($4 \cdot Q_{in}$) to the aerobic/anoxic compartment contained 6 mg/L of DO. If one assumes that 1 mg oxygen allows removal of 2 mg COD of VFA, approximately 27.6 mg COD/L of equivalent VFA is lost due to this oxygen input during the anoxic phase (total anoxic time was 23 minutes for every 40-minute cycle), which resulted in incomplete denitrification as observed in the measurement campaign (section 4.3.5). Second, as a consequence, the recirculation flow from the anoxic to the anaerobic compartment returned a high amount of nitrate (0.7-2 mg NO_3-N/L, $8 \cdot Q_{in}$ for 12 minutes during every 40-minute cycle) to the anaerobic compartment. If one assumes that 1 mg NO_3-N consumes 5.7 mg COD equivalent of acetate, denitrification in the

anaerobic compartment can consume approximately 10-27 mg COD/L of VFA, leaving insufficient VFA for phosphorus removal. The poor EBPR performance was confirmed by 1) the VFA measurement in the anaerobic compartment (only 3.3 mg COD/L); and 2) a batch phosphorus release test with excess acetate supply showed a much higher phosphorus release rate than that observed in the MBR.

However, it should be noted that the COD : nutrient ratio of this MBR influent is lower than that of real municipal wastewater, for which a better nutrient removal can be expected. Separating the aerobic/anoxic compartment to independent aerobic and anoxic compartments (e.g., a UCT configuration) may improve EBPR as well. It appears that separating aerobic and anoxic compartments is essential for MBRs, while it is less significant for CAS processes. Typical MBRs have a higher DO mass flow returning from the membrane tanks (submerged MBRs) or from the membrane loops (side-stream MBRs with air-lift concept). This high DO mass flow is therefore more suitable to be returned to the separated aerobic zone. However, in CAS systems, the return sludge from the underflow of a secondary clarifier typically has a much lower or even zero DO concentration.

4.3.3 Influent wastewater characterization

The influent wastewater was characterised in terms of ASM2d components and used as model input (**Table 4-3**). The VFA (S_A) were measured directly. The estimation of inter soluble COD (S_I) will be discussed in section 4.3.4. The fermentable soluble COD was estimated as $S_F = SCOD - S_A - S_I$. The inert particulate COD (X_I) used the value obtained previously for the same synthetic wastewater (Insel et al., 2006). The main nitrogen source of the synthetic wastewater was urea (organic nitrogen). However, as the soluble organic nitrogen is not defined in ASM2d, the urea organic nitrogen was included in the ammonium fraction (the ammonification process is assumed not to be a rate-limiting step). The nitrate and oxygen present in the influent wastewater were determined directly from measurements.

Table 4-3 Summary of influent characterisation as ASM2d fractions

COD fraction		Nitrogen fraction		Phosphorus fraction	
S_I (mg/L)	4	S_{NH} (mg/L)	46.1	S_{PO4} (mg/L)	11.1
S_A (mg/L)	41.2	S_{NO3} (mg/L)	2.94	$i_{P,SI}$	0
S_F (mg/L)	113	$i_{N,SI}$	0.01	$i_{P,SF}$	0
X_I (mg/L)	18	$i_{N,SF}$	0.03	$i_{P,XI}$	0.01
X_S (mg/L)	281	$i_{N,XI}$	0.02	$i_{P,XS}$	0.005
X_{TSS} (mg/L)	219	$i_{N,XS}$	0.035		
S_O (mg/L)	6.5				

4.3.4 Estimation of inter soluble COD (S_I)

The characterisation of soluble inert COD (S_I) in the MBR exhibited differences with the CAS process. The influent S_I is often estimated as 90% of the effluent SCOD in a CAS process (Henze, 1992; Roeleveld and van Loosdrecht, 2002). However, the soluble effluent organic matter (EfOM) present in a CAS system is mostly composed of SMP, and not S_I originating from the influent (Grady et al., 1972; Daigger and Grady, 1977). The true S_I present in municipal wastewater is mostly composed of natural organic matter (NOM), whose main composition is humic substances, that are typically refractory in biological treatment processes (Klavins et al., 1999). Estimating S_I as 90% of EfOM does not reflect the true amount of S_I in the influent, but rather helps to close the COD mass balance. This is because the ASM model does not include a description of SMP production (Henze et al., 2000).

It is hypothesized that the S_I present in the influent are primary humic substances due to their refractory characteristics and low MW. Humic substances have MW in the rang of a few hundred to a few thousand Da (Croue et al., 2000), which can pass the MF or UF membrane easily (Lesjean et al., 2005; Rosenberger et al., 2006) compared with the pore size of MBR membranes (0.03-0.4 μm). It is also hypothesized that the biological wastewater treatment process may not produce humic substances under common range of SRT conditions.

The S_I present in the influent was estimated using a direct method by measuring the influent and confirmed by an indirect method by measuring the effluent. The DOC (mostly humic substances) of tap water used in making the synthetic influent was measured as 1.6±0.4 mg DOC/L. A LC-OCD (liquid chromatography - organic

carbon detection) analysis of the MBR effluent provides an indirect estimation of S_I. LC-OCD is able to quantify the humic substances concentration and exclude biopolymers and LMW acids. The humic substances concentration measured in MBR effluent (1.46, 1.61 and 1.71 mg DOC/L in 3 grab samples) were consistent with that in the MBR influent, suggesting that the S_I present in the influent were primary humic substances and no humic substances were produced in the biological wastewater treatment. If one assumes the DOC/COD ratio of humic substances to be 0.4, the approximate S_I present in the MBR influent is estimated to be 4 mg COD/L.

4.3.5 Measurement campaign

The measurement campaign results of the dynamic in-cycle behaviour of the MBR system are summarized in **Table 4-4** and **Figure 4-3**. The effluent ammonium concentration was always below 0.2 mg N/L and the nitrite concentration in all 3 compartments and effluent was below 0.2 mg N/L, suggesting complete nitrification. It appears sufficient to describe both nitrification and denitrification as one step as in ASM2d without introducing nitrite as an intermediate.

The SCOD concentration in the bioreactor was quite high (62.8-106 mg/L) and increased from the anaerobic to the aerobic/anoxic compartment and to the membrane loop. The build up of a high concentration of SCOD suggests that first, a large portion of SCOD is actually refractory (see also the low BOD values in Table 4-2); second, the biodegradability of the MBR sludge water cannot be evaluated by its size (e.g., using 0.45 or 0.1 µm) as it has been suggested in some influent wastewater characterisation protocols for CAS processes (e.g., Roeleveld and van Loosdrecht, 2002).

The refractory characteristics of SMP can also be verified by a SCOD mass balance over the three bioreactors. The time weighted recirculation flows from the aerobic/anoxic compartment to the membrane loop to and from the aerobic/anoxic to the anaerobic compartment were 5 and 2.4 times the influent flow rate, respectively. Assuming that the SCOD is refractory (no reaction term), the $SCOD_{anaerobic}$ can be estimated using the transport term from $SCOD_{in}$ and $SCOD_{aerobic/anoxic}$ to be 114.3 mg/L. The difference with the measurement (69.2 − 114.3 = − 45.1 mg COD/L) can be attributed to the reaction term (net consumption of SCOD due to the uptake of

readily biodegradable SCOD present in the influent and produced by hydrolysis). In a similar way, the $SCOD_{mem}$ can be estimated using the transport term from $SCOD_{aerobic/anoxic}$ and $SCOD_{eff}$ to be 102.8 mg/L. The difference with the measurement $(104 - 102.8 = 1.8$ mg COD/L) is so small that the COD mass balance can be considered as closed. Thus, the conversion term, that is the biodegradation of SCOD in the membrane loop, should be negligible. In summary, the SCOD present in the membrane loop (aerobic compartment) is refractory (mostly probably SMP), whereas the SCOD present in the anaerobic compartment is the mixture of refractory SCOD (SMP) and readily biodegradable SCOD.

Table 4-4 Summary of measurement campaign results during one aerobic/anoxic cycle (in mg/L)

Phase	Time (min)	SCOD	PT	PS	VFA*	NH_4^+-N	NO_2^--N	NO_3^--N	TN	PO_4^{3-}-P
					Anaerobic compartment					
Aerobic	0	73.5	11.4	23.2	4.2	8.7	0.053	0.13	12.9	12.7
	9	75.9	10.7	21.8	3.7	10.2	0.043		14.1	15.3
	17	66.3	10.8	20.6	1.9	11.9	0.056	0.15	15.8	18.3
Anoxic	22	65.6	9.9	21.4		14.1	0.043		17.2	20.8
mixing	28	62.8	10.8	19.0	3.2	15.7	0.044	0.13	18.7	22.7
Anoxic	34	70.9	10.5	21.8	3.3	11.9	0.061		15.6	19.0
recirculation	40	69.1	9.6	23.3	-1.1	10.8	0.045	0.18	15.0	14.2
Average		**69.2**	**10.7**	**21.3**	**3.3**	**12.1**	**0.050**	**0.14**	**15.7**	**18.1**
					Aerobic/anoxic compartment					
Aerobic	0	81.7	10.5	27.4	0.95	3.2	0.242	1.7	9.4	8.2
	9					1.3	0.325	3.5	10.9	7.9
	17	85.6	10.8	29.5		0.2	0.137	5.2	11.5	7.5
Anoxic	22					0.2	0.137	4.7	9.9	7.4
mixing	28	85.8	10.5	29.7		0.4	0.049	3.7	9.7	7.3
Anoxic	34					2.6	0.157	2.0	9.7	9.4
recirculation	40	81.6	10.2	26.8		4.4	0.125	0.7	10.9	10.7
Average		**84.4**	**10.6**	**28.9**		**1.3**	**0.175**	**3.5**	**10.2**	**7.9**
					Membrane loop					
Aerobic	0	102	11.2	35.4		0.16	0.027	4.2	11.3	5.4
	17	104	10.8	37.1		0.16	0.021	5.0	11.8	5.4
Anoxic mixing	28	106	11.8	38.5		0.15	0.036	4.7	12.1	5.0
Anoxic recirculation	40	104	11.4	35.6		0.17	0.035	4.4	12.2	6.4
Average		**104**	**11.3**	**37.0**		**0.16**	**0.028**	**4.6**	**11.7**	**5.3**
					Effluent					
Proportional (CIP tank)		13.6	6.4	4.4		0.16	0.17	5.0	7.3	5.6
Proportional (on-line)	0-40	15.0	6.6	4.1		0.14	0.12	5.2	7.2	5.9

* VFA presented as COD concentration

4.3.6 MBR hydraulic model

A description MBR configuration in mathematical models is presented in Figure 4-1. Two MBR bioreactor compartments and the membrane loop are considered as three completely mixed biological reactors. Tracer tests using sodium hydroxide were carried to test the mixing condition. It was concluded that there was not short circuiting or dead zones present in all bioreactor.
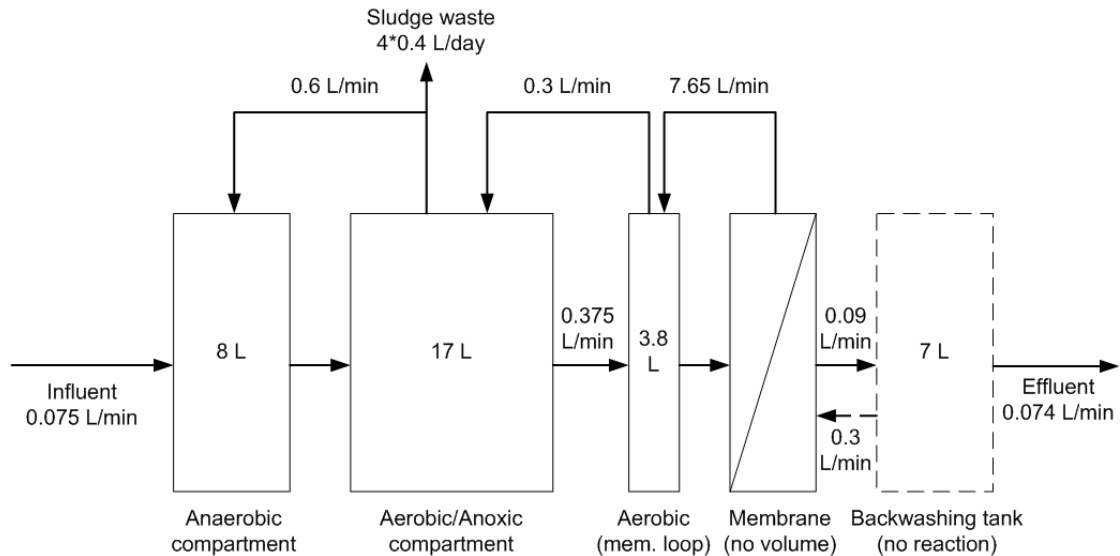
Figure 4-1 Description MBR configuration in model (dashed line is backwashing part of the complete hydraulic model)

The membrane was described as an idea biomass separator without volume and biological reaction. All particulate compounds (X) were assumed completely retained and all soluble compounds (S) could pass without retention. The particle retention of colloidal compounds (e.g., SMP) is overlooked in this chapter, but studied in Chapter 6.

In this lab-scale MBR, for every 7.5 minutes of filtration, the membrane was backwashed for 18 sec and relaxed for 7 sec. The membrane backwashing with permeate complicated the MBR hydraulic condition by introducing mixing of permeate with sludge. Backwashing and relaxation are unique features of most MBRs compared with CAS systems. Two MBR hydraulic models, including and excluding membrane cleanings, were constructed and evaluated with estimated ASM2d parameters obtained in section 4.3.7. The simulation results with the same ASM2d parameters but different hydraulic models are compared in Table 4-2.

Including hydraulic cleaning yields a slight improvement in fitting the effluent quality with respect to nitrate (7.8, 8.7 and 7.0 mg/L) and phosphate (5.6, 5.3 and 5.6 mg/L) for including hydraulic cleaning, without hydraulic cleaning and measurement, respectively. However, including hydraulic cleaning increases the complexity of the membrane model and reduces the simulation speed. In this MBR model, the decrease in simulation speed is 65% using an adaptive step size numerical integrator RK4ASC. This is due to the very short duration of the relaxation and backwashing period (7 and 18 seconds, respectively, in this MBR). Hence, in view of the objective of this study, the inclusion of the hydraulic cleanings of the MBR in the model was not deemed necessary.

4.3.7 ASM2d parameter estimation

The ASM2d model structure developed for CAS processes is used for MBR modelling. The ASM2d parameter estimation used the traditional experience and process knowledge based approach. Further, the sequential methodology proposed by Hulsbeek (2002) and extended by Insel (2006) was used to calibrate the parameters of the biomass decay rate, nitrification, denitrification, and biological phosphorus removal. The parameters calibrated from the previous steps were transferred into the next step. Finally, an overall evaluation of the obtained parameter set was performed. The decay rate of the autotrophic biomass was obtained from the dedicated batch tests. The other parameters were adjusted to fit the 4-month average data under steady state condition and the in-cycle dynamic measurements obtained from the measurement campaign.

4.3.7.1 Estimation of decay rate for autotrophic biomass

A batch experiment was performed to estimate the decay rate of autotrophic biomass (b_{aut}). The exponential decrease in the corrected exogenous OUR is presented in Figure 4-2. The obtained b_{aut} was low (only 0.0315 1/d) at 15 °C. Using the default temperature conversion factors ($\theta = 1.116$) in ASM2d, the decay rate at 20 °C was estimated to be 0.055 1/d, which is still significantly lower than the default ASM2d value (0.15 1/d).

The plot shows an exponential decay line with the equation:

$$OUR_{exo} = 0.938e^{-0.0315\,t}$$

Y-axis: Corrected exogenous OUR (mg/L/min), X-axis: Time (day)
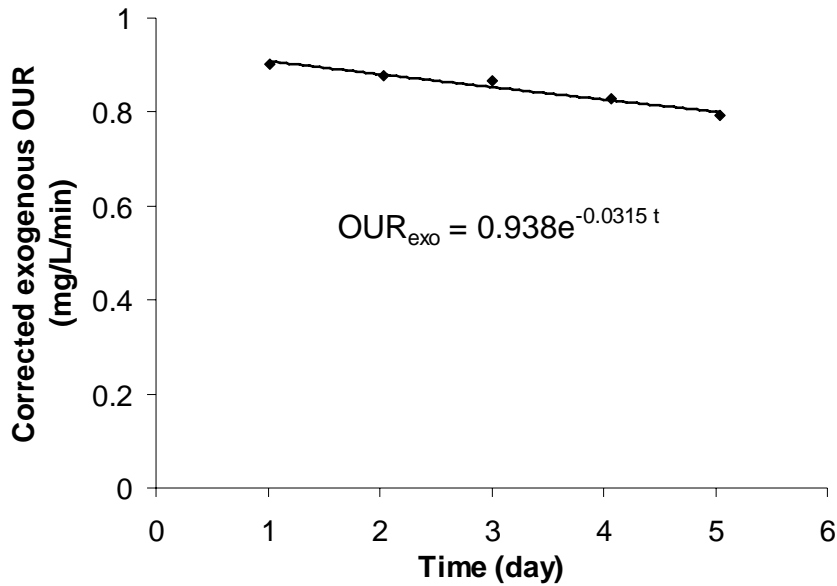
Figure 4-2 Exponential decrease in exogenous OUR in baut determination

However, it should be noted that this low decay value was obtained under alternating aeration conditions (49.4 min aerobic with DO setpoint of 2 mg/L and 70.6 min anoxic). It has been know that the decay rate under anoxic conditions can be significantly lower than that under aerobic conditions. Manser et al. (2006) has reported that the aerobic decay rates of AOB, NOB and heterotrophic bacteria for CAS and MBR processes were not significantly different, i.e., 0.15 ± 0.02, 0.15 ± 0.01 and 0.28 ± 0.05 1/d for CAS and 0.14 ± 0.01, 0.14 ± 0.01 and 0.23 ± 0.03 1/d for MBR. However, anoxic decay rates were significantly lower than the aerobic decay rates, i.e., 0.015 ± 0.004, <0.001 and 0.033 ± 0.002 1/d for CAS and 0.01 ± 0.003, 0.02 ± 0.009 and 0.064 ± 0.002 1/d for MBR. If one assumes $b_{aut,aero} = 0.15$ 1/d and $b_{aut,anoxic} = 0.015$ 1/d, the decay rate under this alternating aeration condition would be 0.071 1/d, which is close to the batch experimental results (0.055 1/d).

4.3.7.2 Estimation of decay rate for heterotrophic biomass

A simulation with the ASM2d default b_H value (0.4 1/d) resulted in a total sludge COD concentration of 10.83 g/L in the aerobic compartment, which is in excellent agreement with the measured value (10.90 g/L). Thus, the default b_H value was adopted without adjustment.

4.3.7.3 Experience and process-knowledge based model calibration

A simulation with default parameter values overestimated the ammonium concentration in the reactor and effluent. To improve the modelled nitrification, the oxygen half-saturation coefficient for autotrophic biomass ($K_{O,aut}$) was reduced from 0.5 to 0.2 mg/L. Manser et al. (2005a) has reported $K_{O,AOB} = 0.18\pm0.04$ mg O_2/L and $K_{O,NOB} = 0.13\pm0.06$ mg O_2/L in a pilot MBR and attributed the high oxygen affinity of the MBR sludge to the small floc sizes (35 μm in 50% percentile) and reduced oxygen diffusion limitation. The mean floc size in this lab-scale MBR was also small, i.e., 30-50 μm, which can be regarded as both an advantage (improved mass transfer) and a disadvantage (higher risks of membrane fouling).

However, the decrease in $K_{O,aut}$ was not sufficient to reduce the ammonium concentration to the measurement values, thus the ammonium half-saturation coefficient ($K_{NH4,aut}$) was decreased from 1 to 0.2 mg N/L, which is consistent with values of $K_{NH4} = 0.13\pm0.05$ mg N/L and $K_{NO2} = 0.17\pm0.06$ mg N/L reported for MBR sludge (Manser et al., 2005b).

As the simulation overestimated the nitrate concentration, while it underestimated the phosphorus concentration, which suggests that more VFA should be used in denitrification by ordinary heterotrophic biomass rather than for PHA formation by PAOs. The possible approaches to reallocate VFA are: 1) increase the denitrification rate, e.g., by reducing the reduction factor for denitrification ($\eta_{NO3,het}$); 2) reduce the PHA uptake by PAOs, e.g., by reducing the PHA storage rate (q_{PHA}); 3) reduce the fermentation rate to reduce S_A production in the anaerobic compartment, e.g., by decreasing the fermentation rate (q_{fe}), or by increasing the half saturation coefficient (K_{fe}); and 4) reduce the aerobic and anoxic phosphorus uptake rate, e.g., by reducing the aerobic phosphate uptake (q_{pp} and $\eta_{NO3,PAO}$). Approaches 1 and 2 are straight forward, whereas approaches 3 and 4 have indirect consequences. All approaches are evaluated below.

Using approach 1, $\eta_{NO3,het}$ was increased from 0.8 to 1. The denitrification was improved but this was not sufficient to allow a good fit. Thus, $\eta_{NO3,het} = 1$ was used in the next steps. Using approach 2, q_{PHA} was increased from 3 to 5 1/d, but this was still

not sufficient. Finally, approaches 3 and 4 were applied together by trial and error, yielding q_{fe} = 1 1/d, q_{pp} = 1.1 1/d and $\eta_{NO3,PAO}$ = 0.4.
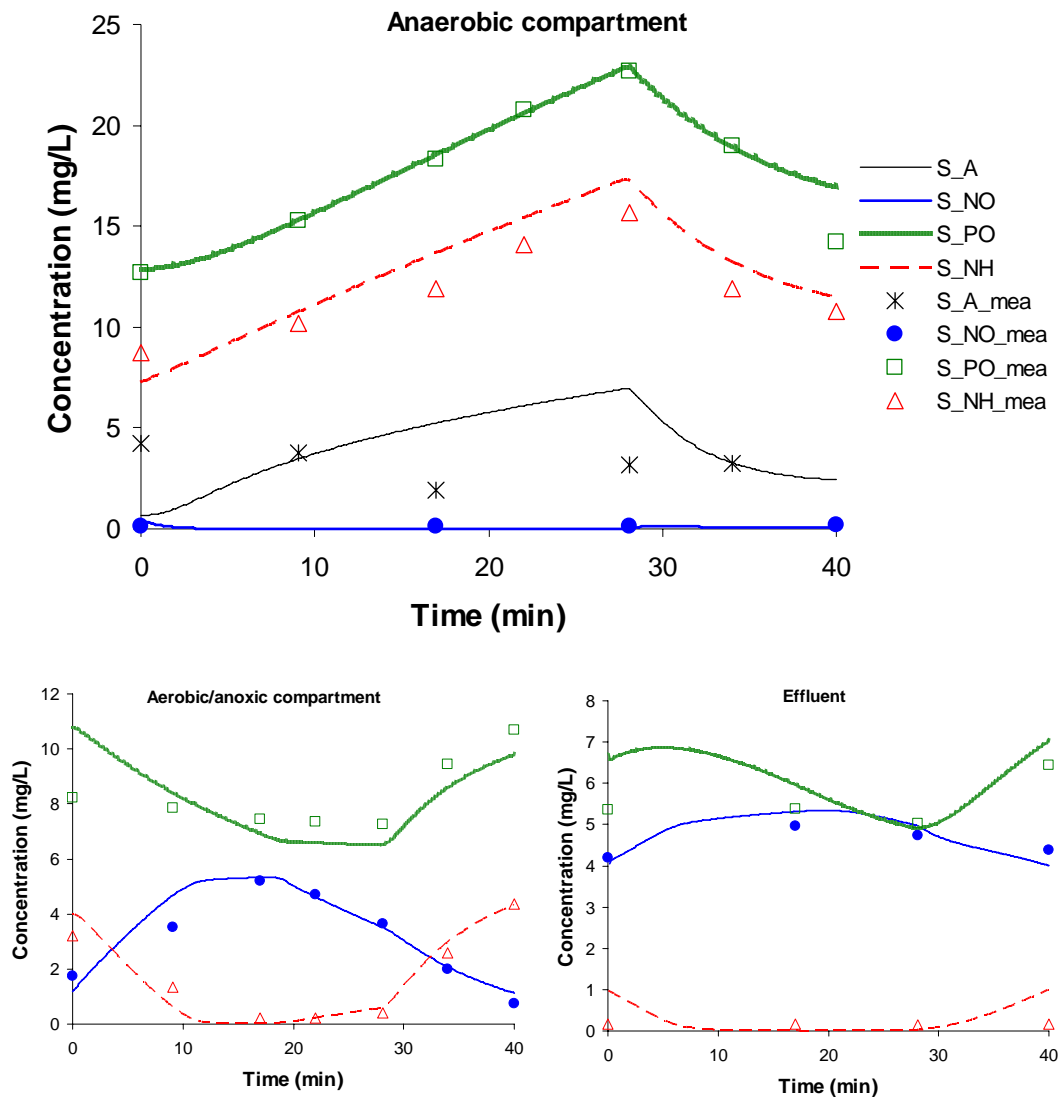
Figure 4-3 Comparison of the simulation and measurement data during one aerobic/anoxic cycle

Table 4-5 Summary of calibrated ASM2d parameters (20 °C)

Parameter name	Symbol	Unit	Default	Calibrated
Decay rate of nitrifiers	b_{aut}	1/d	0.15	0.055
Maximum growth rate of nitrifiers	μ_{aut}	1/d	1	0.6
Oxygen half-saturation coefficient of nitrifiers	$K_{O,aut}$	mg O_2/L	0.5	0.2
Ammonium half-saturation coefficient of nitrifiers	$K_{NH4,aut}$	mg N/L	1	0.2
Reduction factor of anoxic growth of heterotrophs	$\eta_{NO3,het}$	-	0.8	1
Fermentation rate of acetate production	q_{fe}	1/d	3	1
PHA storage rate	q_{PHA}	1/d	3	5
Phosphate uptake rate	q_{pp}	1/d	1.5	1.1
Reduction factor of anaerobic hydrolysis	$\eta_{NO3,PAO}$	-	0.6	0.4

An overall evaluation of the model fit to the results of the measurement campaign suggests that the nitrification rate was too high. Thus, the maximum growth rate of the nitrifiers (μ_{aut}) was reduced from 1 to 0.6 1/d. This adjustment has almost no influence on the nitrifier concentration and only leads to a little increase in the effluent ammonium concentration. After some additional slight adjustments, the model was able to fit both the 4-month average steady state measurements (Table 4-2) and the in-cycle dynamics obtained in the measurement campaign (**Figure 4-3**). The calibrated ASM2d parameters are summarized in **Table 4-5**. A slight adjustment of the initial conditions (initial state variable in WEST) was performed to fit the measurement campaign data.

4.3.7.4 Impact of SMP on autotrophic biomass

The MBR sludge exhibited a lower specific growth rate in the dynamic model calibration, which might be related to the high SMP concentration present in the MBR sludge water. Two comparative batch tests were carried out to evaluate the impact of SMP on nitrification. Washed sludge with a reduced SMP concentration (SCOD = 24 vs. 86 mg COD/L) showed a slightly lower endogenous respiration rate (0.57 ± 0.01 vs. 0.60 ± 0.01, mg O_2/(L·min)) than the raw sludge, which is normal due to the loss of unflocculated sludge during the washing process. However, the washed sludge exhibited a higher exogenous respiration rate (0.69 ± 0.07 vs. 0.62 ± 0.06, mg O_2/(L·min) with excess ammonium substrate) than the raw sludge, suggesting that nitrifiers are more active at reduced SMP concentration in the washed sludge.

The negative impact of SMP on biological removal has been reported in CAS systems. A SMP concentration of approximately 200 mg COD/L inhibits nitrification (Chudoba, 1985a). More recently, A SMP concentration of approximately 10-20 mg DOC/L inhibits both nitrification and anaerobic acetate uptake of PAO (Ichihashi et al., 2006). Due to the retention by membrane in MBRs, SMP can accumulate to a higher concentration than in CAS systems. Hence, nitrifiers and PAO may be less active in MBRs. However, the standard deviations of these two batch tests were quite high and further studies are needed to be conclusive. In addition, other factors in MBRs, e.g., high shear rate, may also impose negative impacts on nitrifers.

4.3.8 Comparison of the modelling approach between MBR and CAS processes

According to the above lab-scale MBR calibration study, the difference in the modelling approach between the MBR and CAS process can be summarized as follows.

4.3.8.1 Membrane vs. secondary clarifier model

The membrane in MBRs can be modelled as an idea settler with complete retention of particulate compounds. Hence, the modelling of biomass separation in an activated sludge process is much easier in MBRs than in CAS systems.

4.3.8.2 Impact of membrane hydraulic cleaning

Including membrane hydraulic cleaning (backwashing and relaxation) in MBR modelling has only a slight improvement in describing the hydraulic conditions with respect to prediction of effluent quality. However, the cost is that the model complexity is increased and simulation speed is significantly reduced. If the accuracy requirement of model prediction is not high, membrane hydraulic cleaning can be overlooked.

4.3.8.3 Verification of SRT

A MBR system has a well defined SRT with complete biomass retention, whereas the SRT of a CAS system is influenced by the settling properties of the activated sludge. A well defined SRT is a significant advantage for the modelling of an activated sludge process. However, the calculation of SRT in MBRs should use the total sludge mass, whereas a simplified SRT calculation method of using sludge volume, often in CAS systems, should be avoid. This is due to the fact that the sludge concentration in MBR bioreactors is often lower in the front and higher at the rear (e.g., 7.54, 10.9, and 13.5 g COD/L for anaerobic compartment, aerobic/anoxic compartment and membrane loop, respectively in this MBR). However, the sludge concentration in a CAS system is more uniformly distributed due to the fact that a concentrated sludge is often

returned from the underflow of a secondary clarifier to the front of the bioreactor, which balances the sludge concentration over the whole reactor.

4.3.8.4 Affinity constant of biomass

Half-saturation coefficients of MBR sludge may be lower, e.g., for oxygen and ammonium in the Monod terms. This may be related to the smaller flocs in MBRs, which are less diffusion limited with respect to substrate transport (Manser et al., 2005b; Sin et al., 2005). Thus, simultaneous nitrification and denitrification might be difficult to achieve in MBRs.

4.3.8.5 Impact of soluble microbial products

MBRs tend to accumulate a high concentration of SMP due to their refractory characteristics and HMW (high molecular weight) (approximately 89.7% retention in this lab-scale MBR). The impacts of SMP accumulation are discussed as follows.

First, 0.45 μm is not a suitable criterion to classify particulate COD and soluble COD due to the abundance of SMP in MBRs. The biochemical method, e.g., using a respirometer, is more appropriate to applied in MBRs rather than the physical method simply by size (Vanrolleghem et al., 1999).

Second, SMP can not be regarded as any of the 5 COD components (S_I, S_A, S_F, X_I and X_S) in the ASM2d model. SMP are less than 0.45 μm and refractory. However, they can not be regarded as inert soluble COD fraction (S_I) due to the fact that they can be partially retained by the membrane. To close the COD mass balance, a simple solution is to overlook the SMP and include them as X_I, if the aim of the study is only for biological nutrient removal. Only in the case that membrane fouling is studied, the SMP should be considered as an additional COD component as in Chapter 6.

Finally, a high SMP concentration, e.g., 86 mg COD/L present in the MBR sludge water appears to inhibit the nitrifiers. The specific growth rate of nitrifers may be reduced in MBRs compared with CAS systems. However, more studies are needed to be conclusive.

4.3.8.6 Influent wastewater characterisation

The characterisation of influent inert particulate COD (X_I) is easier in MBRs than in CAS systems, due to a higher sensitivity of the reactor MLSS concentration to the influent X_I. MBRs often operate under conditions of high SRT/HRT ratio, which accumulates all particulate solids in the bioreactor including X_I (Jiang et al., 2005b).

4.4 Conclusions

A lab-scale MBR was constructed for biological nutrient removal. Phosphorus and nitrogen mass balance was closed, indicating a good data quality and SRT control. An excellent COD removal was achieved (97.6%), which was attributed to both biodegradation and physical retention of colloidal compound by the membrane. However, the enhanced biological phosphorus removal was not satisfied due to the high nutrient contents present in the influent and the intermittent operation of the aerobic/anoxic compartment reducing the utilization efficiency of volatile fatty acids.

With respect to the MBR hydraulic model, the membrane can be modelled as an idea biomass separator without volume and biological reaction. Including the membrane cleaning (backwashing and relaxation) into the MBR hydraulic model slightly improves the accuracy in effluent quality prediction, whereas it significantly decreases simulation speed. It is not necessary to include the hydraulic model, if the requirement for model accuracy is not high.

MBR has a well defined SRT independent from the settling properties. The ASM2d model structure developed for conventional activated sludge (CAS) processes can be directly used for MBR modelling. Most default ASM2d parameters suggested for CAS processes hold for MBR as well. However, the MBR sludge exhibited a lower oxygen and ammonium half-saturation coefficients ($K_{O,aut}$=0.2 mg O_2/L and $K_{NH,aut}$=0.2 mg N/L), probably due to the smaller sludge flocs. The characterisation of influent inert particulate COD (X_I) is easier in MBRs than in CAS systems.

MBRs tend to accumulate a high concentration of soluble microbial products (SMP), that are colloidal and refractory in biological treatment processes. Readaily and slowly biodegradable COD should be not classified based on size, e.g., 0.45 μm. Instead, chemical biological methods are more stuiable. To close the COD mass balance, SMP can be overlooked and treated as X_I, if the aim of the study is for biological nutrient removal. A high SMP concentration present in the MBR sludge water appears to inhibit the nitrifiers in a certain extent. Hence, the specific growth rate of nitrifers may be reduced in MBRs compared with that in CAS systems. However, more studies are needed to be conclusive.

5.

Characterisation of soluble microbial products (SMP)

5.1 Introduction

The interest in soluble microbial products (SMP) was first raised in studies of the lowest achievable effluent organic matter (EfOM) concentration in a biological wastewater treatment process. Many experimental results showed that the original influent substrate only contributed to a small fraction of EfOM. Rather, the majority of the EfOM was composed of soluble organic matter of microbial origin, which was later defined as SMP (Grady et al., 1972; Daigger and Grady, 1977; Chudoba, 1985b).

The generation of SMP is typically divided into two categories: BAP (biomass associated products), associated with biomass decay, and UAP (utilization associated products), associated with substrate uptake and biomass growth. Strong experimental evidence for the existence of these two categories was provided by Namkung and Rittmann (1986), who used labelled tracers in an aerobic biofilm reactor and measured the two types of SMP separately. However, the term of SMP is vague and is poorly defined, although widely used. This is partially due to the difficulty in identifying SMP composition experimentally, but also due to the complexities of influent substrate composition, microbial metabolism and microbial behaviour in response to various influent and operational conditions under steady state and dynamic conditions.

Chemically, SMP is a pool of complex organic matter, e.g., proteins, polysaccharides, humic substances, nucleic acids, organic acids, amino acids and extracellular enzymes, etc. (Painter, 1973; Hejzlar and Chudoba, 1986a; Hejzlar and Chudoba, 1986b; Dignac et al., 2000). The molecular weight (MW) distribution of SMP varies widely from very low (<0.5 kDa) to very high (>100 kDa). In addition, the distribution is typically bimodal with a peak in the LMW (low molecular weight) region (<1 kDa)

and a peak in the HMW (high molecular weight) region (>10 kDa) (Namkung and Rittmann, 1986; Boero et al., 1996; Huang et al., 2000). Boero et al. (1996) used phenol and glucose (labelled with ^{14}C) as substrate to differentiate UAP and BAP. The resulting MWD showed that UAP was mostly composed of small molecules (86% and 76% <1 kDa for phenol and glucose, respectively) and BAP was mostly composed of large molecules (47% and 52% >10 kDa for phenol and glucose, respectively). Pribyl et al. (1997) reported an apparent trend of increase in high molecular fraction of SMP with increasing SRTs.

Some studies have shown that SMP are biodegradable. Gaudy and Blachly (1985) reported that over 90% of the residual soluble COD in batch or continuous flow treatability studies was subject to biological degradation. In the tests, there was an initial build up of SMP up to 1570 mg COD/L, corresponding to 5% of the influent COD in mass fraction, and a subsequent SMP degradation down to 324 mg COD/L. However, others have reported that SMP are refractory. Pribyl et al. (1997) reported a BOD_5/COD ratio of SMP in the range of 0.014-0.082 and no clear trend that HMW (high molecular weight) SMP was more resistant to biodegradation. Barker et al. (1999) studied the aerobic and anaerobic biodegradability of SMP produced in various anaerobic processes. The results showed that the HMW compounds were more readily degraded aerobically and the LMW compounds were more readily degraded anaerobically. In MBR systems, SMP, especially the HMW fraction, often accumulate during the start-up stage due to retention by the membrane. However, they were partially degraded afterwards (Huang et al., 2000; Shin and Kang, 2003; Ji and Zhou, 2006).

The term EPS refers to extracellular polymeric substances. A distinction between EPS and SMP is not clearly defined. It is generally accepted that EPS can be classified according to the phase in activated sludge, i.e., the bound EPS associated with flocs and soluble EPS present in sludge water (the soluble and colloidal fraction of activated sludge). The latter is often referred to as SMP (Laspidou and Rittmann, 2002a). Direct comparison study of MBR and CAS systems have reported the bound EPS in a MBR sludge is not different from that of a CAS (conventional activated sludge) sludge, but the MBR sludge exhibits a significantly higher SMP level and a lower critical flux than the CAS sludge (Cabassud et al., 2004; Masse et al., 2006).

This suggests that fouling in the MBR is more closely associated with the SMP rather than EPS.

Membrane fouling is a main drawback of the MBR system, which limits the rapid commercialization of MBR technology. Recent advances in MBR fouling studies have shown that MBR fouling is mostly related to the organic components in sludge water, i.e., colloidal and soluble compounds. Lesjean et al. (2005) and Rosenberger et al. (2006) used size exclusion chromatography (SEC) to analyze the sludge water phase and concluded that the large organic molecules present in the sludge water phase (i.e., polysaccharides, proteins and organic colloids) impacted MBR fouling. Rojas et al. (2005) reported no correlation between bound EPS with the filtration resistance. Instead, a change in the filtration resistance was explained as a function of COD in the supernatant, and more specifically as a function of protein concentration. Fan et al. (2006) reported that the critical flux in a pilot MBR was closely correlated with the colloidal TOC (total organic carbon) concentration in the sludge water, i.e., a high colloidal TOC concentration reduced critical flux and resulted in more rapid membrane fouling. Rosenberger et al. (2005) summarized 6 MBR case studies of different European research groups. The results showed a clear relevance of liquid phase constituents, either colloidal or soluble, with membrane fouling. Reid et al. (2006) studied the influence of salinity on membrane permeability in a MBR system and showed that the membrane permeability was inversely correlated with the SMP carbohydrate level.

The MBR fouling studies of Rosenberger et al. (Lesjean et al., 2005; Rosenberger et al., 2005; Rosenberger et al., 2006) used a new analytical method, i.e., LC-OCD (liquid chromatography - organic carbon detection) in sludge water characterisation. However, their study did not track the biological origin of SMP in MBRs and did not distinguish BAP and UAP. The MW, hydrophobicity, organic nitrogen content and biodegradability of BAP and UAP were not studied separately. Membranes used in MBRs can partially retain SMP (de Silva et al., 1998; Huang et al., 2000; Shin and Kang, 2003; Ji and Zhou, 2006). However, the interaction of BAP and UAP with membranes and the effectiveness of BW (backwashing) in SMP cleaning were unclear. The objectives of this study were 1) to produce BAP and UAP separately; 2) to study the characteristics of BAP and UAP, i.e., the composition, MW, hydrophobicity, and

biodegradability; and 3) to identify the fractions of BAP and UAP which are correlated with membrane fouling.

In this chapter, first, a lab-scale MBR is summarized shortly, from which both MBR sludge and SMP samples were taken. Second, the batch experiments to produce BAP and UAP and the batch filtration tests to filter BAP and UAP are described. Third, the methods used in separating and characterising SMP are presented. Fourth, the comparison of particle size distribution of MBR and SBR sludge is presented showing a major difference in the colloidal range. Fifth, the characterisation of SMP, BAP and UAP are presented and compared. Both feed, and permeate are analyzed and characteristics of the SMP fraction retained by the membrane (resulting in membrane fouling) is highlighted. Finally, extracted EPS is characterised in comparison with SMP. The characteristics of SMP concluded from this chapter is the background of SMP modelling in Chapter 6, 7 and 8. The experimental results of the BAP and UAP production batches are used in Chapter 6 for BAP and UAP model calibration, respectively.

5.2 Materials and methods

5.2.1 Lab-scale MBR system

A side-steam lab-scale MBR system is setup for biological COD, nitrogen and phosphorus removal. A municipal-like synthetic influent was adapted from Boeije et al. (1999) with modifications. To challenge the MBR capability in nutrient removal, the nutrient : COD ratio was set at a ratio higher than real municipal wastewater (COD : N : P = 100 : 13.7 : 2.76). The lab MBR has an influent flow rate of 108 L/day and operates under constant flux filtration conditions (31.8 L/(m^2·h)). The HRT, total SRT and aerobic SRT are controlled at 6.4 hrs, 17 days and 7.2 days, respectively. The system temperature is controlled at 15 °C using a cooling machine.

A tubular UF module with a total membrane surface area of 0.17 m^2 (X-Flow, the Netherlands) is used. The PVDF membrane has a nominal pore size of 0.03 μm and a tube diameter of 5.2 mm. The membrane is operated under the air lift mode and both sludge and air crossflow velocities are 0.5 m/s. The membrane loop (3.8 L) is also

considered as a completely mixed aerobic reactor. The membrane was backwashed for 18 sec at 106 L/(m^2·h) every 7.5 minutes of filtration. A computer code was programmed using software LabVIEW 7.1 (National Instruments, USA) for automated data acquisition and control. The details of the lab-scale MBR are presented in Chapter 3.

5.2.2 Batch experiments for BAP and UAP production

Fresh sludge was taken from the aerobic/anoxic compartment of the MBR, washed and used in BAP and UAP batches. Both BAP and UAP batches were conducted under conditions of constant temperature (15 °C) and controlled pH (7.5). The BAP batch was conducted under starvation conditions without external substrate addition. Alternating aeration was conducted to maintain the same aerobic:anoxic time ratio (49.4 minutes aerobic with DO setpoint of 2 mg/L, 70.6 minutes anoxic) as the lab-scale MBR. The SMP produced in the BAP batch was dominated by BAP since no external substrate was added. The UAP batch was spiked with acetate (end concentration 1000 mg/L) under completely aerobic conditions with a DO setpoint of 2 mg/L. A reference batch was conducted in parallel under the same conditions as the UAP batch but without acetate addition. The net UAP production is the difference between the UAP and the reference batch, which eliminates the impact of BAP. More details of sludge washing and the batch experiments are described in section 3.3.

5.2.3 Batch filtration experiments

The BAP, UAP and SMP samples were filtered using a stirred cell unit (Stirred Cell 8200, Millipore, USA) operating under constant pressure (TMP = 14.3 kPa) and unstirred (dead-end) conditions. A flat sheet 0.03 μm PVDF membrane was manufactured (X-flow, the Netherlands) with exactly the same material, structure and morphology as the tubular one used in the lab and full-scale MBRs. More details of constant flux filtration are presented in section 3.4. Each filtration run lasted for 10 hours, and at the end, the permeate was collected for analysis (see section 5.2.5).

The sludge water separated directly from the lab-scale MBR was also filtered using a constant flux filtration unit equipped with a pen membrane module (0.0049 m^2) made

by X-Flow (the Netherlands). The membrane module used the same PVDF membrane tubes as the one used in lab and full-scale MBRs. The filtration was performed at the same constant flux as the lab-scale MBR, i.e., 31.8 L/(m^2·h). The membrane was backwashed at 31.8 L/(m^2·h) automatically for 45 sec every 450 sec filtration. A pressure sensor collected the TMP every second, with data saved in a MS-Excel sheet. This operational scheme created the same net flux as the lab-scale MBR, i.e., 26.0 L/(m^2·h). Each constant flux batch filtration started with Milli-Q water to estimate the clean membrane resistance. When a constant pressure was reached, the feed was switched from Milli-Q water to sludge water. Each filtration run lasted for 2 hours, and the permeate and backwash waters were collected for analysis (see section 5.2.5). After 2 hrs filtration, the feed was again switched from sludge water to Milli-Q water until TMP was stabilized. The TMP difference between the sludge water feed and Milli-Q water feed was the contribution of concentration polarization. Afterwards, a prolonged backwashing (20 minutes) was applied at 31.8 L/(m^2·h), and finally a Milli-Q water filtration was again performed. The difference of TMP before and after the prolonged backwashing provided an indication of the fouling reversibility.

5.2.4 Separation of sludge water from sludge samples

The sludge water was separated by centrifugation and one or two-step filtration. First, the sludge was centrifuged (Sorvall RC-5B, Du Pont Instruments) at 2000 rpm (534 G) for 5 minutes to remove suspended solids. Afterwards, if the sludge sample volume is small (e.g., 20 mL), the collected supernatant was filtered directly using a Millex 0.45μm PVDF filter (Millipore, USA). If the volume is large (a few litres for filterability test), the collected supernatant was first filtered through a glass microfibre filter (GF/C, 1.2μm, Whatman, UK) and followed by the second step filtration using a flat sheet microfiltration membrane (DURAPORE 0.45 μm PVDF, Millipore, USA) on a stirred cell (Stirred Cell 8200, Millipore, USA). All filters were pre-rinsed with Milli-Q water before use to remove residual TOC (see section 3.5 for the procedures of rinsing filters). The two-step filtration avoided the build up of a thick filter cake. The final permeate is defined as the sludge water. All samples were stored at 4 °C for a maximum of 4 days before analysis.

5.2.5 Sample analysis

The collected samples (SMP, BAP and UAP) were analysed for COD (or TOC), NH_4^+-N, NO_3^--N, NO_2^--N, TN (total nitrogen), proteins, and polysaccharides. Some samples were analyzed using LC-OCD. The COD, NH_4^+-N, NO_3^--N, NO_2^--N and TN concentrations were measured using colorimetric methods. Proteins were measured using the Lowry method (Lowry et al., 1951; Raunkjaer et al., 1994) and polysaccharides were measured using the phenol method (Dubois et al., 1956) with corrections of nitrate absorbance. The BOD was measured using an Oxitop (WTW, Germany) at 20 °C. The EPS was extracted using the cation exchange method adapted from Frølund et al. (1995). The extraction was performed at 600 rpm for 2 hrs and the extracted EPS was filtered using a Millex 0.45μm PVDF filter. The average organic carbon oxidation number was calculated using the method of Stumm and Morgan (1981).

The LC-OCD analysis was performed by a commercial lab (DOC-LABOR Dr. Huber, Germany, Huber and Frimmel, 1991; Huber and Frimmel, 1992). Both fine and coarse size exclusion chromatography (SEC) columns (Alltech, Germany) were used. The SEC column was filled with Toyopearl resin (HW-50S or HW-65S with pores size of 12.5 and 100 nm respectively). The HW50S column has a good resolution in a LMW region (<20 kDa) and the HW65S column has a good resolution in a HMW region (50-2000 kDa). Therefore the combination provided a clear MW profile of SMP. Three detectors were installed in series in a sequence of UVD, OCD and OND. The UV detector (UVD, Knauer K200, Germany) measures the SAC (spectral adsorption coefficient) at 254 nm. The OCD detector oxidizes all organic matter in a thin film UV reactor, thus the organic carbon present in the sample can be quantified from the amount of produced CO_2 (OCD, DOC-LABOR, Germany). Afterwards a second capillary UV reactor was connected to ensure than all organic nitrogen (Norg.) is oxidized into nitrate. Finally a UVD (Knauer K2001, Germany) was equipped to quantify the amount of nitrate from SAC, due to the fact that nitrate is the only strongly UV-absorbing compound (measured at 220 nm) potentially present after oxidation.

The size-exclusion chromatograph separates compounds according to their molecular size. In a properly operated chromatographic column, the larger molecular compounds elute before the smaller ones. However, the interpretation of LC-OCD chromatograms should be interpreted with caution. First, inorganic colloidal compounds (e.g., polyelectrolytes, polyhydroxides and oxidhydrates of Fe, Al or Si) also absorb UV at 254 nm and unfortunately their elution time is close to that of the biopolymers. In this sample, it is slightly earlier at 28 minutes. Theoretically, polysaccharides have no UV adsorption at all, and some proteins can have a low UV adsorption, e.g., the SUVA of amino acid such as L-tryptophan or L-Tyrosine is about 1.7 L/(mg·m), but BSA (bovine serum albumin) has a very low SUVA as 0.1-0.2 L/(mg·m) (Nam, 2006). Thus, the biopolymer fraction normally exhibits low UV adsorption. Second, if a large amount of nitrate is present in the sample, the OND will not be able to differentiate the nitrate produced after oxidation of Norg. Thus, Norg. chromatograms in this region (after 55 minutes) have to be interpreted with caution.

The LC-OCD chromatograms showed very precise and reproducible results. A UAP sample was analyzed two times in consecutive days using the HW-65S column; the maximum relative error, defined as $|OC_1-OC_2|/OC_1$, in time series (every 5 sec) was only 3%, and in the region of main OC peaks, the relative error was less than 1%.

To compare the particle size distribution (PSD) of the MBR sludge with a CAS sludge, both MBR and SBR sludges were measured using MastersizerS (Malvern,UK). Both reactors treat the same synthetic influent and the operational conditions are similar. The SBR has a SRT of 15 days and a HRT of 12 hours and the anaerobic, aerobic, anoxic, settling and decanting time during one cycle (6 hours) are 60, 130, 110, 40 and 20 minutes, respectively. More details of the SBR reactor are provided in Insel et al. (2006).

5.3 Results and discussion

5.3.1 Comparison of particle size distribution of MBR and SBR sludge

The PSD of MBR and SBR sludge are compared in Figure 5-1. Both sludges exhibited the same main PSD peak in the 30-50 μm range. However, the MBR sludge

had an additional peak in the colloidal range, i.e., 0.1-1 µm. The particles in this range may be bacterial cells or cell fragments. This is consistent with other studies. Sperandio et al. (2005) and Masse et al. (2006) reported the second peak was in the 1-10 µm range and Wisniewski et al. (2000) reported the second peak between 1-2 µm. The most fundamental difference between the two reactors was the biomass separation, i.e., gravity settling vs. membrane separation. The second submicron particle peak present in the MBR sludge suggests that the small size particles can be abundant in MBRs due to the lack of selection pressure as in a CAS process, where the unsettled small-size particles are washed out through effluent. However, it should be noted that the submicron particles measured using MastersizerS may not be reliable due to the uncertainty in the optical properties (i.e., the refractive index) of particles in biological systems. Thus, a new technology, LC-OCD, has been applied to characterise the sludge water phase below.
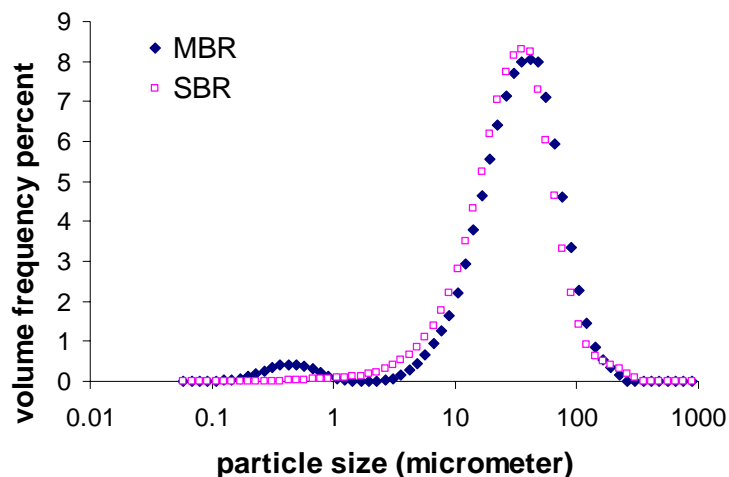
Figure 5-1 Comparison of particle size distribution of MBR and SBR sludge

5.3.2 Characterisation of SMP

The SMP obtained from the lab-scale MBR was filtered through the UF membrane using the unstirred cell. The LC-OCD chromatograms (HW50S column) of the SMP feed, SMP permeate and the effluent of the lab-scale MBR are presented in Figure 5-2. In all three chromatograms of MBR samples, a clear, large peak appeared at approximately 30 minutes, which is the biopolymer peak. The biopolymer fraction has a MW of larger than 20 kDa, the upper limit of separation, according to the calibration of the HW50S column. The biopolymer fraction contained 69.8% of the DOC within the overall sample.
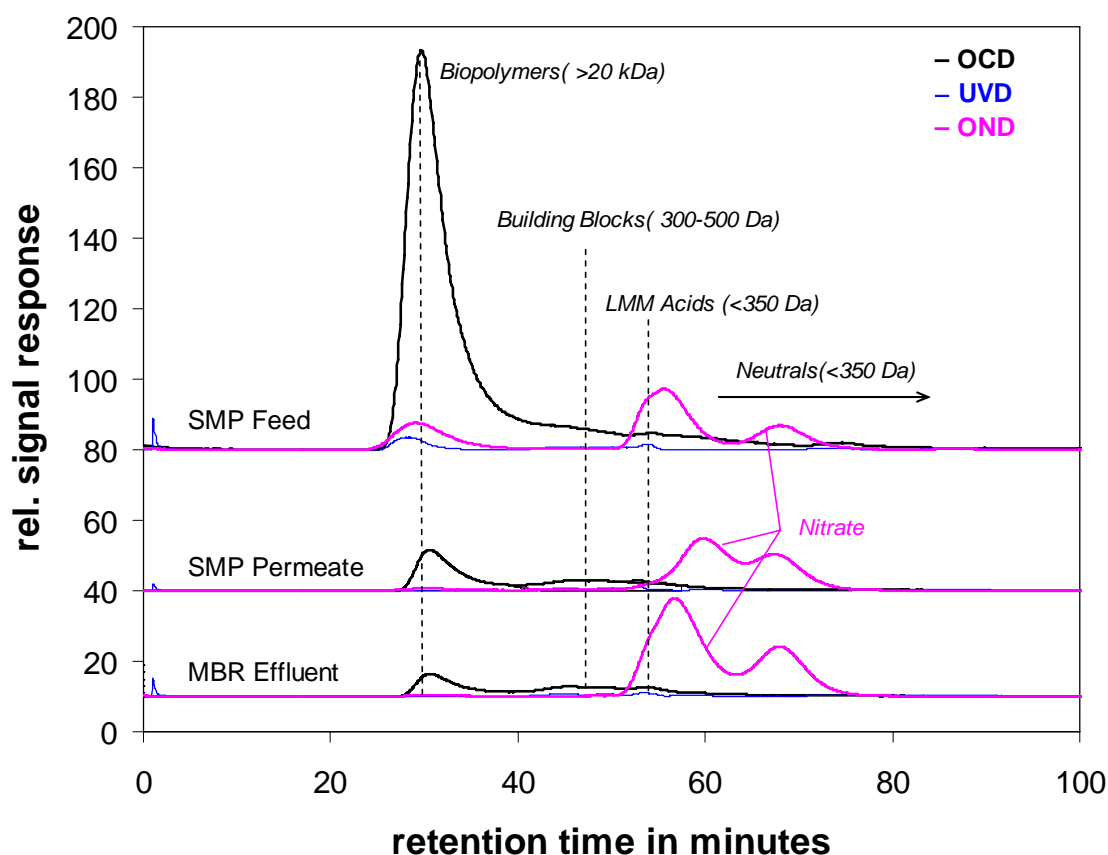
Figure 5-2 LC-OCD chromatogram of SMP feed and permeate from batch filtration and MBR effluent (HW50S column)

The UVD also showed peaks in the biopolymer region. It should be noted that inorganic colloidal compounds (e.g., polyelectrolytes, polyhydroxides and oxidhydrates of Fe, Al or Si) also absorbs UV at 254 nm and unfortunately their elution time is close to that of the biopolymers. A lumped SAC (spectral adsorption coefficient) of biopolymers and inorganic colloids was estimated by integration of the UV signal. The true SUVA (UV_{254}/DOC) of biopolymers should be lower than the lumped value, i.e., 0.15, 0.17 and 0.39 L/(mg·m) for SMP feed, permeate and MBR effluent respectively. The very low SUVA of this fraction suggested that the biopolymers had few aromatic or double carbon bounds and they are strongly hydrophilic.

The Norg. also showed a peak in the biopolymer region, and the organic nitrogen content of biopolymers was estimated as the ratio of Norg./OC, i.e., 5.9%, 6.3% and 5.2% for SMP feed, permeate and MBR effluent respectively. The low nitrogen

contents, low SUVA values and high molecular weights suggested that the biopolymers are most likely mixtures of polysaccharides and proteins. If one assumes that the biopolymer is only composed of polysaccharides and proteins, and uses BSA (bovine serum albumin) to represent protein and dextran to represent polysaccharide, the SMP feed, permeate and MBR effluent would contain 20%, 22% and 18% of protein, respectively. The existence of polysaccharides and proteins were also confirmed by the colorimetric method (Table 5-1).

Table 5-1 Summary of the characteristics of SMP, BAP, UAP, MBR effluent and EPS (batch filtrations were performed in unstirred cell, LC-OCD analyzes were performed with HW50S column)

Item	Fraction	BAP feed	BAP perm	UAP feed	UAP perm	SMP feed	SMP perm	MBR eff	MBR EPS
Organic carbon (mg/L)	Overall sample	77.4	51.8	12.4	10.3	40.2	6.13	4.66	158.3
	Biopolymer	48.4	26.1	5.58	1.42	28.0	2.87	1.711	44.6
	Building blocks	11.2	10.4	1.78	1.54	3.93	1.71	1.612	27.4
	LMW acids	1.17	0.879	0.098	0.165	0.075	0.108	0.127	3.85
	Neutrals	6.36	4.62	3.13	3.53	2.64	0.712	0.628	40.4
SUVA UV_{254}/DOC (L/(mg·m))	Overall sample	0.46	0.63	0.50	0.56	0.20	0.66	0.70	2.15
	Biopolymer+inorg.	0.15	0.17	0.072	0.061	0.12	0.11	0.39	1.25
	BB+LMWA+NT	n.a.	n.a.	0.74	0.80	0.55	1.44	2.01	3.30
Norg. content of biopolymers		5.9%	6.3%	5.6%	6.0%	5.5%	5.8%	5.2%	10.8%
(mg/L)	COD	243	74.4	41.60	29.40	62.9	bdl	12.3	564
	Proteins	22.8	13.9	14.6	12.3	11.6	9.1	8.3	131.3
	Polysaccharides	93.4	62.4	10.1	3.5	24.2	5.9	4.2	88.6
	BOD_5	6.75	n.a.	n.a.	n.a.	1.7	n.a.	2.8	n.a.
	BOD_{17}	12.1	n.a.	n.a.	n.a.	4.6	n.a.	4.5	n.a.
	BOD_{28}	18.1	n.a.	n.a.	n.a.	11.5	n.a.	6.2	n.a.
Mean oxidation number		-0.71	1.85	-1.04	-0.29	1.65	n.a.	0.04	-1.34

1) bdl=below detection limit, BB=building blocks, LMWA=low molecular weight acid, NT=neutral, SMP feed=sludge water of MBR, SMP perm=permeate from collected from unstirred cell batch filtration, MBR EPS=bound EPS extracted from MBR waste sludge;
2) Humic substances were below detection limit and trace humic substances were lumped into building blocks;
3) The TOC of overall sample was determined in the column bypass. The other 4 fractions are estimated by the integration of each chromatogram peak. The sum of the 4 fractions is less than the TOC due to the non-chromatographic DOC (e.g., retained in the column).

In Figure 5-2, for the small compounds eluted after the biopolymers, there were no clear peaks of both OC and UV chromatograms in the retention time of humic substances, building blocks, low molecular acids or neutrals. The UV adsorption of these small molecular compound fractions was lumped together and the SUVA of

these small molecules in the SMP feed sample was 0.55 L/(mg·m), which suggests a hydrophilic character of these small molecules (Table 5-1).

The retention of each fraction by the membrane can be illustrated by comparing the three chromatograms of the SMP feed, permeate and MBR effluent in Table 5-1. There are a few interesting points as follows. First, the UF membrane (0.03 μm and 200 kDa) retained a very large portion of SMP. The retention percentages were 84.8% (overall sample) and 89.8% (biopolymer fraction) in the batch filtration, which is consistent with Lesjean et al., (2005), Rosenberger et al. (2005); and Rosenberger et al. (2006). However, it was surprising that there was some retention of even small molecules (e.g., building blocks and neutrals). This additional retention can be attributed to membrane fouling, which reduced the MWCO (molecular weight cut off) of the membrane and improved solute removal (Chang et al., 2001; Lee et al., 2001b). Second, the COD retention percentage of the sludge water in the lab-scale MBR was 89.7% (obtained by the average of 25 samples; membrane inlet and permeate COD were 107.4 ± 28 and 11.0 ± 3.1 mg/L respectively). This was slightly higher than that in the above batch SMP filtration (84.8% removal). The higher retention percentage in the continuous system was probably due to the fact that a fouled membrane used in the lab-scale MBR had an actual MWCO smaller than a virgin membrane used in the batch filtration. Third, the SMP permeate exhibited a higher SUVA value than the SMP feed. Considering the hydrophilic nature of the UF membrane, the change in SUVA value suggested that the hydrophilic fraction of SMP had a higher retention percentage than the hydrophobic fraction, and was probably more prone to adsorption in membrane pores, resulting in membrane fouling. Fourth, the organic nitrogen content of biopolymers in the permeate (5.8%) was slightly higher than the feed (5.5%), which suggested that the retention of polysaccharides appeared to be higher than proteins. Finally, the mean oxidation number of permeate was always higher than the feed, which suggested that the membrane selectively removed more reduced compounds, and that reduced compounds had a higher fouling potential than oxidized ones, e.g., ketone-like versus carboxylic-like compounds. The higher fouling potential of reduced compounds was confirmed by a filterability test of 3 fractions of electrolysed SMP. The raw SMP was electrolysed using a 1-2 V of DC power and an oxidized portion and a reduced portion of SMP was collected separately. Together

with the raw SMP, the 3 types SMP were filtered using the unstirred cell. The results showed that the filterability was in the order of reduced SMP, raw SMP and oxidized SMP from poor to improved filterability.

The biopolymer peak of the SMP sample (sludge water collected from the MBR) was fractionated into more detail (2000 kDa, 200 kDa and 50 kDa) using the HW65S column (Figure 5-3). The largest peak of biopolymer was at 2000 kDa, which corresponds to a colloidal diameter of approximately 0.2 μm. The existence of this very HMW biopolymer peak is consistent with the second peak of the MBR sludge PSD measured using the MastersizerS (Figure 5-1). The OC and Norg. exhibited consistent peaks in the biopolymer region, which suggests the existence of very HMW proteins within the SMP in addition to polysaccharides. However, the UV peak appeared earlier than the OC peak at 2000 kDa. This can be attributed to inorganic colloids that absorb UV as discussed above.
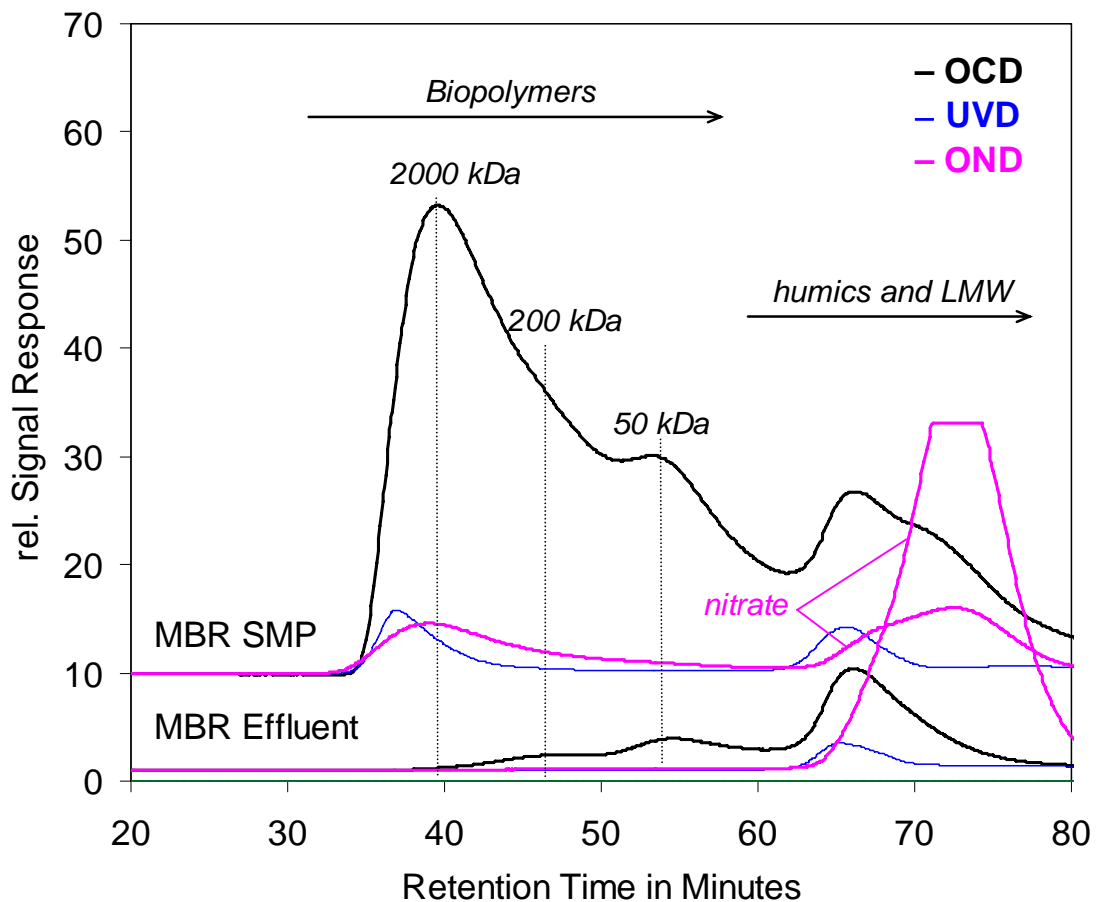
Figure 5-3 LC-OCD chromatogram of SMP and effluent collected online (HW65S column)

A more detailed removal picture of the three designated biopolymer fractions using the column HW65S is presented in Table 5-2. The OC removal was 100%, 80.2% and 80.0% for 2000 kDa, 200 kDa and 50 kDa, respectively. However, the Norg. removal was not proportional to OC, i.e., 100%, 14.3% and 0%. It appears that the lower MW proteins (200 kDa and 50 kDa) had a higher passage than the same MW polysaccharides.

Table 5-2 LC-OCD analyses of the biopolymer fraction of MBR SMP and effluent (column HW65S)

	2000 kDa		200 kDa		50 kDa		Humics etc. LMW[1]	Sum of biopolymer[2]	
	OC	Norg.	OC	Norg.	OC	Norg.	OC	OC	Norg.
MBR SMP (mg/L)	21	1.32	3.18	0.07	4.65	0.11	12.47	28.83	1.5
MBR effluent (mg/L)	0.00	0.00	0.63	0.06	0.93	0.11	4.74	1.56	0.17
removal	100%	100%	80.2%	14.3%	80.0%	0.0%	62.0%	94.6%	88.7%

1) [1] Sum of humic substances, building blocks, LMW acids and neutrals
2) [2] Sum of 3 biopolymer fractions, i.e., 2000, 200 and 50 kDa
3) The Norg. of LMW compound was biased due to the inorganic nitrate present in the sample (see section 5.2.5) and not presented here

The BOD values (5, 17 and 28 days at 20 °C) of SMP and MBR effluent were very low (Table 5-1). It should be noted that ATU was used in the BOD tests. As a result, all oxygen consumption could be attributed to the biodegradation of organic carbon. The BOD_5/COD values were only 0.027 and 0.23 for SMP and MBR effluent, respectively, which suggests that the biodegradabilities of SMP and MBR effluent were very poor. The SMP retention percentage by the membrane is always lower than 100%, thus the retention time of SMP in the bioreactor should always be less than the solid retention time (17 days in the lab-scale MBR). However, the BOD_{17} value was still very low (only 4.6 and 4.5 mg/L from SMP and MBR effluent, respectively), which suggests that these selectively retained SMP were hardly degradable in the bioreactor.

5.3.3 Characterisation of BAP

BAP was produced in a batch experiment without external substrate addition. Thus, the soluble and colloidal compounds produced in the batch were mostly associated with the biomass decay, i.e., the so called BAP. The soluble COD, polysaccharide and

protein concentrations were continuously measured during 19 days and the results are presented in Figure 5-4. The detailed modelling of the BAP production process will be presented in Chapter 6.
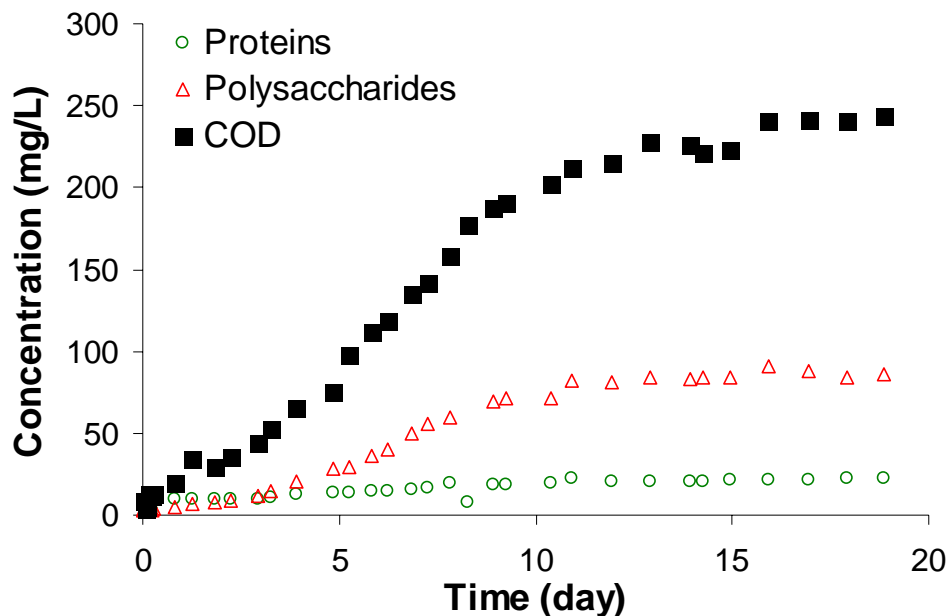
Figure 5-4 Evolution of proteins, polysaccharides and soluble COD in BAP batch experiment

The LC-OCD chromatograms (HW50S column) of the BAP feed (collected on day 19) and permeate filtered using the unstirred constant pressure filtration unit are presented in Figure 5-5. BAP was mostly composed of biopolymers (62.5%) with a small amount of building blocks, LMW acids and neutrals. The shape of the BAP chromatogram (the retention times and relative height of the peaks) was very similar to that of the SMP in Figure 5-2. In addition, the organic nitrogen content of the biopolymers was 5.9 and 6.3% in the BAP feed and permeate respectively, which were similar to those of SMP.

However, more LMW compounds were detected in the BAP sample compared with the corresonding SMP sample. The sum of building blocks, LMW acids and neutrals accounted for 24.2% of the DOC, compared to 16.5% in SMP sample. Unfortunately, the UV after 70 minutes had a systematic error due to the very high nitrate concentration, thus the results cannot be used to calculate SUVA.
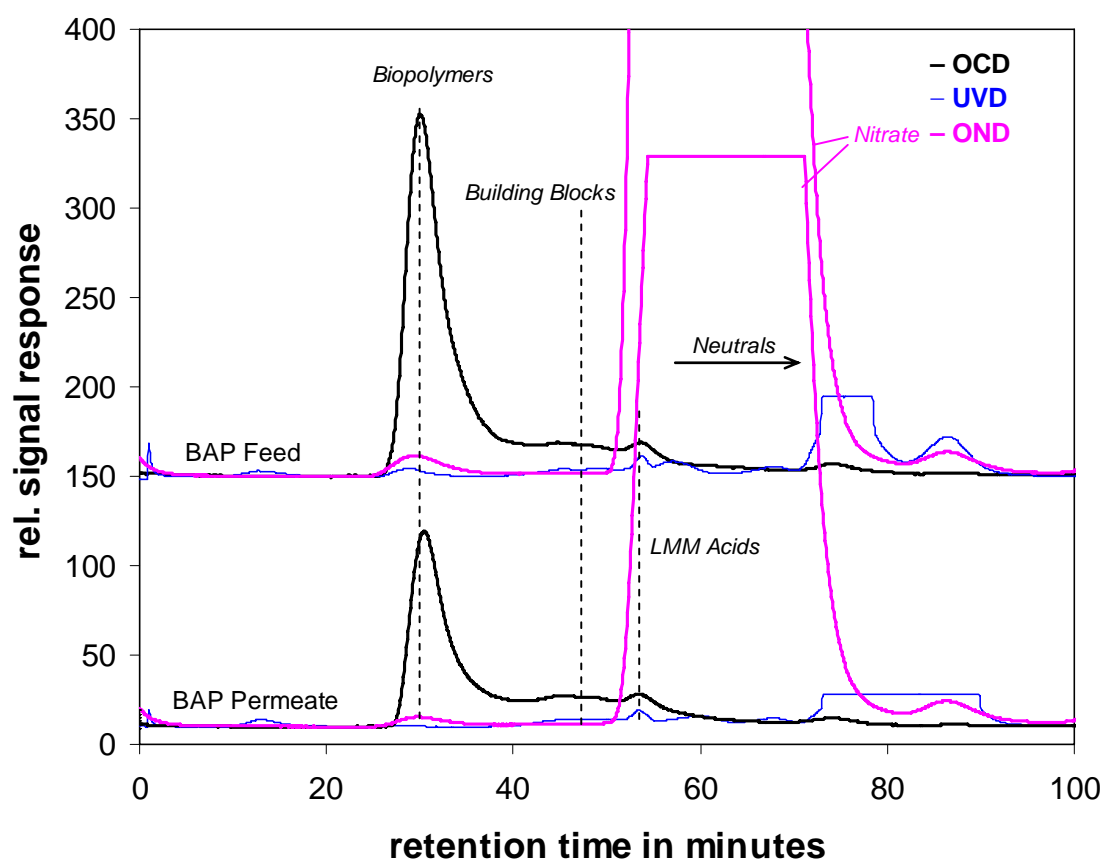
Figure 5-5 LC-OCD chromatogram of BAP feed and permeate from batch filtration (HW50S column)

Comparing the two chromatograms of the BAP feed and permeate, the DOC retention percentage of the overall sample (33.1%) and biopolymers fraction (46.1%) were lower than that of SMP sample (84.8% and 89.8%). This is probably due to the fact that the biopolymers present in the SMP sample directly collected from the lab-scale MBR were selectively retained by the UF membrane (retaining the larger biopolymers and allowing the passage of the smaller ones). However, the biopolymers collected in the BAP batch after 19 days did not reflect the above size selection criteria; as a result, all molecular size compounds may remain in the batch reactor, as long as they are not rapidly biodegraded. The SUVA, organic nitrogen content of biopolymers and mean oxidation number of permeate were higher than the feed BAP (Table 5-1), suggesting that the membrane selectively removed the hydrophilic and more reduced compounds.

The BOD values of BAP (5, 17 and 28 days) at 20 °C were 6.8, 12.1 and 18.1 mg/L, respectively, which still resulted in very low BOD/COD ratios as 0.028, 0.050 and

0.074, respectively. The biodegradability of BAP was very poor, although the BAP includes more small molecular fractions than the SMP samples.

The BAP produced in the above designed batch experiments showed similar characteristics (MW distribution, hydrophobicity and organic nitrogen content) with the SMP fractionated directly from the lab-scale MBR (Table 5-1). These similarities support the hypothesis that BAP is an important constituent of SMP. In addition, it also proves the success of the above experimental design in BAP production.

5.3.4 Characterisation of UAP

UAP was produced in a designed UAP production batch experiment using acetate as a substrate. The soluble COD, polysaccharide and protein concentrations were continuously measured during 23.2 hours. The soluble COD reached 29.4 and 24.1 mg/L by the end of UAP batch experiment (23.2 hrs) for the UAP and the reference batch, respectively. The release of SMP (24.1 mg COD/L in 23.2 hrs) in the reference batch was mostly BAP, since no substrate was added and the added ATU was almost completely biodegraded (see below). The amount of BAP released in this reference batch was consistent with that in the previous BAP batch (19.7 mg COD/L in 19.3 hrs). Thus the colloidal and macroorganic compounds obtained in the UAP batch were actually a mixture of UAP and BAP.

The net UAP production was estimated as the difference between the UAP and the reference batch with respect to COD, polysaccharides and proteins. The maximum net polysaccharide and protein concentrations reached 4.0 and 6.2 mg/L, respectively, at 2-3 hours after acetate addition. However, their concentrations decreased quickly after the depletion of substrate due to simultaneous biodegradation. After 23.2 hours, the net proteins, polysaccharides and soluble COD concentrations were 1.4, 1.2 and 5.6 mg/L, respectively. The increase in SMP after the substrate depletion was consistent with the SMP profile in a SBR reactor (Pribyl et al., 1997). It should be noted that the net UAP production was not high even compared with the measurement error. The mean standard deviations of the colorimetric methods were 0.68 and 0.88 mg/L for polysaccharides and proteins, respectively. Thus, the polysaccharide and protein concentrations presented here are more qualitative than quantitative.

To obtain a more accurate quantification of UAP, the UAP and reference samples at time 0 (before acetate addition), 2 hr, 6.7 hr and 23.2 hr and the UAP permeate of the batch UAP filtration were analyzed by LC-OCD using the HW50S column (Figure 5-6). Both high and low MW compounds increased during the 23.2 hours. By 23.2 hours, the UAP and reference samples contained 45.1% and 39.6% of biopolymer, respectively, which is considerably lower than that in the SMP and BAP samples (69.8% and 62.5%, respectively). However the UAP and reference samples contained more LMW compounds. The sum of building blocks, LMW acids and neutrals accounted for 40.4% and 40.3% of the DOC, compared to 24.2% and 16.5% in SMP and BAP samples, respectively.
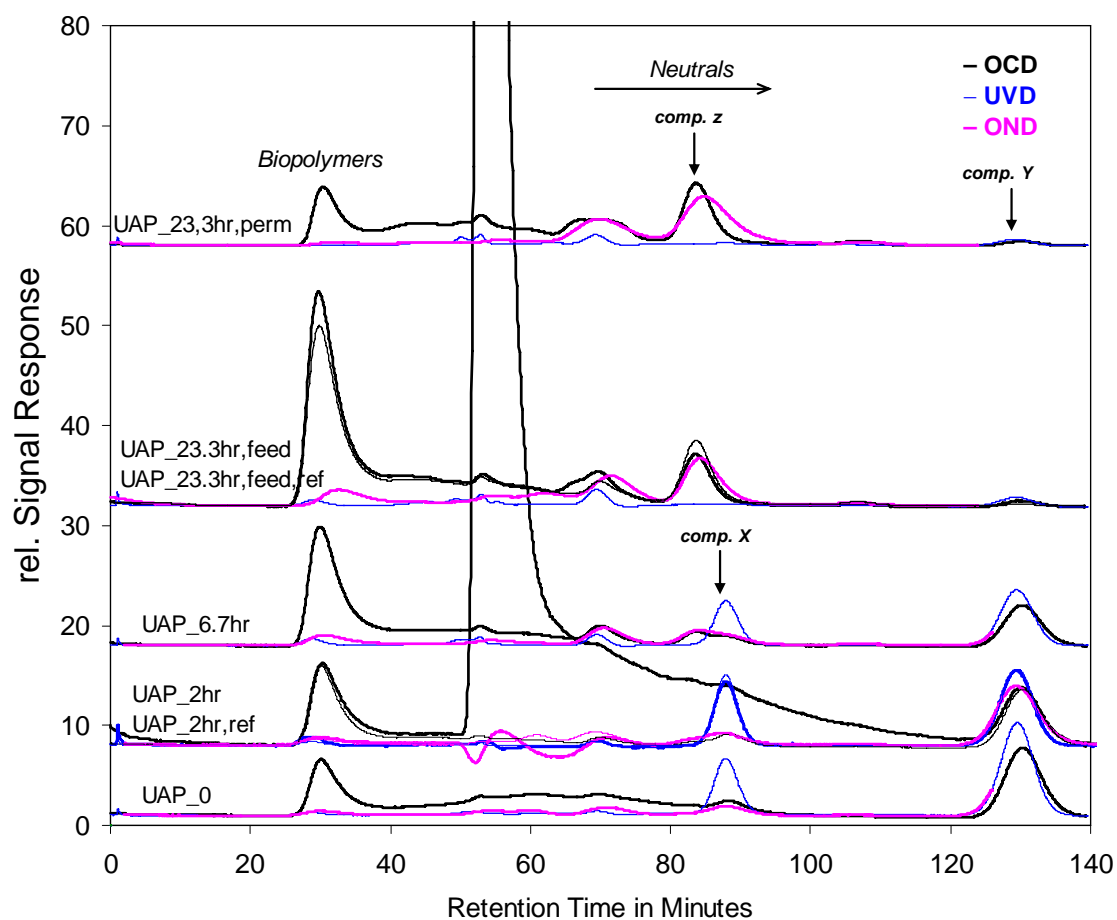
Figure 5-6 Time series of UAP LC-OCD chromatogram (the thick line is the UAP batch with 1000 mg COD/L acetate addition, the thin line is the reference batch without acetate addition) (HW50S column)

The true UAP should be the area between the two chromatograms (see chromatograms at 2, 6.7 and 23.2 hr in Figure 5-6). Close examination suggests that acetate addition did stimulate the production of biopolymers and some LMW compounds. More explicitly, the net UAP production was calculated as the difference of DOC between the UAP and the reference batches in chromatograms (Figure 5-7). There is a trend that the MW of UAP increases as a function of time (the growth phase of biomass). The fraction of HMW UAP increased even as substrate was depleted (the biopolymer peak at 23.3 hr was much larger than those at 2 and 6.7 hrs).
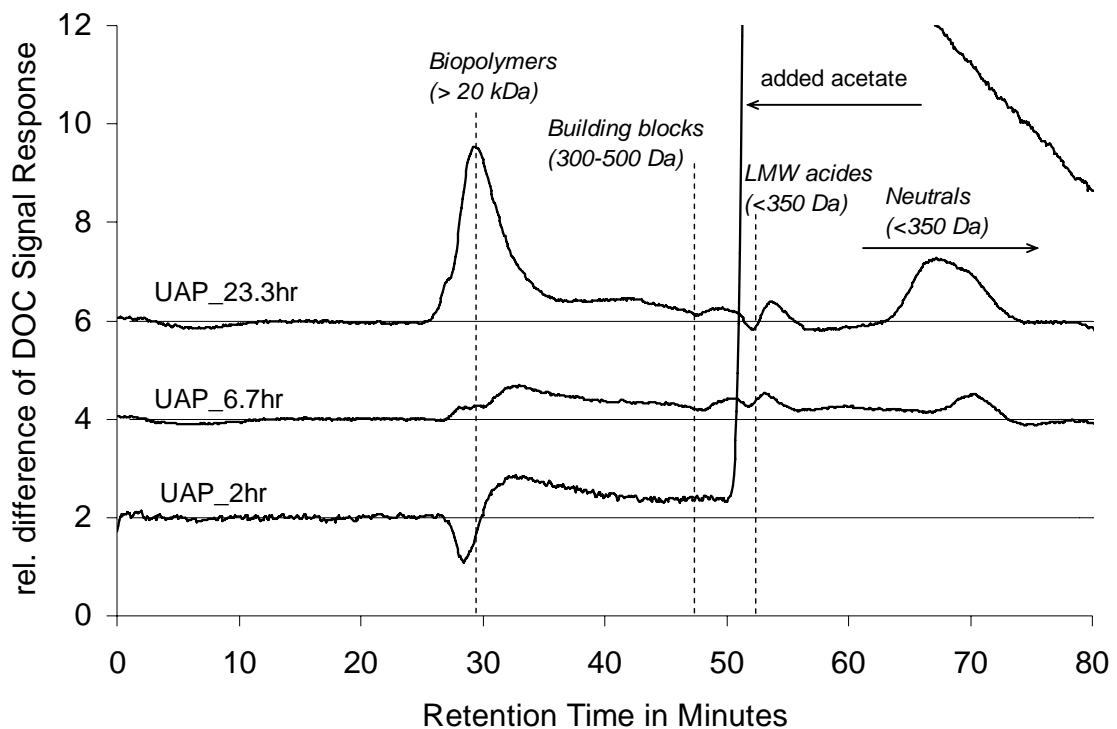
Figure 5-7 The difference of DOC between The UAP and the reference batches measured using LC-OCD (HW50S column)

The increase in MW of UAP is consistent with the study of Boero et al. (1996), who used phenol and glucose as substrate, but did not differentiate UAP from SMP. It is hypothesized that there are two types of UAP produced in the batch process associated with biomass decay according to two stages of cell growth. In phase 1, heterotrophic biomass uptake readily biodegradable substrate and store them as PHA (polyhydroxyalkanoates), and in phase 2, the cells utilize the stored PHA and proliferation takes place (van Loosdrecht et al., 1997). The UAP produced in the cell proliferation phase (UAP$_{pro}$, after 3.85 hr) exhibited higher MW than that produced in

the storage phase (UAP_{sto}, within 3.85 hr). In addition, UAP_{pro} is probably more difficult to biodegrade, since these components remained after one day, while the UAP_{sto} produced in the storage phase was degraded quickly. The storage phenomenon was confirmed by a very high apparent yield (Y_H= 0.83) estimated from the OUR (Spanjers and Vanrolleghem, 1995).

The net biopolymer productions (UAP subtracted from the reference batch) at 2, 6.7 and 23.2 hr were 0.623, 0.436 and 0.743 mg DOC/L, respectively, which corresponds to 0.166%, 0.116% and 0.198% of the DOC of the feed acetate (UAP/substrate(S_0) ratio). This percentage is much lower than some reference values. Boero et al. (1996) used labelled ^{14}C and obtained a maximum of 25% and 3% of UAP/S_0 in an aerobic batch test using phenol and glucose as substrate, respectively. However, after 7 hours, these ratios were decreased to 5.7% and 1.7%, respectively, due to UAP biodegradation. The lower UAP/S_0 obtained in the UAP batch test in this study was probably due to the fact that only a very simple substrate, acetate, was used here. If a more complex substrate (e.g., protein or starch) would have been used, the biomass would have to undergo additional metabolic pathways and prepare certain extracellular enzymes for the hydrolysis of complex molecules, which might produce additional UAP. Therefore, the UAP produced with the acetate as substrate in this thesis is hypothesized to be the minimum UAP production.

There are a few peaks (compounds X, Y and Z) in the LMW range in Figure 5-6, which were not observed previously in the SMP and BAP samples. The compound Y (130 minutes) showed a strong UV adsorption and a high nitrogen content. However, its concentration decreased with time. Y is hypothesized to be ATU according to its molecular formula. This peak was confirmed afterwards by the injection of an ATU standard into the LC-OCD. Compound Z (retention time 85 minutes) showed no UV adsorption but high organic nitrogen content. It did not exist initially, but appeared in the samples after 23.2 hr. Z is hypothesized to be urea as an intermediate product of ATU biodegradation. However, injection of a urea standard into LC-OCD showed a peak at a different elution time, i.e., 75 minutes. Thus Z is not urea. Further studies are needed to identify Z (amino acid-like compound). Compound X (retention time 88 minutes) showed a very strong UV adsorption and a certain amount of organic nitrogen. It appeared initially but disappeared afterwards. X is probably aromatic

amino acid-like compounds produced during the cell lysis due to the toxicity of ATU. The presence of amino acid-like compounds has been reported in UAP samples (Hejzlar and Chudoba, 1986a).

The UAP sample collected at 23.2 hr (actually a mixture of UAP and BAP) was filtered in the unstirred cell. The DOC retention percentage of the overall sample (16.9%) was considerably lower than the retention of the SMP (84.8%) and the BAP (33.1%). The lower retention percentage was consistent with the lower percentage of biopolymer fraction present in the UAP sample, suggesting that the UAP sample may have lower fouling potential than the SMP and the BAP sample.

To obtain a better resolution of the biopolymer peak, the UAP samples were also analyzed using the HW65S column (Table 5-3). Comparing the retention percentage of the biopolymer fraction in the lab-scale MBR (Table 5-2) with the batch filtration of UAP sample (Table 5-3), the on-line SMP filtration in the lab-scale MBR exhibited much higher retention of biopolymers than that in the batch filtration, i.e., 100%, 80.2% and 80.0% versus 98.5%, 45.9% and 46.2% for 2000 kDa, 200 kDa and 50 kDa fractions of biopolymers respectively. This additional retention in the lab-scale MBR can be attributed to membrane fouling, which reduced the MWCO of the membrane (Chang et al., 2001; Lee et al., 2001b).

Table 5-3 LC-OCD analyses of the biopolymer fraction of UAP feed and UAP perm (column HW65S)

	2000 kDa OC	200 kDa OC	50 kDa OC	Humics etc. LMW[1] OC	Sum of biopolymer[2] OC	Norg.
UAP feed (mg/L)	4.60	0.98	0.52	7.26	6.1	0.33
UAP perm (mg/L)	0.07	0.53	0.28	6.05	0.88	0.07
removal	98.5%	45.9%	46.2%	16.7%	85.6%	78.8%

1) [1] Sum of humic substances, building blocks, LMW acids and neutrals
2) [2] Sum of 3 biopolymer fractions, i.e., 2000, 200 and 50 kDa
3) The Norg. of LMW compound was biased due to the inorganic nitrate present in the sample (see section 5.2.5) and not presented here

The SUVA, organic nitrogen content of biopolymer, and mean oxidation number of permeate were higher than the feed UAP, suggesting that the membrane selectively removed the hydrophilic and more reduced compounds (Table 5-1). The MW distribution, hydrophilicity, and organic content of UAP sample were similar to those

of SMP sample. These similarities therefore support the hypothesis that UAP is an important constituent of SMP.

5.3.5 Filtration behaviour of SMP and characterisation of backwash water

A sludge water sample (mostly contain SMP) was collected during a biologically unstable period of the lab-scale MBR and filtered using the automated constant flux filtration unit. The SMP sample was filtered on a constant flux filtration unit. The filtration characteristics are summarized in Table 5-4. Rinsing with Milli-Q water after 2 hrs filtration removed 17% of the total resistance. A further prolonged backwashing removed most foulants and there was only 3.6% remaining as irreversible. However, the very small amount of irreversible foulant was equivalent to 63% of clean membrane resistance, which was still very significant.

Table 5-4 Filtration of SMP under constant flux conditions, 31.8 L/(m^2·h)

Clean membrane resistance (1/m)	3.44×10^{11}
Resistance after 2 hr filtration (1/m)	6.47×10^{12}
Resistance after Milli-Q washing (1/m)	5.39×10^{12}
Resistance after BW (1/m)	5.62×10^{11}
% reversible by rinsing	17%
% irreversible fouling by BW	3.6%
irreversible fouling resistance /clean membrane resistance	63%

The SMP feed, permeate and collected backwash water during the 2 hours filtration were analyzed using LC-OCD (Figure 5-8). An integration of OC in the chromatograms suggests that the overall SMP feed contained 68.6% of biopolymers with respect to TOC, which was similar to the previous SMP sample (69.8%). However, the retention percentage of overall sample and biopolymer fraction (>20 kDa) were considerably lower (63.3% and 69.5% versus 84.8% and 89.8%, respectively). The lower retention suggests that the SMP collected under unstable conditions contained less HMW compounds. The biopolymer fraction in the backwash water (85.6%) was higher than that in the SMP feed (68.6%), which clearly demonstrated that biopolymers were retained by the membrane as foulants and most of them can be removed by backwashing.
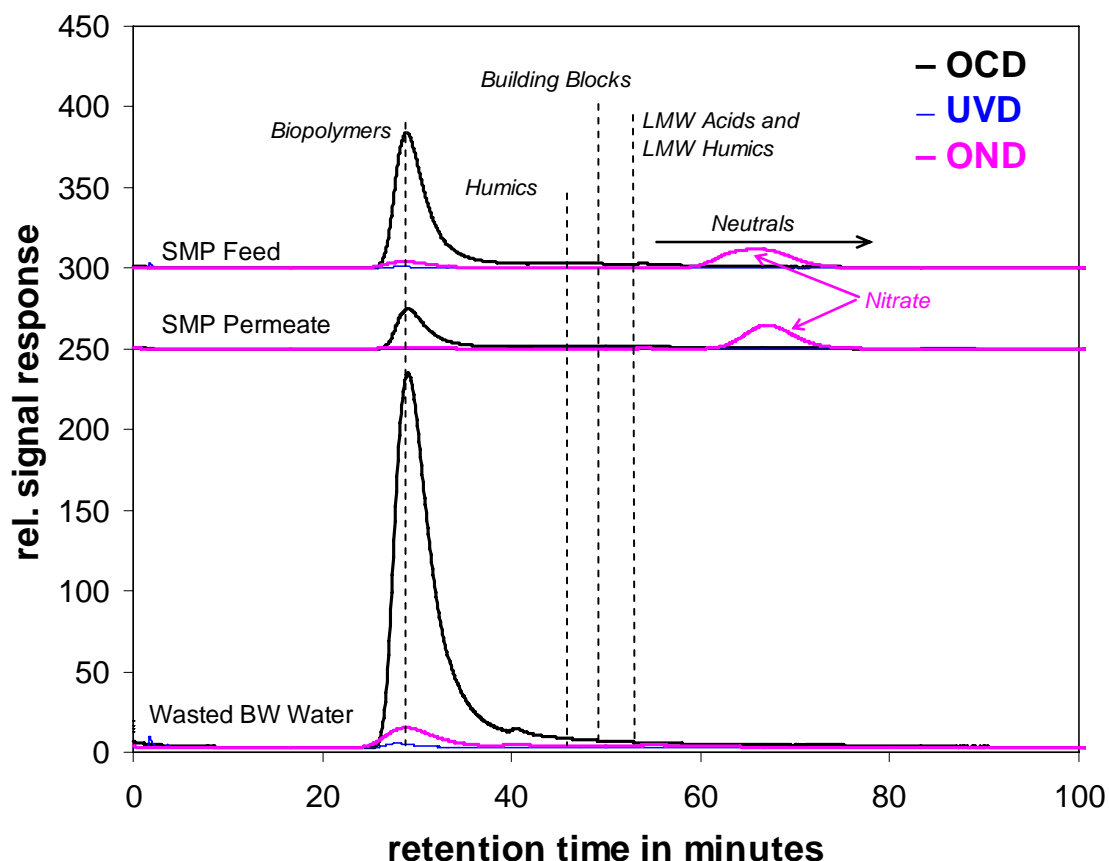
Figure 5-8 LC-OCD chromatograms of SMP feed, permeate and wasted backwash water (HW50S column)

5.3.6 Characterisation of EPS

The LC-OCD chromatogram of extracted bound EPS is presented in Figure 5-9. The main fraction of EPS was still biopolymers (28.2%). However, it contains much more humic substances, building blocks (17.3%), LMW acids (2.4%) and neutrals (25.5%) etc. The SUVA of overall sample, and LMW compounds (sum of humic substances, building blocks, LMW acids and neutrals) were 2.15 and 3.30 L/(mg·m), respectively, suggesting the bound EPS was more hydrophobic (aromatic) than the soluble EPS (SMP). In addition, the extracted EPS was much more complex than the soluble EPS (SMP) with many OC, UV and Norg. peaks in different MW sizes. The hypothesis that "soluble EPS and SMP are indeed identical" and "bound EPS are hydrolyzed to biomass-associated products (BAP)" in the unified EPS and SMP theory (Laspidou and Rittmann, 2002a) are questionable. The previous LC-OCD study of Rosenberger et al. (2006) reported that the sludge water exhibited similar chromatograms as the

extracted bound EPS, only in much smaller quantities. It should be noted that the chromatograms used in this study were equipped with an organic nitrogen detector in addition to an OCD and UVD, which provides opportunities to capture more information.
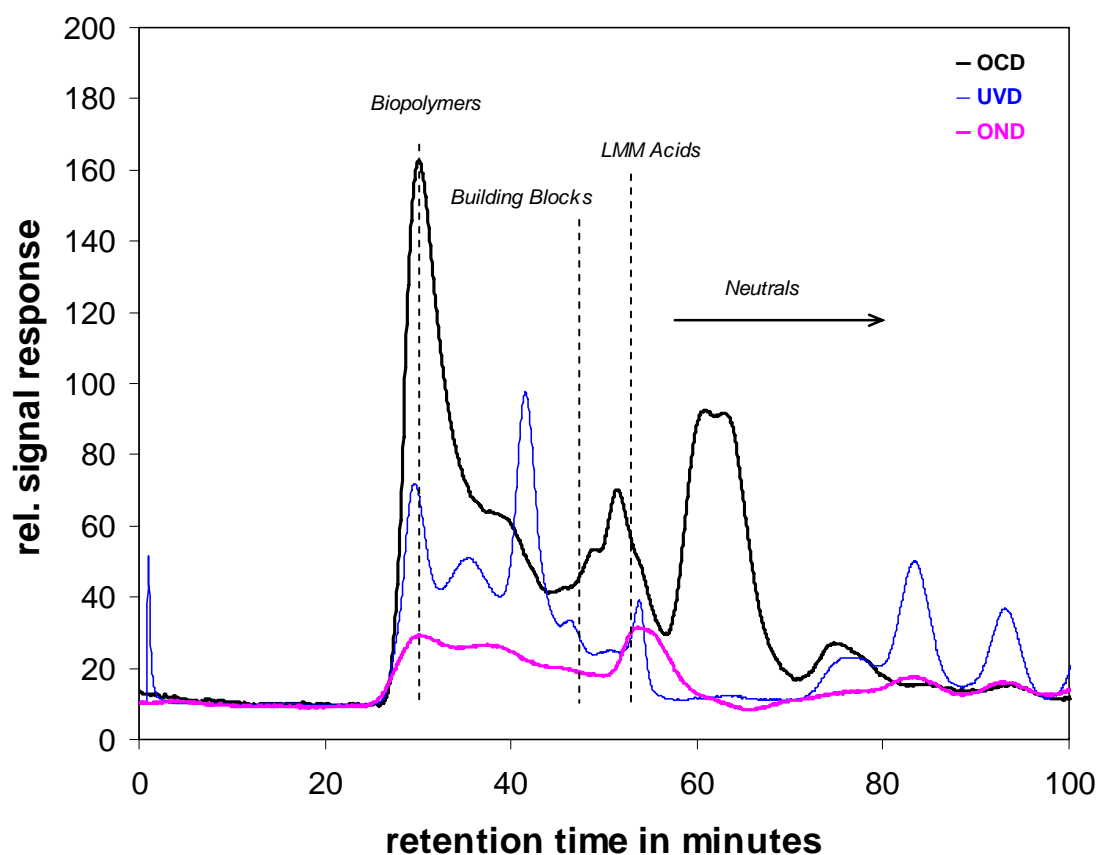
Figure 5-9 LC-OCD chromatograms of extracted EPS (HW50S column)

5.4 Conclusions

BAP and UAP were produced in well designed batch experiments and characterised using a new and powerful tool, LC-OCD. SMP (including BAP and UAP) were mostly composed of biopolymers and a certain amount of small molecules, e.g., building blocks, low molecular weight acids and neutrals. The biopolymer fraction exhibited a very wide MW distribution and the largest portion of biopolymers had a MW of 2000 kDa. The UAP produced during the biomass growth phase exhibited a lower MW than the BAP. Biopolymers were mostly polysaccharides and proteins, and there were probably more polysaccharides than proteins according to the nitrogen

contents (5-7%). The sludge water (mostly SMP) collected in the lab-scale MBR contained a much higher biopolymer fraction than those of BAP and UAP produced in batches, which was attributed to the selective retention of HMW colloids and macromolecular organic compounds by the UF membrane. All sludge water samples (SMP, BAP and UAP) exhibited hydrophilic characteristics, with very low SUVA values.

The BAP collected from the batch BAP reactor and the SMP collected from the MBR reactor showed very low BOD_5/COD ratios. Extending the incubation time up to 28 days obtained only little improvement in biodegradability. The HMW and poor biodegradability of SMP suggest that the retention time of SMP in MBRs can be much longer than the hydraulic retention time, which provides opportunities for them to build up a high concentration in MBRs.

The permeate of the batch BAP, UAP and MBR SMP contained a lower percentage of biopolymers, and the retention of proteins appears to be lower than polysaccharides (higher organic nitrogen content observed in the permeate). In addition, the permeate exhibited more hydrophobic (higher SUVA values) characteristics and was more oxidized (higher mean oxidation number), suggesting the compounds retained by the membrane (potential foulants) were more hydrophilic and more reduced. The retention of biopolymers by a membrane during constant flux filtration and the effectiveness of their removal by periodical backwashing were confirmed by a direct analysis of MBR feed, permeate and backwash water using LC-OCD.

6.
Modelling the production and degradation of
soluble microbial products (SMP)

6.1 Introduction

Recent studies on MBR fouling have reported a significant impact of the biology on membrane fouling. MBR fouling is influenced by DO (dissolved oxygen), SRT (solid retention time), HRT (hydraulic retention time), MLSS (mixed liquor suspended solids), and F/M (food to microorganism ratio) etc. As a general trend, a high DO leads to a better filterability and a lower fouling rate. This has been explained by either a lower specific cake resistance of the fouling layer (Kang et al., 2003; Kim et al., 2006) or a decreased amount of smaller flocs (Jin et al., 2006; Kim et al., 2006). A higher SRT leads to a better filterability in the range of SRTs of 2-10 days (Trussell et al., 2006), 8-80 days (Nuengjamnong et al., 2005) and 10-80 days (Liang et al., 2007). The higher fouling under low SRTs is either attributed to the lower amount of SMP (Liang et al., 2007) or the lower amount of bound EPS (Nuengjamnong et al., 2005). However, further increasing SRTs from 30 to 100 days has been reported to intensify the membrane fouling due to the accumulation of foulants and the higher sludge viscosity (Han et al., 2005). Decreasing HRTs leads to a higher fouling rate in the range of HRTs of 4-10 hrs due to an increase in EPS concentrations (Chae et al., 2006). However, from the viewpoint of both membrane fouling control and economical design, HRT should not be too high, and an optimal HRT of 12 hrs has been suggested (Tay et al., 2003). A higher MLSS simply implies a greater presence of associated SMP while F/M ratio is closely related to the SRT and can be expected to affect the relative proportions of UAP versus BAP components (Hejzlar and Chudoba, 1986a). A recurring problem of almost all literature results is that rarely is one operational parameter varied at a time while all others are held constant.

Unstable operation accelerates MBR fouling. In a large pilot MBR, a large amount of waste sludge withdrawal (increase F/M ratio) has triggered MBR fouling due to an

increase in SMP (polysaccharides) concentration (Drews et al., 2006). A pulse of acetate in the feed can deteriorate the MBR sludge filterability (Evenblij et al., 2005). Spikes of glucose and reduction of HRT have also increase UAP and BAP production, respectively in anaerobic chemostats (Aquino and Stuckey, 2004).

The above literature reports suggest that the biological operational parameters of MBRs, e.g., DO setpoint, SRT, HRT, and waste sludge rate, etc., impact membrane fouling indirectly through changes in SMP, EPS, and floc size, etc. In addition, the change of one operational parameter often impacts another, e.g., increasing SRTs by reducing sludge wastage results in an increase in sludge concentration, viscosity, and oxygen demand but reduce the shear rate on the membrane surface. Thus, fundamental studies are needed to identify the major foulants and predict the foulant concentrate, preferably using a mathematical model. The significance of SMP on MBR fouling has been widely reported as reviewed in Chapter 5. The existing SMP models are reviewed as follows.

Rittmann and coworkers have presented a series of SMP models (Namkung and Rittmann, 1986; Rittmann et al., 1987; Furumai and Rittmann, 1992; de Silva et al., 1998; Urbain et al., 1998). Recently, their SMP studies are summarized and presented as a uniformed SMP and EPS theory (Laspidou and Rittmann, 2002b; Laspidou and Rittmann, 2002a). In their model, the UAP is produced proportional to the substrate utilization rate, with a stoichiometric parameter k_1. The EPS production is also directly proportional to the substrate utilization rate, with a stoichiometric parameter k_{EPS}. However, the BAP is not directly associated with the biomass decay as the others have done. Instead it is described as a hydrolysis product of EPS with k_{hyd} as a first-order rate coefficient. This approach actually decouples BAP from the biomass decay process. The same yield (Y_p) coefficients are assigned to biomass growth on UAP and BAP. However, different degradation rates using a Monod kinetic structure (q_{UAP}, K_{UAP} and q_{BAP}, K_{BAP}) were assigned to UAP and BAP, respectively. The uniformed theory totally introduces 8 SMP associated parameters. However, the approaches of parameter estimation are not presented and most of their model parameters either used parameter values obtained in a biofilm system (Namkung and Rittmann, 1986) or other literature values.

Boero et al. (1991,1996) performed a SMP mass balance using radio active ^{14}C tracer by monitoring the amount of carbon dioxide in the off-gas. The batch SMP experiments with phenol and glucose as substrate are divided into three regions, i.e., i) the original substrate is degraded generating cell mass, so called SMP (equivalent to UAP) and CO_2; ii) the original substrate is depleted, but SMP is partially degraded while some SMP remain non-biodegradable (SMP_{ND}); and iii) so called SMP_E (equivalent to BAP) and CO_2 are produced during the endogenous phase throughout the batch process, but dominate after the depletion of the original substrate and the biodegradable SMP. The behaviour of the SMP produced in the three regions is described as follows. SMP_E are assumed to be non-biodegradable in their model. With respect to stoichiometric relationship, SMP are produced proportional to substrate using a stoichiometric parameter Y_{SMPS}. SMP_S can be used directly for biomass growth with a yield coefficient Y_{XSMPS}. The generation of SMP_E uses a stoichiometric relationship with biomass decay (Y_{SMPEX}). With respect to kinetics, the degradation of SMP_S uses a first-order rate with respect to the degradable fraction of SMP_S, i.e., SMP_{SD} and biomass concentration ($d SMP_S/dt = -k_{SMPS}S_{MPSD}C_{MLX}$). In summary, Boero's model introduces only 3 stoichiometric and 1 kinetic SMP-associated parameters. The model is calibrated yielding Y_{SMPS}=0.13 and 0.025; Y_{SMPEX}=0.039 and 0.036; and k_{SMPS}=0.051 and 0.015 1/d for phenol and glucose, respectively. The substrate specific parameters suggests that phenol produces a much higher percentage of UAP than glucose, but the UAP produced with phenol as substrate are more biodegradable (77.1% vs. 47.5%) and have a higher degradation rate (0.051 vs. 0.015 1/d). The yields of BAP production from phenol and glucose are both very low as 0.026 and 0.036, respectively. Comparing with Rittmann's model, Boero's model is much simpler and uses mass balance based stoichiometric parameters to replace kinetic parameters if possible.

The SMP concept has also been incorporated into ASM1 (Orhon et al., 1989; Artan et al., 1990). Firstly, a very simple SMP model including only BAP (assuming UAP are negligible) is derived (Orhon et al., 1989). The so called S_P (equivalent to SMP) are assumed non-biodegradable and produced proportional to the hydrolysis of particulate COD (X_S) with a stoichiometric parameter β=0.1. However, the assumptions of no UAP production and the non-biodegradable characteristics of SMP have been

questioned (Grady, 1989). In their further developed model (Artan et al., 1990), a UAP production proportional to the biomass growth is introduced into the model with a stoichiometric parameter α. In addition, the parameter β is changed into a variable linear to the effluent soluble COD as $\beta = a + bS_S$. However, this approach mixes the concepts of UAP, BAP and their degradation, which creates strong parameter correlations. Ultimately, the model lacks experimental support.

Lu et al. have incorporated a very complex SMP model into ASM1 (Lu et al., 2001) and ASM3 (Lu et al., 2002) in MBR studies. However, the COD of their SMP model is not balanced. Although 8 SMP related parameters are tuned to fit the steady state soluble COD (SCOD) concentration in the bioreactor by trial and error, the experimental results are not convincing in demonstrating the validity of the model structure and parameter values. Ahn et al. also have adapted similar SMP models into a MBR study, however their model also suffers the lack of appropriate calibration (Lee et al., 2002; Cho et al., 2003; Ahn et al., 2006).

The above review of existing SMP models exhibits very heterogeneous SMP model structures in both CAS (conventional activated sludge) process and MBR system. Most models include the production and degradation of both BAP and UAP. Different parameters have been assigned to each process. However, some models only considered BAP production and assume BAP to be non-biodegradable. The difficulty in modelling SMP arises from 1) a poor understanding of the mechanism and pathway of SMP production; 2) the problem in distinguishing SMP from other soluble organic matters, e.g., influent substrate and hydrolysis products, if only COD or DOC data are measured; and 3) the heterogeneous characteristics of SMP (MW, biodegradability). Most models appear to have reasonable model structures, however, almost all of them suffer from a lack of experimental results demonstrating the validity of the model structure and allowing parameter estimation. This suggests that the development of a SMP model should consider model parameter estimations with limited experimental results.

SMP can build up a high concentration in MBRs (Huang et al., 2000; Shin and Kang, 2003). In addition, SMP are attributed to be the main foulant in MBRs (Lesjean et al.,

2005; Rojas et al., 2005; Rosenberger et al., 2005; Rosenberger et al., 2006). Thus, the predicting SMP concentration present in MBRs has significant importantce in MBR fouling study. However, modelling SMP in MBRs is subject to new challenges, i.e., the partially SMP retention by the membrane (increased retention time in the bioreactor), higher concentration (up to a few hundred mg/L), and long SRT, but short HRT commonly applied in MBRs. The objective of this study is 1) to develop an ASM2dSMP model by integrating SMP into the ASM2d model; and 2) to calibrate the SMP model using well designed SMP production experiments.

In this chapter, first, a lab-scale MBR and batch experiments used for BAP and UAP model calibration are described. Second, a BAP and a UAP model are developed based on the existing SMP models, respectively. The batch experimental results are used for the model parameter estimation. Third, the SMP model is incorporated into the ASM2d model (Henze et al., 1999) as ASM2dSMP. The ASM2dSMP model is validated using independent experimental results of a lab-scale MBR. Finally, the impact of the MBR operational conditions, e.g., SRT, HRT and SRT/HRT ratio, on the SMP concentration is evaluated using the calibrated ASM2dSMP model. The estimated ASM2d model parameter set conducted in Chapter 4 are adopted in the ASM2dSMP model. The predicted SMP concentration in the bioreactor using the ASM2dSMP model can be used as model input in Chapter 8 to predict the MBR fouling rate.

6.2 Materials and methods

A lab-scale MBR was set up for COD and biological nutrient removal. The reactor was fed on synthetic wastewater with SRT=17 days and HRT=6.4 hrs. A tubular membrane with a nominal pore size of 0.03 μm was used for biomass separation. More details of the MBR setup are given in section 3.1.

Fresh sludge was taken from the aerobic/anoxic compartment of the MBR, washed and used in BAP and UAP batches. Both BAP and UAP batches were conducted under conditions of constant temperature (15 °C) and controlled pH (7.5). The BAP batch experiment was conducted under starvation conditions without external substrate addition. Alternating aeration was conducted to keep the same

aerobic:anoxic time ratio (49.4 minutes aerobic with a DO setpoint of 2 mg/L, 70.6 minutes anoxic) as the lab-scale MBR. The SMP produced in the BAP batch was dominated by BAP since no external substrate was added. The UAP batch experiment was spiked with acetate (end concentration 1000 mg/L) under completely aerobic conditions with a DO setpoint of 2 mg/L. A reference batch was conducted in parallel under the same conditions as the UAP batch but without acetate addition. Thus, the net UAP production is the difference between the UAP batch and reference batch, which eliminates the impact of BAP. More details of the procedure of washing the sludge and the batch experiment are given in section 3.3. The correction of remaining acetate in the UAP batch used the method described below.

In the UAP batch, the external substrate acetate is also measured as SCOD. To eliminate the acetate from the measured SCOD and obtain the net UAP, two approaches have been applied: 1) use LC-OCD (Liquid Chromatography – Organic Carbon Detection) to differentiate SMP from acetate due to the fact that SMP have larger MW than acetate (see Chapter 5). 2) measure the protein and polysaccharide concentration and estimate SMP using Eq.(6.1). The UAP_{COD}, UAP_{PT} and UAP_{PS} are the net UAP concentrations (UAP batch results minus those from the reference batch) as COD, proteins and polysaccharides, respectively. The constants 1.5 and 1.07 are conversion factors from polysaccharides and proteins to COD, respectively, assuming that BSA (bovine serum albumin) represents proteins and dextran represents polysaccharides. The value of 0.64 is a correction factor accounting for the underestimation of polysaccharides and proteins using the colorimetric methods obtained from the relationship of 4 months of measurements in the lab-scale MBR. This is due to the fact that not all polysaccharides and proteins can be quantitatively measured by the colorimetric method (Rosenberger et al., 2005).

$$UAP_{COD} = (1.5UAP_{PT} + 1.07UAP_{PS})/0.64 \qquad\qquad (6.1)$$

The SCOD was obtained using a 0.45 μm filter (DURAPORE 0.45 μm PVDF, Millipore, USA). Proteins and polysaccharides were measured using colorimetric methods (Lowry et al., 1951; Raunkjaer et al., 1994 and Dubois et al., 1956, respectively). The LC-OCD separates the soluble organic matter components according to their molecular weight (MW) and measures them as organic carbon, UV

absorbance at 254 nm and organic nitrogen. The LC-OCD analysis was performed by a commercial lab DOC-LABOR (Dr. Huber, Germany, Huber and Frimmel, 1991; Huber and Frimmel, 1992). More details of sample preparation and analysis can be found in Chapter 5.

Software WEST and Tornado (MOSTforWATER NV, Kortrijk, Belgium) were used to perform model simulations and parameter estimations.

6.3 SMP model development and parameter estimation

BAP and UAP in MBRs are considered separately and their respective models are derived below. The overall strategy is to develop a simple but adequate SMP model with minimum parameter correlation, i.e., an identifiable model. The existing SMP model structures reviewed above were adapted and modified to fit the experimental results. The general assumptions are: 1) SMP are defined to have a size < 0.45 μm and thus LMW SMP can be partially retained by the membrane; 2) both BAP and UAP are produced in the MBR system and their relative significance is determined by the influent characteristics and operational conditions; and 3) both BAP and UAP are biodegradable, with the same yield coefficient (Y_H) but a lower degradation rate than influent substrate.

6.3.1 BAP model and calibration

The production of BAP can be described either as proportional to the biomass decay with a stoichiometric parameter (Boero et al., 1991; Boero et al., 1996) or with a separate rate constant of BAP production (e.g., Rittmann et al., Lu et al.). Basically, both approaches are similar. Due to its simplicity, the former approach is adopted here by introducing a stoichiometric parameter f_{BAP} into the biomass decay concept (death-regeneration) in ASM2d (Henze et al., 2000). Thus, in the BAP model, biomass lysis produces BAP, inert particulate COD (X_I) and slowly biodegradable COD (X_S) (Table 6-1).

Table 6-1 Stoichiometric and kinetics of BAP model (only new items to ASM2d are presented)

Processes	S_F	S_{BAP}	S_I	X_I	X_S	X_H	X_{PAO}	X_{AUT}	rate
Aerobic Hydrolysis of BAP	$1-f_{SI}$	-1	f_{SI}						$k_{h,BAP}\dfrac{S_O}{K_O+S_O}S_{BAP}X_H$
Anoxic Hydrolysis of BAP	$1-f_{SI}$	-1	f_{SI}						$k_{h,BAP}\eta_{HNO3}\dfrac{K_O}{K_O+S_O}\dfrac{S_{NO3}}{K_{NO3}+S_{NO3}}S_{BAP}X_H$
Anaerobic Hydrolysis of BAP	$1-f_{SI}$	-1	f_{SI}						$k_{h,BAP}\eta_{fe}\dfrac{K_O}{K_O+S_O}\dfrac{K_{NO3}}{K_{NO3}+S_{NO3}}S_{BAP}X_H$
Lysis of X_H		f_{BAP}		f_{XI}	$1-f_{XI}-f_{BAP}$	-1			$b_H X_H$
Lysis of X_{PAO}		f_{BAP}		f_{XI}	$1-f_{XI}-f_{BAP}$		-1		$b_{PAO}X_{PAO}\dfrac{S_{ALK}}{K_{ALK}+S_{ALK}}$
Lysis of X_{AUT}		f_{BAP}		f_{XI}	$1-f_{XI}-f_{BAP}$			-1	$b_{AUT}X_{AUT}$

Most early SMP studies assume that biomass can grow on BAP directly (Eq.(6.2)). However, the LC-OCD studies in Chapter 5 suggest that most BAP has a molecular weight (MW) larger than 20 kDa. It is highly unlikely that such large molecules can directly pass the cell membrane without an extracellar hydrolysis process. Typically, the degradation of slowly biodegradable substrate requires a series of steps, as follows: 1) adsorption and storage on the active cell surface; 2) extracelluar enzymatic breakdown of the complex organic molecules to simpler ones; and 3) uptake of the hydrolyzed products. The hydrolysis (step 2) is typically the rate limiting step (Dold et al., 1980). Thus, the first step of BAP biodegradation is more likely hydrolysis and production of readily biodegradable COD, i.e., S_F in ASM2d. The hydrolysis of S_{BAP} is described as Monod type of surface reaction, as in ASM2d (Eq.(6.3)), or as a simple first order reactions with respect to BAP and biomass concentration (Eq.(6.4)).

Direct growth: $\quad r_{S_{BAP}}=-\mu_{BAP}\dfrac{S_{BAP}}{K_{BAP}+S_{BAP}}X_H$ $\qquad\qquad\qquad$ (6.2)

Hydrolysis with Monod type surface reaction: $\quad r_{S_{BAP}}=-k_{h,BAP}\dfrac{S_{BAP}/X_H}{K_{BAP}+S_{BAP}/X_H}X_H$ $\qquad$ (6.3)

Hydrolysis with first order kinetics: $\quad r_{S_{BAP}}=-k_{h,BAP}S_{BAP}X_H$ $\qquad\qquad\qquad$ (6.4)

All three forms of the BAP degradation models (Eq.(6.2)-(6.4)) were evaluated using the experimental results with respect to goodness of fit and identifiability (whether a reasonable estimation of parameter set is allowed) of the model parameters. A Simplex algorithm was used to estimate the parameters. Theoretically, the Monod

shape of BAP hydrolysis models (Eq.(6.2)-(6.3)) has been well known for strong parameter correlation between the reaction rate ($k_{h,BAP}$) and the half-saturation coefficient (K_{BAP}). The first order hydrolysis model, Eq.(6.4), is the easiest structure with only one parameter to estimate.

The parameter estimation of the 3 models is evaluated as follows. First, the complete BAP model using Monod shape structure (Eq.(6.2) and (6.3)) requires 3 parameters, i.e., f_{BAP}, μ_{BAP}, K_{BAP} and f_{BAP}, $k_{h,BAP}$, K_{BAP}. Fitting of the Monod type model encountered difficulties with the Simplex algorithm ending in local minima. This is attributed to the strong parameter correlations. However, the complete BAP model using the first order hydrolysis shape (Eq.(6.4)) only requires 2 parameters to be estimated. It was easy to converge to the same results during the optimisation, even when different initial parameter values were used (Figure 6-1). Thus, the simple first order BAP hydrolysis model was adopted. The confidence level of the parameters was calculated from the parameter estimation error covariance matrix. The Hessian matrix was numerically estimated using the method of Nelder and Mead (1965), resulting in a narrow 95% confidence interval, i.e., $f_{BAP}=0.0215 \pm 0.0021$ and $k_{h,BAP}=(7.41\pm0.54) \times10^{-7}$ 1/d.
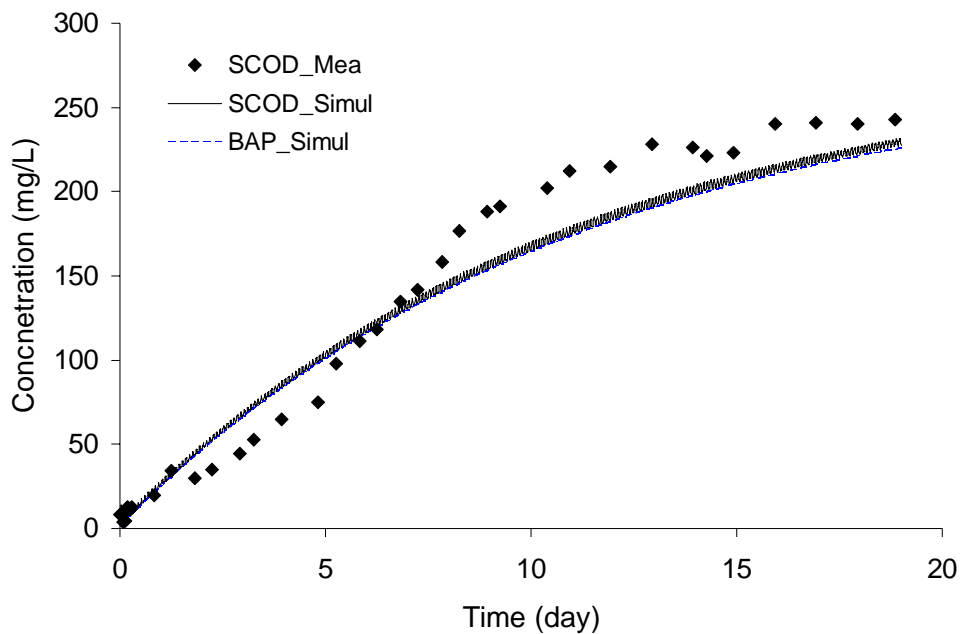
Figure 6-1 Comparison of simulated and measured SCOD in BAP batch

6.3.2 UAP model and calibration

The net UAP production, calculated as the difference of SCOD between the UAP and the reference batch, is presented in Figure 6-2. The UAP was produced immediately after the addition of acetate but the degradation process took place simultaneously. There was net accumulation of UAP between 0-4 hrs, but most of these UAP components were degraded afterwards from 4-8 hrs.
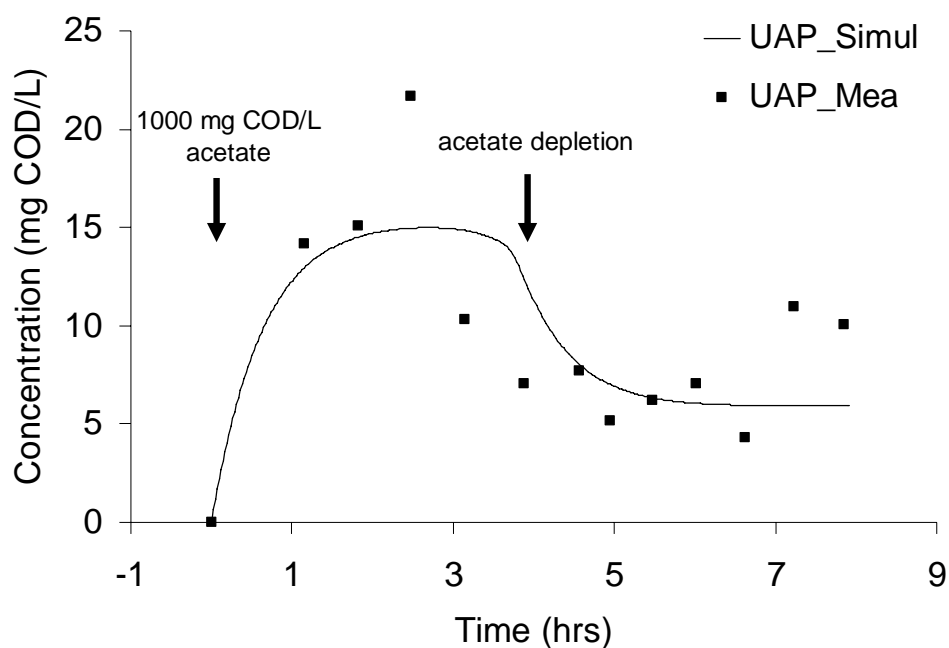
Figure 6-2 Comparison of simulated and measured UAP in UAP batch

The net UAP production, calculated as the difference in DOC signal between the UAP and the reference batch, was also measured using LC-OCD and presented in Figure 6-3. The MW of UAP exhibited a wide range from < 1 kDa to > 20 kDa. The fraction of high MW UAP increased even when substrate was depleted (the biopolymer peak at 23.3 hr was much larger than those at 2 and 6.7 hrs).
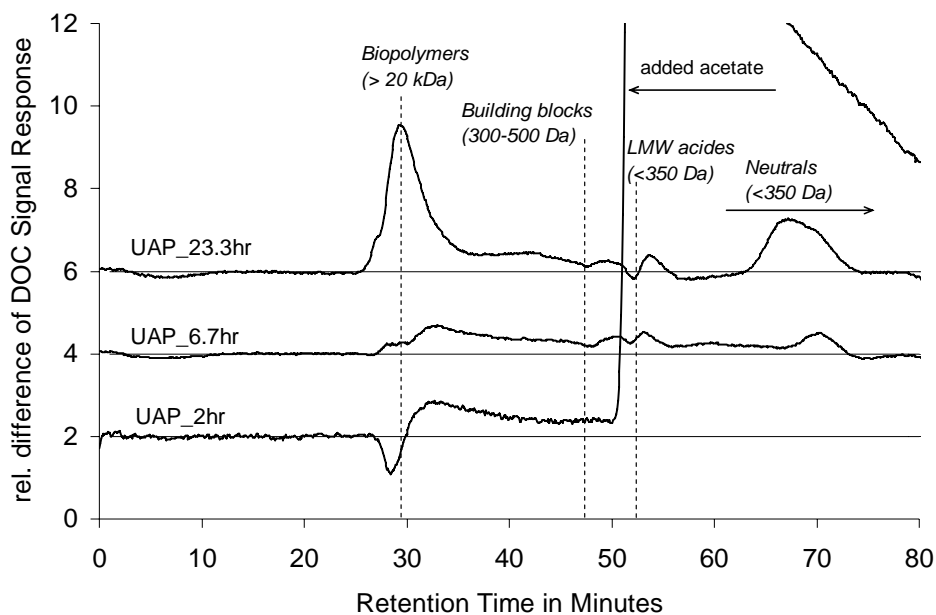
Figure 6-3 Differences of DOC signal between the UAP and the reference batches (net UAP production) measured by LC-OCD

The increase in MW of UAP is consistent with the study of Boero et al. (1996), who used phenol and glucose as substrate. Accoridng to the MW and appearant biodegradability, it is hypothesized that there are two types of UAP produced in the batch process corresponding to two stages of cell growth. In phase 1, heterotrophic biomass take up the readily biodegradable substrate and store them for instance as PHA (polyhydroxyalkanoates), and in phase 2, the cells utilize the stored material and proliferation takes place (van Loosdrecht et al., 1997). Figure 6-3 suggests that the UAP produced in the cell proliferation phase (UAP_{pro}, after 3.85 hr) exhibits higher MW than that produced in the storage phase (UAP_{sto}, before 3.85 hr). In addition, UAP_{pro} is probably more difficult to biodegrade, since these compounds remained in the reactor after one day, while the UAP_{sto} produced in the storage phase was degraded quickly. In this study, a simple substrate, acetate, was used, which is a well known substrate that can easily be stored in the cell as PHB (polyhydroxybutyrate) (van Loosdrecht et al., 1997). The storage phenomenon in the UAP batch was confirmed by a very high apparent yield (Y_H= 0.83) estimated from the OUR (Spanjers and Vanrolleghem, 1995). Unfortunately, the amount of data available in the cell proliferation phase, i.e., from 8 to 24 hrs, is not suffcent to construct a UAP_{pro} model. Thus, only the modelling of UAP_{sto} is presented below according to the net UAP concentration up to 8 hrs.

All UAP models reviewed above describe the UAP production proportional to substrate utilization by introducing a stoichiometric parameter (f_{UAP}). This concept is adopted in the UAP model of this thesis. Thus, substrate is utilized to produce either new cell (Y_H) or UAP (f_{UAP}), or oxidized into CO_2 ($1- Y_H - f_{UAP}$) for energy production (
Table 6-2).

Most SMP studies assume that biomass can directly grow on UAP. Either the same UAP degradation rate as the BAP (Rittmann et al., 1987; Furumai and Rittmann, 1992; Furumai et al., 1998; Lu et al., 2001; Lu et al., 2002) or a separate UAP degradation rate using the Monod shape (Boero et al., 1991; Boero et al., 1996; de Silva et al., 1998; Urbain et al., 1998; Laspidou and Rittmann, 2002b) is assigned. The experimental results of this study clearly demonstrated that the UAP_{sto} with lower MW is biodegradable and probably more readily biodegradable than BAP. Thus, a separate first order kinetic parameter was assigned for the hydrolysis of UAP (Eq.(6.5)). In summary, The UAP model developed in this thesis only used 2 parameters to describe the production and degradation of UAP.

Hydrolysis of first order to UAP: $r_{S_{UAP}} = - k_{h,UAP} S_{UAP} X_H$ (6.5)

The parameter estimation with its 95% of confidence interval resulted in f_{UAP}=0.0963 ± 0.0387 and $k_{h,BAP}$=0.0102 ± 0.0044 1/d, respectively (Figure 6-2). This UAP model and parameters should be applied with caution for the following reasons: 1) the measured UAP had a quite high standard deviation; 2) only UAP_{sto} was included in the model; 3) the simplest substrate, i.e., acetate, was used, while UAP production is substrate specific (Boero et al., 1991; Boero et al., 1996); and 4) a low S_0/X_0 (substrate/MLSS) ratio, i.e., 0.097 in a batch lasting approximately 1 day, was used, which is close to the common F/M ratio of nitrifying activated sludge. It can be expected that a higher S_0/X_0 (substrate/MLSS) ratio will produce a higher percentage of UAP due to more intensive cell proliferation (Hejzlar and Chudoba, 1986a). Further studies are needed to differentiate the UAP produced in the different phases and with more complex substrates, e.g., starch or protein.

Table 6-2 Stoichiometric and kinetics of UAP model (only new items to ASM2d are presented)

Processes	S_O	S_F	S_A	S_{UAP}	S_{NO}	S_I	X_H	X_{PAO}	X_{AUT}	rate
Aerobic Hydrolysis of UAP		$1\text{-}f_{SI}$		-1		f_{SI}				$k_{h,UAP}\dfrac{S_O}{K_O+S_O}S_{UAP}X_H$
Anoxic Hydrolysis of UAP		$1\text{-}f_{SI}$		-1		f_{SI}				$k_{h,UAP}\eta_{HNO3}\dfrac{K_O}{K_O+S_O}\dfrac{S_{NO3}}{K_{NO3}+S_{NO3}}S_{UAP}X_H$
Anaerobic Hydrolysis of UAP		$1\text{-}f_{SI}$		-1		f_{SI}				$k_{h,UAP}\eta_{fe}\dfrac{K_O}{K_O+S_O}\dfrac{K_{NO3}}{K_{NO3}+S_{NO3}}S_{UAP}X_H$
Aerobic growth of X_H on S_F	$-\dfrac{1\text{-}Y_H\text{-}f_{UAP}}{Y_H}$	$-\dfrac{1}{Y_H}$		$\dfrac{f_{UAP}}{Y_H}$			1			$\mu_H\dfrac{S_O}{K_O+S_O}\dfrac{S_F}{K_F+S_F}\dfrac{S_F}{S_A+S_F}\dfrac{S_{NH}}{K_{NH}+S_{NH}}\dfrac{S_{PO}}{K_{PO}+S_{PO}}\dfrac{S_{ALK}}{K_{ALK}+S_{ALK}}X_H$
Aerobic growth of X_H on S_A	$-\dfrac{1\text{-}Y_H\text{-}f_{UAP}}{Y_H}$		$-\dfrac{1}{Y_H}$	$\dfrac{f_{UAP}}{Y_H}$			1			$\mu_H\dfrac{S_O}{K_O+S_O}\dfrac{S_A}{K_A+S_A}\dfrac{S_A}{S_F+S_A}\dfrac{S_{NH}}{K_{NH}+S_{NH}}\dfrac{S_{PO}}{K_{PO}+S_{PO}}\dfrac{S_{ALK}}{K_{ALK}+S_{ALK}}X_H$
Anoxic growth of X_H on S_F		$-\dfrac{1}{Y_H}$		$\dfrac{f_{UAP}}{Y_H}$	$-\dfrac{1\text{-}Y_H\text{-}f_{UAP}}{2.86\,Y_H}$		1			$\mu_H\eta_{NO3}\dfrac{K_O}{K_O+S_O}\dfrac{S_{NO3}}{K_{NO3}+S_{NO3}}\dfrac{S_F}{K_F+S_F}\dfrac{S_F}{S_F+S_A}\dfrac{S_{NH4}}{K_{NH4}+S_{NH4}}\dfrac{S_{PO4}}{K_{PO4}+S_{PO4}}\dfrac{S_{ALK}}{K_{ALK}+S_{ALK}}X_H$
Anoxic growth of X_H on S_A			$-\dfrac{1}{Y_H}$	$\dfrac{f_{UAP}}{Y_H}$	$-\dfrac{1\text{-}Y_H\text{-}f_{UAP}}{2.86\,Y_H}$		1			$\mu_H\eta_{NO3}\dfrac{K_O}{K_O+S_O}\dfrac{S_{NO3}}{K_{NO3}+S_{NO3}}\dfrac{S_A}{K_A+S_A}\dfrac{S_A}{S_F+S_A}\dfrac{S_{NH4}}{K_{NH4}+S_{NH4}}\dfrac{S_{PO4}}{K_{PO4}+S_{PO4}}\dfrac{S_{ALK}}{K_{ALK}+S_{ALK}}X_H$
Aerobic growth of X_{PAO}	$-\dfrac{1\text{-}Y_H\text{-}f_{UAP}}{Y_H}$			$\dfrac{f_{UAP}}{Y_H}$				1		$\mu_{PAO}\dfrac{S_O}{K_O+S_O}\dfrac{S_{PO}}{K_P+S_{PO}}\dfrac{S_{NH}}{K_{NH}+S_{NH}}\dfrac{S_{ALK}}{K_{ALK}+S_{ALK}}\dfrac{X_{PHA}/X_{PAO}}{K_{PHA}+X_{PHA}/X_{PAO}}X_{PAO}$
Anoxic growth of X_{PAO} on NO_3^+				$\dfrac{f_{UAP}}{Y_H}$	$-\dfrac{1\text{-}Y_H\text{-}f_{UAP}}{2.86\,Y_H}$			1		$\eta_{NO3}\mu_{PAO}\dfrac{K_O}{K_O+S_O}\dfrac{S_{NO3}}{K_{NO3}+S_{NO3}}\dfrac{S_{PO}}{K_P+S_{PO}}\dfrac{S_{NH}}{K_{NH}+S_{NH}}\dfrac{S_{ALK}}{K_{ALK}+S_{ALK}}\dfrac{X_{PHA}/X_{PAO}}{K_{PHA}+X_{PHA}/X_{PAO}}X_{PAO}$
Growth of X_{AUT}	$-\dfrac{4.57-Y_A-f_{UAP}}{Y_A}$			$\dfrac{f_{UAP}}{Y_H}$	$\dfrac{1}{Y_A}$				1	$\mu_{AUT}\dfrac{S_O}{K_{OAUT}+S_O}\dfrac{S_{NH}}{K_{NHAUT}+S_{NH}}\dfrac{S_{PO}}{K_{PO}+S_{PO}}\dfrac{S_{ALK}}{K_{ALK}+S_{ALK}}X_{AUT}$

Table 6-3 Comparison of SMP model parameters

	Decay model	b_H	k_2 (1/d, BAP)	f_{BAP} (-)	f_{UAP} (-)	μ_{SMP}	μ_{BAP}	μ_{UAP}	K_{SMP}	K_{BAP}	K_{UAP}	note
Namkung and Rittmann, 1986	endo.	0.15	0.017		0.19							biofilm model
Rittmann et al., 1987	endo.	0.1	0.2		0.18	2.5[C]						Tracer [14]C
Furumai and Rittmann, 1992	endo.	0.1	0.1		0.2	0.5[C]						
Furumai et al., 1998	endo.	0.1	0.1		0.2	0.5[C]						
Urbain et al., 1998[M]	endo.	0.1	0.1		0.2		0.348[C]	0.228[C]		70	24	
de Silva et al., 1998[M]	endo.	0.1	0.1		0.2		0.348[C]	0.228[C]		70	24	
Laspidou and Rittmann, 2002b	endo.	0.74	0.17		0.05		0.0315[C]	0.57[C]		85	100	Unified theory
Boero et al., 1991	endo.		phenol	0.039	0.13			0.028[C]				Tracer [14]C
			glucose	0.037	0.025			0.0078[C]				
Lu et al., 2001[M]	regrow	0.22	0.398		0.38	0.7			30			ASM1
Lu et al., 2002[M]	endo.	0.2	0.01		0.3	2.5			60			ASM3
This study[M]	regrow			0.0215	0.0963		7.41×10^{-7} [H]	0.0102 [H]				ASM2dSMP

[M] in MBR
[H] first order hydrolysis rate
[C] growth rate of biomass was converted from substrate utilization rate using ($\mu=Y_q$)

6.4 Comparison of the SMP model with literature

The SMP model parameters obtained in this study are compared with literature values in

Table 6-3. All model parameters showed a large variation. The production rate of BAP ($k2$) varied from 0.01 to 0.398 1/d, and the fraction of UAP production with respect to substrate varied from 0.025 to 0.2. This can be partially attributed to the diversity of the studied biological systems (biofilm, activated sludge process, and MBR) and substrates (phenol, glucose and acetate, etc.). Another important cause of the diversity is the poor identifiability of the model structures. Some models, e.g., Lu et al. (2001, 2002), introduced 8 parameters, but the experimental results were limited to SCOD measurement, which lumps together BAP, UAP, inert soluble COD and readily biodegradable COD.

Thus, the development of the SMP model in this study aimed at obtaining the simplest adequate model, by minimising parameter correlations. To solve parameter estimation problems, new experiments were conceived. Batch experiments were introduced for BAP and UAP separately to reduce the correlation between BAP and UAP and increase the amount of experimental results under dynamic conditions. The model structure development was based on the observation of dynamic batch experiments, which demonstrated that individual rates should be assigned to BAP and UAP production and degradation. A biomass growth model using Monod kinetics was evaluated not to be identifiable. Instead, a first order hydrolysis model was adopted. Eventually, only 4 additional SMP related parameters were adopted allowing reasonable parameter confidence bounds.

6.5 SMP model validation in a lab-scale MBR

The SMP model was incorporated into the ASM2d model (Henze et al., 1999) as ASM2dSMP, which is able to describe COD, nitrogen and phosphorus removal as well as SMP. The ASM2dSMP was validated using independent experimental results of a lab-scale MBR. The calibrated ASM2dSMP parameters used for model validation are listed in Table 6-4.

Table 6-4 Calibrated parameters of ASM2dSMP and comparison with the default ASM2d parameter values

Parameter	Unit	ASM2d_calibrated value	method	ASM2dSMP_calibrated value	method	ASM2d_default
b_{AUT}	1/d	0.055	batch test	0.055	batch test	0.15
$i_{N,XS}$	gN /gCOD	0.035	measure	0.035	measure	0.04
$i_{P,SF}$	gP /gCOD	0	measure	0	measure	0.01
$i_{P,XS}$	gP /gCOD	0.005	measure	0.005	measure	0.01
$K_{NH,AUT}$	mg N/L	0.2	fit	0.2	fit	1
$K_{O,AUT}$	mg O2/L	0.2	fit	0.2	fit	0.5
μ_{AUT}	1/d	0.6	fit	0.6	fit	1
$\eta_{NO,Het}$	-	1	fit	1	fit	0.8
$\eta_{NO,PAO}$	-	0.4	fit	0.6	fit	0.6
Q_{fe}	1/d	1	fit	3	fit	3
Q_{PHA}	1/d	5	fit	6	fit	3
Q_{PP}	1/d	1.1	fit	1.3	fit	1.5
Y_H	mg COD/mg COD	0.625	default	0.57	mass balance	0.625
Y_{PAO}	mg COD/mg COD	0.625	default	0.57	mass balance	0.625
f_{BAP}	-	n.a.		0.0215	batch test	n.a.
$k_{h,BAP}$	1/d	n.a.		7.41×10^{-7}	batch test	n.a.
f_{UAP}	-	n.a.		0.0963	batch test	n.a.
$k_{h,UAP}$	1/d	n.a.		0.0102	batch test	n.a.
$f_{nf,SMP}$	-	n.a.		0.07	measure + fit	n.a.
$i_{N,SMP}$	gN /gCOD	n.a.		0.07	assume	n.a.
$i_{P,SMP}$	gP /gCOD	n.a.		0.02	assume	n.a.

Note: fit = fit the parameter to the results of measurement campaign and 4-month average effluent

Most ASM2d-related parameters were adapted directly from the calibrated ASM2d model presented in Chapter 4 . However, a few parameters were adjusted. First, the parameters obtained from the batch experiments were directly transferred without adjustment.

Second, the retention percentage of SMP by the membrane was estimated to be 93.2% by assuming S_I =4 mg/L as in Chapter 4. To obtain a better fitting of SCOD in the membrane loop, the retention percentage was slightly decreased to 91.9%, i.e., the non-retained SMP fraction, $f_{nr,SMP}$ is increased to 0.081. This adjustment is acceptable given the uncertainty in the influent S_I. A S_I of 2.5 mg/L will result in $f_{nr,SMP}$ = 0.081.

Third, the yield of X_H and X_{PAO} growth had to be adjusted according to the COD mass balance as a result of the change from ASM2d to ASM2dSMP. In ASM2dSMP, a

portion of the influent substrate COD was directed to UAP production, allowing the X_H and X_{PAO} to grow on UAP after its hydrolysis. Thus, if Y_H and Y_{PAO} remain the same, the actual biomass yield will increase and the fraction of oxidized COD will decrease. To compensate for this change in the COD mass balance, Y_H and Y_{PAO} were decreased from 0.625 to 0.57 according to Eq.(6.6). The validity of this adjustment follows the fact that the same simulated total waste sludge COD is obtained in both models (see Table 4-2).

Fourth, The PAO-related parameters ($\eta_{NO,PAO}$, Q_{PHA}, Q_{fe}, Q_{PHA}, Q_{PP}) were adjusted to increase the anaerobic acetate uptake and the aerobic/anoxic phosphorus uptake. It should be noted that the calibrated ASM2d model in Chapter 4 had a reduced biological phosphorus removal to fit the effluent and in-cycle measurements. The production of UAP in the ASM2dSMP model delayed the production of acetate available for PAO uptake and enabled to restore some PAO-related parameters to their default ASM2d values. It appears that the reduced fermentation rate and aerobic/anoxic phosphorus uptake rate obtained in the calibration of ASM2d model were compensating for overlooking the UAP generation. However, further studies are needed to draw a strong conclusion.

$$Y_{ASM2d,SMP} = \frac{Y_{ASM2d}}{(1+f_{UAP})} \tag{6.6}$$

The comparison of ASM2dSMP model predictions with ASM2d and experimental results is presented in **Table 6-5**. The simulated total COD of sludge and effluent SCOD, NH_4^+-N, NO_3^--N and PO_4^{3-}-P using ASM2dSMP showed excellent agreement with measurement results. However, the ASM2d failed in predicting the SCOD concentration in the bioreactor, e.g., the predicted SCOD in the membrane loop (4.5 mg/L) was well below the measurement (87.4 mg/L). However, the prediction using ASM2dSMP (92.5 mg/L) was very good.

Table 6-5 Comparison of ASM2dSMP model simulation with experimental results

Sample	Item (Unit)	Values			
		4-month average	Standard deviation	Simulation (ASM2d)	Simulation (ASM2dSMP)
Waste sludge	Total COD (g COD/L)	10.90	0.65	10.83	10.85
Sludge water[1] (from waste sludge)	SCOD (mg COD/L)	87.4	22.7	4.5	92.5
	BAP (mg COD/L)	n.a.	n.a.	n.a.	77.5
	UAP (mg COD/L)	n.a.	n.a.	n.a.	10.5
Sludge water[1] (from membrane loop)	SCOD (mg COD/L)	107.4	33.4	5.0	107.5
	BAP (mg COD/L)	n.a.	n.a.	n.a.	90.8
	UAP (mg COD/L)	n.a.	n.a.	n.a.	11.6
Effluent	COD (mg COD/L)	11.0	3.1	5.0	13.2
	BAP (mg COD/L)	n.a.	n.a.	n.a.	7.3
	UAP (mg COD/L)	n.a.	n.a.	n.a.	0.9
	TN (mg N/L)	10.2	2.8	8.8	9.6
	NH_4^+-N (mg N/L)	0.18	0.42	0.18	0.4
	NO_3^--N (mg N/L)	7.03	1.71	8.6	8.6
	NO_2^--N (mg N/L)	0.30	0.21	n.a.	n.a.
	Norg.[2] (mg N/L)	2.61	1.43	0.0	0.6
	PO_4^{3-}-P (mg P/L)	5.63	2.21	5.3	5.7

[1] sludge water = sludge filtrate using 0.45μm membrane filter

[2] Norg. = TN – NH_4^+-N – NO_2^--N – NO_3^--N

6.6 Impact of operational conditions on SMP build up in MBRs

The production of SMP is determined in a large extent by the operational conditions of an activated sludge process. SRT may have the largest impact. Rittmann et al. (1987) reported that the SMP/S_0 ratio had a minimum value at a SRT of 2 days. This model was validated by the experimental results of Grady et al. (1972) and Siber and Eckenfelder (1980). More recently, Pribyl et al. (1997) reported a minimum SMP/S_0 ratio of 5-15 days in both SBR and CFSR reactors.

The definition of BAP and UAP suggests that operating an activated sludge process under low SRTs may result in UAP-dominated SMP, while operating under long SRTs may result in BAP-dominated SMP. This hypothesis was evaluated using the lab-scale MBR and the calibrated ASM2dSMP model. The influent flow rate, concentration, internal recirculation rate, and DO setpoint were fixed. However, the

amount of sludge wastage (approach 1) and the volume of the three compartments (approach 2) were varied proportionally. Approach 1 fixed the HRT, but varied the SRT and the SRT/HRT ratio; while approach 2 fixed the SRT/HRT ratio, but varied the SRT and HRT. The oxygen transfer coefficient $K_L a$ was adjusted in some simulations to ensure that the DO setpoint (2 mg/L) was reached. The simulation was performed for 500 days to reach steady state.

The steady state concentrations of BAP, UAP and SCOD in the membrane loop and the total sludge concentration are presented in Figure 6-4. Under fixed HRT and varying SRT/HRT ratio conditions (left), the SMP concentration increases when the SRT is increased in spite of the fixed HRT. However, under the fixed SRT/HRT ratio conditions (right), the SMP concentration increased in spite of the decreasing sludge concentration. In addition, operating a MBR under a lower SRT increases UAP production but decreases BAP production. However, the MBR system is dominated by BAP at SRTs above 2 days, which suggests that MBRs should not operate at too long SRTs from the viewpoint of controlling the SMP concentration and minimizing membrane fouling. In conclusion this simulation clearly supports the hypothesis that SRT strongly affects the SMP concentration in the MBR system.
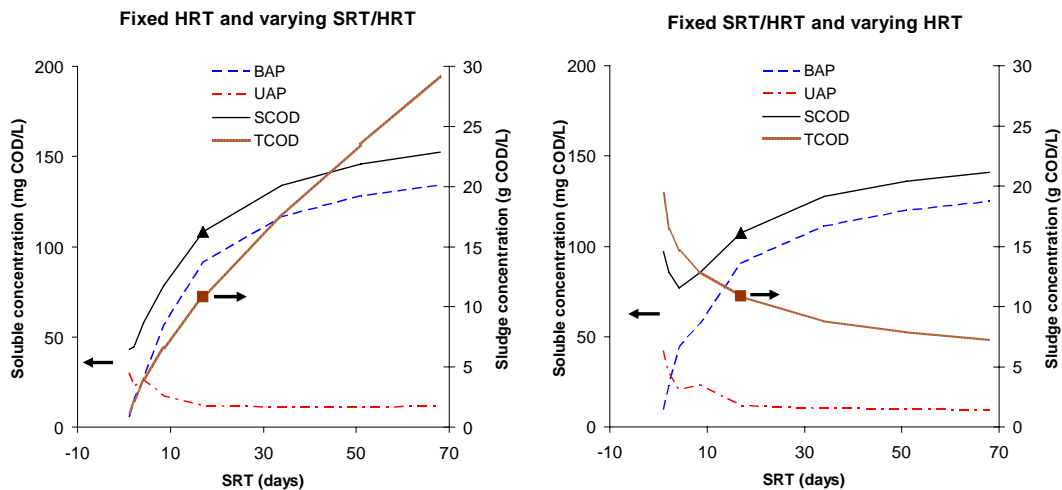

Figure 6-4 The impact of SRT on SMP and sludge concentration (lines = simulation results, ▲ = measured SCOD, ■ = measured TCOD)

However, it should be noted that the simulated SMP concentrations were obtained under steady state conditions. Stressed conditions may stimulate the production of

SMP, e.g., periodical waste sludge (leading to a sudden increase in sludge loading) (Drews et al., 2006), nutrient (nitrogen and phosphorus) deficiency (Aquino and Stuckey, 2003), copper addition (2 mg/L) (Holakoo et al., 2006), high salinity (Reid et al., 2006), and high monovalent-to-divalent cation ratio (Murthy and Novak, 2001), etc. Maintaining a large amount of sludge and higher SRT conditions in MBR systems may provide a better stability under dynamic and stressed conditions and improve the robustness of the system.

6.7 Conclusions

The development of the SMP model in this study aimed at obtaining the simplest adequate model, by minimising parameter correlations. A BAP and UAP model was developed based on the existing SMP models, and care was taken of the identifiability of model structures. Batch experiments were designed for BAP and UAP model calibration separately to reduce the correlation between BAP and UAP and increase the amount of experimental results under dynamic conditions. In total, 4 additional SMP related parameters were adopted allowing reasonable parameter confidence bounds. The parameter estimation of the BAP model resulted in a narrow 95% confidence interval, i.e., $f_{BAP} = 0.0215 \pm 0.0021$ and $k_{h,BAP} = (7.41 \pm 0.54) \times 10^{-7}$ 1/d, while the parameter estimation of the UAP model resulted in $f_{UAP} = 0.0963 \pm 0.0387$ and $k_{h,BAP} = 0.0102 \pm 0.0044$ 1/d.

The SMP model was incorporated into the ASM2d model as ASM2dSMP and validated using independent experimental results of the lab-scale MBR. The SMP-related parameters obtained from the batch experiments were directly transferred to the continuous MBR without adjustment. The retention percentage of SMP by the membrane was slightly decreased from 93.2% to 91.9% to obtain a better fitting of SCOD in the membrane loop, given the uncertainty in the estimation of SMP retention percentage. The simulated SCOD concentration (107.5 mg/L) was very close to the measurement (107.4 mg/L) by introducing the BAP and UAP concept, while the standard ASM2d model failed in predicting the SCOD (the simulated SCOD was only 5.0 mg/L). The ASM2dSMP model was also capable of simulating the nitrogen and phosphorus removal with some adjustment of biomass yields (to balance the COD) and PAO-related parameters (to increase the anaerobic acetate uptake and

the aerobic/anoxic phosphorus uptake). Many PAO-related parameters in the ASM2dSMP model could be restored to their default ASM2d values. It appears that the reduced rates of the anaerobic acetate uptake and the aerobic/anoxic phosphorus uptake obtained in the calibration of the ASM2d model was for the purpose of compensating overlooking the UAP generation. However, further studies are needed to draw a strong conclusion.

Finally, the impact of the MBR biology on the SMP concentration was evaluated using the ASM2dSMP model. Simulations suggests that SRT exhibits a strong impact on the SMP concentration in the MBR system, while, the impact of HRT and SRT/HRT ratio is indirect. Operating a MBR under lower SRT conditions increases UAP production but decreases BAP production. The lab-scale MBR system is dominated by BAP at SRTs above 2 days, which suggests that MBRs should not be operated at too long SRTs from the viewpoint of controlling the SMP concentration and minimizing membrane fouling.

However, the limitation of the model should also be addressed. The UAP experiment used acetate as a substrate and two types of UAP, i.e., UAP_{sto} produced during acetate storage and UAP_{pro} produced during cell proliferation, were identified. However, only UAP_{sto} was modelled and the simulated UAP concentration using the ASM2dSMP model can be considered as the minimum amount of UAP produced by biomass, which cannot reflect a complete UAP picture. UAP studies using more complex substrate are recommended, and UAP_{pro} should also be studied in the model in the future.

7.

Hydrodynamic control of submicron particle deposition[1]

7.1 Introduction

Membrane fouling and high energy consumption are the main drawbacks of membrane bioreactors (MBR). It is generally accepted that biology, membrane characteristics, configuration, and operational conditions of membrane modules all play important roles in membrane fouling control. Hydrodynamic methods, e.g. crossflow filtration, have been applied in membrane fouling control in many micro and ultrafiltration processes. In MBR processes, intensive coarse bubble aeration is often applied in submerged MBRs, while high velocity sludge recirculation (or a mixture of sludge and air) is often applied in side-stream MBRs. However, these hydrodynamic foulilng control methods are also attributed to the high energy consumptions in MBRs.

The composition of activated sludge in MBRs is very complex, and includes natural organic matter (hundreds to thousands Da) introduced from potable water, SMP (or called soluble EPS) produced by the biomass (a few thousand Da to a few million Da), viruses and single bacterial cells (a few dozen nm to a few μm) and protozoa and flocs (a few μm to a few hundred μm) etc. Some early studies on the relative contribution of each sludge fraction (solutes, colloids and particulates) to membrane fouling appeared contradictive, Wisniewski and Grasmick (1998) reported 52%, 25% and 23%; Defrance et al. (2000) reported 5%, 30% and 65%; and Bouhabila et al. (2001) reported 25%, 50% and 24% respectively. However, more recent studies revealed that the SMP in the sludge water phase were closely correlated with MBR fouling. Rojas

et al. (2005) reported that the change in the filtration resistance was positively correlated with the COD in the sludge supernatant, and specifically the protein concentration. Lesjean et al. (2005) and Rosenberger et al. (2006) used size exclusion chromatography (SEC) to analyze the sludge water phase and concluded that the large organic molecules present in the sludge water phase (i.e., polysaccharides, proteins and organic colloids)   impacted the MBR fouling. Rosenberger et al. (2006) summarized 6 MBR case studies of different European research groups. The results showed a clear relevance of sludge liquid phase constituents, either colloidal or soluble, with membrane fouling. te Poele et al. (2004) fractionated sludge water into a series of fractions according to their sizes and concluded that the colloidal particles in a range of 0.1-0.45 µm had the most significant contribution to the filterability of WWTP effluent. The significance of SMP (in colloidal range) in connection with membrane fouling requires the study of submicron particle deposition under MBR operational conditions.

The hydrodynamics of tubular membrane systems were intensively studied in the 1980's and 1990's. An excellent review was provided by Belfort et al. (1994) on particle backtransport mechanisms and models, including the concentration polarisation (Brownian diffusion) model, the shear-induced diffusion model and the inertial lift model. Tardieu et al. (1998) applied these models to compare fouling rates at different crossflow velocities and filtration fluxes in a side-stream MBR equipped with tubular membranes. The simulation showed that increasing crossflow velocity improved particle backtransport and reduced membrane fouling. The simulation results were confirmed by experiments (Tardieu et al., 1998; Tardieu et al., 1999). Tardieu et al. focussed on fouling resulting from large particles (above one micrometer), and less attention was paid to the colloidal particles and macromolecules. In addition, Tardieu et al. employed crossflow velocities in the range 2-4 m/s and TMP's up to 2 bar. However, the new generation of side-stream MBRs in operation today usually employ a suction pump on the permeate side of the membrane, allowing operating the membrane at low TMP (0.05-0.2 bar) and low CF (0.5-1 m/s) to save energy (Gander et al., 2000; Jiang et al., 2003). For example, the new concept air lift is applied with reduced energy consumption (Cui et al., 1997).

This study attempts to correlate the deposition of submicron particles with membrane fouling in the new generation of energy efficient side-stream MBRs. LC-OCD was employed to determine the particle size distribution of submicron particles (Huber and Frimmel, 1991). The objectives of this study are to 1) to evaluate the deposition of submicron particles (mostly SMP) under crossflow conditions; 2) further develop existing hydrodynamic models by incorporating energy consumption into them; 3) quantify the cost-effectiveness of crossflow in the control of submicron particle deposition and 4) optimize the operational conditions of side-stream MBR systems using the improved model.

In this chapter, first, an existing hydrodynamic model is further developed by incorporating energy consumption. Second, a lab-scale MBR and the methods used in separating SMP are described. Third, the method and conditions of simulation and sensitivity analysis are presented. Fourth, the impact of crossflow velocity and particle radius on particle deposition is highlighted. Sensitivity analysis was used as a tool to identify the most influential operational variables. Thereafter, a theoretical optimization of MBR operation is performed aiming at finding optimal operational conditions to maximize the energy efficiency. Finally, operating a MBR under the minimum crossflow velocity conditions, suggested by the theoretical optimisation, is evaluated under practical considerations. It should be noted that only a very simple hydrodynamic model (physical aspects), without considering the interactions between the SMP and flocs, are proposed to provide a rough estimation of SMP deposition.

The biological and chemical aspects of SMP have been discussed in Chapter 5 and 6. The physical aspectics of SMP deposition will be studied in this chapter. Combining the physical and biological aspects of SMP yields the integrated MBR fouling model presented in Chapter 8 (Figure 1-1).

7.2 Theory

7.2.1 Flow in the membrane tube

The Reynolds number (Re) of the sludge circulating in a membrane tube can be estimated by $\rho_f U D / \eta_f$, where U is the crossflow velocity (m/s), D is the membrane

tube diameter (m) and η_f is the feed sludge viscosity (Pa s) (White, 1986). The specific density of feed activated sludge (ρ_f, kg/m^3) can be estimated by DS + 1000(1-DS/ρ_{DS}), where ρ_s (kg/ m^3) is the specific density of dry solids, ρ_{DS}=1250 kg/m^3 (Tchobanoglous et al., 2003) and DS (g/l) is the dry solid contents of the activated sludge.

An activated sludge leads to typical non-Newtonian flow. The sludge viscosity decreases with increasing shear rate and approaches a constant, the "limit viscosity". Considering the high shear rate (typically >1000 1/s calculated in the subsequent sections of this paper) in the membrane tube of side-stream MBRs, the "limit viscosity" often applies. The activated sludge viscosity can be expressed as a function of the dry solid contents, which can be determined by an exponential law (Eq.(7.1), Tixier et al., 2003).

$$\eta_f = 9.968 \times 10^{-4} e^{0.0934DS} \tag{7.1}$$

To evaluate the validity of this empirical equation under high SMP conditions, a series of experiments was conducted to compare the viscosity of a whole MBR sludge, washed sludge (replace the sludge water with the synthetic inorganic solution making MBR influent), SMP (87.4 mg COD/L) and tap water. It was found the whole sludge and the washed sludge showed almost the same viscosity and the sludge water and tap water showed almost the same viscosity. Thus, Eq.(7.1) including DS only appears valid for MBR sludge with high SMP concentrations.

The temperature effect on viscosity can be estimated by Eq.(7.2) (White, 1986), where T_0 and T are the absolute temperature in the field and standard condition (293.15 K); η_{f0} and η_f are the corresponding viscosity; $a = -1.94$; $b = -4.80$ and $c = 6.74$. However, it should be noted that Eq.(7.1) and (7.2) are empirical and not optimised for this study. The actual sludge viscosity may deviate from the values derived from them.

$$\ln \frac{\eta_f}{\eta_{f0}} \approx a + b\left(\frac{T_0}{T}\right) + c\left(\frac{T_0}{T}\right)^2 \tag{7.2}$$

7.2.2 Headloss, shear stress and shear rate in the membrane tube

The headloss of feed sludge passing through the membrane tube (h_f, m water column) can be estimated by $f\dfrac{L}{D}\dfrac{U^2}{2g}$, where f is the Darcy friction factor determined by Eq.(7.3) and Eq.(7.4) and L is the membrane tube length (m) (White, 1986).

$$f = 64/\text{Re} \qquad\qquad (\text{Re} < 2300) \qquad\qquad (7.3)$$
$$f = 0.316\text{Re}^{-1/4} \qquad\qquad (\text{Re} > 2300) \qquad\qquad (7.4)$$

The wall shear stress (τ_w, Pa) and shear rate (γ_w, 1/s) at the surface of the membrane can be estimated from Eq.(7.5) and (7.6) (White, 1986).

$$\tau_w = f\rho_f U^2/8 \qquad\qquad\qquad\qquad (7.5)$$
$$\gamma_w = \tau_w / \eta_f \qquad\qquad\qquad\qquad (7.6)$$

7.2.3 Energy consumption of the membrane module

Only energy consumption associated with the membrane (module) in the side-stream MBR is considered in this study. Energy consumption in the biological process is beyond the scope of this study. Energy consumption due to the crossflow in the membrane tube and the suction pump (E_c and E_f, Watt) can be estimated using Eq.(7.7) and (7.8), where Q_f and Q_p are the volumetric flow rates through the membrane tube (m^3/s); ρ_p is the density of permeate (kg/m^3); ΔP_f is the pressure difference during filtration (Pa).

$$E_c = Q_f \rho_f g h_f \qquad\qquad\qquad\qquad (7.7)$$
$$E_f = Q_p \Delta P_f \qquad\qquad\qquad\qquad (7.8)$$

The specific energy consumption to obtain a net unit volume of filtrate ($\hat{E}_c$, J/m^3) due to the crossflow can be estimated by Eq.(7.9), where J_f is the filtration flux (gross flux, m/s); J_{BW} is the backwashing flux (m/s); t_f and t_{BW} are the duration of one filtration and backwashing cycle (s); t_{tot} is the total cycle time (filtration + backwashing) (s); and A is the total membrane surface area (m^2).

$$\hat{E}_c = \frac{Q_f \rho_f g h_f t_{tot}}{\int\limits_{t=0}^{t_f} J_f * A * dt - \int\limits_{t=0}^{t_{BW}} J_{BW} * A * dt} \qquad (7.9)$$

Similarly, the specific energy consumption to obtain a net unit volume of filtrate ($\hat{E}_f$, J/m^3) due to filtration (suction and backwashing) can be estimated using Eq.(7.10), where ΔP_{BW} is the pressure difference during backwashing (Pa).

$$\hat{E}_f = \frac{\int\limits_{t=0}^{t_f} J_f * A * \Delta P_f * dt + \int\limits_{t=0}^{t_{BW}} J_{BW} * A * \Delta P_{BW} * dt}{\int\limits_{t=0}^{t_f} J_f * A * dt - \int\limits_{t=0}^{t_{BW}} J_{BW} * A * dt} \qquad (7.10)$$

The specific total energy consumption of the membrane filtration module ($\hat{E}_{tot}$, J/m^3) can be easily obtained by the sum of $\hat{E}_c$ and $\hat{E}_f$.

7.2.4 Particle backtransport velocity

When particles enter the membrane tube and come close to the membrane surface, two forces are imposed on particles, i.e., the convective force towards the membrane surface (due to the drag force of permeation flow) and the shear force (due to crossflow velocity). The particle backtransport mechanisms include concentration polarisation (Brownian diffusion, influencing small colloids), shear-induced diffusion and inertial lift (influencing big particles) (Davis, 1992; Belfort et al., 1994). However, recent investigations reported that particle-particle and particle-membrane interactions (including entropy, van der Waals interactions and electrostatic interactions) may also play important roles in particle transportation to/from the membrane surface, especially in concentrated solutions of colloidal particles (Davis, 1992; Bowen and Sharif, 1998).

Brownian diffusion is a random movement resulting from the bombardment of particles by water molecules. The Brownian diffusion coefficient D_B (m^2/s) can be estimated from the Stokes-Einstein relationship (Eq.(7.11)) (Davis, 1992), where k is

the Boltzmann constant (1.38×10^{-23} kg m^2/s^2), T is the absolute temperature (K) and *a* is the particle radius (m), assuming spherical particles.

$$D_B = \frac{kT}{6\pi\eta_f a} \tag{7.11}$$

Trettin and Doshi derived the particle backtransport velocity due to Brownian diffusion J_B (m/s) for a dilute solution under laminar flow (Eq.(7.12), Belfort et al., 1994), where Φ_b and Φ_w are the particle volume fraction in the bulk and at the edge of the cake layer respectively (-). Combining Eq.(7.11) and (7.12) yields Eq.(7.13).

$$J_B = 1.31(\frac{\gamma_w D_B^2}{L}\frac{\Phi_w}{\Phi_b})^{1/3} \tag{7.12}$$

$$J_B = 0.185(\frac{\gamma_w k^2 T^2}{\eta_f^2 a^2 L}\frac{\Phi_w}{\Phi_b})^{1/3} \tag{7.13}$$

The Brownian diffusion model underestimates the particle backtransport, and the deviation is more pronounced for large particles and at high shear rate conditions (Belfort et al., 1994). A possible explanation for this phenomenon may be that some other backtransport mechanisms are not included in the model. To solve the problem, a possible mechanism, the shear-induced hydrodynamic diffusivity model, was introduced by Zydney and Colton (1986). Shear-induced diffusion occurs because individual particles undergo random displacements from the streamlines in a shear flow as they interact with and tumble over other particles. Davis and Sherwood (1990) further developed the shear-induced diffusion model, and the backtransport velocity due to shear-induced diffusion (J_s) for a dilute solution ($\Phi_b < 0.1$) is as follows:

$$J_s = 0.072\gamma_w(\frac{a^4}{L}\frac{\Phi_w}{\Phi_b})^{1/3} \tag{7.14}$$

In addition, an inertial lift mechanism was also proposed by Belfort and co-workers (Green and Belfort, 1980; Drew et al., 1991). Inertial lift involves a lateral migration of particles, which transports particles away from the membrane. The backtransport

velocity due to inertial lift (J_I) of spherical particles in a dilute suspension under fast laminar flow conditions (channel Reynolds numbers large compared to unity) can be estimated as follows (Belfort et al., 1994):

$$J_I = 0.036 \frac{\rho_f a^3 \gamma_w^2}{\eta_f} \qquad (7.15)$$

These three particle backtransport mechanisms work simultaneously, and the total backtransport velocity (J_{tot}) is assumed to be the sum of them. The contribution of the individual mechanisms to the total backtransport velocity mainly depends on particle size and crossflow velocity etc., which will be illustrated in section 7.5.1.

However, it should be noted that MBR sludge exhibits a wide particle size distribution; the particles are not sphere and rigid and they may deform, aggregate and break up; the particle particle interactions (e.g. electrical forces) may play a role for colloidal particles. All these aspects are not considered in these simple hydrodynamic models. Thus care should be taken in use of these simple models.

7.3 Experimental

A side-stream lab-scale MBR system for biological COD, nitrogen and phosphorus removal equipped with a tubular UF module with a total membrane surface area of $0.17 \, m^2$ (X-Flow, the Netherlands) was designed and built for this study. The PVDF membrane had a nominal pore size of 0.03 μm, a tube diameter of 5.2 mm and a length of 1 m. The only differences between this lab-scale X-Flow module and a full-scale module are the tube length (3 m in a full-scale) and the number of tubes in a module (600 in full-scale).

The sludge water phase was fractionated by centrifugation and subsequent filtration. Firstly, the sludge was centrifuged at 2000 rpm (534 G) for 5 minutes to remove large flocs. The supernatant was first filtered through a glass microfibre filter (GF/C, 1.2μm, Whatman, UK) and thereafter, the second filtration step was performed using a flat sheet microfiltration membrane (DURAPORE 0.45 μm PVDF, Millipore, USA) in a

stirred cell (Stirred Cell 8200, Millipore, USA). The two-step filtration avoided the build up of a thick filter cake. The final permeate is defined as the water phase of the sludge including colloids, macroorganic matters and solutes.

The sludge was filtered using a stirred cell unit (Stirred Cell 8200, Millipore, USA). However, the stirred cell unit was not stirred during operation in order to have dead-end filtration. A flat sheet 0.03 μm PVDF membrane was specially made for these batch filtration tests (X-flow, the Netherlands) with exactly the same material, structure and morphology as the tubular membrane employed in the lab and full-scale MBR systems. The feed was supplied by a constant head high level tank (TMP = 14.3 KPa, which close to the practical TMP applied in full-scale MBRs.

The particle size distribution of MBR sludge flocs was measured using a MastersizerS (Malvern, UK). The sub-micron particles in the sludge water were measured using LC-OCD by a commercial lab, DOC-LABOR (Dr. Huber, Germany, Huber and Frimmel, 1991). A coarse size exclusion chromatography (SEC) column (Alltech, Germany) was used filled with Toyopearl resin (HW-65S with pores size of 100 nm).

In order to compare filtration performances, an indicator, i.e., the specific resistance to filtration (SRF) is defined as the increase in filtration resistance (1/m) when one mgCOD (or TOC) is delivered to one m^2 of membrane surface area. The SRF only counts the delivered COD or TOC in the sludge water phase (< 0.45 μm). However, the particulate phase (> 0.45 μm) is not considered as "delivered COD", since these particles have a low tendency to deposit and exhibit a low correlation with MBR fouling (Lesjean et al., 2005; Rojas et al., 2005; Rosenberger et al., 2005; Rosenberger et al., 2006). Therefore, the difference in SRF in the batch and on-line filtration should be mainly due to the hydrodynamic conditions, i.e., CF in the experiment.

7.4 Simulation and sensitivity analysis

A tubular UF membrane module used in full-scale MBRs (F4385 membrane, 38PRV module, X-Flow, the Netherlands) was used as a reference tubular membrane in the model simulation. This UF membrane (nominal pore size = 0.03 μm) module comprised 600 membrane tubes. Each membrane tube was 3 m long and the inner

diameter was 5.2 mm. The other operational parameters and variables of the simulation were summarized in Table 7-1 and Table 7-2.

Table 7-1 Fixed operational variables or parameters in the simulation

Parameter/variable	Reference values
Φ_w/Φ_b	60
Filtration flux	30 L/(m²·h)
BW flux	6×30 L/(m²·h)
Filtration TMP	0.1 bar
BW TMP	0.6 bar
Filtration/BW mode	300 seconds filtration/8 seconds BW

Table 7-2 The reference value and range of simulation of operational variables

Variables	Reference value	Range of simulation
T	15°C	5-30 °C
DS	10 g/L	2-30 g/L
a	0.1μm	0.01-100 μm
U	1 m/s	0.2-4 m/s
D	5.2 mm	2-10 mm
L	3 m	1-5 m

In Table 7-1, the concentration polarisation factor Φ_w/Φ_b was difficult to measure and it is assumed to be 60. At the critical condition of filter cake formation, the Φ_w equals the cake packing density (Φ_c). If one assumes $\Phi_w = \Phi_c = 0.6$ and $\Phi_b = 0.01$ (DS=10 g/l), $\Phi_w/\Phi_b = 60$ will be obtained. However, it should be noted that: 1) the Φ_w/Φ_b ratio can vary depending on the extent of concentration polarisation and bulk sludge DS; and 2) the Φ_w/Φ_b ratio is not a sensitive parameter, due to the fact that the backtransport velocity increases with the Φ_w/Φ_b ratio to a power of just 1/3 as in Eq.(7.12)-(7.14)). A small error in Φ_w/Φ_b ratio will not significantly influence the simulation results according to the sensitivity analysis (result not shown).

The absolute sensitivity (AS) and relative sensitivity (RS) were evaluated using Eq.(7.16) and (7.17), where, y and Δy are the model output variables and their variation; x and Δx are the model input parameters/variables and their variations.

$$AS = \frac{\Delta y}{\Delta x} \tag{7.16}$$

$$RS = \frac{\Delta y / y}{\Delta x / x} \tag{7.17}$$

RS is more attractive than AS because the magnitude of RS associated with each parameter is comparable. RS eliminates the influence of unit and absolute values of different parameters by considering their relative changes only. The criteria to evaluate RS are listed below.

RS<0.25,   the parameter has no significant influence on a model output;

$0.25 \leq RS < 1$,   the parameter is influential on a certain model output;

$1 \leq RS < 2$,   the parameter is very influential on a certain model output;

$RS \geq 2$,   the parameter is extremely influential on a certain model output.

7.5 Results

7.5.1 Impact of crossflow velocity and particle radius

The Reynolds number, headloss and specific energy consumption are summarized in Table 7-3. At crossflow velocities above 0.23 m/s, which cover almost all MBR operational conditions, the specific energy consumption due to crossflow ($\hat{E}_c$) is considerably higher than the energy consumption of filtration ($\hat{E}_f$). This can be predicted according to the equations of Re, f and h_f, where the specific energy consumption due to crossflow ($\hat{E}_c$) increases with the crossflow velocity to the power of 2.75 under turbulent flow conditions (U>1.1 m/s). Theoretical calculation shows the specific total energy consumption ($\hat{E}_{tot}$) in this membrane module is 0.245 kWh/m^3 (U=1 m/s). However, if one assumes that the overall efficiency of the pumps and electrical motors is 50%, the actual $\hat{E}_{tot}$ will be 0.49 kWh/m^3. This value is higher than the typical energy consumption in submerged MBRs (0.2-0.4 kWh/m^3, Churchouse, 2002). The high energy consumption is a drawback of side-stream MBR systems (Gander et al., 2000).

Table 7-3 The impact of crossflow velocity on the hydrodynamics and specific energy consumption (D=5.2 mm, L=3 m, DS=10 g/L, T=15 °C)

Crossflow velocity (m/s)	Re	Headloss (bar)	$\hat{E}_c$	$\hat{E}_f$ (at 30 L/m²·h) kWh/m³	$\hat{E}_{tot}$
0.23	466	0.010	0.004	0.004	0.008
0.50	1030	0.040	0.036	0.004	0.040
0.75	1540	0.082	0.108	0.004	0.112
1.00	2060	0.136	0.241	0.004	0.245
2.00	4111	0.456	1.610	0.004	1.614
3.00	6171	0.928	4.920	0.004	4.924
4.00	8222	1.533	10.832	0.004	10.836

The headloss along the membrane tube increases significantly with increasing CF velocity, which can result in a considerable heterogeneous distribution of TMP due to the decrease in feed pressure from the inlet to outlet. The local fluxes at the outlet may be considerably lower than the inlet, which cannot simply be measured by the global observation, e.g., flux and TMP. The headloss is estimated as 0.16 bar under the reference conditions. Consequently, the TMP at the outlet of the membrane tube is 0.16 bar lower than the inlet. The heterogeneous distribution of TMP is another disadvantage of high CF in addition to the energy consumption. However, this problem can be counterbalanced by introducing air into the feed (air lift) in vertical membrane module systems, which reduces the gravity head inside the tube near the inlet (bottom) (Cui et al., 1997).

Figure 7-1 illustrates the particle backtransport velocity as a function of the feed sludge crossflow velocity and particle radius. To compare it with the permeation velocity, the filtration flux is also plotted, i.e., 30 L/(m²·h) (the equivalent log10 value is -5.1 m/s).

The shaded area in the lower figure is the region, in which the permeation velocity exceeds the backtransport velocity, and hence, in which case the particles have a higher likelihood to deposit. The critical particle size, on which the permeation and backtransport velocity are balanced, at U=1 m/s is 1.5 μm. Increasing the CF up to 4m/s reduced the critical particle size down to 0.3 μm. On the other hand, for particles larger than 10 μm, even very low crossflow velocities (0.3 m/s) can keep them in

suspension. Fortunately, the majority of MBR sludge particles are larger (in dimension) than 10 μm (Zhang et al., 1997; Defrance et al., 2000), although some studies reported small particle sizes (1-2 μm) (Wisniewski et al., 2000).
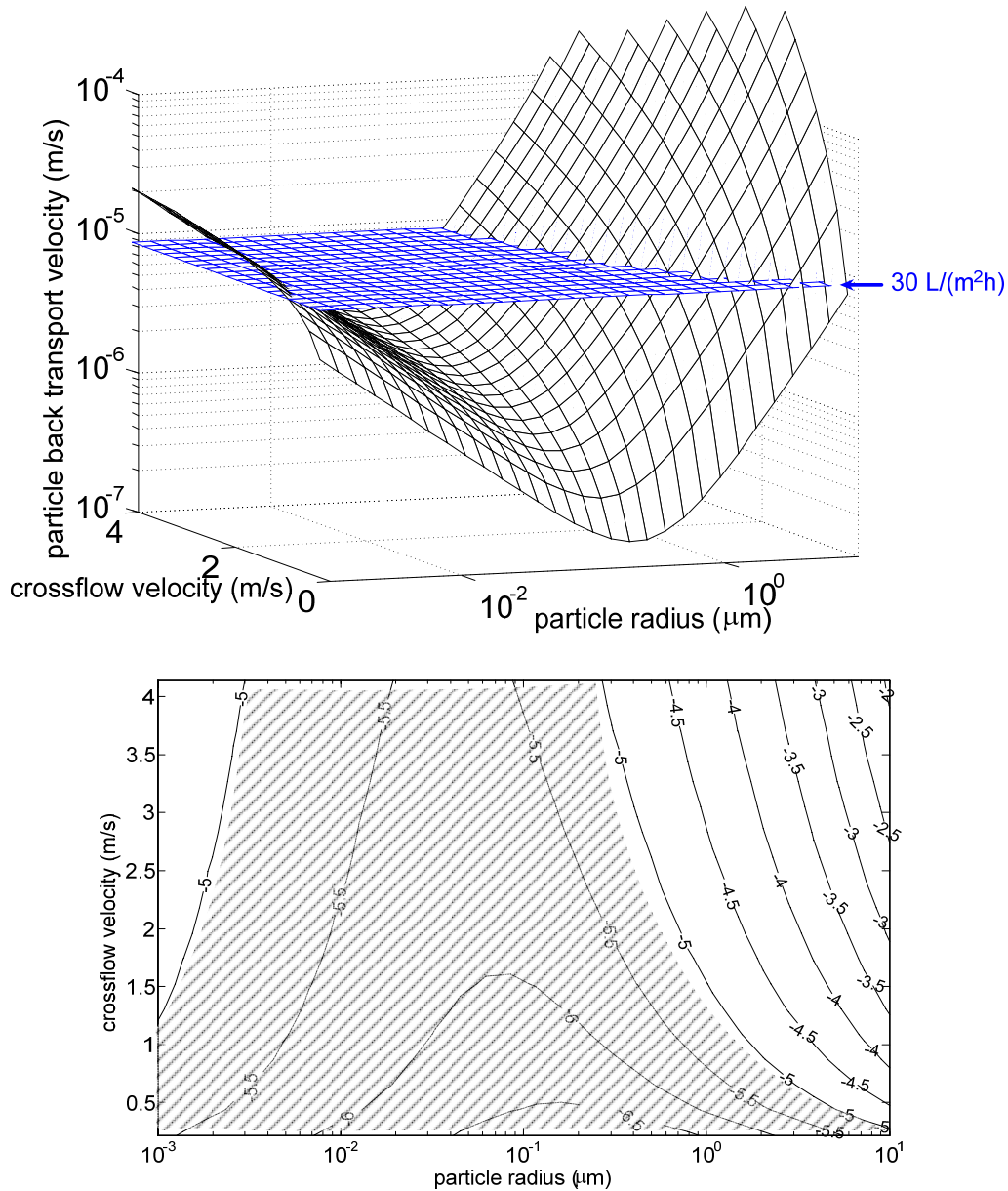
Figure 7-1 The influence of crossflow velocity and particle size on the particle backtransport (D=5.2 mm, L=3 m, DS=10 g/L, T=15 °C, the numbers in the lower figure are the log10 values of backtransport velocities)

The above theoretical simulation suggests that submicron particles have a high likelihood to deposit, and simply increasing CF may not completely prevent their deposition. The worst region is when the particle radii are around 0.1 μm and CF below 0.5 m/s. The colloidal particles (<0.45 μm) in a MBR, e.g., SMP, are mostly

produced due to microbial activity during the biomass growth and decay phases (Namkung and Rittmann, 1986; Rittmann et al., 1987). The operation of the MBR biology should therefore aim at reducing the SMP production or improve its degradation.

Figure 7-2 illustrates the particle backtransport velocities for three particle radii (0.01, 0.1 and 1 µm) as a function of the specific total energy consumption as the crossflow velocity is varied. A specific total energy consumption higher than 2 kWh/m^3 (in corresponding CF is 2.2 m/s) hardly improves the particle backtransport velocity, suggesting that for submicron particles, increasing the crossflow velocity would have less gain (controlling particle deposition) above a certain value. This phenomenon may be explained by the fact that the backtransport mechanism of small colloidal particles is mainly controlled by Brownian diffusion, and is therefore not sensitive to the shear rate (only a power of 0.33 in Eq.(7.13)).
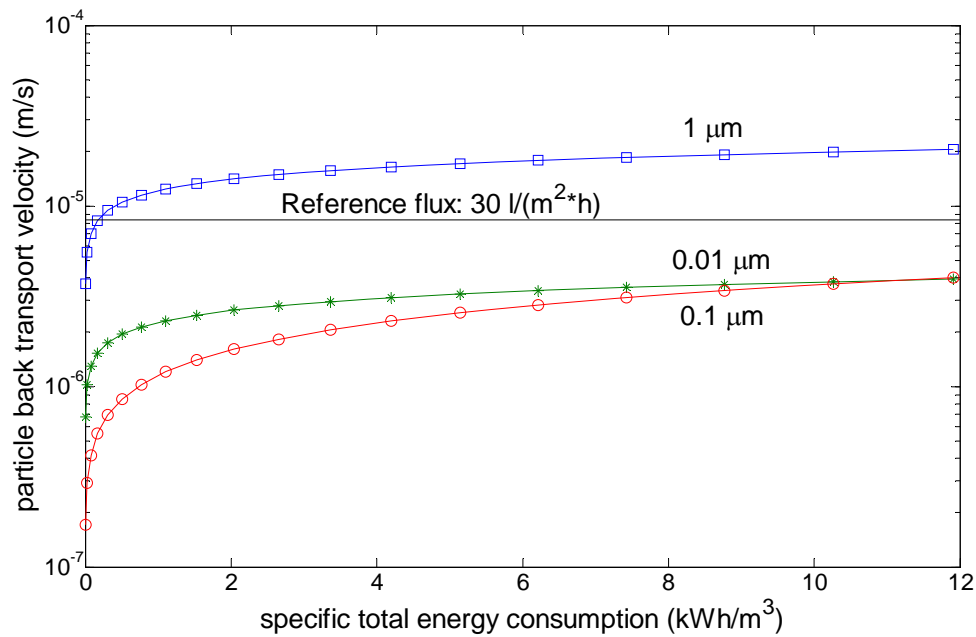
Figure 7-2 The influence of specific total energy consumption (by varying crossflow velocities) on the particle backtransport velocity for three particle radii (□ 0.01 µm; ∗ 0.1 µm; ○ 1 µm) (D=5.2 mm, L=3 m, DS=10 g/L, T=15 °C)

7.5.2 Sensitivity analysis

The influence of design/operational variables on the headloss of the recirculating flow (h_f), the specific total energy consumption ($\hat{E}_{tot}$) and the particle backtransport velocity (J_{tot}) is quantified using relative sensitivity (RS) or absolute sensitivity (AS) in Table 7-4. A positive sensitivity indicates a positive correlation, and larger RS values indicate higher influence, and vice versa. Comparing the magnitudes of RS, the crossflow velocity and the dry solid contents have the most significant impact on the particle backtransport velocity. In the case that the sign of $\hat{E}_{tot}$ and J_{tot} are opposite, e.g., for the DS case, one can minimise DS to achieve a reduced energy consumption and improved particle backtransport. However, in the cases that $\hat{E}_{tot}$ and J_{tot} have the same sign, e.g., increasing the CF the particle backtransport is improved at the expense of more energy. Consequently, an optimisation is needed. Detailed optimizations are given in sections 7.5.4-7.5.5.

Table 7-4 The sensitivity of headloss, specific energy consumption and backtransport velocity with respect to operational variables (at conditions in Table 7-1 and Table 7-2)

MBR Variable	Headloss (h_f)	Specific energy consumption ($\hat{E}_{tot}$)	Backtransport velocity (J_{tot})	Other
Particle radius (a)	Null	Null	0.079	
Crossflow velocity (U)	1.75	2.69	0.59	
Membrane tube diameter (D)	-1.24	-0.24	-0.14	+ Membrane manufacture cost
Membrane length (L)	1	0	-0.32	- Membrane manufacture cost
Dry solid contents (DS)	0.23	0.23	-0.85	- Construction cost of bioreactor
Temperature (T)	- 92 Pa	- 0.0016 kWh	7.54×10^{-8} m/s	- Particle breaking up

* All sensitivities are RS except for the temperature, which is AS

The RS of $\hat{E}_{tot}$ and J_{tot} with respect to the crossflow velocity is plotted in Figure 7-3. The RS of J_{tot} (0.58-0.61) is much lower than the one of $\hat{E}_{tot}$ (1.4-2.8), which suggests that the relative improvement in particle backtransport is less than the relative increase in energy consumption. Fortunately, the RS of J_{tot} remains high even at high crossflow velocities. Thus, increasing the crossflow velocity is still effective in fouling control throughout the crossflow velocity range (0.2-4 m/s). In order to adapt to the variation of fluxes (e.g., the diurnal flow rate profile of typical municipal WWTPs), side-stream MBRs can/should incorporate a certain control of the crossflow velocity, e.g., for long-term operation, a low CF at low fluxes (low to average flows)

may be applied to save energy, and for short periods of operation, a high CF may be applied to handle high fluxes (peak flows). However, in submerged MBRs, the efficiency of coarse bubble aeration on fouling control generally decreases with increasing aeration density and eventually may saturate (Howell et al., 2004). The flexibility of CF control to handle membrane fouling in high flux conditions is an advantage of side-stream MBRs compared to the submerged ones.

Finally, the sensitivity of the particle backtransport velocity on various particle radii is plotted in Figure 7-4. The sensitivity of the particle backtransport with respect to bigger particles is much higher than the submicron particles, and the most insensitive sizes have radii of approximately 0.1 μm. The colloids below 0.1 μm have negative sensitivities, which is due to the dominance of Brownian diffusion.
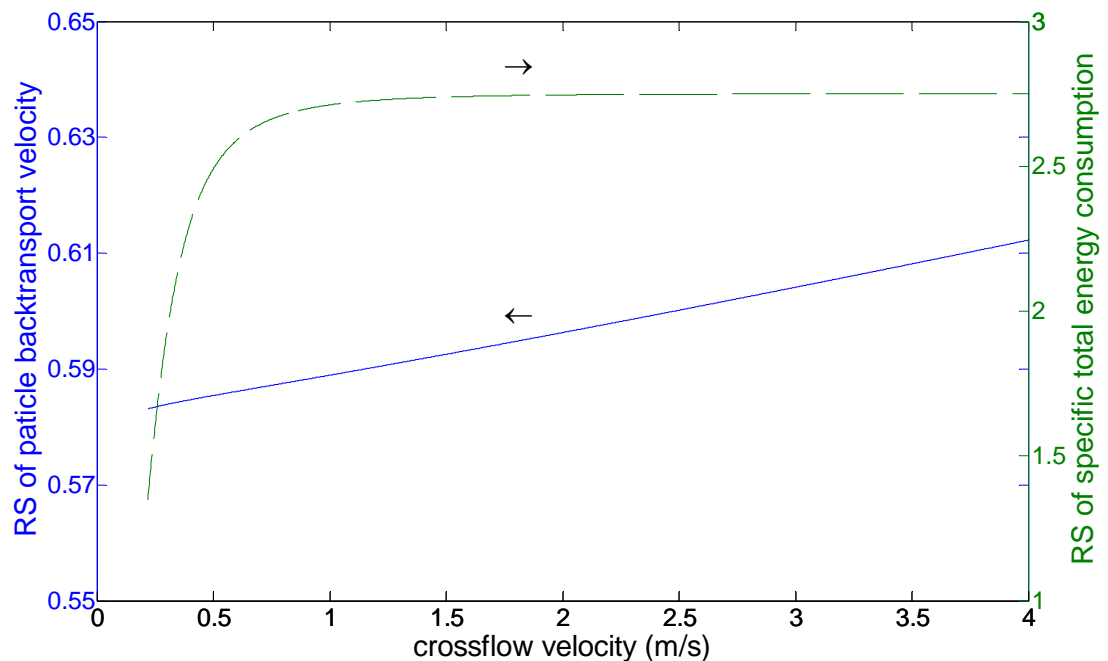
Figure 7-3 The relative sensitivity (RS) of particle backtransport and specific total energy consumption with respect to crossflow velocities (a=0.1 μm, DS=10 g/L, D=5.2 mm, L=3 m, T=15 °C)
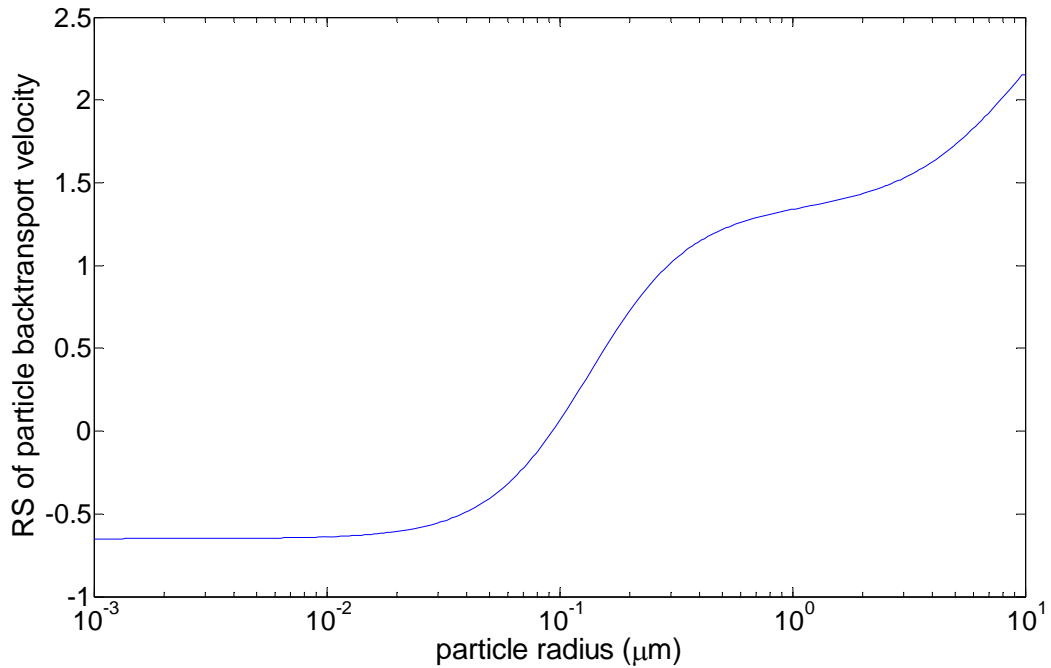
Figure 7-4 The relative sensitivity (RS) of the particle backtransport velocity with respect to particle radii (U=1 m/s, DS=10 g/L, D=5.2 mm, L=3 m, T=15°C)

7.5.3 Particle size distribution in a lab-scale MBR

The particle size distribution (PSD) of the lab-scale MBR sludge is presented in Figure 7-5. The MBR sludge had a main peak at around 40 μm (flocs) and a second peak at 0.1-1 μm (colloids). The colloidal peak may be bacteria cell or cell fragments. Many MBR studies showed a similar bimodal PSD. Sperandio et al. (2005) and Masse et al. (2006) reported the second peak was in the 1-10 μm range and Wisniewski et al. (2000) reported the second peak in around 1-2 μm. This study showed a second peak at even lower sizes. However, it should be noted that the submicron particle measurement using Malvern may not be reliable due to the uncertainty in the optical properties (i.e., the refractive index) of particles in biological systems.
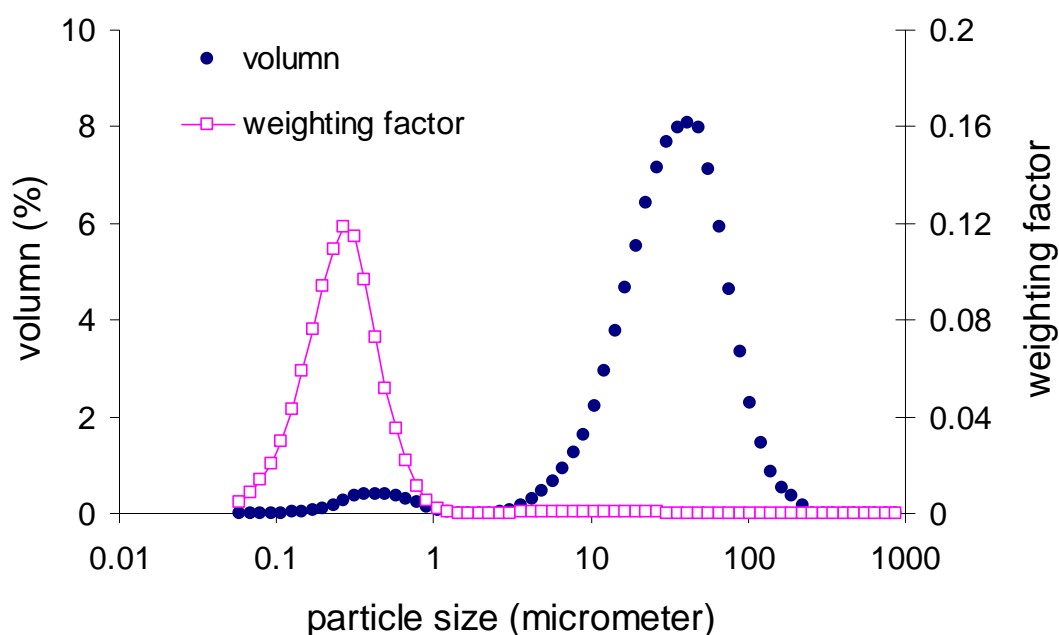
Figure 7-5 Particle size distribution and particle size weighting factor of lab-scale MBR sludge

To confirm the PSD of submicron particles, a LC-OCD was used to measure the sludge water (Figure 7-6). The SEC (size exclusion chromatography) separates particles according to their sizes. The results suggested most submicron organic particles were biopolymers. The DOC of the 3 biopolymer fractions, i.e., 2000 kDa (i.e., approximately 0.2 μm), 200 kDa (0.02 μm) and 50 kDa (0.005 μm) were 21.0, 3.18 and 4.65 mgDOC/L respectively. The very small colloids, e.g., humic substances, low molecular weight (LMW) acids and neutrals (< 2 kDa) amount to 12.5 mgDOC/L. The sum of the submicron particles (<0.45 μm) measured using Malvern was approximately 187 mg/L. This value was in the same magnitude with the estimation using the TOC of sludge water, i.e., 48.2 mgTOC/L, if one assumes the carbon content of particles is 44% (polysaccharide).
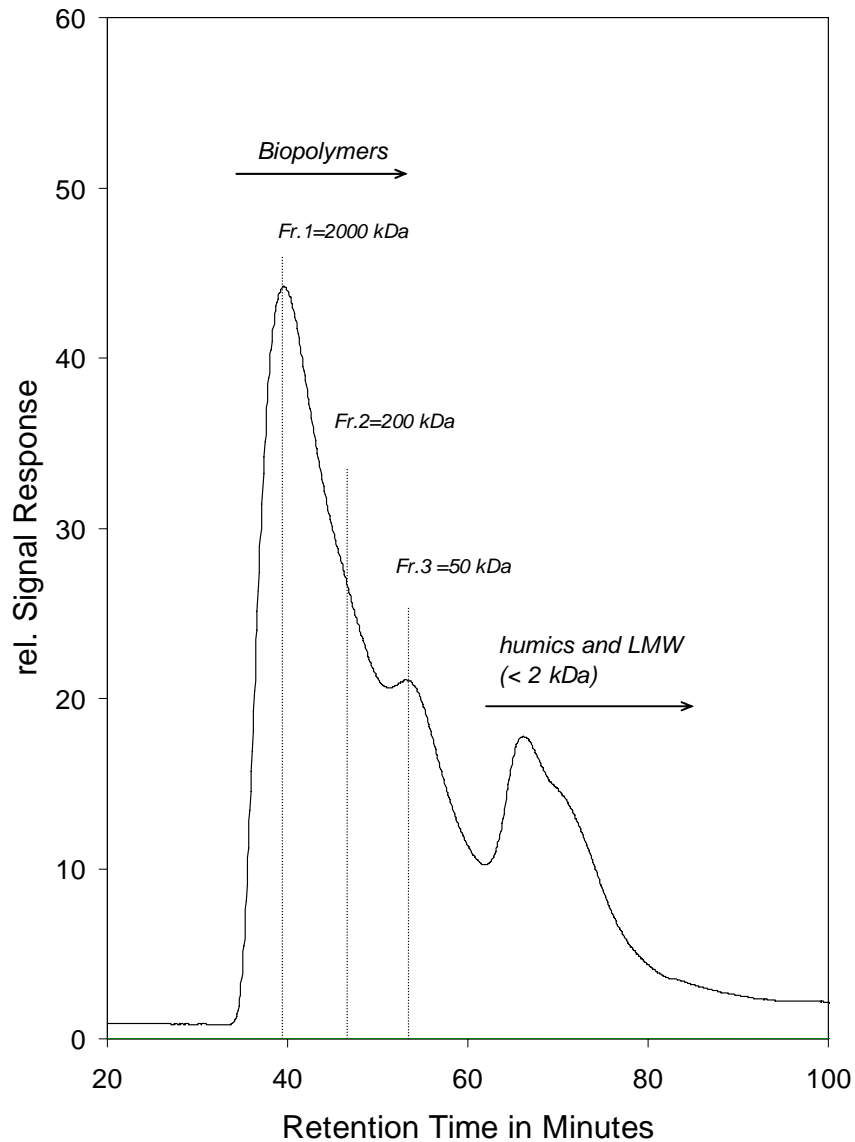
Figure 7-6 LC-OCD chromatogram of SMP (PSD of submicron particles) of lab-scale MBR sludge water

7.5.4 Theoretical optimization of MBR operation

Particle backtransport velocity and energy consumption should be optimised to maximize the energy efficiency in a side-stream MBR. An objective function (OBJ), Eq.(7.18), is constructed to maximize the gain of particle backtransport velocity (J_{tot}) for the specific expense of energy ($\hat{E}_{tot}$) under various operational conditions (U, DS, D, L and T). If the PSD of a MBR sludge (based on volume) is known, a weighting factor (w_i Eq.(7.19)) can be included into the OBJ. The w_i is assumed inversely

proportional to the square of the particle size based on the cake filtration mechanism (Kozeny-Carman relationship) (Mulder, 1996).

$$OBJ = \sum_{w_i=a_{min}}^{a_{max}} w_i * J_{tot,i} / \hat{E}_{tot} \tag{7.18}$$

Where i is a particle size class in a specific size range; a_{min} and a_{max} are the smallest and largest particle class radii; $J_{tot,i}$ is the backtransport velocity of class i particles.

$$w_i = \frac{p_i}{a_i^2} \tag{7.19}$$

Where p_i is the percentage of a specific particle class i; a_i is its particle class size.

Using the PSD of the lab-scale MBR sludge, the weighting factor (w_i) is plotted as a function of particle diameter (Figure 7-5). It is interesting to see that high weighting factors lie in the range of the submicron particles, although the peak of the PSD is at around 40 μm. This suggests that the submicron particles had a high filter cake formation potential even when their quantity (in terms of volume) was low. It should be noted that the above calculation of w_i does not consider hydrodynamic effects, as they have been included in $J_{tot,i}$. In addition to the weighting factor, another criterion is included in the optimisation, i.e., the particles with backtransport velocities larger than the filtration flux are assigned a zero weighting factor, since they are unlikely to deposit.

A non-linear optimization with five operational variable constraints, (U, DS, D, L and T) was formulated to maximize the objective function Eq.(7.18). A non-linear programming (NLP) problem was solved using GAMS software (Brooke, 1998). The operational variables were constrained in the practical MBR operational range, i.e., U=0.5-4 m/s, DS = 5-30 g/L, D=2-10 mm, L=1-5 m, and T=5-30°C. The particle size is an independent variable, thus a series of optimization steps were performed for each particle size (0.01-100 μm). Consequently no weighting factors are used in this theoretical optimization. The optimization results showed that the optimal operation

conditions of five variables all coincide with the boundary conditions (i.e., U=0.5 m/s, DS= 5g/L, D=2 mm, L=1 m and T=30°C) in spite of the particle sizes.

The optimisation of crossflow velocity can be illustrated more clearly in Figure 7-7. This simulation used the PSD and weighting factor in the lab-scale MBR and typical MBR operational conditions (DS= 10g/L, D=5.2 mm, L=3 m, T=15°C). The result shows that operating at a low CF and allowing a certain degree of fouling maximizes the OBJ. Operating at high crossflow velocity and high energy consumption to achieve high flux is not economical in long-term operation.
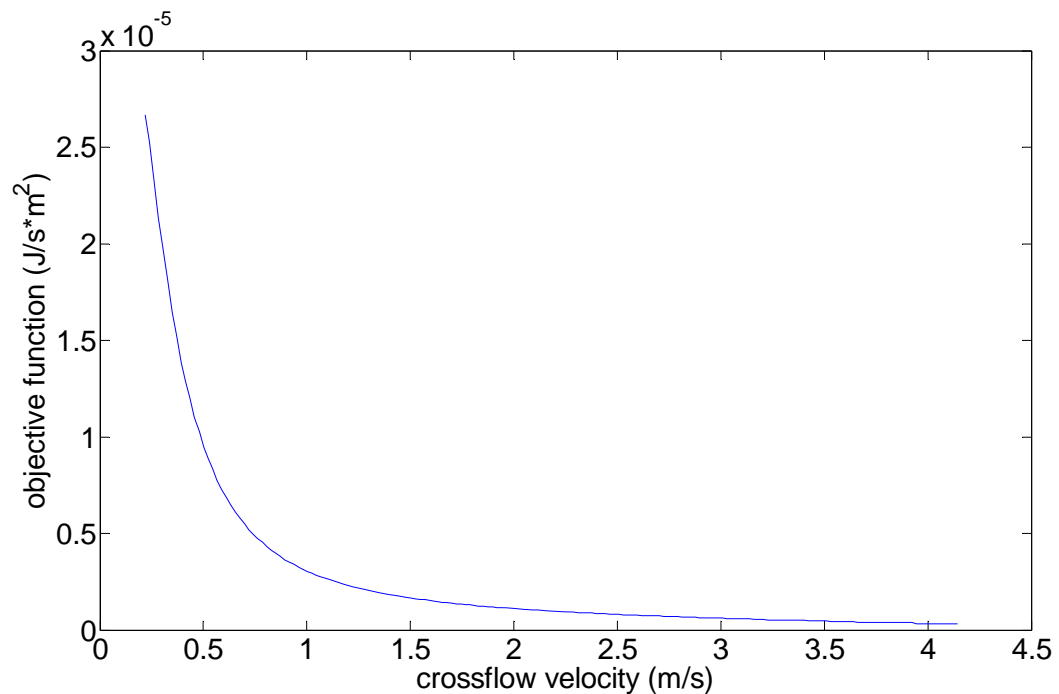
Figure 7-7 Optimizing of crossflow velocity using the PSD of a lab-scale MBR sludge (DS= 10g/L, D=5.2 mm, L=3 m, T=15 °C)

7.5.5 Practical optimization of crossflow velocity in a lab-scale MBR

The influence of CF on particle deposition and membrane fouling was investigated in a lab-scale MBR system (U=0.5-1.5 m/s), and the results were compared with the non-stirred cell batch filtration system in Table 7-5. There are a few interesting points: 1) Generally, increasing CF reduced the SRF, which was more pronounced at high flux and high fouling rate conditions (e.g., 50 L/(m^2·h)). However, a too high CF was not always beneficial with respect to fouling control (e.g., the SRF doubled as CF

increased from 1 to 1.5 m/s at 40 L/(m^2·h)). This strange behaviour may be due to the heterogeneous distribution of TMP. It was estimated using the above developed model that the TMP at the membrane inlet was 4.5-9.2 kPa higher than at the outlet, as the CF was increased from 1 to 1.5m/s. The higher TMP in the membrane inlet created a higher flux, which probably exceeded the critical flux (Fane et al., 2002). 2) At 40 L/(m^2·h), doubling the CF from 0.5 to 1 m/s reduced the SRF by a factor of 20, although the backtransport velocity of 0.2 μm particles (the main fraction of SMP) was merely doubled. This suggested that a critical CF value probably exists, below which, the fouling was significantly intensified, and above which, fouling was not further reduced. In this lab-scale MBR, this critical CF was between 0.75-1 m/s at 40 L/(m^2·h), which may be connected to the change from laminar to turbulent flow (Re increased from 1030 to 2060 as CF increased from 0.75-1 m/s). 3) The permeation velocities at 40 and 50 L/(m^2·h), i.e., 1.1 and 1.4×10^{-5} m/s respectively, were actually much higher than the backtransport velocities, predicted by the sum effects of the Brownian diffusion, shear-induced diffusion and inertial lift. It appears that either other hydrodynamic mechanisms controlled particle deposition, or that other physical/chemical factors played a role, e.g., the electrostatic repulsion between colloidal particles.

Dead-end and on-line crossflow MBR filtration were compared using the SRF and theoretical calculation of particle backtransport velocity (Table 7-5). The SRF at U=0.5 m/s was just 53% of the SRF in dead-end filtration, i.e., the 0.5 m/s CF only reduced 47% of the membrane fouling. This suggests that the CF was too low to effectively control the deposition of colloidal particles in the sludge water phase. In the dead-end batch filtration, an ultimate filtration flux was stabilized at 3.30 L/(m^2·h) in 10 hours. According to the classical concentration polarization model (Mulder, 1996; Chen et al., 1997), at a critical cake formation condition, the particle backtransport velocity can be assumed to equal this ultimate permeation flux, i.e., 9.17×10^{-7} m/s. Consequently, the actual particle backtransport velocity in the batch filtration should be lower than this value, since a cake was built up. However, it should be noted that the estimation of particle backtransport presented here is rather rough. A more précise model considering other factors should be considered in the future, e.g., looking at combined effects of different particle sizes.

Table 7-5 The impact of hydrodynamic condition (dead-end vs. various CF velocities) on MBR fouling

crossflow velocity (m/s)	Re	Specific resistance to filtration (dR/dCOD_delivered, m/mgCOD)		backtransport velocity of 0.2 μm particles (m/s)
		40 L/(m²·hr)	50 L/(m²·hr)	
0	0	3.81×10^9 (in dead-end batch filtration)		$< 9.17\times10^{-7}$
0.5	1030	20.3×10^8	n.a.	4.92×10^{-7}
0.75	1540	5.90×10^8	n.a.	6.91×10^{-7}
1	2060	1.03×10^8	15.1×10^8	9.06×10^{-7}
1.5	3081	2.23×10^8	7.15×10^8	13.8×10^{-7}

7.6 Conclusions

A simple integrated hydrodynamic model based on strong assumptions was developed to study the sensitivity of MBR operational parameters and minimise the energy consumption. The model is able to predict the effects of feed sludge particle size (a), dry solid contents (DS), crossflow velocity (U), membrane tube dimension (D and L) and temperature (T) on the particle transportation and energy consumption. The theoretical simulation focused on submicron particles and the crossflow velocity in a full-scale tubular membrane module. The results showed the submicron particles had a high likelihood to deposit, and the worst fouling region was with particle radii around 0.1 μm and crossflow (CF) velocity below 0.5 m/s. Simply increasing CF did not completely prevent colloidal particle deposition. The sensitivity analysis concluded the impact of CF is significant, while other operational variables (DS, D, L and T) were less influential.

The particle size distribution showed that a lab-scale MBR sludge had a second peak at 0.1-1 μm in the colloidal region in addition to a main peak at 40 μm, which was confirmed by LC-OCD measurement of sludge water with a high biopolymer fraction at 2000 kDa. In the optimisation, the submicron particles received high weighting factors (high filter cake formation potential) although their quantity was small. The theoretical optimisation considering the typical PSD suggested that cost-effective operation of an MBR is at the lowest possible crossflow velocity. However, the practical optimisation in a lab-scale MBR concluded that the crossflow velocity should neither be too low such that dead-end conditions are approached, nor too high

to result in heterogeneous TMP distribution and increased energy consumption. A critical CF value probably exists, below which, the fouling is significantly intensified, and above which, fouling is not further reduced. In this lab-scale MBR, this critical CF was between 0.75-1 m/s at 40 L/(m^2·h).

7.7 Recommendations

The models presented here assumed ideal particles and no particle-particle interactions. However, the flocs and submicron particles are not perfect spheres, and some may even be porous. They may deform, aggregate and break up in both the bulk and boundary layer and inside the filter cake. The particle size distribution may be shifted and more soluble microbial products may be relased, e.g. from extracellular polymeric substances, as the shear rate increases. The contributions of all these effects to the hydrodynamic models presented in this chapter are unknown and will need to be addressed in future model structures and analyses.

A control algorithm for the crossflow velocity can be developed based on this study, e.g., for long-term low flux operation, low CF can be used to save energy and for short-term high flux (fouling) conditions, high CF can be employed to handle flux peaks. Finally, this study indicated the difficulty in controlling the deposition of submicron particles using only a hydrodynamic approach, therefore operation of MBR biology should aim at reducing the SMP production and improve SMP degradation, to reduce the fraction of particles in the colloidal range.

Modelling the impact of soluble microbial products (SMP) on MBR fouling

8.1 Introduction

MBR fouling is a complex phenomenon. Identifying the major fraction of MBR sludge responsible for membrane fouling has been widely studied in literature. A summary of 13 MBR studies by Judd (2006) reported very heterogeneous results. However, an overall trend suggested that the sludge water (colloidal and soluble) fraction exhibited a higher contribution to membrane fouling than the suspended solids fraction.

Early MBR studies attempted to correlate MBR fouling with some bulk variables, e.g., MLSS (Cicek et al., 1999; Chang and Kim, 2005), viscosity (Ueda et al., 1996), floc size distribution (Wisniewski and Grasmick, 1998), etc. More recent studies have showen that MBR fouling is microbial in origin, and thus SMP (soluble microbial products) and EPS (extracellular polymeric substances) have been attributed to high fouling potentials. SMP and EPS are often measured using bulk variables, e.g., as COD and TOC, or more specifically, as colorimetric determinations of polysaccharides and proteins. Most MBR studies attributed the high fouling potential of SMP to its polysaccharide fraction (Chu and Li, 2005; Lesjean et al., 2005; Rosenberger et al., 2006; Zhang et al., 2006a). However, others attributed SMP related fouling to proteins (Rojas et al., 2005).

SMP are traditionally classified into BAP (biomass associated products) and UAP (utilization associated products). The relative concentrations of BAP and UAP are related to the biomass growth phase. It has been reported that BAP dominates under starvation conditions and UAP dominates under growth conditions (Namkung and Rittmann, 1986). The characterisation of BAP and UAP was performed in Chapter 5, however, their respective filtration behaviours are not clear.

MBRs are routinely operated under sub-critical flux conditions. Typical long-term filtration behaviours (TMP vs. time) between two chemical cleanings can be classified into three stages, as follows. The initial conditioning stage (in hours) arises due to the adsorption of colloidal and macromolecular organic matter (Zhang et al., 2006a). This adsorption is coupled with membrane pore blocking (Jiang et al., 2005a) and often difficult to clean hydraulically (Ognier et al., 2002). After the initial conditioning stage, the active adsorption sites on the membrane surface and pores have been covered with macromolecular organic matter; The second stage (from days to weeks) is a slow fouling process in which hydraulic cleaning, e.g., crossflow and backwashing, is able to control the particle deposition and results in a low fouling rate (Brookes et al., 2006; Ye et al., 2006; Zhang et al., 2006a); In the third phase (in days), MBRs exhibit a sudden TMP jump, roughly exponential in shape (Le-Clech et al., 2003a). This is attributed to the loss of membrane surface area (Ognier et al., 2004) or to the heterogeneous distribution of TMP (Cho and Fane, 2002; Ye et al., 2005a), resulting in a higher local flux above the global critical flux.

Many studies have been conducted to understand MBR fouling under sub-critical flux conditions, and some have proposed mathematical models to describe the 3 stage TMP changes. Ognier et al. (2004) attributed the gradual increase of TMP in stages 1 and 2 to the loss of membrane surface area due to foulant adsorption. It was hypothesised that the increase in local filtration flux above a critical flux resulted in the rapid fouling in stage 3. A simple pore blocking model was proposed to describe the loss of available membrane pores. However, no model simulations were performed and no comparison between model simulations and experimental results was conducted. Cho and Fane (2002) attributed the gradual increase of TMP in stages 1 and 2 to fouling due to soluble EPS (SMP), and rapid fouling in stage 3 to the deposition of biomass. The development of fouling layers along the membrane module varied with location. When the local flux exceeded the critical flux, stage 3 commenced. Ye et al. (2006) applied a combined pore blocking and cake filtration model originally developed by Ho and Zydney (2000) to model the TMP transition in an unstirred batch filtration test. Alginates were used as a model soluble EPS. The model was able to fit the experimental results, suggesting that the fouling mechanism might be due to standard pore blocking in the early stage, followed by cake filtration.

Typical MBRs operate under crossflow conditions either with sludge or mixture of sludge/air flushing tubular membranes in side-stream configuration or with coarse bubbles agitating the submerged membrane. Crossflow filtration reduces membrane fouling by promoting particle backtransport (Belfort et al., 1994; Tardieu et al., 1998). In addition, many MBRs apply relaxation and backwashing to clean the deposited foulant. In contrast, most of the above studies were conducted under batch filtration conditions, and some even used synthetic foulants. None of their models therefore considered the field conditions in MBRs, i.e., crossflow, periodical backwashing/relaxation, and actual MBR sludge. For better understanding and optimisation, it is however essential to try to model the filtration behaviour in MBRs under field conditions and to predict the amount of hydraulically irreversible fouling and the chemical cleaning frequency from both theoretical and practical points of view.

The objectives of this study were: 1) to quantify the impact of SMP, BAP and UAP on MBR fouling; and 2) to develop a mathematical model to simulate the accumulation of irreversible fouling and TMP change over both short-term (within one filtration cycle) and long-term (between two chemical cleanings) operation.

In this chapter, first, the development of filtration models describing both irreversible and reversible fouling is presented. Second, a lab-scale MBR and the methods used in evaluating membrane fouling are described. Third, the very high fouling potential of SMP is quantified using a modified fouling index and specific cake resistance. Fourth, the filtration model is calibrated and validated in a lab-scale MBR to simulate the TMP vs. time profile. Finally, the impact of SMP concentration and filtration flux on membrane fouling is evaluated using model simulations. To perform a dynamic simulation, the model presented in this chapter requires the SMP concentration, predicted in Chapter 6, as model input. In addition, the influence of hydrodynamic conditions discussed in Chapter 7 is also used in this chapter.

8.2 Model development

A mathematical model is developed in this section to simulate the filtration behaviour. Membrane fouling is differentiated as reversible and irreversible with respect to

hydraulic cleaning. To simplify the model, the irreversible fouling is assumed to be attributed to the complete blocking of membrane pores only, and the absorption of colloids (standard blocking) is lumped into complete blocking from the modelling point of view. The validity of using a complete blocking model to describe the irreversible fouling is described in section 8.4.4. The initial TMP immediately after a backwashing is used to quantify the amount of irreversible fouling. Cake filtration is assumed to be the dominant filtration mechanism during one filtration cycle (between two backwashings) and completely reversible by backwashing. Pore blocking is associated with the initial rapid TMP increase and assumed partially irreversible. To simplify the model, short-term pore blocking within one filtration cycle is not included in the model and is lumped into irreversible resistance or cake resistance. An integrated model including both long-term irreversible fouling due to pore blocking and short-term reversible fouling due to cake filtration is presented in section 8.2.2.

Sludge water is defined as the colloidal macromolecular organic fraction of MBR sludge obtained using a 0.45 μm filter (see section 3.2.4). The major organic component of sludge water is SMP and it is therefore assumed to be the main foulant in MBRs participating in both irreversible and reversible cake build up. Supporting evidence includes: 1) the SMP size ranges from a few hundred Da to a few million Da (see Chapter 5), which covers the membrane pore size of a MBR; and 2) SMP has a strong correlation with MBR fouling (Lesjean et al., 2005; Rojas et al., 2005; Rosenberger et al., 2005; Rosenberger et al., 2006).

8.2.1 Modelling the accumulation of irreversible resistance under crossflow and periodical backwashing/relaxation conditions

Complete blocking assumes that each particle arriving at the membrane participates in pore blocking with no superposition of particles (no filter cake formation). The traditional complete blocking filtration law was modified to describe the accumulation of irreversible resistance in a MBR system. The derivation of the model is presented in this section and the model calibration and validation are presented in sections 8.4.4, 8.4.5 and 8.4.6.

Traditionally, the loss of available membrane surface area is assumed to be proportional to the filtration volume V_t as in Eq.(8.1) (Hermia, 1982). However, this approach does not consider the impact of foulant concentration on membrane fouling. Therefore, it is more explicit to use Eq.(8.2) in a differential form by taking into account the foulant concentration in the MBR sludge.

$$A(t) = A_0 - \sigma V_t \tag{8.1}$$

$$\frac{dA_t}{dV_t} = -\sigma_{COD} C_b(t) \tag{8.2}$$

Where A_0, $A(t)$ — available membrane surface area at time 0 and t (m^2)

σ — blocked membrane surface area per unit filtration volume (m^2/m^3)

σ_{COD} — hydraulically irreversibly blocked membrane surface area per kg mass of COD in sludge water (m^2/kg COD)

$C_b(t)$— COD concentration of the bulk sludge water at time t (kg COD/m^3)

$V(t)$ — filtration volume (m^3)

Combining filtration flow rate $Q(t) = \dfrac{dV(t)}{dt}$ (m^3/s) with (8.2) yields

$$\frac{dA_t}{dt} = -\sigma_{COD} C_b(t) Q(t) \tag{8.3}$$

Many MBRs apply hydraulic cleaning, e.g., relaxation, forward fluxing and backwashing, which can partially remove the deposited foulants and reopen the membrane pores that have been completely blocked during the filtration phase. However, some hydraulically irreversible fouling resistance (R_{irr}) can accumulate with time and result in irreversible loss of available membrane surface area. To describe the R_{irr}, the parameter σ_{COD} is defined here as the hydraulically irreversibly blocked membrane surface area per kg of delivered COD in sludge water. The term "irreversibly" used here is defined as the residual fouling, which cannot be removed by the routine hydraulic cleaning mentioned above, but it is very possibly reversible by chemical cleaning.

The effect of reduced particle deposition under crossflow conditions and periodical backwashing are also lumped into the parameter σ_{COD}, thus no additional parameters describing the percentage of particle deposition are introduced into the model. This approach reduces model complexity and potential parameter correlation. However, the cost is that the model is not able to describe the dynamic impact of crossflow velocity and backwashing on membrane fouling.

According to Darcy's law, the available membrane surface area can be expressed as follows:

$$\Delta P(t) = \frac{\eta_p R_m Q(t)}{A(t)} \tag{8.4}$$

Where: η_p — viscosity of permeate (Pa s)

R_m — membrane resistance (m^{-1})

$\Delta P(t)$ — TMP at time t (Pa)

$Q(t)$ and $C_b(t)$ can be measured experimentally. Thus, the dynamic TMP can be obtained by solving Eqs. (8.3) and (8.4). In addition, an explicit expression of R_{irr} (Eq.(8.6)) can be obtained by combining Eq.(8.4) with the resistance in series model Eq.(8.5). The dynamic R_{irr} can be obtained by solving Eqs. (8.3) and (8.6).

$$\frac{Q(t)}{A_0} = \frac{\Delta P(t)}{\eta_p [R_m + R_{irr}(t)]} \tag{8.5}$$

$$R_{irr}(t) = R_m \frac{A_0}{A(t)} - R_m \tag{8.6}$$

Under steady state conditions, by assuming constant flux (Q) and constant COD concentration of sludge water (C_b), an explicit expression of TMP and R_{irr} can be derived as Eqs. (8.7) and (8.8).

$$\frac{1}{\Delta P(t)} = \frac{1}{\Delta P_0} - \frac{\sigma_{COD} C_b}{\eta_p R_m} t \tag{8.7}$$

$$R_{irr}(t) = R_m \frac{A_0}{A_0 - \sigma_{COD} C_b Q t} - R_m \tag{8.8}$$

This adapted dynamic complete blocking model only introduces one parameter σ_{COD}, which can be calibrated by curve fitting given Q, C_b and R_{irr} (see section 8.4.4). Dynamic $R_{irr}(t)$ can be estimated experimentally from the starting TMP immediately after backwashing, given that R_m is known from a clean water test (Jiang et al., 2003; Jiang et al., 2005a).

8.2.2 Integrated modelling of MBR fouling

Cake filtration assumes that each particle locates on others already arrived and there is no room for direct obstruction of membrane pores. A cake filtration model is integrated into the above developed complete blocking model. The complete blocking model describes the irreversible fouling due to the membrane history (i.e., the starting point of a filtration cycle after backwashing), while the cake filtration model describes the reversible fouling during a filtration cycle (between two backwashing).

Due to the loss of available membrane surface area, the observed filtration flux or global flux (J_G, L/(m^2·h)) defined as $Q(t)/A_0$ cannot represent the actual filtration flux or local flux ($J_L(t)$, L/(m^2·h)). The local flux is higher than the global flux and can be described as being inversely proportional to the available membrane surface area as in Eq.(8.9).

$$J_L(t) = J_G(t) \cdot A_0/A(t) \tag{8.9}$$

The filtration behaviour during one filtration cycle is the combined effects of membrane resistance (R_m), hydraulically irreversible resistance ($R_{irr}(t)$), blocking resistance ($R_b(t)$) and cake resistance ($R_c(t)$) as in Eq.(8.10). In one filtration cycle, the sum of R_m and $R_{irr}(t)$ can be estimated from Eq.(8.8). Practically, $R_b(t)$ is difficult to measure experimentally, due to the fact that the filtration behaviour in the initial few seconds after backwashing is the combined effects of pump start up and pore blocking. Since the long-term irreversible fouling has been modelled in section 8.2.1, to simplify the integrated model, $R_b(t)$ is omitted here by lumping it into R_{irr} and R_c.

$$\Delta P(t) = \eta_p J_G(t)[R_m + R_{irr}(t) + R_b(t) + R_c(t)] \tag{8.10}$$

The last term in Eq.(8.10), $R_c(t)$, can be estimated from the deposited cake mass as in Eq.(8.11). It is assumed that: 1) the cake resistance after a backwashing is zero and builds up during the filtration cycle; 2) the cake resistance reaches a maximum value before the next backwashing and it can be completely removed by backwashing. This approach simplifies the model by assuming all filter cakes are reversible for backwashing and lumps a small amount of hydraulically irreversible cake resistance into the irreversible blocking resistance; and 3) the filter cake is assumed incompressible due to the low TMP applied in modern MBRs (typically below 0.2 bar (Judd, 2006)). However, the model can be easily extended to compressible cake situations by introducing a pressure-dependent specific cake resistance, e.g., $\alpha = \alpha_0 \Delta P(t)^n$.

$$R_c(t) = \alpha \; \frac{w(t)}{A_0} \tag{8.11}$$

Where α — specific cake resistance assuming incompressible cake (m/kg)

w — filter cake mass (kg) estimated in Eq.(8.12) under dynamic conditions

$$\frac{dw(t)}{dt} = C_d(t)Q(t) \tag{8.12}$$

Where $C_d(t)$ — deposited COD concentration, which is the amount of COD in the sludge water able to deposit and form a cake under crossflow conditions (kg COD/m^3)

Only a portion of colloidal and macromolecular organic matter can deposit and form a filter cake due to the particle backtransport under crossflow conditions. The cake-forming particles likely have larger sizes than the membrane pore sizes, and their backtransport velocities are more sensitive to crossflow velocities (see Chapter 7). Thus, Eq.(8.13) is introduced to estimate the percentage of particle deposition, and assume it is empirically proportional to $(J_L/J_m)^n$. J_m and n are empirical parameters with physical meaning. J_m is the critical filtration flux, above which all COD in the sludge water can deposit, which is equivalent to a dead-end filtration of sludge water. If J_L is lower than J_m, only a portion of the COD $(J_L/J_m)^n$ in the sludge water is able to

deposit. J_m and n are influenced by the hydrodynamic conditions of the MBR and particle size distribution (PSD) of submicron colloids in the sludge water.

$$C_d(t)= C_b(t) [J_L(t)/J_m]^n \qquad\qquad (8.13)$$

The cake filtration model only introduces 3 parameters (α, J_m and n). α can be measured experimentally using an unstirred cell (see section 8.3). J_m and n can be determined by curve fitting as demonstrated in section 8.4.5. $C_b(t)$ and $Q(t)$ can be measured experimentally. Combining Eqs. (8.9)-(8.13) and solving differential equations, the dynamic TMP can be simulated as a function of time. Under constant flux and constant COD concentration of sludge water, substituting $V(t)/A_0$ by $J_G t$, an explicit form of TMP can be written as Eq.(8.14). The first pressure term on the right side represents the TMP overcoming the membrane resistance and the long-term irreversible blocking resistance, and the second pressure term on the right side represents the TMP overcoming the short-term reversible cake resistance. During the simulation of long-term MBR operation between two chemical cleanings, the first term always increases due to the accumulation of irreversible resistance, while the second term shows a cyclical behaviour due to the dynamic build up and removal of the filter cake. This behaviour is demonstrated using experimental results in section 8.4.4-8.4.5.

$$\Delta P(t) = \eta_p J_G(R_m+ R_{irr}(t)) + \eta_p J_G^2 \alpha C_b[J_L(t)/J_m]^n\, t \qquad\qquad (8.14)$$

8.3 Materials and methods

A side-steam lab-scale MBR system is setup for biological COD, nitrogen and phosphorus removal. The lab MBR has an influent flow rate of 108 L/day and operates under constant flux filtration conditions (31.8 L/(m^2·h)). The HRT, total SRT and aerobic SRT are controlled at 6.4 hrs, 17 days and 7.2 days, respectively. A tubular UF module with a total membrane surface area of 0.17 m^2 (X-Flow, the Netherlands) is used. The PVDF membrane has a nominal pore size of 0.03 µm and a tube diameter of 5.2 mm. The membrane is operated under the air lift mode and both sludge and air crossflow velocities are 0.5 m/s. The membrane loop (3.8 L) is also considered as a completely mixed aerobic reactor. The membrane was backwashed

for 18 sec at 106 L/(m^2·h) every 7.5 minutes of filtration. The details of the lab-scale MBR are presented in section 3.1.

The production of BAP was conducted under starvation conditions without external substrate addition. The production of UAP was spiked with 1000 mg COD/L (end concentration) sodium acetate. More details of BAP and UAP batches are described in section 3.3. The BAP, UAP and SMP samples were filtered using a stirred cell unit (Stirred Cell 8200, Millipore, USA) operating under constant pressure (TMP = 14.3 kPa) and unstirred (dead-end) conditions. A flat sheet 0.03 μm PVDF membrane was manufactured (X-flow, the Netherlands) with exactly the same material, structure and morphology as the tubular one used in the lab and full-scale MBRs. More details of constant pressure batch filtration are presented in section 3.4.

Specific cake resistance (α) in the batch filtrations was estimated using Eq.(8.11). The mass of filter cake was estimated using mass balances of COD or DOC, since the feed and the permeate COD were measured. It is hypothesized that the blocking resistance was negligible compared with cake resistance during a long time dead-end batch filtration (10 hours). Thus, the cake resistance can be estimated using the total filtration resistance minus the clean membrane resistance.

The modified fouling index (MFI) was developed to estimate the fouling potential of feed water to membrane filtration systems (Schippers and Verdouw, 1980) using a 0.45 μm MF membrane. The MFI is based on the mechanism of cake filtration as in Eq.(8.15), whereby, the slope $\dfrac{\eta I}{2\Delta P A_0{}^2}$ is called the MFI. The fouling index I, in the MFI, is defined as the product of the specific resistance (α) of the cake deposited and the concentration of particles (C_b) in the feed water. An advantage of using the fouling index I as a lumped parameter is that in most cases it is impossible to determine C_b and α accurately. A high MFI value of feed water is an indication of high filter cake forming potential.

$$\frac{t}{V} = \frac{\eta R_m}{\Delta P A_0} + \frac{\eta I}{2\Delta P A_0{}^2} V \qquad (8.15)$$

Recently, the MFI-UF was further developed by using a UF membrane (Boerlage et al., 2002). To compare the MFI-UF values with other studies, the MFI-UF was calculated and normalized to a standard set of conditions as in Eq.(8.16), i.e., 20 °C, TMP = 2 bar, membrane surface area $A_0 = 13.8 \times 10^{-4}$ m^2). All MFI-UF discussed in the following sections of this chapter refer to the MFI-UF normalized to the standard condition.

$$\text{MFI-UF} = \frac{\eta_{20} I}{2 \Delta P_0 A_0^2} = \frac{\eta_{20}}{\eta_T} (\frac{\Delta P}{\Delta P_0})^{1-\omega} (\frac{A}{A_0})^2 \frac{d(t/V)}{dV} \tag{8.16}$$

SUR (specific ultrafiltration resistance) is another indicator of cake forming potential (Roorda and van der Graaf, 2005), which is similar to MFI as follows:

$$SUR = MFI \frac{2 \Delta P A^2}{\eta_T} \tag{8.17}$$

In order to compare the filtration performance of different feed concentrations, a new parameter, specific resistance to filtration (SRF), is defined as the increase in filtration resistance (1/m) when one kg COD (or DOC) present in the sludge water (< 0.45 μm) is delivered to one m^2 of membrane surface area. The SRF only considers the delivered COD or DOC in the sludge water. However, the particulate COD (> 0.45 μm) is not considered as "delivered COD", due to the fact that particulates in MBR sludge have a low tendency to deposit and exhibit a low correlation with MBR fouling (Lesjean et al., 2005; Rojas et al., 2005; Rosenberger et al., 2005; Rosenberger et al., 2006).

8.4 Results and discussion

8.4.1 Fouling potential of BAP, UAP and SMP

To evaluate the filtration behaviour of BAP, UAP and SMP, the three samples were filtered using the unstirred cell operating under constant pressure conditions. The filtration flux and MFI-UF of the UAP filtration are plotted in Figure 8-1. The flux-

time curve showed a typical shape of constant pressure filtration. The flux undergoes a rapid initial decline, followed by a long tail, and eventually stabilized at 6.14 L/(m²·h) after 10 hours. The initial flux of the UAP sample was 104 L/(m²·h) at 14.3 kPa, which was obtained 90 seconds after the start up of the filtration. This initial flux was much lower than the clean water flux (164 L/(m²·h) obtained using Milli-Q water. Thus, in the initial 90 seconds, 37% of membrane permeability was lost probably due to the adsorption of SMP and pore blocking (Ognier et al., 2002; Zhang et al., 2006a).
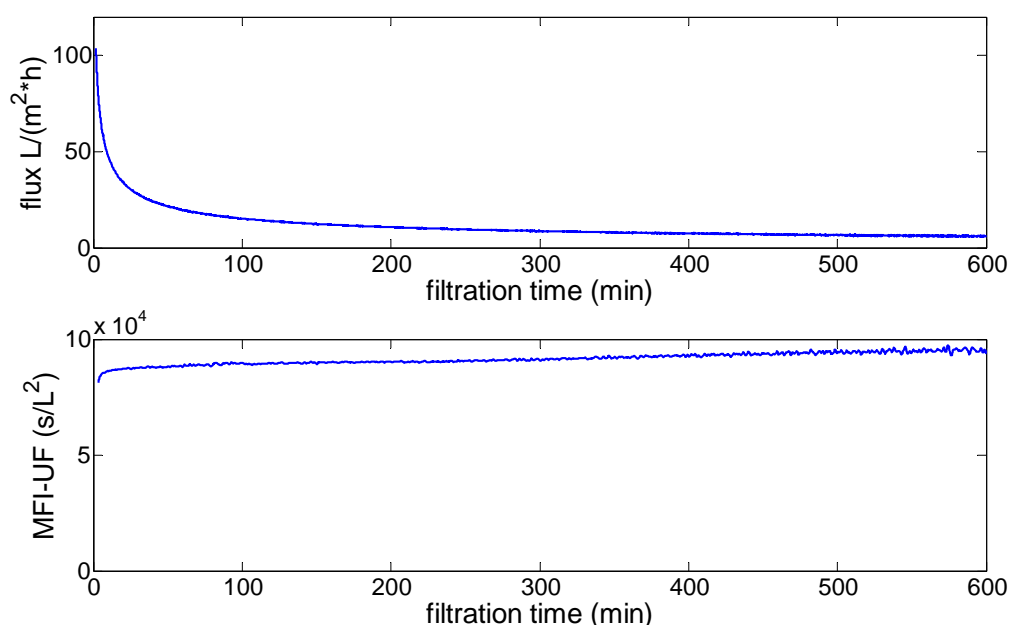
Figure 8-1 Flux and MFI-UF of UAP sample under non-stireed constant pressure filtration (TMP=14.3 kPa)

The MFI-UF showed a slight increase except for the rapid increase in the initial 5 minutes. The MFI is based on the cake filtration mechanism and theoretically it should be constant if cake filtration holds. The slight increase might be due to the depth filtration, i.e., the filter cake was rearranged and became more compact. The mean MFI-UF values of the last half hour filtration were 4.27×10^5, 9.53×10^4, and 2.91×10^5 s/L² for BAP, UAP and SMP filtration, respectively. Roorda et al. (2005) reported that the SUR values of effluent collected from 8 Dutch WWTPs (wastewater treatment plants) were in a range of $5-29 \times 10^{12}$ 1/m² using a 150 kDa capillary membrane, which corresponded to MFI-UF values of $6.6-38 \times 10^3$ s/L² at standard MFI-UF test conditions presented in section 8.3. The MFI-UF of SMP in this MBR is

7.8-44 times higher than that of EfOM (effluent organic matter) from WWTPs. Given that the COD levels of MBR sludge water and EfOM are of the same general magnitude, i.e., (60-120 mg/L), the very high MFI-UF of SMP samples suggest that the "quality" of the macromolecular organic matter in the MBR sludge water is much worse (i.e., poorer filterability) than that of the EfOM from WWTPs. This difference in filterability may be attributed to the fact that the organic components in MBR sludge water are mostly in the size of colloids and macromolecular organic matter. However, the EfOM still contains abundant unsettled flocs (Tchobanoglous et al., 2003).

The specific resistance to filtration (SRF) and specific cake resistance (α) of BAP, UAP and SMP filtrations are summarized in Table 8-1. The comparison of SRF values suggests that the SMP sample collected in the lab-scale MBR exhibited a higher fouling potential than the BAP and UAP samples produced in the batch experiments. Given the fact that the SMP sample contained a higher fraction of biopolymers (> 20 kDa) (69.8% vs. 62.5% and 45.1% with respect to DOC) and a higher overall DOC retention percentage (84.8% vs. 33.1% and 16.9%) than the BAP and UAP samples (see Chapter 5), the higher fouling potential of the SMP sample can be attributed to its biopolymer fraction, which was retained by the membrane (pore blocking or cake formation). This is consistent with earlier studies (Lesjean et al., 2005; Rojas et al., 2005; Rosenberger et al., 2005; Rosenberger et al., 2006), with an improvement in fundamental understanding of SMP fouling by differentiating BAP and UAP.

However, the specific cake resistance (α) showed an opposite trend. The BAP and UAP samples exhibited higher specific cake resistances than that of the SMP sample. This is probably due to the fact that BAP and UAP samples contained more smaller size colloidal and macromolecular organic matter (see Chapter 5), which can also be deduced from the retention percentage by the membrane (Table 8-1). In addition, the BAP and UAP filtration may incur more pore blocking given their smaller molecular sizes. Thus, the specific cake resistances obtained in the batch filtrations of BAP and UAP actually included a certain amount of blocking resistances.

Table 8-1 Specific resistance to filtration (SRF) and specific cake resistance (α) of SMP samples under non-stireed constant pressure filtration (TMP=14.3 kPa)

parameter	BAP	UAP	SMP
SRF_{COD} (m/kg COD)	1.40×10^{15}	1.73×10^{15}	3.81×10^{15}
SRF_{DOC} (m/kg DOC)	4.39×10^{15}	5.82×10^{15}	5.95×10^{15}
α_{COD} (m/kg COD)	1.93×10^{15}	5.39×10^{15}	3.58×10^{15}
α_{DOC} (m/kg DOC)	12.7×10^{15}	31.4×10^{15}	6.61×10^{15}
Removed by membrane (%COD)	69.4%	29.3%	95.2%
Removed by membrane (%DOC)	33.1%	16.9%	84.8%

Lee and co-workers obtained a α of mixed liquor of a MBR sludge in the range of $0.2\text{-}2 \times 10^{12}$ m/kg (Lee et al., 2001b; Jin et al., 2006). The α of the SMP sample in this study is 2,000-20,000 times higher than that of MLSS; however, it is consistent with that of sludge water (3×10^{15} m/kg) obtained in an anoxic MBR (Ognier et al., 2002). The measured α in this study is compared with a theoretical calculating using the Carman-Kozeny equation. If one assumes a particle diameter = 0.2 µm (Chapter 5), cake porosity = 0.65 (Jin et al., 2006), and particle density = 1250 kg/m^3 (Tchobanoglous et al., 2003), theoretical specific cake resistance should be 4.6×10^{12} m/kg, which is 3 orders lower than the measured value (3.58×10^{15} m/kg). To fit the measured α, the cake porosity has to be decreased to 0.1. This cake porosity is consistent with a filtration of 200 nm alginate particles as model soluble EPS (Ye et al., 2005b). This theoretical calculation of the specific cake resistance suggests that the void in the filter cake formed by SMP has probably been filled by other smaller SMP and has resulted in a very compact cake layer and a very high specific cake resistance.

After each batch filtration of BAP, UAP and SMP samples, the cake formed on the flat sheet membrane was carefully removed manually. The membrane was put back into the unstirred cell, and Milli-Q water was filtered to determine the flux again. The difference between the filtration resistance after the removal of the filter cake and the clean membrane resistance provides a rough estimation of the blocking resistance. The results showed that the blocking resistance accounted for approximately 108%, 134% and 40% of the clean membrane resistance for BAP, UAP and SMP respectively. The highest blocking resistance was obtained in the UAP filtration, which can be attributed to the fact that a higher fraction of low molecular compounds

exists, which can be attributed to the highest fraction low molecular compound of the UAP sample (see Chapter 5).

The comparison of the filtration characteristics of BAP, UAP and SMP concluded that SMP directly collected from the lab-scale MBR exhibited the highest retention (removal) percentage and fouling potential. This was attributed to a higher proportion of biopolymer fraction. The UAP and BAP obtained in batches experiments exhibited a lower fouling potential, but a higher pore blocking potential and a higher specific cake resistance. Molecular sizes of BAP, UAP and SMP played a dominant role in determining the filtration characteristics. However, the larger molecular size of the SMP sample is actually due to the selective retention of larger molecular weight compounds in the bioreactor and the washout of smaller molecules through the permeate in a continuously operating MBR system. In the batch BAP and UAP experiments, all molecular size compounds remained in the reactor until final harvesting. The hypothesis that SMP is composed of BAP and UAP appears true, but the above size selection pressure offsets the sizes of the SMP directly collected from the bioreactor.

8.4.2 Comparison of the batch filtration with on-line filtration in the lab-scale MBR

The specific resistance to filtration (SRF) defined above was applied here to compare the on-line filtration in the lab-scale MBR with the batch filtration. Given the normalization using the delivered COD, the difference in SRF can be mainly attributed to the feed water quality instead of quantity (e.g., the percentage of biopolymer) and the difference in hydrodynamic conditions between dead-end and crossflow filtration.

The average values of SRF (5 minute-10 hr in the batch and 60-450 sec in the lab-scale MBR) are presented in Figure 8-2. The SRF obtained in on-line MBR filtration representing low, moderate and high fouling conditions (4, 18 and 25 days after a chemical cleaning, respectively) are compared in the same figure.
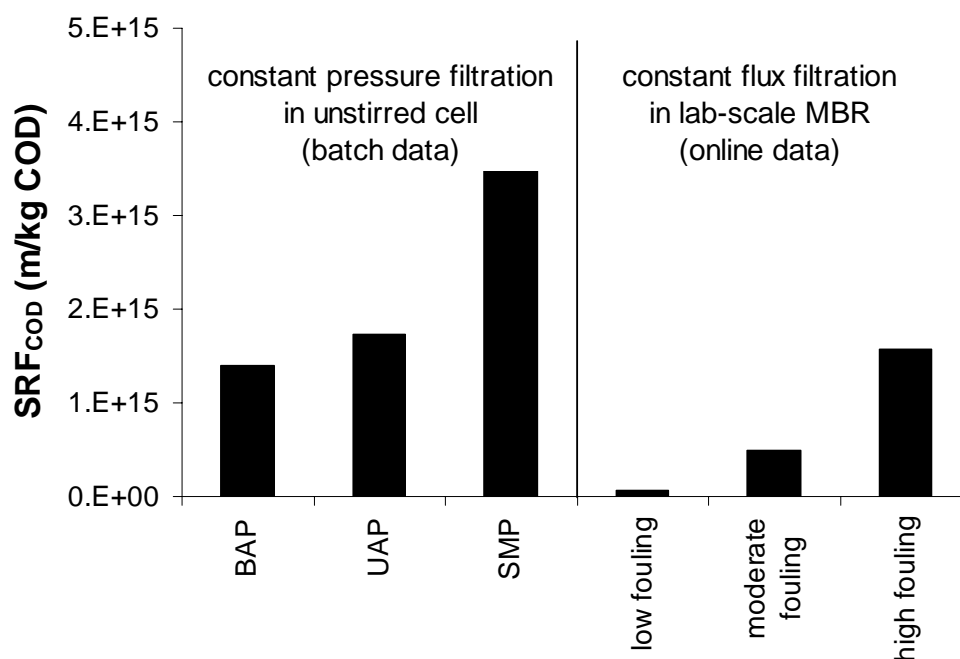
Figure 8-2 Comparison of specific resistance to filtration (SRF) of batch SMP filtration and on-line lab-scale MBR filtration (TMP_cons_press = 14.3 kPa; TMP_cons_flux = 5.2, 8.6 and 28.8 kPa for low, moderate and high fouling respectively)

In the lab-scale MBR, the SRF under high fouling conditions (1.57×10^{15} m/kg COD) was much higher than under low and moderate fouling conditions (5.60×10^{13} and 4.94×10^{14} m/kg COD, respectively). The feed sludge characteristics (e.g., MLSS, SMP concentration and temperature) were similar and the membrane operational conditions (e.g., the hydrodynamics) were exactly the same during this period. The difference of SRF should therefore only be related to the history of the membrane (the accumulation of hydraulically irreversible fouling with time), which is explained as follows: 1) the membrane surface porosity was reduced due to the accumulation of membrane foulant and the actual local filtration flux, from the micro perspective, was increased possibly above the critical flux (Cho and Fane, 2002; Fane et al., 2002; Ognier et al., 2004); and 2) the deposited foulant modified the surface characteristics of the membrane, e.g., the previously deposited biopolymers changed the membrane surface to be more hydrophilic. As a result, the other biopolymers or hydrophilic macromolecular organic matter can easily absorb onto the previously deposited hydrophilic foulant (Chang et al., 2001).

Comparing the SRF obtained in the batch SMP filtration with the on-line filtration of the lab-scale MBR showed that the average SRF in the batch SMP filtration was 68, 7.7 and 2.4 times higher than those in the lab-scale MBR filtration under low, moderate and high fouling conditions, respectively. This difference is due to the combined effects of hydrodynamics and membrane history. If the membrane was only fouled slightly or moderately, the crossflow on the membrane feed side (0.5 m/s sludge and 0.5 m/s air in this lab-scale MBR) was effective in controlling membrane fouling. However, if the membrane had a strong fouling history, the actual local filtration flux can be much higher than the global flux and extend beyond the critical flux. Thus, the crossflow was not able to control the SMP deposition anymore and the SRF could approach that of a dead-end filtration. The history of the membrane is further studied in the following sections of this chapter using a modelling approach.

8.4.3 Correlation analysis of the lab-scale MBR

The importance of membrane history of fouling properties was also illustrated by a correlation analysis between the starting resistance (defined as the total resistance at 10 sec after the start of a filtration cycle, i.e., R_m+R_{irr}) and the reversible fouling resistance (defined as the increase in filtration resistance from 10 to 450 sec, R_c). Eight months of data from the lab-scale MBR (one data point every second) were used in the statistical study. The result showed that the correlation between the starting resistance and the reversible fouling resistance was significant with a correlation coefficient of 0.72 and a p value of 2.2×10^{-17} (a p value less than 0.05 can be considered as statistically significant). This is consistent with the previous relationship that the membrane history (included in the starting resistance in relationship with the irreversible fouling) can significantly influence the SRF (related to the reversible resistance). The correlation analysis was also extended to other variables (e.g., MLSS, MLVSS, SMP, EPS, effluent COD, COD retention percentage by the membrane). However, none of these, including SMP, exhibited a clear correlation with membrane fouling. This is probably due to the fact that the long-term impact of SMP resulted in an accumulation of irreversible resistance, which overwhelmed the short-term impact of SMP concentration on MBR fouling.

8.4.4 Simulating the accumulation of irreversible fouling

The developed integrated model is able to simulate the TMP under conditions of varying flux and varying SMP concentration. However, the lab-scale MBR was operated under constant flux condition and no operational parameters were changed. Thus, only steady state (with respect to biology) experimental results were available for model calibration. The sludge concentration, SMP concentration and effluent quality during the period of model calibration (25 days) and model validation (24 days) was stable. The mean COD concentrations of the sludge water collected from the membrane loop (the feed of the membrane) were 119 ± 33 and 100 ± 29 mg COD /L for model calibration and validation period, respectively.

The SRF in the lab-scale MBR showed that the filtration behaviour depended significantly on the membrane history. The long-term irreversible fouling (membrane history) may be attributed to either complete blocking, standard blocking, intermittent blocking, cake filtration or a combination of above. Only the derivation of the complete blocking model is presented in section 8.2.1. The derivation of other models can be inferred from Hermia (1982). Each of these four models has only one parameter to estimate.

Four models were proposed individually to fit the TMP_{start}, which was arbitrarily defined as the TMP at 10 sec after the start of a filtration cycle, as a rough estimation of $R_m + R_{irr}$. A non-linear curve fitting was performed in Matlab (Mathworks, USA) and two parameters were estimated (TMP_{start} at day 1 as the initial condition and another model related parameter). The cake filtration model resulted in a linear relationship between TMP and time, which was obviously not able to fit the curve. The fitting using standard blocking and intermediate blocking are presented in Figure 8-3 and the best fitting using complete blocking model is presented in Figure 8-4.
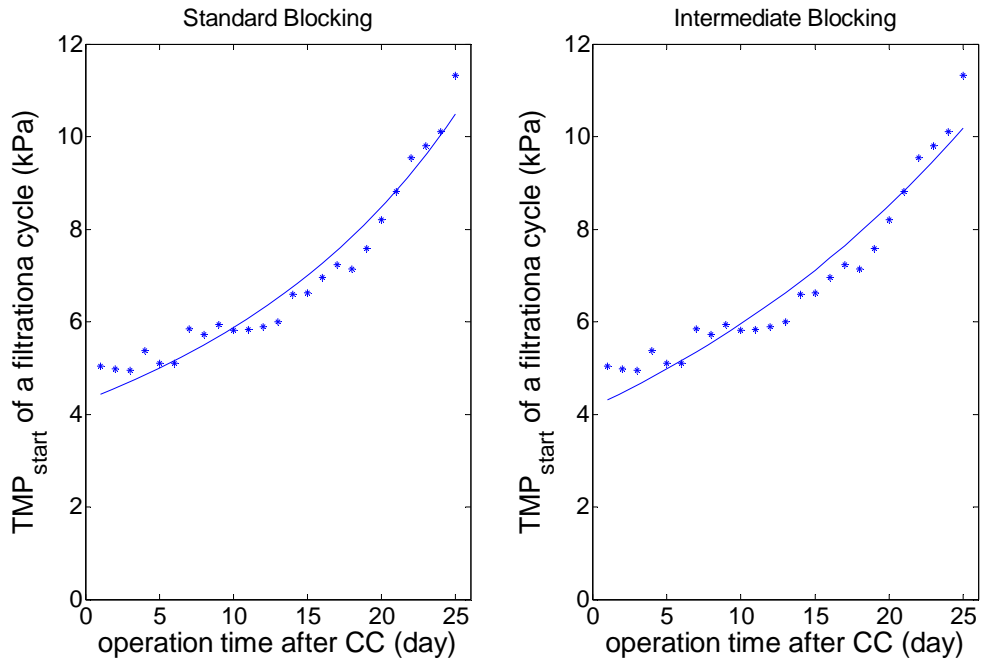
Figure 8-3 Comparision of simulated and measured starting point of TMP after backwashing in 25 days ("*" = measured TMP$_{start}$; "—" = simulated TMP$_{start}$ using standard blocking and intermediate blocking model, one measurement point represents one day)
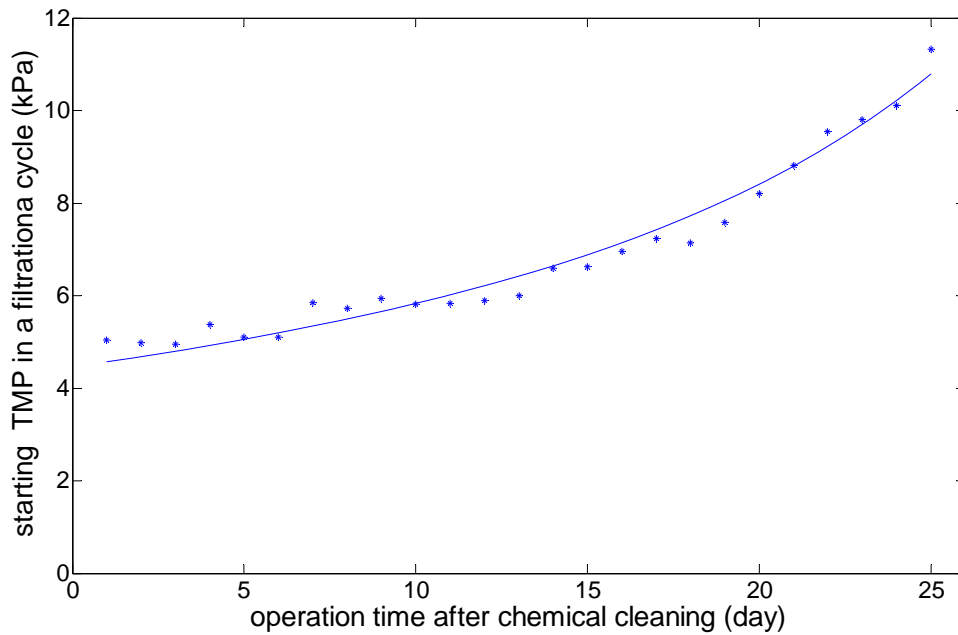
Figure 8-4 Comparision of simulated and measured starting point of TMP after backwashing in 25 days ("*" = measured TMP$_{start}$; "—" = simulated TMP$_{start}$ using complete blocking model, one measurement point represents one day)

The mean value of the relative error $|TMP_{simulated} - TMP_{start}|/TMP_{start}$ between the measured and the simulated TMP$_{start}$ are 0.051, 0.062, and 0.040 for standard blocking, intermediate blocking and complete blocking model, respectively. The sum of squre

erros are 3.9×10^6, 5.8×10^6, and 2.4×10^6 Pa^2 for standard blocking, intermediate blocking and complete blocking model, respectively. In addition, the residuals of the curve fitting using standard blocking and intermediate blocking model are not random. However, the residuals of the curve fitting using the complete blocking model appear random with model deviations less than the measurement error. Thus, the complete blocking model is applied in the following sections to describe the increase in irreversible fouling between two chemical cleanings of the lab-scale MBR. The estimated parameters are: TMP_{start} = 4463 Pa, and σ_{COD} = 0.2582 m^2/kg COD.

It should be noted that the estimated parameter σ_{COD} is the hydraulically irreversibly blocked membrane surface area by 1 kg of delivered COD. Thus, the complete blocking model adopted here described the loss of available membrane surface area and the increase in R_{irr} well, under real MBR operational conditions, i.e., crossflow, periodical relaxation and backwashing, and using real MBR sludge.

8.4.5 Simulating the filtration behaviour between two chemical cleanings

A cake filtration model was combined with the complete blocking model to simulate the TMP vs. time curve during the 450 sec filtration cycles. However, the start-up of the suction pumps and the initial pore blocking are not included in the model. Three filtrations cycles on day 4, 18, and 25 representing low, moderate and high fouling membrane history conditions were used to calibrate the cake filtration part of the model. The parameters TMP_{start} = 4463 Pa and σ_{COD} = 0.2582 m^2/kg COD estimated above were directly transferred into the integrated model. The specific cake resistance (α) used the value estimated in the unstirred cell batch filtration, i.e., 3.58×10^{15} m/kg (see Table 8-1). The other two parameters, i.e., the critical local flux, J_m and the power parameter, n, were estimated using curve fitting as in Figure 8-5.
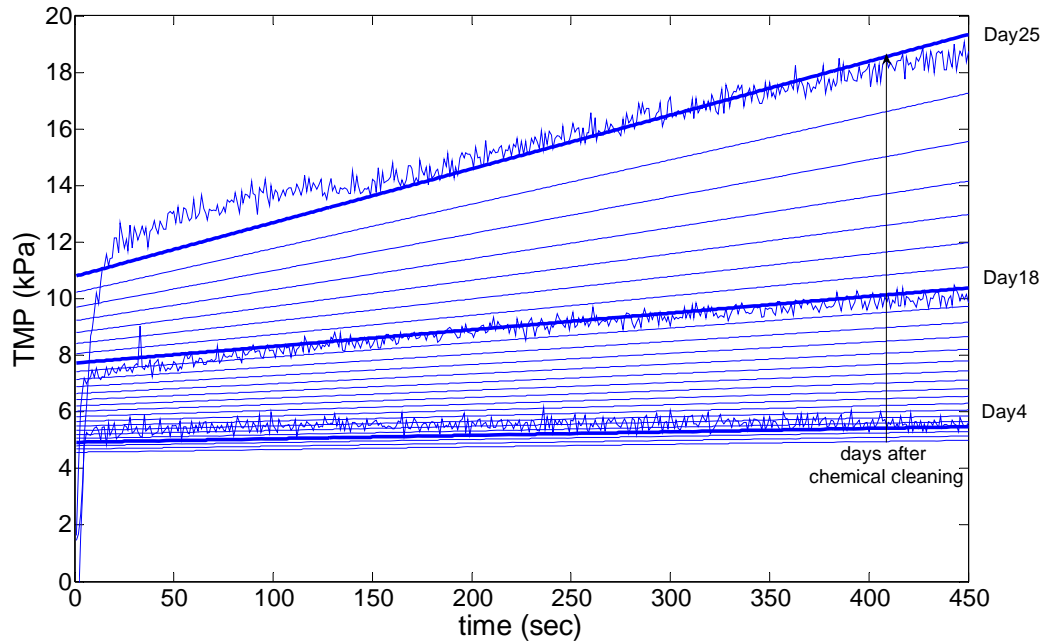
Figure 8-5 Comparision of simulated and measured TMP during a filtration cycle in 25 days (noisy line = measured TMP on day 4, 18 and 25; thin straight line = simulated TMP using the integrated model from day 1 through day 25; thick straight line = simulated TMP using the integrated model on day 4, 18 and 25, one line represents one filtration cycle on a certain day)

The sum of the SSE of the 3 cycles from (40 to 450 seconds) by omitting the initial blocking state were minimized resulting in $J_m = 94.3$ L/(m^2·h) and n=3.5. The mean values of the relative error between the measured and the simulated TMPs are: 0.067, 0.037, 0.023 for day 4, 18 and 25, respectively, which is again very satisfactory. It should be noted that the specific cake resistance (α) in the lab-scale MBR may differ from the one obtained in the dead-end filtration test. An adjustment of α may therefore be performed to obtain a better fitting, if necessary. However, the α obtained in the unstirred cell batch filtration appears to be adequate in this case.

8.4.6 Validation of the integrated filtration model

The integrated model developed above was validated using a set of MBR data collected in a different period. The parameters σ_{COD}, α, J_m and n estimated above were used directly in the model validation simulation. However, in the validation data set, the TMP$_{start}$ was much higher than the one in the calibration data set. Thus, the TMP$_{start}$ had to be calibrated (TMP$_{start}$ = 8981 Pa). This small adjustment only increased the intercept, but showed no impact on the shape of the simulated TMP$_{start}$.

The simulated and observed TMP$_{start}$ are compared in Figure 8-6, clearly showing the model overestimated the TMP$_{start}$ after day 10. The mean value of the relative error between the measured and the simulated TMP$_{start}$ was 0.12. The deviation of the simulated TMP$_{start}$ from the measurement is attributed to the status of the membrane at the time of the period of model validation. A chemically cleaned membrane was used to collect the calibration data set, whereas, a virgin membrane was used during the collection of validation data set. It appears that the TMP$_{start}$ using the virgin membrane barely increased during the initial 10 days.

Figure 8-6 Validation of simulated and measured starting point of TMP after backwashing in 24 days ("*" = measured TMP$_{start}$; "—" = simulated TMP$_{start}$ using complete blocking model, one measurement point represents one day)

The short-term TMP evolution between two backwashings during this period was also validated. The measured and simulated TMP vs. time are presented in Figure 8-7. In most filtration cycles, the model overestimated the TMP during the initial 60-140 sec, while it underestimated the TMP afterwards. The mean values of the relative error between the measured and the simulated TMPs are: 0.089, 0.084 and 0.031 for day 8, 16 and 24, respectively.
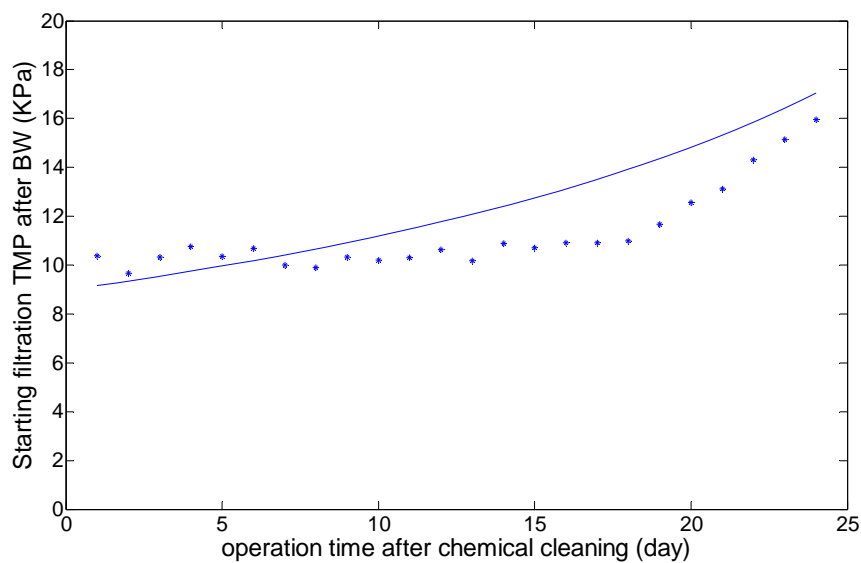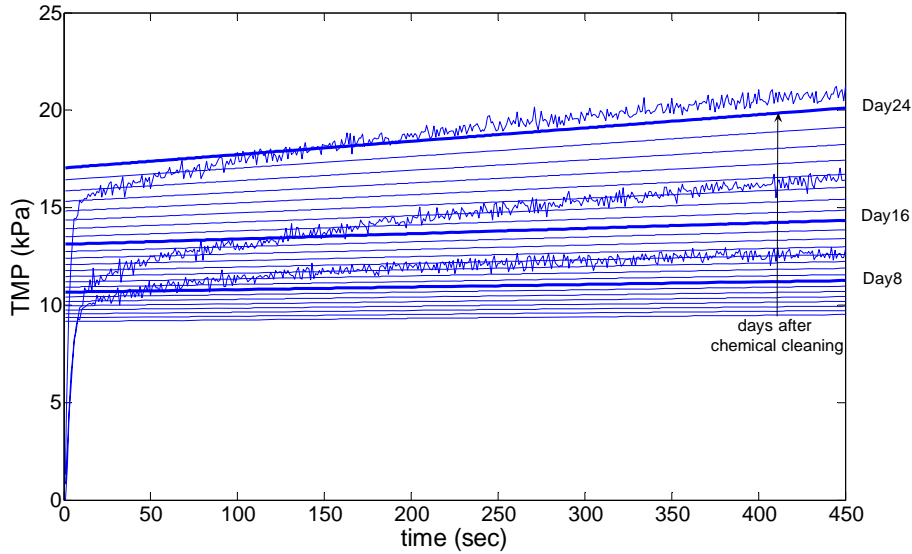
Figure 8-7 Validating of simulated and measured TMP during a filtration cycle in 24 days (noisy line = measured TMP on day 8, 16 and 24; thin straight line = simulated TMP using the integrated model from day 1 through day 24; thick straight line = simulated TMP using the integrated model on day 8, 16 and 24, one line represents one filtration cycle on a certain day)

The model calibration using the 25-day data set was successful but the subsequent model validation using the different 24-day data set was not good. The integrated model well described the 3 stage filtration behaviour and the importance of membrane history (the amount of irreversible fouling). In the initial 2 stage operation (from days to weeks), both reversible fouling rate ($\dfrac{dTMP}{dt}$) during one filtration cycle and irreversible fouling rate ($\dfrac{dTMP_{start}}{dt}$) were low. However, when the membrane becomes old due to the accumulation of irreversible resistance, both fouling rates accelerate rapidly and reach an upper limit of chemical cleaning TMP within days. The membrane history can be well described by the irreversibly complete blockage of available membrane surface area. In addition, the cake filtration model well described the increase in TMP in a filtration cycle (except for the initial blocking stage). If a membrane is clean, a large membrane surface area can result in a low local filtration flux below the critical flux, thus the formation of a filter cake is slow. However, if the membrane is old, only a small membrane surface area is available for filtration. Thus the actual local filtration flux can be higher than the critical flux and result in a rapid build up of a filter cake in one filtration cycle.

8.4.7 Predicting the impact of SMP concentration and filtration flux on MBR fouling

The impact of SMP on MBR fouling can be illustrated using the developed model. Using the above calibrated parameters of the MBR data sets (TMP$_{start}$ = 4463 Pa, σ_{COD} = 0.2582 m^2/kg COD, α = 3.58×10^{15} m/kg, J$_m$ = 94.3 L/(m^2·h) and n=3.5), filtration behaviours at two SMP concentrations (50% and 150% of reference conditions, 119 mg COD/L) are simulated in Figure 8-8. A TMP of 20 kPa is assumed as an upper limit for chemical cleaning TMP. Under the reference conditions (C$_b$=119 mg/L, J=31.8 L/(m^2·h)), it takes 25 days for the TMP to reach 20 kPa. Halving the SMP to 59.5 mg/L allows the MBR to operate for 55 days without chemical cleaning. However, a 50% increase in the SMP concentration (178.5 mg COD/L) decreased the chemical cleaning interval to only 15 days.
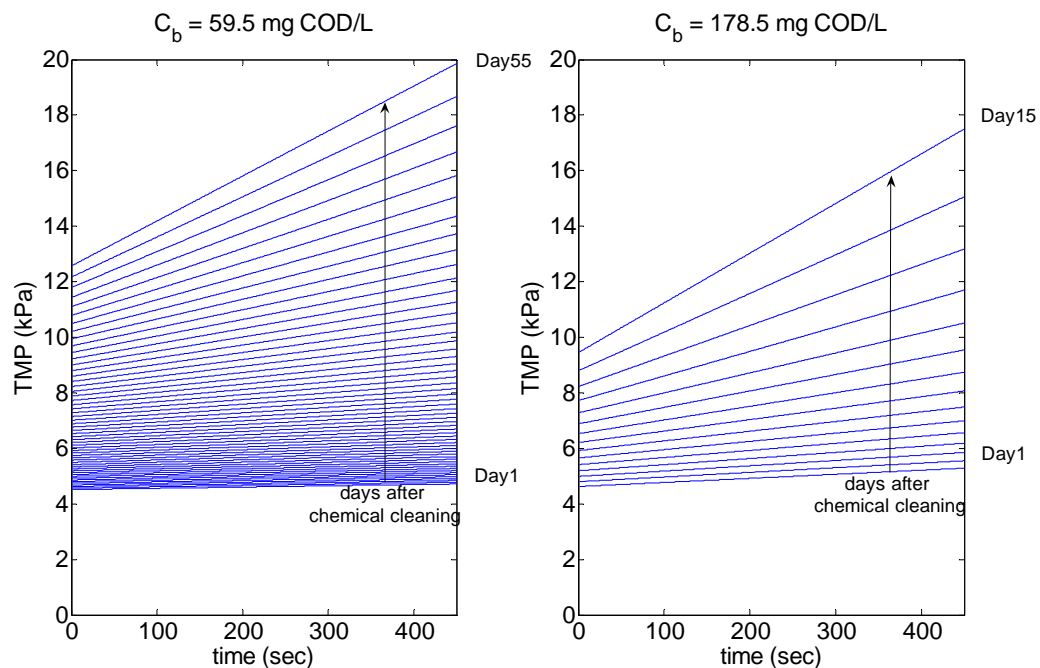
Figure 8-8 Simulating the impact of SMP concentration on TMP increase and chemical cleaning requency under constant flux conditions (J$_G$=31.8 L/(m^2·h))

Similarly, filtration behaviours at two filtration fluxes (50% and 150% of reference conditions, 31.8 L/(m^2·h)) are simulated in Figure 8-9. Under the reference conditions (J$_G$=31.8 L/(m^2·h), C$_b$=119 mg/L), it takes 25 days for the TMP to reach 20 kPa. Halving the flux to 15.9 L/(m^2·h) allows the MBR to operate 64 days without

chemical cleaning. However, a 50% increase in flux (47.7 L/(m²·h)) decreased the chemical cleaning interval to a mere 8 days.
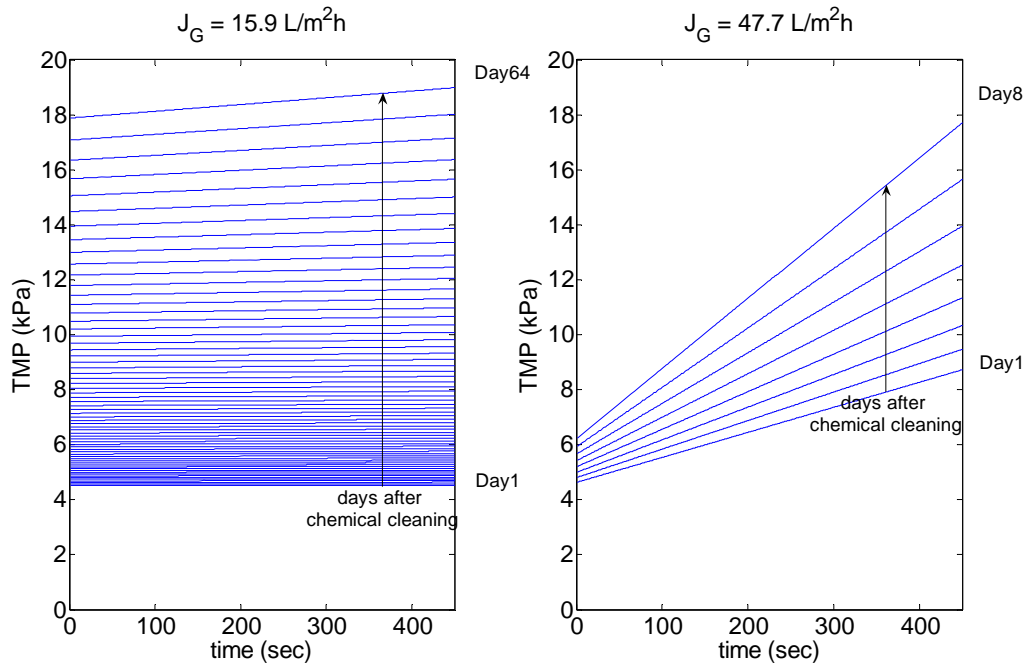
Figure 8-9 Simulating the impact of filtration flux on TMP increase and chemical cleaning requency under constant SMP concentration conditions (C_b=119 mg COD/L)

Comparing the significance of SMP concentration and filtration flux on the chemical cleaning frequency showed interesting results. Given the same SMP mass flux delivered to the membrane (C_bJ_G, 59.5×31.8 vs. 119×15.9 mg COD/h), decreasing filtration flux allows the MBR operating 64 days without chemical cleaning, while decreasing bulk SMP concentration only extended the chemical cleaning frequency to 55 days. Clearly, filtration flux has a higher impact than SMP concentration. This can be attributed to the fact that a lower flux reduces the particle permeation velocity and consequently reduces the likelihood of SMP deposition (see Chapter 7). Thus, reducing flux reduces the percentage of foulants (SMP) that can actually reach the membrane in addition to decreasing filtration volume. However, reducing SMP concentration has no direct impact on hydrodynamic conditions. This comparison of the impact of filtration flux with the SMP concentration demonstrates the ability of the model that is able to predict the impact of hydrodynamic conditions. However, the model does not include the crossflow velocity as input variable. Its ability in describing hydrodynamics is still limited to constant crossflow conditions.

197

The prediction of chemical cleaning frequency has practical significance, e.g., 1) to predict the life time of the membrane, which is influenced by the cumulative chemical exposure during chemical cleanings; and 2) to assistant in the design of a MBR system. The determination of filtration flux and the amount of membrane modules to purchase can be determined based on an economy analysis. An economic analysis using this model is possible, but beyond the scope of this fundamental study due to the fact that many assumptions have to be made, e.g., the cost of the membrane, the tolerance of cumulative chemical exposure of the membrane, and the price of the membrane when the membrane needs to be replaced.

8.5 Conclusions

SMP, BAP and UAP exhibited very high fouling potentials. The MFI-UF of SMP in a lab-scale MBR was 7.8 to 44 times higher than that of secondary effluent of wastewater treatment plants. The specific cake resistance of the SMP sample was approximately 2,000 to 20,000 times higher than that of a MBR sludge, which was attributed to a very low cake porosity (0.10) as estimated using the Carman-Kozeny equation.

SMP directly collected from the lab-scale MBR exhibited the highest retention (removal) percentage and fouling potential. This was attributed to a higher portion of biopolymer fraction. The UAP and BAP obtained in batches experiments exhibited a lower fouling potential, but a higher pore blocking potential and a higher specific cake resistance. Molecular sizes of BAP, UAP and SMP played a dominant role in determining the filtration characteristics.

A heavily fouled membrane showed a much higher fouling rate than a slightly or moderately fouled membrane. This was attributed to the membrane history that the hydraulically irreversible fouling reduced the available membrane surface area and resulted in a higher local flux. In a statistical analysis of the lab-scale MBR, the only variable that significantly correlated with the reversible fouling in the lab-scale MBR was the membrane history (the amount of irreversible fouling).

A dynamic model combining the complete blocking and cake filtration model was developed. The model considers the typical MBR operational conditions: crossflow, periodical backwashing and relaxation. It was calibrated under the lab-scale MBR conditions and able to predict both the short-term TMP increase in one filtration cycle (except for the first a few seconds of the filtration) and long-term TMP increase between two chemical cleanings. It should be noted that the assumptions made in the model development are not unique for MBRs. Thus, the integrated model can be applied to any MF and UF filtration system.

Simulations using this model demonstrated that a 50% decrease in SMP concentration or flux reduced the chemical cleaning frequency from 25 days to 65 or 55 days, respectively. This illustrated and quantified the importance of SMP concentration and flux on long-term MBR fouling. However, given the same SMP mass flux delivered to the membrane ($C_b J_G$, 59.5×31.8 vs. 119×15.9 mg COD/h), filtration flux has a higher impact on membrane fouling than SMP concentration, which is attributed to the fact that reducing flux reduces the percentage of foulants (SMP) that can actually reach the membrane in addition to decreasing filtration volume.

Finally, the integrated model has its limitations. First, in full-scale MBRs, many other factors can influence the filtration process, e.g., influent wastewater concentration and flow rate, temperature, hydrodynamic conditions, effectiveness of chemical cleaning and the deterioration of membrane polymer structure etc. These factors are not considered or well described in the model. Second, the model was calibrated under conditions of constant flux and constant COD concentration of sludge water, thus, the validity of this model under dynamic conditions needs to be further studied. Third, although the model is able to describe the short-term and long-term filtration behaviour in this lab-scale MBR, the parameters obtained in this study are specific for this MBR and its operational conditions, thus, the extrapolation to other systems should be with caution. Finally, only a very simple steady state hydrodynamic model is incorporated into the membrane fouling model. A more detailed hydrodynamic model including the influence of crossflow velocity should be combined to simulate the fouling under varying hydrodynamic conditions. Optimisation and energy saving can be studied with this more advanced model.

9.
General conclusions

The goal of this thesis was to characterise the foulants in MBRs and develop a mathematical model to predict both the membrane fouling and effluent quality. The study focused on the interactions between the MBR biology and the membrane fouling. The impact of membrane separation on biology is straight-forward and described in Chapter 4. However, the impact of biology on membrane fouling is very complex, requiring multidisciplinary interactions clearly visible in the work obtained in Chapter 5-8.

Impact of membrane separation on biology

A fully automated lab-scale MBR was constructed and modelled using the ASM2d model. The excellent COD removal was attributed to both biodegradation and physical retention by the UF (ultrafiltration) membrane with a total removal percentage of 97.6%. However, the removal of total nitrogen and phosphorus was only 83.7% and 49.3%, respectively, due to the higher nutrient contents present in the influent and the coupled aerobic/anoxic compartment reducing the utilization efficiency of volatile fatty acids.

With respect to the MBR hydraulic model, the membrane can be modelled as an idea biomass separator without volume and biological reaction. Including the membrane cleaning (backwashing and relaxation) into the MBR hydraulic model slightly improved the accuracy in effluent quality prediction, whereas it significantly decreased simulation speed. It is not necessary to include the hydraulic model, if the requirement for model accuracy is not high.

MBR has a well defined SRT independent from the settling properties. The ASM2d model structure developed for conventional activated sludge (CAS) processes can be directly used for MBR modelling. Most default ASM2d parameters suggested for

CAS processes hold for MBR as well. However, the MBR sludge exhibited a lower oxygen and ammonium half-saturation coefficients ($K_{O,aut}$=0.2 mg O_2/L and $K_{NH,aut}$=0.2 mg N/L), probably due to the smaller sludge flocs (30-50 μm). The characterisation of influent inert particulate COD (X_I) is easier in MBRs than in CAS systems.

MBRs tend to accumulate a high concentration of soluble microbial products (SMP), that are colloidal and refractory in biological treatment processes. Readaily and slowly biodegradable COD should be not classified based on size, e.g., 0.45 µm. Instead, chemical biological methods are more stuiable. To close the COD mass balance, SMP can be overlooked and treated as X_I, if the aim of the study is for biological nutrient removal. A high SMP concentration present in the MBR sludge water appears to inhibit the nitrifiers in a certain extent. Hence, the specific growth rate of nitrifers may be reduced in MBRs compared with that in CAS systems. However, more studies are needed to be conclusive.

An ASM2dSMP model was developed with the capability of simulating both SMP concentration and nutrient removal. The introduction of SMP into the ASM2d model allowed restoring some PAO (phosphorus accumulating organism)-related parameters to their default ASM2d values. It appears that the reduced fermentation rate and aerobic/anoxic phosphorus uptake rate obtained in the calibration of the ASM2d model were compensating for the overlooking UAP (utilization associated product) generation. However, this remains as a hypothesis and more studies are needed to be conclusive.

It appears that the accumulation of SMP in the bioreactor may have a certain impact on ASM modelling. However, the evidence provided in thesis is not convincing enough to draw a solid conclusion. In this aspect, if the aim of MBR modelling is to describe COD and biological nutrient removal, the SMP may be overlooked and compensated for tuning of some related parameters. It can be stated that the significance of SMP is mostly related to MBR fouling as described below.

Impact of biology on membrane fouling

The impact of biology on membrane fouling is very complex. Dissolved oxygen concentration (Kang et al., 2003; Kim et al., 2006), sludge retention time (Han et al., 2005; Nuengjamnong et al., 2005; Trussell et al., 2006) and hydraulic retention time (Tay et al., 2003; Chae et al., 2006), etc. can all influence MBR fouling. SMP are recognized as the main constituent of activated sludge affecting MBR fouling and it is hypothesized that the variation of a MBR's biology impacts the MBR fouling in an indirect way by changing the SMP concentration and composition. A complete picture of the impact of SMP on membrane fouling has been established in this PhD thesis, i.e., the characterisation of SMP, prediction of SMP concentration in bioreactors, deposition of SMP under crossflow conditions, and prediction of fouling rate due to the deposited SMP.

Significance of SMP with respect to membrane fouling

SMP are composed of BAP (biomass associated products produced during biomass decay) and UAP (utilization associated products produced during biomass growth). The SMP collected from the bioreactor are normally a mixture of BAP and UAP. Most MBR studies in literature obtained SMP samples directly from the MBR's bioreactor. This approach does not allow differentiating between BAP and UAP and it is also not possible to correlate membrane fouling with the phase of biomass growth or the phase of biomass decay, as these processes occur simultaneously. In this thesis, batch experiments were successfully conducted to produce BAP and UAP separately. The filterability of the produced BAP and UAP samples collected from these batch experiments were consequently tested using an unstirred cell. The feed and permeate were characterised using a new tool, LC-OCD (liquid chromatography − organic carbon detection).

SMP were mostly composed of biopolymers and a certain amount of small molecules. The biopolymer fraction exhibited a very wide MW distribution and the largest portion of biopolymers exhibited a MW of 2000 kDa. The permeate of batch SMP filtration contained a lower percentage of biopolymer fraction, and the retention of proteins appears lower than that of polysaccharides (a higher organic nitrogen content was observed in the permeate). In addition, the permeate exhibited a higher

hydrophobicity (higher SUVA values) and was more oxidized (higher mean oxidation number). The comparison of the feed and permeate suggests that the biopolymer fraction retained by the membrane was the major fraction related to membrane fouling.

The BAP collected from the batch BAP reactor and the SMP collected from the MBR reactor showed very low BOD_5/COD ratios indicating low biodegradabilities. Extending the incubation time up to 28 days led to only little improvement in biodegradability. The poor biodegradability of BAP is consistent with the very low hydrolysis rate in the calibrated BAP model. Two types of UAP are produced. The UAP produced in the storage phase (UAP_{sto}) is more biodegradable than the UAP produced in the cell proliferation phase (UAP_{pro}). In addition, the UAP_{sto} exhibits lower MW than UAP_{pro}. In general, the UAP produced during the biomass growth phase exhibited a lower molecular weight than the BAP, suggesting UAP has a lower fouling potential than BAP.

SMP, BAP and UAP exhibited very high fouling potentials. The MFI-UF (modified fouling index – UF) of SMP in the lab-scale MBR was 7.8 to 44 times higher than that of secondary effluent of conventional wastewater treatment plants. The specific cake resistance of the SMP sample was approximately 2,000 to 20,000 times higher than that of the MBR sludge, which was attributed to a very low cake porosity (0.10) as estimated using the Carman-Kozeny equation.

Impact of MBR biology on SMP concentration

The separate production and characterisation of BAP and UAP in dedicated batch experiments allow the development of a simple but adequate SMP model that minimises parameter correlation. A BAP and UAP model was developed based on the existing SMP models, respectively and special attention was paid to the identifiability (whether allows a reasonable estimation of parameter set) of the model parameters. In total, only 4 additional SMP-related parameters were adopted, allowing reasonable parameter confidence bounds.

The SMP model was incorporated into the ASM2d model forming a new ASM2dSMP model. The model was validated using independent experimental results of the lab-

scale MBR. The simulated soluble COD concentration (107.5 mg/L) was very close to the measured value (107.4 mg/L) by introducing the BAP and UAP concept, while the standard ASM2d model failed in predicting the soluble COD concentration (the simulated soluble COD was only 5.0 mg/L).

Compared with SMP models published in literature, the proposed model exhibits a much lower parameter correlation, and therefore has more trusted parameter estimations. The ASM2dSMP model can be used as a tool to simulate the SMP concentration under various SRT and HRT conditions aiming at finding optimal operational conditions inducing the lowest SMP concentration as that would reduce the membrane fouling. Simulation results show that SRTs exhibit a strong and direct impact on the SMP concentration, while the impact of HRT and the SRT/HRT ratio is indirect. Operating a MBR under lower SRT conditions increases UAP production but decreases BAP production. The lab-scale MBR system is dominated by BAP at SRTs above 2 days, which suggests that MBRs should not operate at too long SRTs from the viewpoint of controlling the SMP concentration and minimizing membrane fouling.

The simulated impact of SRT seems in contradiction with some reported SRT studies, which showed that a higher SRT leads to a better filterability in the range of SRTs of 2-10 days (Trussell et al., 2006), 8-80 days (Nuengjamnong et al., 2005) and 10-80 days (Liang et al., 2007). It should be noted however that the simulated SMP concentrations were obtained under steady state conditions. Applying dynamic conditions may stimulate the production of SMP (Drews et al., 2006). Field conditions are always dynamic with respect to influent flow rate, characteristics and temperature. Operating under higher SRT conditions may provide a better stability and improve the robustness of the system. On the other hand, increasing SRTs from 30 to 100 days has also been reported to intensify membrane fouling due to the accumulation of foulants and a higher sludge viscosity (Han et al., 2005), which is consistent with the prediction of the ASM2dSMP model derived in this thesis.

Hydrodynamic control of SMP deposition

The deposition of SMP onto the membrane is impacted by the hydrodynamic conditions in the membrane module. An integrated hydrodynamic model was developed by combining particle backtransport and energy consumption in tubular MBR systems. The model is able to predict the effects of feed sludge particle size, dry solid contents, crossflow velocity, membrane tube dimension and temperature on the particle backtransport and energy consumption.

Simulation results showed that submicron particles exhibited a high likelihood to deposit, and the worst fouling conditions are encountered with particle radii around 0.1 μm and a crossflow velocity below 0.5 m/s. Simply increasing the crossflow did not completely prevent colloidal particle deposition. A sensitivity analysis of operational variables and membrane module dimension concluded the impact of crossflow to be significant, while other variables were less influential.

An optimisation study was performed aiming at maximizing the efficiency of energy consumption in particle backtransport. Submicron particles received high weighting factors (high filter cake formation potential) although their quantity was small. The theoretical optimisation considering a typical particle size distribution suggests that cost-effective operation of an MBR is to run it at the lowest possible crossflow velocity. However, the practical optimisation in the lab-scale MBR concluded that the crossflow velocity should neither be too low such that dead-end conditions are approached, nor be too high to result in a heterogeneous TMP distribution along the membrane and increased energy consumption. A critical crossflow value probably exists, below which, fouling is significantly intensified, and above which, fouling is not further reduced. In this lab-scale MBR, this critical crossflow velocity was between 0.75-1 m/s at 40 $L/(m^2 \cdot h)$.

Prediction of the MBR fouling rate

A heavily fouled membrane showed a much higher fouling rate than a slightly or moderately fouled membrane. This was attributed to the membrane history induced by

the accumulation of hydraulically irreversible fouling, which reduced the available membrane surface area and resulted in a higher local flux.

A dynamic model combining the complete blocking model and the cake filtration model was developed. The model considered the typical MBR operational conditions: crossflow, periodical backwashing and relaxation. To reduce the model complexity, a simple steady state hydrodynamic model was incorporated. The integrated model was calibrated and validated under steady state conditions in the lab-scale MBR. With the SMP concentration simulated by the ASM2dSMP model as model input, the integrated model has the power to dynamically predict the impact of MBR operational conditions (e.g., SRT and HRT) on both the short-term TMP increase in one filtration cycle (except for the first few seconds of the filtration) and the long-term TMP increase between two chemical cleanings.

Overall evaluation of SMP with respect to MBR fouling

The role of SMP linking membrane fouling with biology is schematically presented in Figure 9-1. SMP are produced in the MBR during both biomass growth and decay. A large fraction of SMP is poorly biodegradable and retained by the membrane. As a result, a high concentration of SMP can accumulate in MBRs and the main constituent of MBR sludge water is actually SMP. SMP have a very high fouling potential due to their small sizes (comparable with the membrane pore size). Their small size also provides SMP a higher likehood to deposit onto the membrane even under crossflow conditions. The shear rate on the feed side of the membrane surface cannot completely prevent their deposition in the range of common filtration fluxes and crossflow velocities. The deposited SMP can result in both pore blocking and filter cake formation and the fouling can be both reversible and irreversible to hydraulic cleaning. Fouling irreversible to hydraulic cleaning is the most troublesome phenomena, as it reduces the available membrane surface area and results in increased local filtration fluxes. All above SMP-related phenomena are described mathematically in this thesis and a developed integrated model is able to predict the membrane fouling under steady state conditions provided the biological and membrane operational conditions are known.
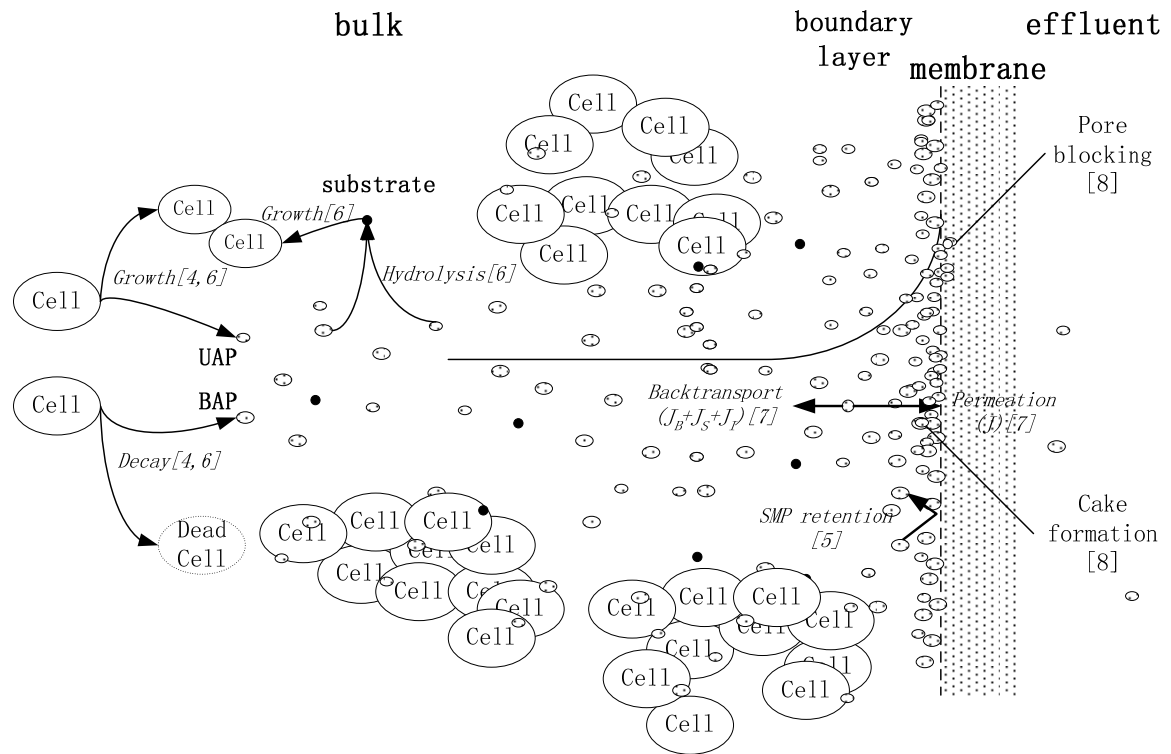
Figure 9-1 The role of SMP linking membrane fouling with biology (the number after the process in brackets is the related chapter number)

10.
Perspectives

This thesis characterised the SMP in MBRs and developed a mathematical model to predict both the membrane fouling and effluent quality. A complete picture of the SMP linking of MBR biology and membrane fouling via SMP is presented. However, the limitations and perspectives of this study are as follows.

First, the main foulant in MBRs should be studied under various hydrodynamic conditions. This thesis deals with SMP and it is defined here as the soluble and colloidal organic compound with sizes less than 0.45 μm. Chapter 8 assumed that the only compound depositing on the membrane is SMP, which appears valid under low fouling conditions. However, if the fouling is significant and the local flux is actually much higher than the critical flux, single cells and small activated sludge flocs may also deposit (Cho and Fane, 2002). Further studies in identifying corresponding foulants under various fouling and hydrodynamic conditions are therefore recommended. Special attention should be given to the deposition of single cells, since they may be abundant under certain conditions.

Second, the characteristics of feed, permeate and backwashing water collected in BAP, UAP and SMP batch filtrations were studied using LC-OCD. The fraction of SMP retained by the membrane was assumed to be the fraction resulting in membrane fouling. However, it is not clear whether and where they are deposited (in the membrane pores or on the membrane surface) and interact with the membrane. Further studies should be focused on the SMP-membrane interaction and the effectiveness of hydraulic cleaning.

Third, this study used batch experiments to produce BAP and UAP separately. The UAP experiment used acetate as substrate and two types of UAP, i.e., UAP_{sto} produced during acetate storage and UAP_{pro} produced during cell proliferation were identified. However, only UAP_{sto} was modelled and the simulated UAP concentration

using the ASM2dSMP model can therefore be regarded as the minimum amount of UAP production, but it cannot reflect a full UAP picture. UAP studies using more complex substrates are recommended, and UAP_{pro} should also be further investigated.

Fourth, to reduce the complexity of the integrated model, only a simple steady state hydrodynamic model was incorporated into the blocking and cake filtration model. A more detailed hydrodynamic model including the influence of crossflow velocity should be considered in the future to simulate the fouling under varying hydrodynamic conditions. In this way, optimisation and energy saving can be studied with this more advanced model.

Finally, the whole SMP study, from the lab-scale MBR to the batch SMP tests, used synthetic municipal-like wastewater as substrate. The results obtained from the study are probably substrate specific. The extrapolation of the model parameters to full-scale MBRs should therefore be done with caution. However, the methods and models developed in this thesis are general, and can be applied to any MBR system. The ASM2dSMP model can also be applied in conventional activated sludge processes and the MBR fouling model can also be applied in other microfiltration and ultrafiltration processes. It is highly recommend to test the methods and models developed in this thesis in pilot and full-scale MBRs under field conditions.

11.

References

Adin, A. (1999) Particle characteristics: A key factor in effluent treatment and reuse. Water Science and Technology 40(4-5), 67-74.

Ahn, Y.T., Choi, Y.K., Jeong, H.S., Chae, S.R. and Shin, H.S. (2006) Modeling of extracellular polymeric substances and soluble microbial products production in a submerged membrane bioreactor at various SRTs. Water Science and Technology 53(7), 209-216.

Aksu, Z. (2005) Application of biosorption for the removal of organic pollutants: A review. Process Biochemistry 40(3-4), 997-1026.

Al-Malack, M.H. (2006) Determination of biokinetic coefficients of an immersed membrane bioreactor. Journal of Membrane Science 271(1-2), 47-58.

APHA (1998) Standard methods for the examination of water and wastewater, 20th ed. , American Public Health Association, Washington, DC.

Aquino, S.F. and Stuckey, D.C. (2003) Production of soluble microbial products (SMP) in anaerobic chemostats under nutrient deficiency. Journal of Environmental Engineering-Asce 129(11), 1007-1014.

Aquino, S.F. and Stuckey, D.C. (2004) The effect of organic and hydraulic shock loads on the production of soluble microbial products in anaerobic digesters. Water Environment Research 76(7), 2628-2636.

Artan, N., Orhon, D. and Baykal, B.B. (1990) Implications of the Task Group Model .1. The Effect of Initial Substrate Concentration. Water Research 24(10), 1251-1258.

ASCE (1993) Measurement of Oxygen Transfer in Clean Water - 2nd Edition, American Society of Civil Engineers, New York.

Baker, J.S. and Dudley, L.Y. (1998) Biofouling in membrane systems - A review. Desalination 118(1-3), 81-89.

Baker, R.W. (2004) Membrane technology and applications, J. Wiley, Chichester ; New York.

Barker, D.J., Mannucchi, G.A., Salvi, S.M.L. and Stuckey, D.C. (1999) Characterisation of soluble residual chemical oxygen demand (COD) in anaerobic wastewater treatment effluents. Water Research 33(11), 2499-2510.

Bartlett, M., Bird, M.R. and Howell, J.A. (1995) An Experimental-Study for the Development of a Qualitative Membrane Cleaning Model. Journal of Membrane Science 105(1-2), 147-157.

BCC (2006) Membrane Bioreactors in the Changing World Water Market (Business Communications Company Inc).

Belfort, G., Davis, R.H. and Zydney, A.L. (1994) The behavior of suspensions and macromolecular solutions in cross-flow microfiltration. Journal of Membrane Science 96(1-2), 1-58.

Bird, M.R. and Bartlett, M. (2002) Measuring and modelling flux recovery during the chemical cleaning of MF membranes for the processing of whey protein concentrate. Journal of Food Engineering 53(2), 143-152.

Bitton, G. (1999) Wastewater microbiology, Wiley-Liss, New York.

Boeije, G., Corstanje, R., Rottiers, A. and Schowanek, D. (1999) Adaptation of the CAS test system and synthetic sewage for biological nutrient removal - Part I: Development of a new synthetic sewage. Chemosphere 38(4), 699-709.

Boerlage, S.F.E., Kennedy, M.D., Dickson, M.R., El-Hodali, D.E.Y. and Schippers, J.C. (2002) The modified fouling index using ultrafiltration membranes (MFI-UF): characterisation, filtration mechanisms and proposed reference membrane. Journal of Membrane Science 197(1-2), 1-21.

Boero, V.J., Eckenfelder, W.W. and Bowers, A.R. (1991) Soluble Microbial Product Formation in Biological-Systems. Water Science and Technology 23(4-6), 1067-1076.

Boero, V.J., Bowers, A.R. and Eckenfelder, W.W. (1996) Molecular weight distribution of soluble microbial products in biological systems. Water Science and Technology 34(5-6), 241-248.

Bonne, P.A.C., Hofman, J.A.M.H. and van der Hoek, J.P. (2000) Scaling control of RO membranes and direct treatment of surface water. Desalination 132(1-3), 109-119.

Bouhabila, E., Ben Aim, R. and Buisson, H. (2001) Fouling characterisation in membrane bioreactors. Separation and Purification Technology 22-3(1-3), 123-132.

Bowen, W.R., Calvo, J.I. and Hernandez, A. (1995) Steps of Membrane Blocking in Flux Decline during Protein Microfiltration. Journal of Membrane Science 101(1-2), 153-165.

Bowen, W.R. and Sharif, A.O. (1998) Hydrodynamic and colloidal interactions effects on the rejection of a particle larger than a pore in microfiltration and ultrafiltration membranes. Chemical Engineering Science 53(5), 879-890.

Brdjanovic, D., Van Loosdrecht, M.C.M., Versteeg, P., Hooijmans, C.M., Alaerts, G.J. and Heijnen, J.J. (2000) Modeling COD, N and P removal in a full-scale wwtp Haarlem Waarderpolder. Water Research 34(3), 846-858.

Brindle, K. and Stephenson, T. (1996) Nitrification in a bubbleless oxygen mass transfer membrane bioreactor. Water Science and Technology 34(9), 261-267.

Brindle, K., Stephenson, T. and Semmens, M.J. (1998) Nitrification and oxygen utilisation in a membrane aeration bioreactor. Journal of Membrane Science 144(1-2), 197-209.

Brockmann, M. and Seyfried, C.F. (1996) Sludge activity and cross-flow microfiltration a non-beneficial relationship. Water Science and Technology 34(9), 205-213.

Broeckmann, A., Busch, J., Wintgens, T. and Marquardt, W. (2006) Modeling of pore blocking and cake layer formation in membrane filtration for wastewater treatment. Desalination 189(1-3), 97-109.

Brooke, A., Kendrick, D., Meeraus, A., Raman, R. (1998) GAMS—A user's guide, GAMS Development Corporation, Washington, USA.

Brookes, A., Jefferson, B., Guglielmi, G. and Judd, S.J. (2006) Sustainable flux fouling in a membrane bioreactor: Impact of flux and MLSS. Separation Science and Technology 41(7), 1279-1291.

Cabassud, C., Masse, A., Espinosa-Bouchot, M.C. and Sperandio, M. (2004) Submerged membrane bioreactors: Interactions between membrane filtration and biological activity. in: Proceedings of Water Environment - Membrane Technology Conference, Seoul, Korea.

Carmen, P.C. (1937) Fluid flow through granular beds. Trans. Inst. Chem. Eng. 15, 150-166.

Casey, E., Glennon, B. and Hamer, G. (1999) Oxygen mass transfer characteristics in a membrane-aerated biofilm reactor. Biotechnology and Bioengineering 62(2), 183-192.

Casey, T.G., Ekama, G.A., Wentzel, M.C. and Marais, G.V. (1995) Filamentous Organism Bulking in Nutrient Removal Activated-Sludge Systems .1. A Historical Overview of Causes and Control. Water Sa 21(3), 231-238.

Chae, S.R., Ahn, Y.T., Kang, S.T. and Shin, H.S. (2006) Mitigated membrane fouling in a vertical submerged membrane bioreactor (VSMBR). Journal of Membrane Science 280(1-2), 572-581.

Chaize, S. and Huyard, A. (1991) Membrane Bioreactor on Domestic Waste-Water Treatment Sludge Production and Modeling Approach. Water Science and Technology 23(7-9), 1591-1600.

Chang, I.S. and Lee, C.H. (1998) Membrane filtration characteristics in membrane-coupled activated sludge system - the effect of physiological states of activated sludge on membrane fouling. Desalination 120(3), 221-233.

Chang, I.S., Bag, S.O. and Lee, C.H. (2001) Effects of membrane fouling on solute rejection during membrane filtration of activated sludge. Process Biochemistry 36(8-9), 855-860.

Chang, I.S. and Kim, S.N. (2005) Wastewater treatment using membrane filtration - effect of biosolids concentration on cake resistance. Process Biochemistry 40(3-4), 1307-1314.

Chen, V., Fane, A.G., Madaeni, S. and Wenten, I.G. (1997) Particle deposition during membrane filtration of colloids: Transition between concentration polarization and cake formation. Journal of Membrane Science 125(1), 109-122.

Chiemchaisri, C., Wong, Y.K., Urase, T. and Yamamoto, K. (1992) Organic Stabilization and Nitrogen Removal in Membrane Separation Bioreactor for Domestic Waste-Water Treatment. Water Science and Technology 25(10), 231-240.

Cho, B.D. and Fane, A.G. (2002) Fouling transients in nominally sub-critical flux operation of a membrane bioreactor. Journal of Membrane Science 209(2), 391-403.

Cho, J., Ahn, K.H., Seo, Y. and Lee, Y. (2003) Modification of ASM no.1 for a submerged membrane bioreactor system: including the effects of soluble microbial products on membrane fouling. Water Science and Technology 47(12), 177-181.

Cho, J.W., Ahn, K.H., Lee, Y.H., Lim, B.R. and Kim, J.Y. (2004) Investigation of biological and fouling characteristics of submerged membrane bioreactor process for wastewater treatment by model sensitivity analysis. Water Science and Technology 49(2), 245-254.

Choo, K.H. and Lee, C.H. (1996) Effect of anaerobic digestion broth composition on membrane permeability. Water Science and Technology 34(9), 173-179.

Chu, H.P. and Li, X.Y. (2005) Membrane fouling in a membrane bioreactor (MBR): Sludge cake formation and fouling characteristics. Biotechnology and Bioengineering 90(3), 323-331.

Chudoba, J. (1985a) Inhibitory Effect of Refractory Organic-Compounds Produced by Activated-Sludge Microorganisms on Microbial Activity and Flocculation. Water Research 19(2), 197-200.

Chudoba, J. (1985b) Quantitative Estimation in COD Units of Refractory Organic-Compounds Produced by Activated-Sludge Microorganisms. Water Research 19(1), 37-43.

Chudoba, J., Hejzlar, J. and Dolezal, M. (1986) Microbial Polymers in the Aquatic Environment .3. Isolation from River, Potable and Underground Water and Analysis. Water Research 20(10), 1223-1227.

Chuichulcherm, S., Nagpal, S., Peeva, L. and Livingston, A. (2001) Treatment of metal-containing wastewaters with a novel extractive membrane reactor using sulfate-reducing bacteria. Journal of Chemical Technology and Biotechnology 76(1), 61-68.

Churchouse, S. (2002) Membrane bioreactors: going from laboratory to large scale—problems to clear solutions. in: Proceedings of Membranes and the Environment, University of Oxford, UK.

Cicek, N., Franco, J.P., Suidan, M.T., Urbain, V. and Manem, J. (1999) Characterization and comparison of a membrane bioreactor and a conventional activated-sludge system in the treatment of wastewater containing high-molecular-weight compounds. Water Environment Research 71(1), 64-70.

Clara, M., Strenn, B., Ausserleitner, M. and Kreuzinger, N. (2004) Comparison of the behaviour of selected micropollutants in a membrane bioreactor and a conventional wastewater treatment plant. Water Science and Technology 50(5), 29-36.

Clara, M., Kreuzinger, N., Strenn, B., Gans, O. and Kroiss, H. (2005a) The solids retention time - a suitable design parameter to evaluate the capacity of wastewater treatment plants to remove micropollutants. Water Research 39(1), 97-106.

Clara, M., Strenn, B., Gans, O., Martinez, E., Kreuzinger, N. and Kroiss, H. (2005b) Removal of selected pharmaceuticals, fragrances and endocrine disrupting compounds in a membrane bioreactor and conventional wastewater treatment plants. Water Research 39(19), 4797-4807.

Combe, C., Molis, E., Lucas, P., Riley, R. and Clark, M.M. (1999) The effect of CA membrane properties on adsorptive fouling by humic acid. Journal of Membrane Science 154(1), 73-87.

Côte, P., Buisson, H. and Praderie, M. (1998) Immersed membranes activated sludge process applied to the treatment of municipal wastewater. Water Science and Technology 38(4-5), 437-442.

Croue, J.-P., Korshin, G.V., Benjamin, M.M. and AWWA Research Foundation. (2000) Characterization of natural organic matter in drinking water, AWWA Research Foundation and American Water Works Association, Denver, CO.

Cui, Z.F., Bellara, S.R. and Homewood, P. (1997) Airlift crossflow membrane filtration - A feasibility study with dextran ultrafiltration. Journal of Membrane Science 128(1), 83-91.

Daigger, G.T. and Grady, C.P.L. (1977) Factors Affecting Effluent Quality from Fill-and-Draw Activated-Sludge Reactors. Journal Water Pollution Control Federation 49(12), 2390-2396.

Davis, R.H. and Sherwood, J.D. (1990) A similarity solution for steady-state cross-flow microfiltration. Chemical Engineering Science 45(11), 3203-3209.

Davis, R.H. (1992) Modeling of Fouling of Cross-Flow Microfiltration Membranes. Separation and Purification Methods 21(2), 75-126.

de Silva, D.G.V., Urbain, V., Abeysinghe, D.H. and Rittmann, B.E. (1998) Advanced analysis of membrane-bioreactor performance with aerobic-anoxic cycling. Water Science and Technology 38(4-5), 505-512.

De Wever, H., Van Roy, S., Dotremont, C., Muller, J. and Knepper, T. (2004) Comparison of linear alkylbenzene sulfonates removal in conventional activated sludge systems and membrane bioreactors. Water Science and Technology 50(5), 219-225.

Debus, O. and Wanner, O. (1992) Degradation of Xylene by a Biofilm Growing on a Gas-Permeable Membrane. Water Science and Technology 26(3-4), 607-616.

Defrance, L. and Jaffrin, M.Y. (1999a) Comparison between filtrations at fixed transmembrane pressure and fixed permeate flux: application to a membrane bioreactor used for wastewater treatment. Journal of Membrane Science 152(2), 203-210.

Defrance, L. and Jaffrin, M.Y. (1999b) Reversibility of fouling formed in activated sludge filtration. Journal of Membrane Science 157(1), 73-84.

Defrance, L., Jaffrin, M.Y., Gupta, B., Paullier, P. and Geaugey, V. (2000) Contribution of various constituents of activated sludge to membrane bioreactor fouling. Bioresource Technology 73(2), 105-112.

Dignac, M.F., Ginestet, P., Rybacki, D., Bruchet, A., Urbain, V. and Scribe, P. (2000) Fate of wastewater organic pollution during activated sludge treatment: Nature of residual organic matter. Water Research 34(17), 4185-4194.

Dochain, D. and Vanrolleghem, P.A. (2001) Dynamical Modelling and Estimation in Wastewater Treatment Processes, IWA Publishing, London, UK.

Dold, P.L., Ekama, G.A. and Marais, G.R. (1980) A General-Model for the Activated-Sludge Process. Progress in Water Technology 12(6), 47-77.

Drew, D.A., Schonberg, J.A. and Belfort, G. (1991) Lateral Inertial Migration of a Small Sphere in Fast Laminar-Flow through a Membrane Duct. Chemical Engineering Science 46(12), 3219-3224.

Drewes, J.E. and Fox, P. (1999) Fate of natural organic matter (NOM) during groundwater recharge using reclaimed water. Water Science and Technology 40(9), 241-248.

Drews, A., Evenblij, H. and Rosenberger, S. (2005) Potential and drawbacks of microbiology-membrane interaction in membrane bioreactors. Environmental Progress 24(4), 426-433.

Drews, A., Vocks, M., Iversen, V., Lesjean, B. and Kraume, M. (2006) Influence of unsteady membrane bioreactor operation on EPS formation and filtration resistance. Desalination 192(1-3), 1-9.

Dubois, M., Gilles, K.A., Hamilton, J.K., Rebers, P.A. and Smith, F. (1956) Colormetric method for determination of sugars and related substances. Analytical Chemistry 28(3), 350-356.

Eckstein, E.C., Bailey, D.G. and Shapiro, A.H. (1977) Self-Diffusion of Particles in Shear-Flow of a Suspension. Journal of Fluid Mechanics 79(Jan20), 191-208.

Eichhorn, P. and Knepper, T.P. (2002) alpha,beta-unsaturated sulfophenylcarboxylates as degradation intermediates of linear alkylbenzenesulfonates: evidence for Omega-oxygenation followed by beta-oxidations by liquid chromatography-mass spectrometry. Environmental Toxicology and Chemistry 21(1), 1-8.

Eikelboom, D.H., Andreadakis, A. and Andreasen, K. (1998) Survey of filamentous populations in nutrient removal plants in four European countries. Water Science and Technology 37(4-5), 281-289.

Ekama, G.A., Dold, P.L. and Marais, G.V. (1986) Procedures for Determining Influent COD Fractions and the Maximum Specific Growth-Rate of Heterotrophs in Activated-Sludge Systems. Water Science and Technology 18(6), 91-114.

Evenblij, H., Verrecht, B., van der Graaf, J.H.J.M. and Van der Bruggen, B. (2005) Manipulating filterability of MBR activated sludge by pulsed substrate addition. Desalination 178(1-3), 193-201.

Fan, F.S., Zhou, H.D. and Husain, H. (2006) Identification of wastewater sludge characteristics to predict critical flux for membrane bioreactor processes. Water Research 40(2), 205-212.

Fane, A.G., Chang, S. and Chardon, E. (2002) Submerged hollow fibre membrane module - design options and operational considerations. Desalination 146(1-3), 231-236.

Fang, H.H.P. and Shi, X.L. (2005) Pore fouling of microfiltration membranes by activated sludge. Journal of Membrane Science 264(1-2), 161-166.

Field, R.W., Wu, D., Howell, J.A. and Gupta, B.B. (1995) Critical Flux Concept for Microfiltration Fouling. Journal of Membrane Science 100(3), 259-272.

Flemming, H.C., Griebe, T. and Schaule, G. (1996) Antifouling strategies in technical systems - A short review. Water Science and Technology 34(5-6), 517-524.

Flemming, H.C. (1997) Reverse osmosis membrane biofouling. Experimental Thermal and Fluid Science 14(4), 382-391.

Frølund, B., Griebe, T. and Nielsen, P.H. (1995) Enzymatic-Activity in the Activated-Sludge Floc Matrix. Applied Microbiology and Biotechnology 43(4), 755-761.

Frølund, B., Palmgren, R., Keiding, K. and Nielsen, P.H. (1996) Extraction of extracellular polymers from activated sludge using a cation exchange resin. Water Research 30(8), 1749-1758.

Furumai, H. and Rittmann, B.E. (1992) Advanced Modeling of Mixed Populations of Heterotrophs and Nitrifiers Considering the Formation and Exchange of Soluble Microbial Products. Water Science and Technology 26(3-4), 493-502.

Furumai, H., Nagasaka, M. and Sato, Y. (1998) Modelling of nitrogen removal in sequencing batch reactors treating domestic sewage. Indian Journal of Engineering and Materials Sciences 5(4), 173-181.

Gander, M., Jefferson, B. and Judd, S. (2000) Aerobic MBRs for domestic wastewater treatment: a review with cost considerations. Separation and Purification Technology 18(2), 119-130.

Gao, M.C., Yang, M., Li, H.Y., Yang, Q.X. and Zhang, Y. (2004) Comparison between a submerged membrane bioreactor and a conventional activated sludge system on treating ammonia-bearing inorganic wastewater. Journal of Biotechnology 108(3), 265-269.

Gaudy, A.F. and Blachly, T.R. (1985) A Study of the Biodegradability of Residual COD. Journal Water Pollution Control Federation 57(4), 332-338.

Gehlert, G. and Hapke, J. (2002) Mathematical modeling of a continuous aerobic membrane bioreactor for the treatment of different kinds of wastewater. Desalination 146(1-3), 405-412.

Ghyoot, W., Vandaele, S. and Verstraete, W. (1999) Nitrogen removal from sludge reject water with a membrane-assisted bioreactor. Water Research 33(1), 23-32.

Grady, C.P.L., Harlow, L.J. and Riesing, R.R. (1972) Effects of Growth-Rate and Influent Substrate Concentration on Effluent Quality from Chemostats Containing Bacteria in Pure and Mixed Culture. Biotechnology and Bioengineering 14(3), 391-&.

Grady, C.P.L. (1989) The Concept of Soluble Residual Product Formation in the Modeling of Activated-Sludge - Discussion. Water Science and Technology 21(12), 1565-1566.

Grady, C.P.L., Daigger, G.T. and Lim, H.C. (1999) Biological wastewater treatment, Marcel Dekker, New York.

Green, G. and Belfort, G. (1980) Fouling of ultrafiltration membranes - Lateral migration and the particle trajectory model. Desalination 35(1-3), 129-147.

Grelier, P., Rosenberger, S. and Tazi-Pain, A. (2006) Influence of sludge retention time on membrane bioreactor hydraulic performance. Desalination 192(1-3), 10-17.

Gujer, W., Henze, M., Mino, T. and van Loosdrecht, M. (1999) Activated Sludge Model No. 3. Water Science and Technology 39(1), 183-193.

Günder, B. (2001) The membrane-coupled activated sludge process in municipal wastewater treatment, Technomic Pub., Lancaster.

Han, S.S., Bae, T.H., Jang, G.G. and Tak, T.M. (2005) Influence of sludge retention time on membrane fouling and bioactivities in membrane bioreactor system. Process Biochemistry 40(7), 2393-2400.

Harada, H., Momonoi, K., Yamazaki, S. and Takizawa, S. (1994) Application of Anaerobic-UF Membrane Reactor for Treatment of a Waste-Water Containing High-Strength Particulate Organics. Water Science and Technology 30(12), 307-319.

Hasar, H. and Kinaci, C. (2004) Empirical model representing microbial activity in a submerged MBR treating strength wastewater. Desalination 170(2), 161-167.

Heberer, T. (2002) Tracking persistent pharmaceutical residues from municipal sewage to drinking water. Journal of Hydrology 266(3-4), 175-189.

Hejzlar, J. and Chudoba, J. (1986a) Microbial Polymers in the Aquatic Environment .1. Production by Activated-Sludge Microorganisms under Different Conditions. Water Research 20(10), 1209-1216.

Hejzlar, J. and Chudoba, J. (1986b) Microbial Polymers in the Aquatic Environment .2. Isolation from Biologically Non-Purified and Purified Municipal Waste-Water and Analysis. Water Research 20(10), 1217-1221.

Henze, M., Grady, J.C.P.L., Gujer, W., Marais, G.V.R. and Matsuo, T. (1987) Activated sludge model No. 1, IAWPRC Scientific and Technical Reports, No. 1, London.

Henze, M. (1992) Characterization of Waste-Water for Modeling of Activated-Sludge Processes. Water Science and Technology 25(6), 1-15.

Henze, M., Gujer, W., Mino, T., Matsuo, T., Wentzel, M.C.M. and Marais, G.V.R. (1995) Activated sludge model No. 2, IAWPRC Scientific and Technical Reports, No. 3, London.

Henze, M., Gujer, W., Mino, T., Matsuo, T., Wentzel, M.C., Marais, G.V.R. and Van Loosdrecht, M.C.M. (1999) Activated Sludge Model No.2d, ASM2d. Water Science and Technology 39(1), 165-182.

Henze, M., Gujer, W., Mino, T. and van Loosdrecht, M. (2000) Activated sludge models: ASM1, ASM2, ASM2d and ASM3, Scientific and Technical Reports No. 9, IWA publishing, London.

Hermans, P.H. and Bredée, H.L. (1936) Principles of the mathematical treatment of constant-pressure filtration. J. Soc. Chem. Ind., 55T, 1-4.

Hermia, J. (1982) Constant Pressure Blocking Filtration Laws - Application to Power-Law Non-Newtonian Fluids. Transactions of the Institution of Chemical Engineers 60(3), 183-187.

Ho, C.C. and Zydney, A.L. (2000) A combined pore blockage and cake filtration model for protein fouling during microfiltration. Journal of Colloid and Interface Science 232(2), 389-399.

Holakoo, L., Nakhla, G., Yanful, E.K. and Bassi, A.S. (2006) Chelating properties and molecular weight distribution of soluble microbial products from an aerobic membrane bioreactor. Water Research 40(8), 1531-1538.

Hong, S.K. and Elimelech, M. (1997) Chemical and physical aspects of natural organic matter (NOM) fouling of nanofiltration membranes. Journal of Membrane Science 132(2), 159-181.

Howe, K.J. and Clark, M.M. (2002) Fouling of microfiltration and ultrafiltration membranes by natural waters. Environmental Science & Technology 36(16), 3571-3576.

Howell, J.A., Chua, H.C. and Arnot, T.C. (2004) In situ manipulation of critical flux in a submerged membrane bioreactor using variable aeration rates, and effects of membrane history. Journal of Membrane Science 242(1-2), 13-19.

Huang, X., Liu, R. and Qian, Y. (2000) Behaviour of soluble microbial products in a membrane bioreactor. Process Biochemistry 36(5), 401-406.

Huang, X., Gui, P. and Qian, Y. (2001) Effect of sludge retention time on microbial behaviour in a submerged membrane bioreactor. Process Biochemistry 36(10), 1001-1006.

Huber, S. and Frimmel, F.H. (1992) A Liquid-Chromatographic System with Multi-Detection for the Direct Analysis of Hydrophilic Organic-Compounds in Natural-Waters. Fresenius Journal of Analytical Chemistry 342(1-2), 198-200.

Huber, S.A. and Frimmel, F.H. (1991) Flow-injection analysis of organic and inorganic carbon in the low-ppb range. Analytical Chemistry 63(19), 2122-2130.

Hulsbeek, J.J.W., Kruit, J., Roeleveld, P.J. and van Loosdrecht, M.C.M. (2002) A practical protocol for dynamic modelling of activated sludge systems. Water Science and Technology 45(6), 127-136.

Ichihashi, O., Satoh, H. and Mino, T. (2006) Effect of soluble microbial products on microbial metabolisms related to nutrient removal. Water Research 40(8), 1627-1633.

Insel, G., Sin, G., Lee, D.S., Nopens, I. and Vanrolleghem, P.A. (2006) A calibration methodology and model-based systems analysis for SBRs removing nutrients under limited aeration conditions. Journal of Chemical Technology and Biotechnology 81(4), 679-687.

Jarusutthirak, C., Amy, G. and Croue, J.P. (2002) Fouling characteristics of wastewater effluent organic matter (EfOM) isolates on NF and UF membranes. Desalination 145(1-3), 247-255.

Jenkins, D., Richard, M.G., Daigger, G.T. and Jenkins, D. (2004) Manual on the causes and control of activated sludge bulking, foaming, and other solids separation problems, Lewis Publishers, Boca Raton, Fla.

Ji, L. and Zhou, J.T. (2006) Influence of aeration on microbial polymers and membrane fouling in submerged membrane bioreactors. Journal of Membrane Science 276(1-2), 168-177.

Jiang, T. (2002) Fouling in Membrane Bioreactor Systems. M.Sc. thesis, UNESCO-IHE institute for water education, Delft.

Jiang, T., Kennedy, M.D., van der Meer, W.G.J., Vanrolleghem, P.A. and Schippers, J.C. (2003) The role of blocking and cake filtration in MBR fouling. Desalination 157(1-3), 335-343.

Jiang, T., Kennedy, M.D., Guinzbourg, B.F., Vanrolleghem, P.A. and Schippers, J.C. (2005a) Optimising the operation of a MBR pilot plant by quantitative analysis of the membrane fouling mechanism. Water Science and Technology 51(6-7), 19-25.

Jiang, T., Liu, X., Kennedy, M.D., Schippers, J.C. and Vanrolleghem, P.A. (2005b) Calibrating a side-stream membrane bioreactor using Activated Sludge Model No. 1. Water Science and Technology 52(10-11), 359-367.

Jin, Y.L., Lee, W.N., Lee, C.H., Chang, I.S., Huang, X. and Swaminathan, T. (2006) Effect of DO concentration on biofilm structure and membrane filterability in submerged membrane bioreactor. Water Research 40(15), 2829-2836.

Jones, M.L., Liehr, S.K., Classen, J.J. and Robarge, W. (2000) Mechanisms of dinitrogen gas formation in anaerobic lagoons. Advances in Environmental Research 4(2), 133-139.

Judd, S. (2006) The MBR book: principles and applications of membrane bioreactors, Elsevier, Boston, MA.

Kang, I.J., Lee, C.H. and Kim, K.J. (2003) Characteristics of microfiltration membranes in a membrane coupled sequencing batch reactor system. Water Research 37(5), 1192-1197.

Kiani, A., Bhave, R.R. and Sirkar, K.K. (1984) Solvent-Extraction with Immobilized Interfaces in a Microporous Hydrophobic Membrane. Journal of Membrane Science 20(2), 125-145.

Kim, H.Y., Yeon, K.M., Lee, C.H., Lee, S. and Swaminathan, T. (2006) Biofilm structure and extracellular polymeric substances in low and high dissolved oxygen membrane bioreactors. Separation Science and Technology 41(7), 1213-1230.

Kim, J.S., Lee, C.H. and Chang, I.S. (2001) Effect of pump shear on the performance of a crossflow membrane bioreactor. Water Research 35(9), 2137-2144.

Kimura, K., Hara, H. and Watanabe, Y. (2005) Removal of pharmaceutical compounds by submerged membrane bioreactors (MBRs). Desalination 178(1-3), 135-140.

Klavins, M., Eglite, L. and Serzane, J. (1999) Methods for analysis of aquatic humic substances. Critical Reviews in Analytical Chemistry 29(3), 187-193.

Krampe, J. and Krauth, K. (2003) Oxygen transfer into activated sludge with high MLSS concentrations. Water Science and Technology 47(11), 297-303.

Kuzmenko, D., Arkhangelsky, E., Belfer, S., Freger, V. and Gitis, V. (2005) Chemical cleaning of UF membranes fouled by BSA. Desalination 179(1-3), 323-333.

Kwon, B., Lee, S., Cho, J., Ahn, H., Lee, D. and Shin, H.S. (2005) Biodegradability, DBP formation, and membrane fouling potential of natural organic matter: Characterization and controllability. Environmental Science & Technology 39(3), 732-739.

LaPara, T.M., Klatt, C.G. and Chen, R. (2006) Adaptations in bacterial catabolic enzyme activity and community structure in membrane-coupled bioreactors fed simple synthetic wastewater. Journal of Biotechnology 121(3), 368-380.

Larson, R.A. and Weber, E.J. (1994) Reaction mechanisms in environmental organic chemistry, Lewis Publishers, Boca Raton.

Laspidou, C.S. and Rittmann, B.E. (2002a) A unified theory for extracellular polymeric substances, soluble microbial products, and active and inert biomass. Water Research 36(11), 2711-2720.

Laspidou, C.S. and Rittmann, B.E. (2002b) Non-steady state modeling of extracellular polymeric substances, soluble microbial products, and active and inert biomass. Water Research 36(8), 1983-1992.

Le-Clech, P., Jefferson, B., Chang, I.S. and Judd, S.J. (2003a) Critical flux determination by the flux-step method in a submerged membrane bioreactor. Journal of Membrane Science 227(1-2), 81-93.

Le-Clech, P., Jefferson, B. and Judd, S.J. (2003b) Impact of aeration, solids concentration and membrane characteristics on the hydraulic performance of a membrane bioreactor. Journal of Membrane Science 218(1-2), 117-129.

Le Clech, P., Jefferson, B., Chang, I.S. and Judd, S.J. (2003) Critical flux determination by the flux-step method in a submerged membrane bioreactor. Journal of Membrane Science 227(1-2), 81-93.

Lee, H., Amy, G., Cho, J.W., Yoon, Y.M., Moon, S.H. and Kim, I.S. (2001a) Cleaning strategies for flux recovery of an ultrafiltration membrane fouled by natural organic matter. Water Research 35(14), 3301-3308.

Lee, J., Ahn, W.Y. and Lee, C.H. (2001b) Comparison of the filtration characteristics between attached and suspended growth microorganisms in submerged membrane bioreactor. Water Research 35(10), 2435-2445.

Lee, N., Amy, G. and Lozier, J. (2005) Understanding natural organic matter fouling in low-pressure membrane filtration. Desalination 178(1-3), 85-93.

Lee, N.H., Amy, G., Croue, J.P. and Buisson, H. (2004) Identification and understanding of fouling in low-pressure membrane (MF/UF) filtration by natural organic matter (NOM). Water Research 38(20), 4511-4523.

Lee, W., Kang, S. and Shin, H. (2003) Sludge characteristics and their contribution to microfiltration in submerged membrane bioreactors. Journal of Membrane Science 216(1-2), 217-227.

Lee, Y., Cho, J., Seo, Y., Lee, J.W. and Ahn, K.H. (2002) Modeling of submerged membrane bioreactor process for wastewater treatment. Desalination 146(1-3), 451-457.

Lesjean, B., Rosenberger, S., Laabs, C., Jekel, M., Gnirss, R. and Amy, G. (2005) Correlation between membrane fouling and soluble/colloidal organic substances in membrane bioreactors for municipal wastewater treatment. Water Science and Technology 51(6-7), 1-8.

Liang, S., C., L. and Song, L.F. (2007) Soluble microbial products in membrane bioreactor operation: Behaviors, characteristics, and fouling potential. Water Research 41, 95-101.

Liu, W., Howell, J.A., Arnot, T.C. and Scott, J.A. (2001) A novel extractive membrane bioreactor for treating biorefractory organic pollutants in the presence of high concentrations of inorganics: application to a synthetic acidic effluent containing high concentrations of chlorophenol and salt. Journal of Membrane Science 181(1), 127-140.

Livingston, A.G. (1994) Extractive Membrane Bioreactors - a New Process Technology for Detoxifying Chemical-Industry Wastewaters. Journal of Chemical Technology and Biotechnology 60(2), 117-124.

Livingston, A.G., Arcangeli, J.P., Boam, A.T., Zhang, S.F., Marangon, M. and dos Santos, L.M.F. (1998) Extractive membrane bioreactors for detoxification of chemical industry wastes: process development. Journal of Membrane Science 151(1), 29-44.

Lobos, J., Wisniewski, C., Heran, M. and Grasmick, A. (2005) Effects of starvation conditions on biomass behaviour for minimization of sludge production in membrane bioreactors. Water Science and Technology 51(6-7), 35-44.

Lowry, O.H., Rosebrough, N.J., Farr, A.L. and Randall, R.J. (1951) Protein measurement with the Folin phenol reagent. Journal of Biological Chemistry 193, 265-275.

Lu, S.G., Imai, T., Ukita, M., Sekine, M., Higuchi, T. and Fukagawa, M. (2001) A model for membrane bioreactor process based on the concept of formation and degradation of soluble microbial products. Water Research 35(8), 2038-2048.

Lu, S.G., Imai, T., Ukita, M., Sekine, M. and Higuchi, T. (2002) Modeling prediction of membrane bioreactor process with the concept of soluble microbial product. Water Science and Technology 46(11-12), 63-69.

Lu, W.M. and Ju, S.C. (1989) Selective Particle Deposition in Cross-Flow Filtration. Separation Science and Technology 24(7-8), 517-540.

Luxmy, B.S., Nakajima, F. and Yamamoto, K. (2000) Predator grazing effect on bacterial size distribution and floc size variation in membrane-separation activated sludge. Water Science and Technology 42(3-4), 211-217.

Luxmy, B.S., Kubo, T. and Yamamoto, K. (2001) Sludge reduction potential of metazoa in membrane bioreactors. Water Science and Technology 44(10), 197-202.

Madaeni, S.S., Fane, A.G. and Wiley, D.E. (1999) Factors influencing critical flux in membrane filtration of activated sludge. Journal of Chemical Technology and Biotechnology 74(6), 539-543.

Mallevialle, J., Odendaal, P. and Wiesner, M. (1996) Water treatment membrane processes, McGraw-Hill, New York.

Manser, R., Gujer, W. and Siegrist, H. (2005a) Membrane bioreactor versus conventional activated sludge system: population dynamics of nitrifiers. Water Science and Technology 52(10-11), 417-425.

Manser, R., Gujer, W. and Siegrist, H. (2005b) Consequences of mass transfer effects on the kinetics of nitrifiers. Water Research 39(19), 4633-4642.

Manser, R., Gujer, W. and Siegrist, H. (2006) Decay processes of nitrifying bacteria in biological wastewater treatment systems. Water Research 40(12), 2416-2426.

Masse, A., Sperandio, M. and Cabassud, C. (2006) Comparison of sludge characteristics and performance of a submerged membrane bioreactor and an activated sludge process at high solids retention time. Water Research 40(12), 2405-2415.

Matsumoto, H., Koyama, Y. and Tanioka, A. (2003) Interaction of proteins with weak amphoteric charged membrane surfaces: effect of pH. Journal of Colloid and Interface Science 264(1), 82-88.

Meijer, S.C.F., van der Spoel, H., Susanti, S., Heijnen, J.J. and van Loosdrecht, M.C.M. (2002) Error diagnostics and data reconciliation for activated sludge modelling using mass balances. Water Science and Technology 45(6), 145-156.

Moloney, C.L. and Field, J.G. (1991) The Size-Based Dynamics of Plankton Food Webs .1. A Simulation-Model of Carbon and Nitrogen Flows. Journal of Plankton Research 13(5), 1003-1038.

Mueller, J.A., Boyle, W.C. and Pöpel, H.J. (2002) Aeration : principles and practice, CRC Press, Boca Raton.

Mulder, M. (1996) Basic principles of membrane technology, Kluwer Academic, Dordrecht; Boston.

MunozAguado, M.J., Wiley, D.E. and Fane, A.G. (1996) Enzymatic and detergent cleaning of a polysulfone ultrafiltration membrane fouled with BSA and whey. Journal of Membrane Science 117(1-2), 175-187.

Murthy, S.N. and Novak, J.T. (2001) Influence of cations on activated-sludge effluent quality. Water Environment Research 73(1), 30-36.

Musvoto, E.V., Lakay, M.T., Casey, T.G., Wentzel, M.C. and Ekama, G.A. (1999) Filamentous organism bulking in nutrient removal activated sludge systems - Paper 8: The effect of nitrate and nitrite. Water Sa 25(4), 397-407.

Nam, S.N. (2006) Contribution of Wastewater to Formation of Disinfection By-Products (DBPs): Contrasting Effluent Organic Matter (EfOM) versus Natural Organic Matter (NOM) Properties, and the Role of EfOM as a DBP Precursor. PhD thesis, University of Colorado.

Namkung, E. and Rittmann, B.E. (1986) Soluble microbial products (SMP) formation kinetics by biofilms. Water Research 20(6), 795-806.

Nelder, J.A. and Mead, R. (1965) A simplex method for function minimization. Computer Journal 7, 308-313.

Nowak, O., Franz, A., Svardal, K., Muller, V. and Kuhn, V. (1999) Parameter estimation for activated sludge models with the help of mass balances. Water Science and Technology 39(4), 113-120.

Nuengjamnong, C., Kweon, J.H., Cho, J., Polprasert, C. and Ahn, K.H. (2005) Membrane fouling caused by extracellular polymeric substances during microfiltration processes. Desalination 179(1-3), 117-124.

Nystrom, M., Kaipia, L. and Luque, S. (1995) Fouling and Retention of Nanofiltration Membranes. Journal of Membrane Science 98(3), 249-262.

Ognier, S., Wisniewski, C. and Grasmick, A. (2002) Influence of macromolecule adsorption during filtration of a membrane bioreactor mixed liquor suspension. Journal of Membrane Science 209(1), 27-37.

Ognier, S., Wisniewski, C. and Grasmick, A. (2004) Membrane bioreactor fouling in sub-critical filtration conditions: a local critical flux concept. Journal of Membrane Science 229(1-2), 171-177.

Orhon, D., Artan, N. and Cimsit, Y. (1989) The Concept of Soluble Residual Product Formation in the Modeling of Activated-Sludge. Water Science and Technology 21(4-5), 339-350.

Painter, H.A. (1973) Organic compounds in solution in sewage effluents. Chem. Ind. September, 818-822.

Pribyl, M., Tucek, F., Wilderer, P.A. and Wanner, J. (1997) Amount and nature of soluble refractory organics produced by activated sludge microorganisms in sequencing batch and continuous flow reactors. Water Science and Technology 35(1), 27-34.

Ramphao, M., Wentzel, M.C., Merritt, R., Ekama, G.A., Young, T. and Buckley, C.A. (2005) Impact of membrane solid-liquid separation on design of biological nutrient removal activated sludge systems. Biotechnology and Bioengineering 89(6), 630-646.

Raunkjaer, K., Hvitvedjacobsen, T. and Nielsen, P.H. (1994) Measurement of Pools of Protein, Carbohydrate and Lipid in Domestic Waste-Water. Water Research 28(2), 251-262.

Reid, E., Liu, X.R. and Judd, S.J. (2006) Effect of high salinity on activated sludge characteristics and membrane permeability in an immersed membrane bioreactor. Journal of Membrane Science 283(1-2), 164-171.

Ren, N.Q., Chen, Z.B., Wang, A.J. and Hu, D.X. (2005) Removal of organic pollutants and analysis of MLSS-COD removal relationship at different HRTs in a submerged membrane bioreactor. International Biodeterioration & Biodegradation 55(4), 279-284.

Rieger, L., Koch, G., Kuhni, M., Gujer, W. and Siegrist, H. (2001) The EAWAG Bio-P module for activated sludge model No. 3. Water Research 35(16), 3887-3903.

Rittmann, B.E., Bae, W., Namkung, E. and Lu, C.J. (1987) A critical-evaluation of microbial product formation in biological processes. Water Science and Technology 19(3-4), 517-528.

Roeleveld, P.J. and van Loosdrecht, M.C.M. (2002) Experience with guidelines for wastewater characterisation in The Netherlands. Water Science and Technology 45(6), 77-87.

Rojas, M.E.H., Van Kaam, R., Schetrite, S. and Albasi, C. (2005) Role and variations of supernatant compounds in submerged membrane bioreactor fouling. Desalination 179(1-3), 95-107.

Roorda, J.H. and van der Graaf, J.H.M. (2005) SUR test used for optimisation of membrane filtration plants treating wastewater effluents. Desalination 179(1-3), 131-150.

Rosenberger, S. and Kraume, M. (2002) Filterability of activated sludge in membrane bioreactors. Desalination 146(1-3), 373-379.

Rosenberger, S., Evenblij, H., te Poele, S.T., Wintgens, T. and Laabs, C. (2005) The importance of liquid phase analyses to understand fouling in membrane assisted activated sludge processes - six case studies of different European research groups. Journal of Membrane Science 263(1-2), 113-126.

Rosenberger, S., Laabs, C., Lesjean, B., Gnirss, R., Amy, G., Jekel, M. and Schrotter, J.C. (2006) Impact of colloidal and soluble organic material on membrane performance in membrane bioreactors for municipal wastewater treatment. Water Research 40(4), 710-720.

Sannigrahi, P. (2005) Composition and Cycling of Natural Organic Matter: Insights from NMR Spectroscopy, Georgia Institute of Technology.

Schafer, A.I., Pihlajamaki, A., Fane, A.G., Waite, T.D. and Nystrom, M. (2004) Natural organic matter removal by nanofiltration: effects of solution chemistry on retention of low molar mass acids versus bulk organic matter. Journal of Membrane Science 242(1-2), 73-85.

Schippers, J.C. and Verdouw, J. (1980) Modified Fouling Index, a Method of Determining the Fouling Characteristics of Water. Desalination 32(1-3), 137-148.

Schleheck, D., Dong, W.B., Denger, K., Heinzle, E. and Cook, A.M. (2000) An alpha-proteobacterium converts linear alkylbenzenesulfonate surfactants into sulfophenylcarboxylates and linear alkyldiphenyletherdisulfonate surfactants into sulfodiphenylethercarboxylates. Applied and Environmental Microbiology 66(5), 1911-1916.

Shimizu, Y., Okuno, Y., Uryu, K., Ohtsubo, S. and Watanabe, A. (1996) Filtration characteristics of hollow fiber microfiltration membranes used in membrane bioreactor for domestic wastewater treatment. Water Research 30(10), 2385-2392.

Shin, H.S. and Kang, S.T. (2003) Characteristics and fates of soluble microbial products in ceramic membrane bioreactor at various sludge retention times. Water Research 37(1), 121-127.

Shukairy, H.M. and Summers, R.S. (1992) The Impact of Preozonation and Biodegradation on Disinfection by-Product Formation. Water Research 26(9), 1217-1227.

Siber, S. and Eckenfelder, W.W. (1980) Effluent Quality Variation from Multicomponent Substrates in the Activated-Sludge Process. Water Research 14(5), 471-476.

Simpson, A.E., Kerr, C.A. and Buckley, C.A. (1987) The Effect of pH on the Nanofiltration of the Carbonate System in Solution. Desalination 64, 305-319.

Sin, G., Guisasola, A., De Pauw, D.J.W., Baeza, J.A., Carrera, J. and Vanrolleghem, P.A. (2005) A new approach for modelling simultaneous storage and growth processes for activated sludge systems under aerobic conditions. Biotechnology and Bioengineering 92(5), 600-613.

Smith, C.W., Di Gregorio, D. and Talcott, R.M. (1969) The use of ultrafiltration membrane for activated sludge separation. in: Proceedings of 24th Annual Purdue Industrial Waste Conference, Purdue University, West Lafayette, Indiana, USA, 1300-1310.

Sonnenschein, C. and Soto, A.M. (1998) An updated review of environmental estrogen and androgen mimics and antagonists. Journal of Steroid Biochemistry and Molecular Biology 65(1-6), 143-150.

Spanjers, H. and Vanrolleghem, P. (1995) Respirometry as a Tool for Rapid Characterization of Waste-Water and Activated-Sludge. Water Science and Technology 31(2), 105-114.

Sperandio, M., Masse, A., Espinosa-Bouchot, M.C. and Cabassud, C. (2005) Characterization of sludge structure and activity in submerged membrane bioreactor. Water Science and Technology 52(10-11), 401-408.

Stephenson, T., Judd, S., Jefferson, B. and Brindle, K. (2000) Membrane bioreactors for wastewater treatment, IWA Pub., London, UK.

Stumm, W. and Morgan, J.J. (1981) Aquatic chemistry : an introduction emphasizing chemical equilibria in natural waters, Wiley, New York.

Tardieu, E., Grasmick, A., Geaugey, V. and Manem, J. (1998) Hydrodynamic control of bioparticle deposition in a MBR applied to wastewater treatment. Journal of Membrane Science 147(1), 1-12.

Tardieu, E., Grasmick, A., Geaugey, V. and Manem, J. (1999) Influence of hydrodynamics on fouling velocity in a recirculated MBR for wastewater treatment. Journal of Membrane Science 156(1), 131-140.

Tarleton, E.S. and Wakeman, R.J. (1994) Understanding Flux Decline in Cross-Flow Microfiltration .2. Effects of Process Parameters. Chemical Engineering Research & Design 72(A3), 431-440.

Tay, J.H., Zeng, J.L. and Sun, D.D. (2003) Effects of hydraulic retention time on system performance of a submerged membrane bioreactor. Separation Science and Technology 38(4), 851-868.

Tchobanoglous, G., Burton, F.L. and Stensel, H.D. (2003) Wastewater engineering: treatment and reuse, McGraw-Hill, Boston.

te Poele, S.T., Roorda, J.H. and van der Graaf, J.H.J.M. (2004) Influence of the size of membrane foulants on the filterability of WWTP-effluent. Water Science and Technology 50(12), 111-118.

te Poele, S.T. and van der Graaf, J. (2005) Enzymatic cleaning in ultrafiltration of wastewater treatment plant effluent. Desalination 179(1-3), 73-81.

Terada, A., Hibiya, K., Nagai, J., Tsuneda, S. and Hirata, A. (2003) Nitrogen removal characteristics and biofilm analysis of a membrane-aerated biofilm reactor applicable to high-strength nitrogenous wastewater treatment. Journal of Bioscience and Bioengineering 95(2), 170-178.

Terada, A., Yamamoto, T., Igarashi, R., Tsuneda, S. and Hirata, A. (2006) Feasibility of a membrane-aerated biofilm reactor to achieve controllable nitrification. Biochemical Engineering Journal 28(2), 123-130.

Tixier, N., Guibaud, G. and Baudu, M. (2003) Determination of some rheological parameters for the characterization of activated sludge. Bioresource Technology 90(2), 215-220.

Trussell, R.S., Merlo, R.P., Hermanowicz, S.W. and D., J. (2004) The effect of organic loading on membrane fouling in a submerged membrane bioreactor treating municipal wastewater. in: Proceedings of WEFTEC, New Orleans, USA.

Trussell, R.S., Merlo, R.P., Hermanowicz, S.W. and Jenkins, D. (2006) The effect of organic loading on process performance and membrane fouling in a submerged membrane bioreactor treating municipal wastewater. Water Research 40(14), 2675-2683.

Ueda, T., Hata, K. and Kikuoka, Y. (1996) Treatment of domestic sewage from rural settlements by a membrane bioreactor. Water Science and Technology 34(9), 189-196.

Ueda, T. and Hata, K. (1999) Domestic wastewater treatment by a submerged membrane bioreactor with gravitational filtration. Water Research 33(12), 2888-2892.

Urbain, V., Mobarry, B., de Silva, V., Stahl, D.A., Rittmann, B.E. and Manem, J. (1998) Integration of performance, molecular biology and modeling to describe the activated sludge process. Water Science and Technology 37(4-5), 223-229.

van der Roest, H.F., Lawrence, D.P. and van Bentem, A.G.N. (2002) Membrane Bioreactors for Municipal Wastewater Treatment, IWA Publishing, London.

van Loosdrecht, M.C.M., Pot, M.A. and Heijnen, J.J. (1997) Importance of bacterial storage polymers in bioprocesses. Water Science and Technology 35(1), 41-47.

Van Loosdrecht, M.C.M. and Henze, M. (1999) Maintenance, endogeneous respiration, lysis, decay and predation. Water Science and Technology 39(1), 107-117.

Van Veldhuizen, H.M., Van Loosdrecht, M.C.M. and Heijnen, J.J. (1999) Modelling biological phosphorus and nitrogen removal in a full scale activated sludge process. Water Research 33(16), 3459-3468.

Vanrolleghem, P.A., Spanjers, H., Petersen, B., Ginestet, P. and Takacs, I. (1999) Estimating (combinations of) Activated Sludge Model No. 1 parameters and components by respirometry. Water Science and Technology 39(1), 195-214.

Vanrolleghem, P.A., Sin, G. and Gernaey, K.V. (2004) Transient response of aerobic and anoxic activated sludge activities to sudden substrate concentration changes. Biotechnology and Bioengineering 86(3), 277-290.

Wen, X.H., Xing, C.H. and Qian, Y. (1999) A kinetic model for the prediction of sludge formation in a membrane bioreactor. Process Biochemistry 35(3-4), 249-254.

White, F.M. (1986) Fluid mechanics, McGraw-Hill, Inc., New York.

Wijmans, J.G., Kaschemekat, J., Davidson, J.E. and Baker, R.W. (1990) Treatment of Organic-Contaminated Waste-Water Streams by Pervaporation. Environmental Progress 9(4), 262-268.

Wintgens, T., Rosen, J., Melin, T., Brepols, C., Drensla, K. and Engelhardt, N. (2003) Modelling of a membrane bioreactor system for municipal wastewater treatment. Journal of Membrane Science 216(1-2), 55-65.

Wintgens, T., Gallenkernper, M. and Melin, T. (2004) Removal of endocrine disrupting compounds with membrane processes in wastewater treatment and reuse. Water Science and Technology 50(5), 1-8.

Wisniewski, C. and Grasmick, A. (1998) Floc size distribution in a membrane bioreactor and consequences for membrane fouling. Colloids and Surfaces a-Physicochemical and Engineering Aspects 138(2-3), 403-411.

Wisniewski, C., Grasmick, A. and Cruz, A.L. (2000) Critical particle size in membrane bioreactors - Case of a denitrifying bacterial suspension. Journal of Membrane Science 178(1-2), 141-150.

Wobus, A., Ulrich, S. and Roske, I. (1995) Degradation of chlorophenols by biofilms on semi-permeable membranes in two types of fixed bed reactors. Water Science and Technology 32(8), 205-212.

Woolard, C.R. and Irvine, R.L. (1994) Biological Treatment of Hypersaline Waste-Water by a Biofilm of Halophilic Bacteria. Water Environment Research 66(3), 230-235.

Yamamoto, K., Hiasa, M., Mahmood, T. and Matsuo, T. (1989) Direct Solid-Liquid Separation Using Hollow Fiber Membrane in an Activated-Sludge Aeration Tank. Water Science and Technology 21(4-5), 43-54.

Yang, W.B., Cicek, N. and Ilg, J. (2006) State-of-the-art of membrane bioreactors: Worldwide research and commercial applications in North America. Journal of Membrane Science 270(1-2), 201-211.

Ye, Y., Le Clech, P., Chen, V. and Fane, A.G. (2005a) Evolution of fouling during crossflow filtration of model EPS solutions. Journal of Membrane Science 264(1-2), 190-199.

Ye, Y., Le Clech, P., Chen, V., Fane, A.G. and Jefferson, B. (2005b) Fouling mechanisms of alginate solutions as model extracellular polymeric substances. Desalination 175(1), 7-20.

Ye, Y., Chen, V. and Fane, A.G. (2006) Modeling long-term subcritical filtration of model EPS solutions. Desalination 191(1-3), 318-327.

Yoon, S.H., Kim, H.S. and Yeom, I.T. (2004) The optimum operational condition of membrane bioreactor (MBR): cost estimation of aeration and sludge treatment. Water Research 38(1), 37-46.

Yuan, W. and Zydney, A.L. (1999) Humic acid fouling during microfiltration. Journal of Membrane Science 157(1), 1-12.

Zeman, L.J. and Zydney, A.L. (1996) Microfiltration and ultrafiltration: principles and applications, M. Dekker, New York.

Zhang, B., Yamamoto, K., Ohgaki, S. and Kamiko, N. (1997) Floc size distribution and bacterial activities in membrane separation activated sludge processes for small-scale wastewater treatment/reclamation. Water Science and Technology 35(6), 37-44.

Zhang, J., Chua, H.C., Zhou, J. and Fane, A.G. (2006a) Factors affecting the membrane performance in submerged membrane bioreactors. Journal of Membrane Science 284(1-2), 54-66.

Zhang, J.S., Chuan, C.H., Zhou, J.T. and Fane, A.G. (2006b) Effect of sludge retention time on membrane bio-fouling intensity in a submerged membrane bioreactor. Separation Science and Technology 41(7), 1313-1329.

Zydney, A.L. and Colton, C.K. (1986) A concentration polarization model for the filtrate flux in cross-flow microfiltration of particulate suspensions. Chemical Engineering Communications 47(1-3), 1-21.

Summary

Membrane bioreactors (MBRs) refer to the combination of membrane technology and high rate biological process technology for wastewater treatment. MBRs produce excellent effluent quality (reusable) and only require a small footprint. Strict EU effluent discharge standards and decreasing membrane costs have been the main driving force for MBR applications in EU countries. However, membrane fouling occurring on the membrane surface and within the pores reduces the long-term stability of the membrane filtration performance. The understanding of MBR fouling is still limited and at this moment, neither the evolution of membrane permeability under certain operating conditions nor the effect of cleaning measures can be predicted. These uncertainties therefore cause considerable difficulties in MBR design and operation.

Recent studies have shown that the colloidal and soluble fraction of the sludge (sludge water) correlates well with MBR fouling. Soluble microbial products (SMP) are the main constituent of MBR sludge water. However, it is not clear how to predict the foulant concentrations, how foulants are deposited onto the membrane, and how to predict the impact of deposited foulants on membrane permeability. The goal of this thesis was therefore to characterize the foulants in MBRs and to develop a mathematical model to predict both membrane fouling and effluent quality. The focus of this study is the interaction between the MBR biology and membrane fouling.

A lab-scale MBR reactor was constructed for biological nutrient removal, equipped with a tubular membrane (0.03 µm) in side-stream configuration. The SRT and HRT were set at 17 days and 6.4 hours, respectively. The sludge obtained from this MBR was used in specifically designed batch experiments to produce BAP (biomass associated products) and UAP (utilization associated products) separately, which allowed their characterisation using a new tool, LC-OCD (liquid chromatography - organic carbon detection). Both BAP and UAP exhibited a very wide molecular weight (MW) distribution. The biopolymer fraction of SMP exhibited a very high

MW and a good correlation with MBR fouling. The UAP produced during the biomass growth phase exhibited a lower MW than the BAP, suggesting UAP has a lower fouling potential than BAP.

The study of the impact of complete sludge retention on MBR biology benefits from the available ASM models. The existing Activated Sludge Model No. 2d (ASM2d) model structure can be directly applied in MBR modelling and most default parameters suggested for conventional activated sludge (CAS) hold for MBR as well. However, the MBR sludge exhibited higher substrate and oxygen affinities due to the smaller floc sizes and reduced diffusion limitation. The comparison of the ASM modelling approach as applied to MBR and CAS processes was discussed.

The impact of MBR biology on membrane fouling is very complex. A new model, called ASM2dSMP, was developed with the power to predict both effluent quality and SMP concentration. Attention was paid in the model development to minimize parameter correlation and to obtain reasonable parameter estimates. The possibility of SMP deposition can be predicted by an extended hydrodynamic model. Simulations under typical MBR operational conditions suggest that the particles with radii around 0.1 μm have the highest likelihood to deposit. The high fouling potential and high deposition possibility of SMP are demonstrated to be the main characteristics correlated with MBR fouling.

The deposited SMP can either irreversibly block the membrane or build up a hydraulically reversible cake layer. This dynamic process under crossflow and periodical backwashing conditions was modelled successfully by a newly developed filtration model. With the SMP concentration simulated by the ASM2dSMP model as input, the filtration model is able to dynamically predict the impact of MBR operational conditions (e.g., SRT and HRT) on both the short-term transmembrane pressure (TMP) increase in one filtration cycle and the long-term TMP increase between two chemical cleanings.

Samenvatting

Membraanbioreactoren (MBRs) combineren membraantechnologie met biologische zuivering om afvalwater te behandelen. MBRs produceren effluenten van een uitstekende kwaliteit (herbruikbaar) en vereisen relatief kleine installaties. De grootste drijvende krachten achter de implementatie van MBR-toepassingen in Europa zijn de dalende membraankosten en de strenge Europese lozingsnormen voor effluenten. De MBR-toepassingen kampen echter nog met één groot probleem: de langetermijnstabiliteit van de membraanfiltratie wordt gereduceerd door membraanvervuiling die optreedt zowel op het membraanoppervlak als in de membraanporiën. De kennis over dergelijke MBR-vervuiling is momenteel nog vrij beperkt en op heden kan noch voorspeld worden hoe de membraanpermeabiliteit evolueert onder bepaalde procescondities noch welk effect bepaalde reinigingstechnieken hebben. Deze onzekerheden veroorzaken aanzienlijke moeilijkheden in het MBR-ontwerp en in de MBR-werking.

Recente studies toonden aan dat de colloïdale en opgeloste fracties van het slib (waterige fractie) gecorreleerd zijn met de MBR-vervuiling. Onderzoek toonde aan dat de hoofdcomponenten van deze waterige fractie opgeloste microbiële producten (SMP) zijn. Desondanks is het niet duidelijk hoe men de concentraties aan vervuilende stoffen kan voorspellen, hoe deze vervuilende stoffen zich afzetten op de membranen en hoe men de impact van deze vervuiling op de membraanpermeabiliteit kan voorspellen. Het doel van deze thesis is bijgevolg het karakteriseren van de vervuilende stoffen in MBRs en de ontwikkeling van een mathematisch model dat zowel de membraanvervuiling als de effluentkwaliteit voorspelt. Deze studie is voornamelijk gefocust op de interactie tussen de MBR-biologie en de membraanvervuiling.

Op laboschaal werd een membraanbioreactor van het zijstroomtype gebouwd die nutriënten biologisch verwijdert en uitgerust is met een tubulair membraan (0.03 μm). De slibverblijftijd (SRT) en de hydraulische verblijftijd (HRT) werden ingesteld op

231

respectievelijk 17 dagen en 6.4 uren. Het slib verkregen uit de MBR werd vervolgens gebruikt voor specifiek ontworpen 'batch' experimenten die biomassageassocieerde producten (BAP) en verbruiksgeassocieerde producten (UAP) afzonderlijk produceerden. Hierdoor werd de karakterisatie van BAP en UAP mogelijk. Deze karakterisatie gebeurde aan de hand van een nieuwe techniek, namelijk LC-OCD (vloeistofchromatografie – organische koolstof detectie). Het moleculair gewicht (MW) van zowel BAP als UAP vertoont een zeer grote spreiding. De fractie aan biopolymeren in SMP heeft een zeer groot MW en vertoont een goede correlatie met de MBR-vervuiling. De UAP, geproduceerd tijdens de fase van biomassagroei, vertonen een lager MW dan de BAP. Dit laatste resultaat wijst op het lagere vervuilingspotentieel van UAP tegenover BAP.

Een studie naar de impact van de volledige slibretentie op de MBR-biologie werd uitgevoerd aan de hand van een model. Een bestaande modelstructuur (Actief Slib Model Nr. 2d - ASM2d) werd hiervoor zonder wijzigingen toegepast, waarbij de meeste standaardparameters voor conventioneel actief slibsystemen (CAS) ook geldig bleken voor het MBR-systeem. Het MBR-slib bezat echter wel een hogere substraat- en zuurstofaffiniteit vanwege de kleinere vlokken en de gereduceerde diffusiebeperking. Een vergelijkende studie werd uitgevoerd tussen de ASM-modelering toegepast op een MBR-systeem en op een CAS-systeem.

De impact van de MBR biologie op de membraanvervuiling is zeer complex. Een nieuw model, ASM2dSMP, werd ontwikkeld. Dit model kan zowel de effluentkwaliteit als de SMP concentratie voorspellen. Extra aandacht werd besteed aan de modelontwikkeling zodat een minimale parametercorrelatie en realistische parameterschattingen werden bekomen. Aan de hand van een uitgebreid hydrodynamisch model werd de kans op SMP-afzetting voorspeld. Simulaties met dit model tonen aan dat onder typische condities in MBRs de slibdeeltjes met een straal van 0.1 µm de hoogste kans hebben om afgezet te worden. Er werd aangetoond dat het grote vervuilingspotentieel en de hoge afzettingskans van SMP het sterkst correleren met de MBR-vervuiling.

Afgezette SMP kunnen ofwel het membraan irreversibel blokkeren ofwel een reversibele hydraulische koeklaag opbouwen. Onder een dwarsstroomconfiguratie en

onder periodische terugspoelcondities werd dit dynamisch proces succesvol gemodelleerd door een nieuw ontwikkeld filtratiemodel. Dit nieuwe filtratiemodel gebruikt de SMP-concentratie berekend uit het ASMP2dSMP model als input. Het filtratiemodel is in staat om dynamische te voorspellen wat de impact is van de werkingscondities van de MBR (vb. SRT en HRT) op zowel de kortetermijntoename van de transmembraandruk (gedurende één filtratiecyclus) als op de langetermijntoename van de transmembraandruk (tussen twee chemische reinigingen).

Appendix A.

Influent composition of Lab-scale MBR

Chemicals	Concentrated (mg/L)	Diluted (mg/L)
NaAc·3H$_2$O	1974.60	131.64
Urea	1376.10	91.74
NH$_4$Cl	191.30	12.75
KH$_2$PO$_4$	351.00	23.40
CaCl$_2$	2526.41	168.43
FeSO$_4$·7H$_2$O	116	7.73
MgHPO$_4$·3H$_2$O	435.3	29.02
MgCl$_2$·6H$_2$O	1199.60	79.97
Peptone	261.20	17.41
Starch	1830.00	122.00
Milk powder	1742.90	116.19
Yeast	783.60	52.24
Soy oil	835.33	55.69
ZnCl$_2$	3.100	0.207
PbCl$_2$	1.500	0.100
MnSO$_4$·H$_2$O	1.600	0.107
NiSO$_4$·6H$_2$O	5.000	0.333
CuCl$_2$·2H$_2$O	8.000	0.533
Cr(NO$_3$)$_3$·9H$_2$O	11.600	0.773
HCl (Hydrochloric Acid)	190 mL in 75L till pH < 3	

Appendix B.

List of equipment used in lab-scale MBR

Equipment	Function	Model	Operation range
Bioreactor			24 L
Membrane	Biomass separation	X-flow, tube F4385, module 11PE	0.17 m^2 (5.2 mm)
Mixer 1	Mixing in anaerobic compartment	Aquarium pump, Project Green	
Mixer 2	Mixing in aerobic/anoxic	Aquarium pump, Project Green	
Pump P1	Influent pump	Watson Marlow 323U/RL (4.8 mm tube)	0.075 L/min
Pump P2	Mixing & recirculation & waste	Watson Marlow 505 U, 501RL head (8 mm tube)	0.6 L/min
Pump P3	Pump bioreactor to membrane	Watson Marlow 505 U, 501RL head (8 mm tube)	0.375 L/min
Pump P4	Sludge recirculation in membrane loop	Seepex BN 2-6L + frequency controller	7.65 L/min
Pump P5	Control permeate/BW flux	Seepex MD 003-12 + frequency controller	0.075 L/min
Air valve V5	Aeration on/off control	Burkert 0330 A3	0-20 L/min
Air flow meter	Read air flow to the bioreactor & membrane	Air flow meter: Dwyer RMA-23-SSV (25, 50LPM)	25,50 L/min
3 way solenoid pinch valve	Various control	Sirai S306 01-Z530A	8 mm silicon tube
Bürkert solenoid valve (V6, V7)	Switch filtration/BW	Bürkert 3/2-way; G 1/4, Universal function, type 330	−0.5-1 bar
Relay	Switch a 24V DC	Finder 95.75	−0.5-1 bar
Pressure sensor 1 (PS1)	Bioreactor level	Honeywell 142PC02D	0-0.1 bar
Pressure sensor 2 (PS2)	Membrane inlet pressure	Honeywell 142PC15D	0-1 bar
Pressure sensor 3 (PS3)	Membrane outlet pressure	Honeywell 142PC15D	0-1 bar
Pressure sensor 4 (PS4)	Permeate pressure	Honeywell 143PC15D	−1-1 bar
DO sensor_Aerobic		METTLER TOLEDO InPro6050	0-10
DO_Aerobic_cable		VP6-ST/5m	
DO_Aerobic_transmitter		Knick stratos-E 2402 oxygen	
pH sensor_Aerobic		METTLER TOLEDO HA 405-DXK-S8/225	2-12
pH_Aerobic_cable		VP6-ST/5m	
pH_Aerobic_Transmitter		Knick stratos-E 2402 pH	
pH sensor_Anaerobic		METTLER TOLEDO Inpro4250	2-12
pH_Anaerobic_cable		VP6-ST/5m	
pH_Anoxic_Transmitter		Knick stratos-E 2402 pH	
ORP sensor_Aerobic		METTLER TOLEDO Pt4805-DXK-58/120	−100-300 mV
ORP_Aerobic_cable		AS9/5m	
ORP_Aerobic_Transmitter		Knick stratos-E 2402 pH	
DAQ-card and connector block	DAQ and process control	NI, DAQ card: PCI-MIO-16XE-50, connector block CB-68LPR	
PC	DAQ and process control	PII 350	
Cooling coil 1(anaerobic)	MBR Temp. Contr.	JULA71507400 coil (diameter 94mm)	15 °C
Cooling coil 2 (aero./anox.)	MBR Temp. Contr.	JULA71507400 coil (diameter 94mm)	15 °C
Cooling coil 3 (membrane)	MBR Temp. Contr.	JULA8970416 (1.3m)	15 °C
Cooling machine	MBR Temp. Contr.	LAUDA WK CLASS WK 1200	15 °C
THERMOSTAT switch	Swith off P1&P5 if P5 dry-run	Farnell order NO 560248	indep. from LabVIEW
Velleman Liquid Level switch	Swith off P1&P5 if level is too high	Velleman Liguid Level Controller K2639	indep. from LabVIEW
UPS	Protect the system from power failure	APC Smart-UPS XL 1000VA	

Appendix C.

DAQ card channel configuration

Device	Description	Physical channel	Channel name	Calibration	Output range
Pressure sensor PS2	Inlet of membrane	AI0	PS2	Auto	1-6 V
Pressure sensor PS3	Outlet of membrane	AI1	PS3	Auto	1-6 V
Pressure sensor PS4	Permeate of membrane	AI2	PS4	Auto	1-6 V
Pressure sensor PS1	Bioreactor depth	AI3	PS1	Auto	1-6 V
pH anaerobic	On-line pH	AI4	pHan	Yes	2-12
ORP aerobic/anoxic	On-line ORP	AI5	ORPan	Yes	-100-300 mV
pH aerobic/anoxic	On-line pH	AI6	pHa	Yes	2-10
DO aerobic/anoxic	On-line DO	AI7	DOa	Yes	0-10
Temperature aerobic/anoxic	Combined with ORP sensor	AI8	Tempa	Yes	5-45
free		AI9			
free		AI10			
free		AI11			
free		AI12			
Measure the pressure sensor excitation voltage	For auto calibration of pressure sensor	AI13	PSSupply	No	Typical 8 V
Electricity failure alarm in	Detect electricity failure	AI14	ElecFail	No	Normal <1 V Alarm >3 V
Over flow alarm In	Detect overflow from bioreactor , safety tank	AI15	AlarmIn	Check battery	Normal <4 V Alarm >4 V
Recirculation pump in membrane loop P4	Control sludge recirculation rate	AO0	P4	Yes	0-10 V
Permeate/BW pump P5	Control effluent and BW flow rate	AO1	P5	Yes	0-10 V
3-way valve to switch influent V1	Time controlled	DIO0	V1	No	Normal off
3-way valve to waste sludge V2	Time controlled	DIO1	V2	No	Normal off
3-way valve to switch aerobic mixing and anaerobic recirculation V3	Time controlled	DIO2	V3	No	Normal off
Aeration valve V4	DO On-off control	DIO3	V4	No	Normal off
3-way valve for BW V6,7	Time controlled	DIO4	V67	No	Normal off
3-way vale for effluent sampling V8	Time controlled	DIO5	V8	No	Normal off
free		DIO6			
Alarm Out	Stop all pumps and set to emergent mode	DIO7	AlarmOut	No	Normal off

AI = analog input, AO = analog output, DIO = Digital input/output
DAQ card model: NI PCI-MIO-16XE-50

Curriculum Vitae

Personal particulars

Tao JIANG
Suzhou, P.R. China, September 26, 1974
tao.jiang@biomath.ugent.be
Chinese

Basic Education

October, 2000 — June, 2002
M.Sc., Sanitary Engineering, graduate with distrinction
UNESCO-IHE Institute for Water education, Delft, the Netherlands
Thesis title: "Fouling in Membrane Bioreactor Systems"

September, 1993 — July, 1997
B.Sc., Environmental Engineering, graduate with distrinction
University of Science & Technology of Suzhou, P.R. China
Thesis title: "Nutrient Removal of a Municipal Wastewater Treatment Plant"

Extra training

Doctoral training course, Ghent University, Belgium, 2003-2004

Employment

From January 2003 to date as research assistant and Ph.D. student at the Department of Applied Mathematics, Biometrics and Process Control (BIOMATH), Ghent University (Belgium), and UNESCO-IHE Institute for Water education, Delft, the Netherlands

From August, 1997 to September, 2000 as government official at Environmental Protection Agency of Suzhou, P.R. China

Research stays abroad

November 1 – December 15, 2005, University of Cape Town and University of Kuwazulu-Natal, South Africa

Publications

Publications in books and in international journals with reading committee

Jiang, T., Kennedy, M.D., van der Meer, W.G.J., Vanrolleghem, P.A. and Schippers, J.C. (2003) The role of blocking and cake filtration in MBR fouling. Desalination 157(1-3), 335-343.

Jiang, T., Kennedy, M.D., Guinzbourg, B.F., Vanrolleghem, P.A. and Schippers, J.C. (2005) Optimising the operation of a MBR pilot plant by quantitative analysis of the membrane fouling mechanism. Water Science and Technology 51(6-7), 19-25.

Jiang, T., Liu, X., Kennedy, M.D., Schippers, J.C. and Vanrolleghem, P.A. (2005) Calibrating a side-stream membrane bioreactor using Activated Sludge Model No. 1. Water Science and Technology 52(10-11), 359-367.

Jiang, T., Kennedy, M.D., Yoo, C.K., Nopens, I., van der Meer, W.G.J., Futselaar, H., Schippers, J.C. and Vanrolleghem, P.A. (2007) Controlling submicron particle deposition in a side-stream membrane bioreactor: a theoretical hydrodynamic modelling approach incorporating energy consumption, Journal of Membrane Science. Journal of Membrane Science (accepted).

Jiang, T., De Schepper, V.C.J., Kennedy, M.D., Nopens, I., van der Meer, W.G.J., Futselaar, H., Amy, G. and Vanrolleghem, P.A. (2007) Modelling the impact of soluble microbial products on MBR fouling: the short-term reversible fouling and long-term irreversible fouling. Journal of Membrane Science (submitted).

Jiang, T., Kennedy, M.D., De Schepper, V.C.J., Nopens, I., van der Meer, W.G.J., Futselaar, H., Vanrolleghem, P.A. and Amy, G. (2007) Characterisation of soluble microbial products in membrane bioreactors: the impact of substrate condition and biomass growth phase. Journal of Membrane Science (submitted).

Jiang, T., Myngheer, S., De Pauw, D.J.W., Spanjers, H., Nopens, I., Kennedy, M.D., Amy, G. and Vanrolleghem, P.A. (2007) Modelling the production and degradation of soluble microbial products in membrane bioreactors. Water Research (submitted).

Jiang, T., Sin, G., Spanjers, H., Nopens, I., Kennedy, M.D., van der Meer, W.G.J., Futselaar, H., Amy, G. and Vanrolleghem, P.A. (2007) Comparison of modelling approach between membrane bioreactor and conventional activated sludge processes. Water Research (submitted).

Publications in conference proceedings
Jiang, T., Kennedy, M.D., van der Meer, W.G.J., Vanrolleghem, P.A. and Schippers, J.C. (2003) The role of blocking and cake filtration in MBR fouling, Malta.

Jiang, T., Kennedy, M.D., van der Meer, W.G.J., Vanrolleghem, P.A. and Schippers, J.C. (2003) Controlling membrane pore blocking and filter cake build-up in side-stream MBR systems, Sydney, Australia.

Jiang, T., Kennedy, M.D., Guinzbourg, B.F., Vanrolleghem, P.A. and Schippers, J.C. (2005) Optimising the operation of a MBR pilot plant by quantitative analysis of the membrane fouling mechanism, Seoul, Korea.

Jiang, T., Liu, X., Kennedy, M.D., Schippers, J.C. and Vanrolleghem, P.A. (2005b) Calibrating a side-stream membrane bioreactor using Activated Sludge Model No. 1, Marrakech, Morocco.

Jiang, T., De Schepper, V., Kennedy, M.D., Futselaar, H., van der Meer, W.G.J., Amy, G.L. and Vanrolleghem, P.A. (2006) Simulating the soluble microbial products in a membrane bioreactor system and their impact on membrane fouling, Beijing, China.

Sin, G., Niville, K., Bachis, G., Jiang, T., Nopens, I., Van Hulle, S.W.H. and Vanrolleghem, P.A. (2007) Nitrite effect on the phosphorus uptake activity of phosphate accumulating organisms (PAO) in pilot-scale SBR and MBR reactors, Baltimore, Maryland, USA.

Congresses and workshops
EUROMBRA workshop, Bio-fouling in Membrane System, July 11-12, 2006, NTNU –Norwegian University of Science and Technology, Trondheim, Norway, platform presentation